Wind Turbines near flood defences

Study on the impact craters of falling nacelles hitting a dike

V.N. Kramer

TU Delft

Witteveen + Bos

Cover photo: *Windpark Noordoostpolder*

Source: http://www.klaaseissens.nl/

Wind Turbines near Flood Defences

Study on the impact craters of falling nacelles hitting a dike

by

V.N. Kramer (Victor)

to obtain the degree of Master of Science in Civil Engineering
at the Delft University of Technology,
to be defended publicly on December 20, 2017 at 16:00.

Student number:	4076508	
Project duration:	February 2017 – December 2017	
Thesis committee:	Prof. dr. ir. M. Kok	TU Delft, chairman
	Dr. ing. M.Z. Voorendt	TU Delft
	Dr. P.J. Vardon	TU Delft
	Ir. G.R. Spaargaren	Witteveen+Bos
	H.A. Schelfhout	Deltares

An electronic version of this thesis is available at `http://repository.tudelft.nl/`

TU Delft

Witteveen + Bos

Summary

Building wind turbines near flood defences has numerous advantages over other locations on land. The water authorities, which own the land of the flood defence, will only permit the turbines if the flood protection assessment satisfies the safety standard after the wind turbines have been constructed. There are three types of failure of a wind turbine: falling over of the turbine, nacelle falling off the tower and blades falling of the rotor. The first two, with their relation to the flood defence, are analyzed in this report. An assessment is made, in which the additional failure probability of the flood defence is determined.

The main white spots in the flood protection assessments are: First, the assessment method of wind turbines near flood defences is a gray area, which leaves room for interpretation. Secondly, the effects of the constant vibrations of wind turbines are unknown, this is currently being researched. Thirdly, the size and depth of the crater which develops after an impact of a nacelle hitting the flood defence. This third white spot is researched in this report.

The models currently used to estimate the penetration depth of the crater give questionable results. They are developed for other purposes than impacts of objects similar to a nacelle, which has a large mass and low impact velocity. Finite elements methods are strong in modeling soil-structure interaction and deformations. However, at modeling large deformations severe mesh distortions will occur. The Material Point Method (MPM) can handle large deformations, which is essential in the case of a nacelle impact. A MPM model is made for the case study of an Enercon E-126 nacelle hitting a sea dike in the north of Groningen.

The Material Point Method turns out to be a good method to determine the size and depth of a crater. The nacelle of the Enercon E-126 turbine can cause at maximum a penetration depth of 3.8 meters on a dry sea dike consisting of sand. There are two impact locations on the dike which can be distinguished: an impact on the crest and an impact on the slope. If the impact is on the crest, both the crest is and large parts of both slopes are affected. The soil below the slopes is lifted up, this causes the revetment to lose its coherence. An impact on the slope will mainly affect the slope and the crest is only limited affected. However, the size and depth of the crater depend largely on the soil characteristics and the potential energy of the nacelle. Those are taken conservative in the model. So, the penetration depth of 3.8 meters is the maximum.

The Expertise Network for Flood Protection gave requirements for wind turbines near flood defences. The case study is again an Enercon E-126 turbine built directly at the inner side of a sea dike in Groningen. Overtopping & overflow, inner slope-instability and instability of the revetment are considered as the governing failure mechanisms for the additional failure probability. When using only conservative assumptions, the flood protection requirements are not satisfied. However, with using more realistic assumptions, the additional failure probability can be determined more precise and therefore be lowered. In the end, the wind turbine can be moved further inland to lower the hitting probability of the flood defence, this will decrease the additional failure probability.

Preface

This thesis report is the result of the graduation project to complete my master degree in Civil Engineering at Delft University of Technology. This is the result of 9 months of hard work in the field of Flood Protection and geotechnical modeling, with which I was not familiar before. The research is supported by Witteveen+Bos and Deltares.

First of all, I would like to express my gratitude to the members of my graduation committee. Their support, ideas and feedback helped during this graduation project. Matthijs Kok, for the scientific approach and chairing the committee. Gerben Spaargaren, for the daily supervision and always having ideas on how to move forward. Mark Voorendt, for the scientific approach as well and the advice on how to write a good report. Harry Schelfhout, for being the expert on the field of flood protection and helping for when I got stuck. Phil Vardon, for helping me with numerical modeling issues.

Furthermore, I would like to thank Witteveen+Bos for giving me the opportunity to work and their office and providing expertise on multiple subjects. I want to thank all my colleagues as well for sharing their knowledge, I always felt very welcome, and I appreciated the nice working environment at the office.

I would like to express my gratitude as well to the colleagues from Deltares which provided the MPM software and helped for me 3 months learning to use program: Alex Rohe and Amine Aboufirass. I appreciated the opportunity as well to see the development of model.

Victor Kramer
Rotterdam, November 2017

Contents

Chapter 1

Introduction

1.1 Background and problem description

The most seen windmill today is the electricity producing wind turbine. In the 1980's, the first large wind turbines were built (Shahan, 2014) and a few years later the first wind farms (group of wind turbines) were constructed. The wind turbines increased in size ever since and can reach heights of 200 meters (Quilter, 2016). Large wind turbines increasingly affect their surroundings.

Most areas in the Netherlands prone to flooding are protected by flood defences: dikes, barriers and dunes. These dikes (also named embankments or levees) are vital to the Dutch flood protection system. Failure of a dike could lead to catastrophic floods, for example in 1953. Therefore, understanding the safety, functioning and vulnerability of dikes is very important.

In the Netherlands the tendency is to build wind turbines together in wind farms. For the onshore wind farms there are multiple advantages to build them near or on dikes:

- Wind turbines in a row and dikes are both line elements in the landscape. For aesthetic reasons, people prefer these elements together in a line compared to other configurations.
- The average wind speed on land is higher near the sea and lakes. So, wind turbines built near the edge of the sea and lakes will generate more electricity (SenterNovem, 2005). This is exactly where the dikes are located in the Netherlands.
- For project developers there are less land owners to deal with when the wind farm is being constructed on or near a dike. The land owners of dikes in the Netherlands are the water authorities and in few cases they also have the land next to it. With less stakeholders involved this will speed up the planning phases in the construction process.
- Relatively few people live close to a dike compared to other parts of the country, so there is less inconvenience for the surrounding.

But there is a turning side. There are risks involved for the dikes, which still must satisfy the flood protection requirements. Therefore, water authorities and Rijkswaterstaat, which must ensure the land behind the dike is safe from the water, are skeptic about these wind turbines near dikes. For example, the wind turbine might affect the stability of the dike body and possibly increases the failure probability due to macro-stability. During a storm the wind turbine tower could buckle and as a result the nacelle can land on the dike as another example. In addition, foundations piles can penetrate a clay layer which can lead to water moving along these piles. This effect might increase when the wind turbine is vibrating. These vibrations could even have an effect on every failure mechanism of the dike (Hölscher, 2016).

All water authorities and Rijkswaterstaat have their own policy for building wind turbines near their dikes. Several water authorities do not permit any positioning of wind turbines in the

core and protection zone of the dike. The policy of Rijkswaterstaat is: "Placing of wind turbines in the core zone & protection zone of a dike will only be approved when the initiator can prove that this has no negative effects on the water retaining function of the dike conform the safety standard in the Water Act (Rijkswaterstaat, 2015)."

A reason why water authorities and Rijkswaterstaat are so reluctant, is that many aspects of this safety assessment are unknown. At the moment the knowledge gaps in these assessments are filled with conservative estimations. In several cases these conservative estimations lead to designs with a minimum distance between the core zone and wind turbine in the order of the wind turbine hub height. When turbines are placed that far from the dike, it will limit the potential advantages mentioned. When more knowledge gaps or white spots are filled in, the water authorities can make a better decision to permit wind turbines near or on the dike.

1.2 Relevance of research on wind turbines near flood defences

In 2013 forty Dutch organizations came to an agreement to show their commitment for a more sustainable society and economy. This agreement is called 'Energieakkoord voor duurzame groei' or 'The Agreement on Energy for Sustainable Growth' (Sociaal-Economische Raad, 2013). The forty organizations consist of employer's associations, trade unions, nature- and environmental organizations, societal organizations, financial organizations and governments. One of the four formulated overarching objectives is: 14% share of renewable energy in the Netherlands' total consumption of energy by 2020. In order to reach this 14% share of renewable energy, onshore wind should provide 6.000 MW in 2020. At the end of 2015 the total installed onshore wind power was only 2.950 MW (RVO, 2016). This implies that only before 2020 3.050 MW of power must be installed.

To achieve these goals, many new wind farms are needed. The Dutch government has a leading role in the spatial planning of the locations of wind farms. The government has chosen preferred locations for large scale wind energy production (Ministerie van Infrastructuur en Milieu, 2014). These are the locations with relatively high average wind speeds and sparsely populated areas (SenterNovem, 2005). These preferred areas are often near dikes. This resulted in many initiatives of placing wind turbine near dikes and consequently more requests at water authorities.

The trend is to build larger wind turbines (NOS, 2016). The larger the wind turbine rotor diameter & higher the hub height, the more energy is produced. This results in turbines tip heights of almost 200 meters (Quilter, 2016). Larger wind turbines produce more energy, but can as well potentially cause more damage. These larger wind turbines have for example more mass, higher hubs and larger foundations. The effects of these increased size of elements on the surrounding will increase and therefore the effect on flood defences will increase as well.

1.3 Structure of the report

This report consists of 2 parts. The first part has 3 chapters: 1. 'Introduction', 2. 'System analysis' and 3. 'Research definition'. The second part is the study of the impact craters caused by a structural failure of the wind turbine.

The system analysis will deal with the total system wind turbine and dike. The goal of this part is to show what is actually happening or could happen during the life cycle of wind turbine near a dike. During the construction, exploitation and dismantling phase the dike can be affected by a wind turbine. These mostly qualitative risk studies of the wind farms in the Netherlands are combined to provide an overview to the system wind turbine and dike. These effects are related to a failure mechanism of the dike. Chapter 2 'System Analysis' ends with an overview

of the system wind turbine - dike related to relative distance from the wind turbine. In addition, the white spots which follow from the system analysis can be found here.

Chapter 3 'Research definition' presents the conclusions from the system analysis and the introduction to the second part of the report. The research questions are related to the depth of crater impact and the Material Point Method.

The second part consists of the impact crater which can be formed when a wind turbine hits a dike. First, models are described which have been used in the past in flood protection assessments in Chapter 4. The Material Point Method is used to assess the crater formation. This method is compared with the other models and methods.

In Chapter 5 'Simulation set-up' the Material Point Method simulations set-ups are outlined.

The results and analysis of the simulations can be found in Chapter 6 'Analysis of simulation results'.

In Chapter 7 'Impact on dike failure probability' the coupling is made back to flood protection. A short flood protection assessment is performed with components which are related to the results of Chapter 6.

The last chapter, consists of conclusions and recommendations for further research.

Chapter 2

System analysis

2.1 Introduction

This system analysis provides an overview of the aspects that are important for placing of a wind turbine near a flood defence. There are many aspects to cope with before the wind turbine can be built. The system of the wind turbine and the effects it potentially has on the surroundings is one part. The other main part is the dike and its failure mechanisms. First these two aspects are dealt with separately before they are combined. The practical side of building wind turbines is treated in this system analysis as well. The goal of the system analysis is to present an overview of the most important factors which have an influence on the location of a wind turbine near a dike for the flood protection aspect.

2.2 Assessment of flood defences

System of flood protection

In the Netherlands, the system of flood protection divides the flood defences in primary and regional flood defences. Primary flood defences protect the land against a flooding from the sea, large rivers and large lakes. Flood defences are: dikes, dams, dunes and other structures such as locks and storm surge barriers (ENW, 2016). Along canals, puddles and small rivers the regional flood defences protect the land against flooding. A breach of a regional flood defence often has less consequences then a breach of a primary flood defence, but as well can have a significant impact.

Until the year 2017 each dike ring had its own exceedance probability as a safety standard. These safety standards were the exceedance probability of a hydraulic load level. From 2017 on, the primary defences have been split into segments with their own safety standard, which is a maximal permissible failure probability, shown in Figure 2.1. The actual failure probability consists out of the probability of a certain load and the probability the flood defence cannot withstand this load. It is important. The English word 'segment' is in Dutch 'traject', the Dutch word 'segment' is used for a small part of the dike with similar characteristics.

The National Government determines the safety standards for the dike segments of primary flood defences. For the regional ones the safety standards are determined by the provinces. But the water boards have the task to manage and take care of the maintenance of the flood defences, excluding a small part of the primary defences which are managed by Rijkswaterstaat.

Figure 2.1: Dike segments of primary flood defences in the Netherlands in 2017 (ENW, 2016)

Procedure assessment WBI 2017

The primary flood defences need to be assessed at least every 12 years to verify whether they still satisfy the safety requirements. Together with the new safety standards the 'Wettelijk Beoordelingsinstrumentuarium 2017' (WBI 2017), or 'statutory assessment instruments 2017' is introduced. The method and standards to assess the flood defences are prescribed in WBI2017. It as well contains the calculation methods, software and manuals (Rijkswaterstaat, 2016c).

A short simplified assessment of a dike segment will be elaborated in this section. The goal of an assessment is to determine if a flood defence satisfies the safety standard. In WBI2017 this assessment results in a safety judgment. The safety standard consists of 2 values: the lower threshold & alert value. If the failure probability is lower than both the lower threshold & alert value, the segment does not have to be reinforced. If the failure probability is higher than the lower threshold value, then the segment has to be reinforced. It is possible that the safety judgment is that the failure probability is in between them and then future reinforcements are considered, see Figure 2.2.

To make rapid safety judgments, there is a filter in WBI2017. This filter is used to determine which check/calculation should be used. The scheme for the general filter can be found in Figure 2.3. First a general filter on segment level will be applied. If it is applicable, immediately a safety judgment can be made. When this general filter on segment level is not applicable, a general filter on section (vak) level is used. A section of a dike is a dike of a certain length with the same characteristics. The filter could lead to a simple check, detailed check per section or/and per segment. Or it could lead to a custom check (toets op maat). These different checks will lead to a check judgment which could lead to an improved check or a safety judgment (Rijkswaterstaat, 2016c).

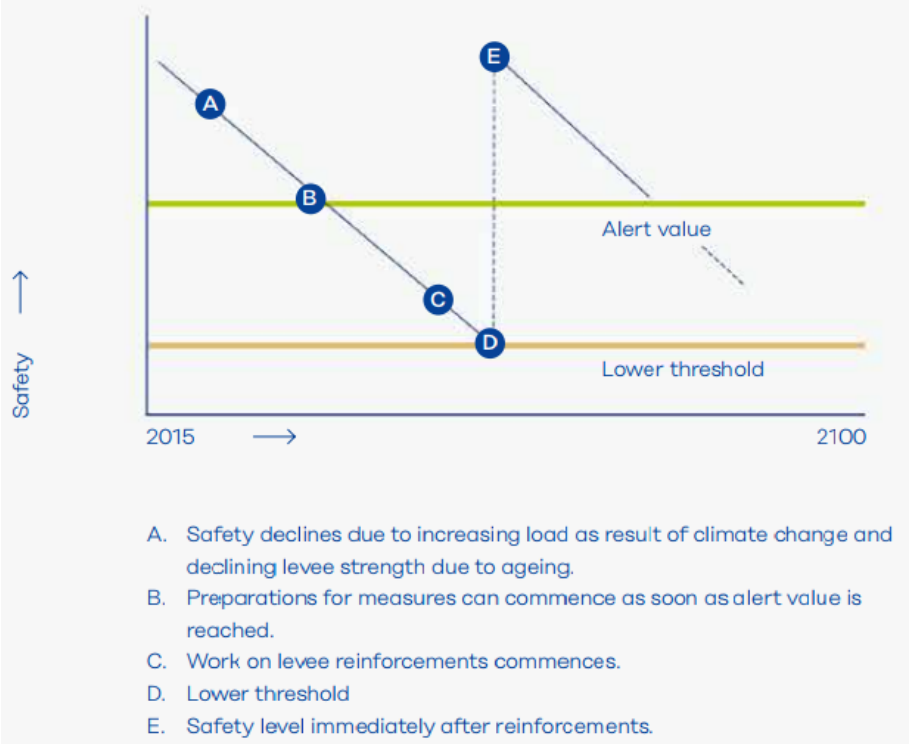

Figure 2.2: Alert value and lower threshold value (ENW, 2016)

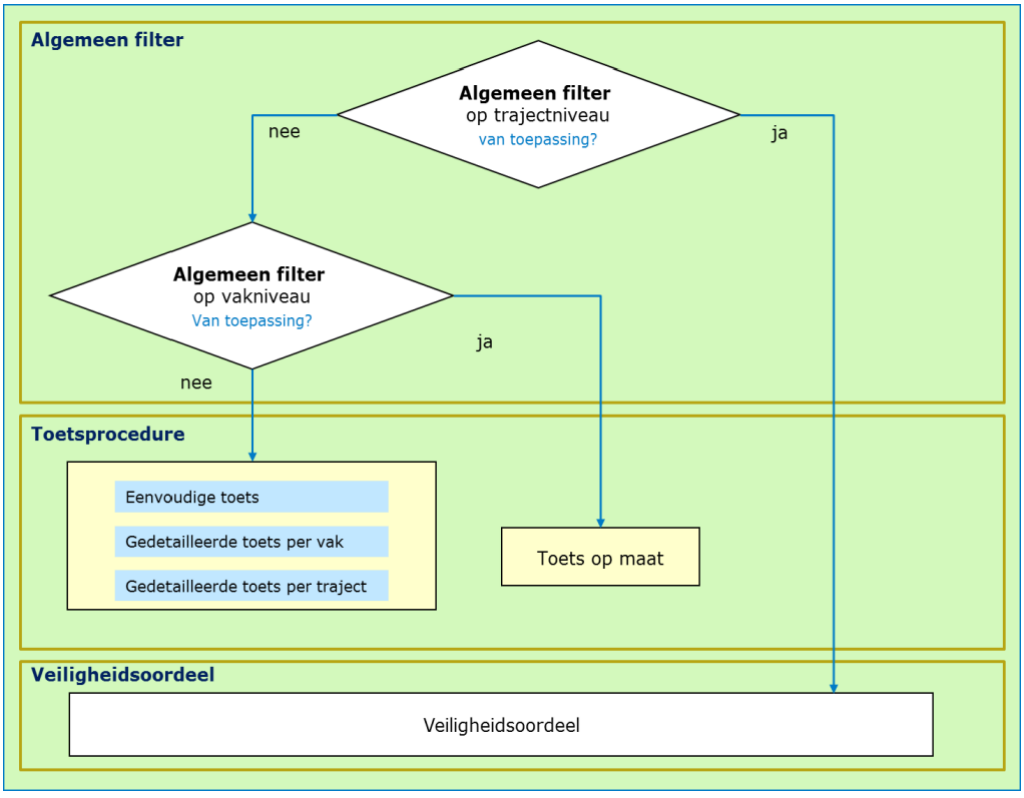

Figure 2.3: General filter WBI 2017 (Rijkswaterstaat, 2016b)

Non-water retaining objects

A wind turbine belongs to the group non-water retaining objects or 'Niet-waterkerend objecten' (NWO's). Other objects in this group are for example buildings, trees and cables. These NWO's can potentially damage a flood defence. The NWO's are split in 4 groups: buildings, vegetation, cables & pipes, other structures. The wind turbine itself is in the group other structures, however, the cables of the wind turbine are in the in the group cables & pipes. For the wind turbine itself is no 'simple check' of 'detailed check' is available, it is assessed by a 'custom check' (Rijkswaterstaat, 2016c).

The 'custom check' makes it possible to do specific analyses: location specific analyses, advanced analyses and expert judgments. In WBI 2017 there is no prescription on how this should be performed. In the future examples on how this could be done will be available. Further in this chapter more will be elaborated on this assessment.

Relevant failure mechanisms of flood defences

Flood defences have the goal of protecting the land behind it against flooding. These defences can 'fail' and 'collapse'. These are two states which look the same, however they are not the same. A collapse is a loss of consistency or large geometrical change. A failure of a defence is an exceeding of the ultimate limit state.

Flood defences can fail according to various mechanisms (Jonkman & Schweckendiek (eds), 2015). For dikes these are shown in Figure 2.4. The ones which could be related to effects of wind turbines are explained in the text.

A. Overflow When the still water level is higher than the crest height of the dike it is called overflow. Water flows over the crest into the protected area. The water flowing down the inner slope can damage the slope. This can for example cause a breach.

B. Wave overtopping In this failure mechanism the still water level remains under the crest height, but waves do overtop the crest. When the discharge of these overtopping waves is high, the inner slope can erode.

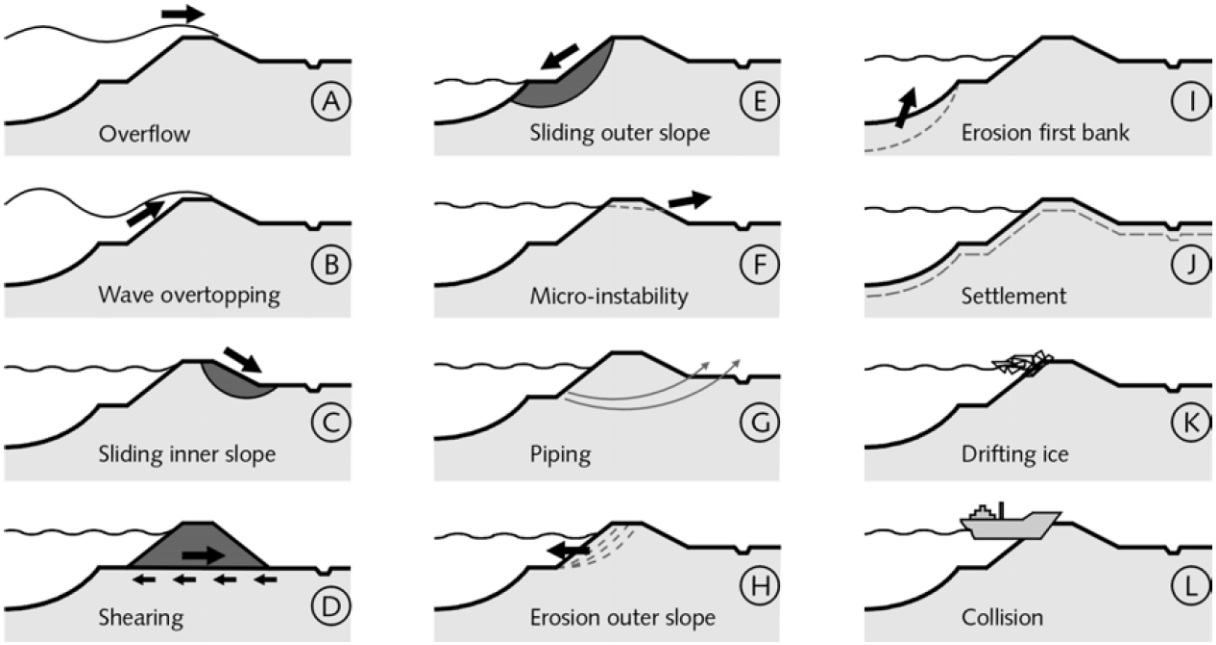

Figure 2.4: Schematic overview of the most relevant failure mechanisms (TAW, 1998)

C. Sliding inner slope (macro-instabiliteit binnenwaarts) Sliding of the inner slope is the most common stability problem for dikes. This typical river dike problem occurs when the dike body is saturated with water. The pore pressures increases, the effective stress decreases. The decreased effective stress has an influence on the shear stress resistance, which can lead to the development of sliding planes in the slope.

E. Sliding outer slope (macro-instabiliteit buitenwaarts) If the outside water level drops very quickly sliding of the inner slope can occur. The pore water inside the dike body cannot follow the rate of change of the water level. The pore pressure in the dike body will be higher than usual and sliding can occur.

G. Piping Piping occurs when there is a hydraulic gradient over a dike for a longer period (days, weeks). If these gradients on the land side are high enough, particles can start eroding due to a flow of water under the dike. If more and more particles erode, a pipe forms under the dike. When this pipe has a significant size, it collapses and the dike fails.

H. Erosion outer slope (revetment failure) The revetment protects the slope from the currents and wave attacks. The revetment is often a grass cover or consists of blocks in case of higher loads. When this revetment fails, the slope is unprotected and can erode.

I. Erosion first bank (foreshore) A flow slide of the foreshore as a result of liquefaction is another failure mechanism. This can occur rather quickly. Relative steep slopes of loosely packed sand ($>$ 1V:4H) will transform into very gentle slopes (i.e. 1V:10H to 1V:20H).

2.3 Wind turbines

The wind turbines which are considered in this study are only large turbines. The characteristics of these large turbines can be found in this section.

Characteristics & components

In the 1980's the large scale production of wind energy started (Hau, 2006). From then on wind turbines can be split into two types: offshore and onshore turbines. Important differences in characteristics are the hub height and foundation structure. This thesis focuses on onshore wind turbines, Figure 2.5 presents an overview of such a turbine. These onshore wind turbines consist several major components:

- Rotor blades: Wind turbines have typically three blades. In too high wind speed the turbine has to be shut down to avoid damage to itself and the surroundings. This can be done by pitching the blades, so the turbine stops rotating. The material of the blades is often fiberglass reinforced polymer (Hau, 2006).
- Rotor hub: The blades are attached in the rotor hub. The hub has the mechanism inside which controls the pitch of the blades. The hub is connected to the tower with the nacelle.
- Nacelle: This is the housing for all the equipment which has to be protected against the environment. The generator and gearbox are the most important parts in the nacelle.
- Tower or mast: Usually manufactured from steel or concrete. Different parts of the tower are connected with each other by bolts. Inside the tower is a ladder or a lift to access the nacelle for maintenance.

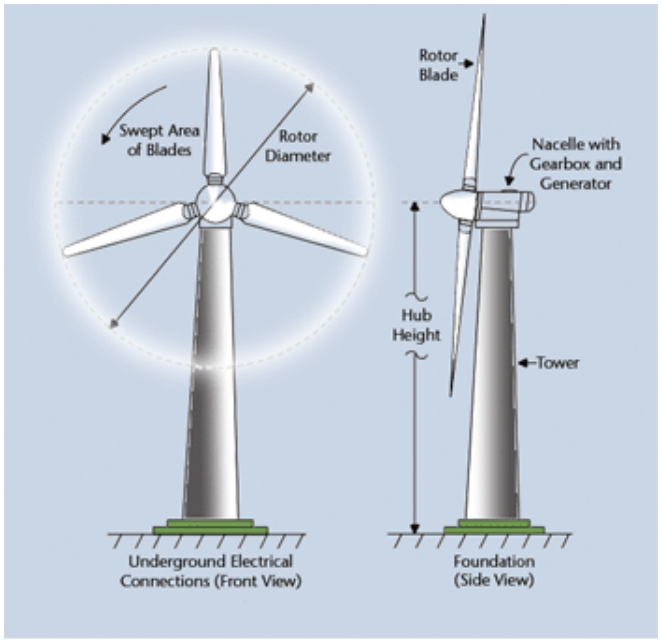

Figure 2.5: Wind turbine components European Commission Research & Innovation (2013)

- Foundation: The foundation transfers the forces from the tower towards the ground. Consists out of a concrete cap and foundation piles. The diameter of the concrete foundation is on average twice the diameter of the base of the tower.
- Cables: Not a part of the turbine itself, however, they could have an influence on the surroundings. The produced energy will be transported though cables in the ground. Multiple cables are bundled in a tube.

Nacelle

The nacelle is a complex component and therefore needs more specification. The nacelle is the housing for different component of the energy conversion process. The size of the nacelle depends only on the size and shape of the parts inside. Each manufacturer uses different equipment and has therefore a nacelle with a different size and shape. Figure 2.6 is an example of a geared wind turbine nacelle with the most important components. The generator is often the largest and heaviest part inside the nacelle. It determines for a large part the mass of the nacelle. In geared wind turbines the gearbox is the second largest and heaviest part in the nacelle. Direct drive wind turbines do not have gearboxes, but have much larger generators (Hau, 2006). At those turbines the generator is located in the nacelle against the rotor hub which is rotating. The increased size makes it able to put more magnets on the generator to maximize energy conversion.

Developments

The technical developments in the wind industry are going fast. The future characteristics of wind turbines can be predicted though. Most studies focus on the increase of the energy output in Mega Watt (MW). This power output in MW can theoretically be coupled with the rotor diameter. The power output is proportional to the swept area by the blades (Hau, 2006). The design of wind turbines is not only on creating the largest diameter, because all the components

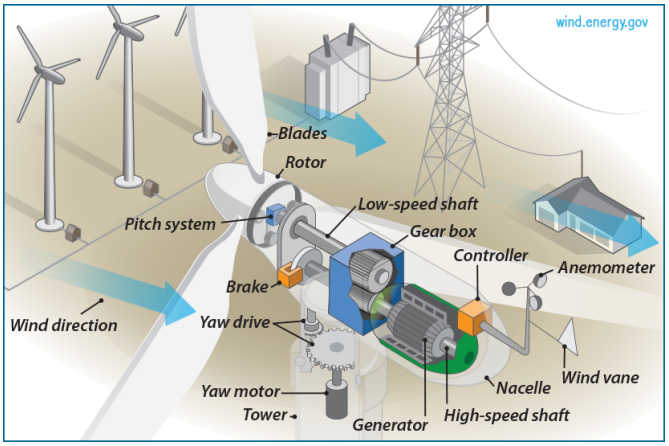

Figure 2.6: Components inside a nacelle (US Department of Energy, 2014)

of the turbine should work together to make it as well a safe, reliable, durable and efficient structure.

At the moment there are multiple companies fabricating turbines and turbines. They use different designs with different characteristics of all sizes. The largest onshore turbine in 2016 is the Enercon E-126 7.5 MW (Quilter, 2016). This turbine is used in Windpark Noordoostpolder in the Netherlands. The turbine has a concrete tower and a tip height of 198.5 m. The dimensions of this gearless turbine are in Table 2.1. There are a handful larger turbines on the market, but they are mostly for offshore solutions, so they are not explicitly considered in this study, although their prototypes are built on land.

For determination of the size of future turbines multiple studies have been done. The one used in this thesis has the advantage that the focus is on the upscaling of different parts of the turbine, so not only the upscaling of Mega Watts. It is a master's thesis, so it is not known what the comments were on the report. Though it is the only study which goes very deep in this material. This thesis on the subject of upscaling has used historical data from 230 different turbines, offshore and onshore, geared and gearless (Sánchez de Lara García, 2013). Because the database consists of all types of turbines, the upscaled wind turbines are as well the average of turbines. Onshore turbines have a relative higher tower than offshore turbines, so the tower height of onshore turbines will be higher than in Table 2.1, but the rest of the characteristics will be very similar. The height tower height of onshore turbines is similar to the rotor diameter. Next to the 3 upscaled turbines (WT), 3 turbines currently in use have been put in the table. The GE Energy 4.1-113 and Areva M5000-135 are used as a reference for offshore wind turbines. In addition, the Enercon E-126 has been added as onshore turbine (Willenbacher, 2012).

Limitations of developments

The development of larger wind turbines can go towards the upscaled WT 3, but there are limitations. The turbine manufacturers often scale their design up for largest turbines. This is possible when mostly the same materials and equipment is used. But this upscaling cannot go on unlimited, due to the scaling laws. For blades for example the analytic scaling predicts flap wise bending moments to increase with R^3 (Ashuri et al., 2016), and edgewise bending moments with R^4. This implies a very high increase in material use and therefore mass increase. So larger component upscaling is possible, but will be very complicated. As well more practical problems will arise with larger turbines (Sánchez de Lara García, 2013):

- The generators used in gearless turbines will increase significantly in size and weight. New generators will have to be developed to solve this problem.

Table 2.1: Current and upscaled wind turbines (Sánchez de Lara García, 2013)

Manufacturer	GE Energy	Areva	Enercon	Upscaled	Upscaled	Upscaled
Type	4.1-113	M5000-135	E-126	WT 1	WT 2	WT 3
Rotor diameter (m)	112.5	135	127	175	200	250
Power output (MW)	4.1	5	7.5	9.48	12.82	21.21
Min rotor speed (rpm)	7	4.5	5	4.87	4.43	3.78
Max rotor speed (rpm)	18	13.5	12.1	9.82	8.77	7.25
Blade length (m)	54.75	-	63.5	85.47	97.76	122.34
Tip speed (m/s)	-	-	80.42	92.51	95.01	99.35
Tower height (m)	85	-	139	123.96	135.96	158.65
Blade mass (t)	12.614	16.5	26.67	38.83	53.91	93.27
Rotor mass (t)	41	62	300	145.63	185.36	277.41
Nacelle mass (t)	214.324	233	348	265.1	338.73	510.2
Top mass (t)	293.166	344.5	650	529.38	707.56	1148.96

- Transport of larger parts will cause problems. The transport of parts by road will be difficult if a blade is almost 100 m in length. In addition, the weight will increase significantly with these larger blades. An option is to assemble the blades at the site, but these blades have not yet been developed.
- Higher towers and hub height imply higher cranes to assemble the blades and nacelle parts.
- The top mass will increase to over 1000 t, this should be reduced. The tower will have to be wider and thicker to withstand these forces from the top. The concrete and steel material quantities will rise exponentially with higher towers and heavier top structures.
- To manufacture blades of 100 m, a mould of that size is needed. The current longest moulds available are in the order of 75 m.

The wind turbines used in this study are only large wind turbines which all could seriously damage a flood defence. Wind turbines with a rotor diameter and hub height of over 100 meters are considered large.

2.4 Effects of wind turbines on the surroundings

This section is an introduction to the risks of section 2.6. A wind turbine has effects on its own surroundings. These effects can be related to visibility, visible physical effects and non-visible physical effects.

The first category of visibility has a large impact in the beginning stages of the project. When a wind farm will be built, especially in the Netherlands, there are many stakeholders. Often, several residents which live close the wind park will see the wind turbines as 'ugly' things which harm their surroundings. The visibility of large white towers can be seen from kilometers away is one of the effects. In addition, the top of the turbines will be lightened in the night. For the people who live very close to the turbines the dynamic shadow from rotating blades can be annoying.

In addition, there are visible physical effects, this means that the effects are above ground. Wind turbines have as well non-visible physical effects on the surroundings. Several of the effects are presented in the Figure 2.7. The figures are schematic and not on scale. Failures of the wind turbine blades (Figure 2.7a), nacelle (Figure 2.7b) and tower (Figure 2.7c) are all structural failures which can occur during the exploitation phase. All the wind turbine parts can break of from the rest of the structure, this can be in parts or with parts together, but they can be traced

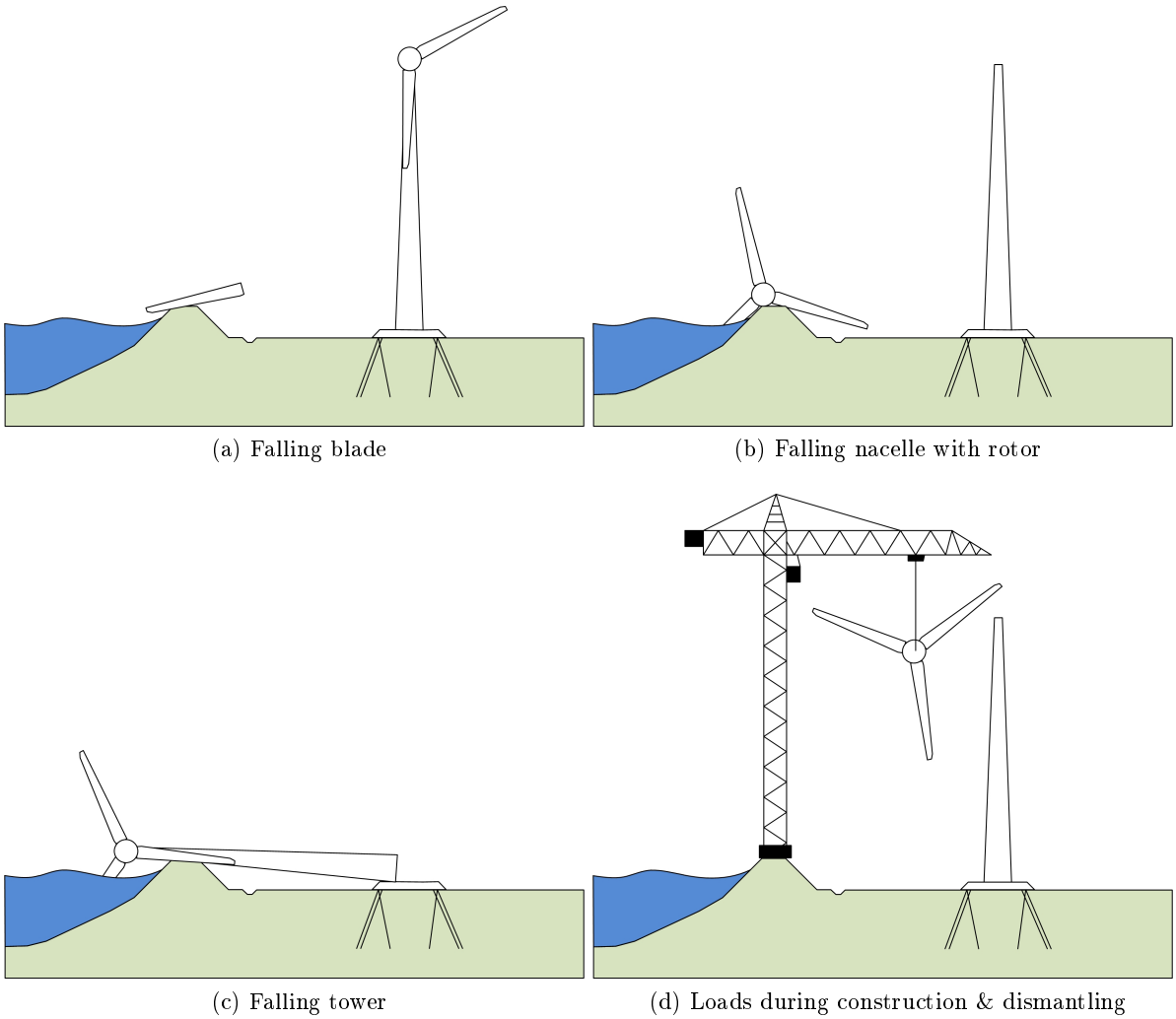

(a) Falling blade

(b) Falling nacelle with rotor

(c) Falling tower

(d) Loads during construction & dismantling

Figure 2.7: Above ground effects of wind turbines on the surroundings

back to three main situations. A blade can completely break off from the rotor hub or only a tip of the rotor hub can break off. The tower can break or buckle at different heights as well. These parts can potentially land on the flood defence and damage it. For the construction of the turbine heavy equipment is needed. This equipment can damage the damage the flood defences, but can as well cause settlements due to the loads it causes (Figure 2.7d).

The non-visible physical effects are mainly related to the vibrations and cables. Different sort of vibrations have an effect on the surroundings. The vibrations (Figure 2.8a) in the construction and dismantling phase are rather well-known, these have their origin in the foundation piles. But the vibrations in the exploitation stage are different, they originate from the rotating blades. The cables of the wind turbine (Figure 2.8b) as well influence the surrounding, they have to be dug and might cross the flood defence.

Failure probabilities of wind turbines

For the effects of Figure 2.7: falling of wind turbine components, failure probabilities have been determined. In the Netherlands the failure probabilities used are currently from the 'Handbook Risk zoning wind turbines v3.1' (Dutch: Handboek risicozonering windturbines or HRW) (RVO, 2014). The HRW describes three methods to determine the failure probabilities. The methodology of the failure probability determination will be described in short and very rough here, the calculation in the book is more complex. The first method is to use the failure data of all

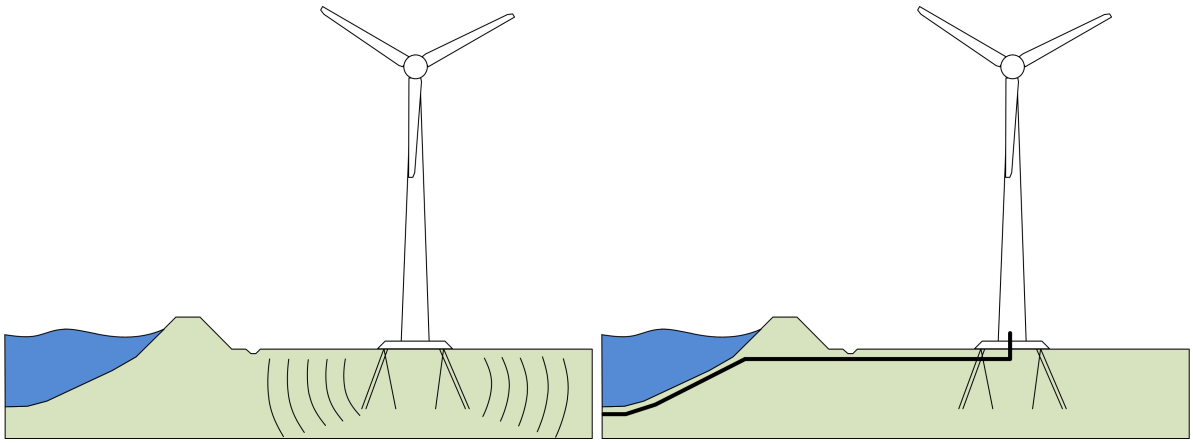

(a) Vibrations (b) Cables

Figure 2.8: Underground effects of wind turbines on the surroundings

wind turbines ever built from 1 MW and larger in the countries around the Netherlands. Sum up the total operational hours of every wind turbine and divide that by the number of failures. The second way is only possible for wind turbine types of which many have been built. The total sweeping hours of all wind turbines could be enough to use its failure statistics the same way as the previous method. To use that data one has to build that exact same turbine type to obtain the same failure probability. The third method is to have certified companies check critical components and connections regularly and provide certificates. The failure probabilities of all the components and all the combined and provide a total failure probability for blades, nacelle and tower.

This is a very rough description of how the HRW determines the failure probabilities. But the HRW mainly use the first method, which probably is an overestimation of the failure probability, because the manufacturers provide failure probabilities in lower orders. This due increased regulation of the inspections and more reliable components used in turbines. In future updates of the HRW the failure probability might decrease for new turbines. One has to keep in mind that larger turbines also cause higher failure consequences.

For the failure probabilities of the foundation of wind turbines no special probability is determined. A failure of a pile foundation is considered negligible.

2.5 Practical considerations for construction of wind turbines near flood defences

Wind turbines which are close to flood defences can be constructed on land or in the water. To build them in the water close to the flood defence can be expensive and does not have a positive effect on the energy production.

Close to the flood defence the water is often still very shallow, so it is not possible for installation vessels to reach those locations. Expensive special equipment is needed for the installation for those wind turbines. In addition, the maintenance causes complications because there is no road towards the turbine. For the wind farm Noordoostpolder (NOP), Nuon wants to know a year before the maintenance of the dike revetment if bridges used to access the turbines need to be removed (Fugro Geoservices b.v., 2012). In addition, the connector cables need extra attention if turbines are built in water: the construction is more complicated and at one point they need to cross the flood defence. Crossing a flood defence can enlarge the external risks.

Figure 2.9: Wind farm Irene Vorrink in Flevoland, wind turbines are on outer side (National Geographic, 2013)

Building of wind turbines in the slope of a dike or dune is as well possible. This could be more expensive, but it does not have to be the case. If an initiator is willing to pay for the extra costs it is possible. This could be the case if the initiator is also the owner of the land. Building wind turbines in the toe ditch is as well possible, but if the ditch has a drainage function this function needs to be assured. This can be done by putting tubes around the foundation which detour the ditch for example.

One of the functions of the protection zone around flood defences is to reserve space for future dike reinforcements. So building wind turbines at a location which might require near future reinforcements might not be possible, but this will probably be clear in the planning stages of a project.

Due to these practical obstacles it is less likely wind turbines will be built on the outside of flood defence. Therefore this thesis focuses on wind turbines on the inner side.

2.6 Risks

Risk analysis studies

The wind turbine and flood defence system have been viewed separately so far in this chapter. When they come together, the additional risk of failure of the flood defence can be determined. Before the use of WBI 2017, the advanced analyses were done for this situation. For this thesis research these analyses are combined to provide an insight of what the real uncertainty and risks are. None of the previous advanced analyses gave a complete picture of the problem. The advanced analyses used in this thesis are wind farms studies in the Netherlands.

- Wind farm Krammer: The construction of the wind farm started in January 2017 (Kra, 2017). Turbines will be built near the Krammer locks. These are at different relative

locations to the flood defences (Royal HaskoningDHV, 2013, 2014).

- Wind farm Afsluitdijk: This wind farm is canceled, instead wind farm Fryslân will be built in the IJsselmeer. The risk analysis study has been done to explore the technical feasibility of building wind turbines on and near the Afsluitdijk. The effect of the turbines on the functioning of the flood defences is as well explored. (Royal HaskoningDHV, 2012).
- Wind farm Eemshaven West: Plan for many wind turbines at the west of the Eemshaven. The turbines might be placed next to the flood defence. For the water board this an interesting case because multiple initiators have different stakes. In addition, the wind turbines of wind farm Oostpolderdijk are in the same dike ring, which causes a complication for the flood protection assessments (Witteveen+Bos, 2016).
- Wind farm Oostpolderdijk: Three wind turbines foundations will be built inside the dike itself. The studies for this wind farm have as well been used for wind farm Eemshaven West (Grontmij, 2016).
- Wind farm Noordoostpolder: Largest onshore wind farm in the Netherlands in operation. The largest 7.5 MW wind turbines have a tip height of 198.5m. They are build 65m from the toe of the dike. A very extensive risk analysis has been performed for this wind farm (Pondera Consult, 2009) (Pondera Consult, 2009) (Fugro Geoservices b.v., 2012) (Fugro Geoservices b.v., 2008).
- Wind farm Haringvlietdam: This wind farm is not constructed, due to multiple objections (Har, 2016). Since 1997 6 600 kW wind turbines are standing on the dam, the plan was to replace them with 4 larger ones with a rotor diameter of 93 meter.

Influence zones of flood defences

In Section 2.2, the relevant failure mechanisms of flood defences have been described. Failure mechanisms could be affected if certain events occur in the influence zone. For piping this is the seeping length from the entry point to the exit point for example. The area between those two points is called the influence zone of a failure mechanism. The influence zone is a zone in which a certain failure mechanism could occur. If something occurs outside an influence zone of certain failure mechanism, it has no influence on that failure mechanism. In Figure 2.10 for the mechanisms overflow & overtopping, sliding inner slope and piping the influence zones have been visualized. For the sliding of the inner slope a distance from the inner toe towards a point where at maximum the sliding circle ends of 4.H is used, this is simplified conservative estimation of the influence zone. This is 4 times the height of the dike, which runs from outer ground level to crest level. This value originates from the experience of many sliding circles (Provincie Zuid-Holland, 2009). The influence zone of piping is chosen in Figure 2.10 as 50.ΔH, which is 50 times the difference between the polder water level and the water level at the safety standard. The value of 50 is a reference value for the location Windpark Noordoostpolder. In WBI2017 the values are roughly between 25 and 70 if there is not a very thick cover layer (Rijkswaterstaat, 2016c).

Risks of wind turbines

Table 2.2 provides a list of risks and possible effects of wind turbines regarding flood protection. These risks are from obtained from the risk analysis studies provided in this paragraph. The effects elaborated in Appendix B. For all effects all sorts of properties and descriptions are provided: distance from flood defence relation, zones, exactly unknowns, when is the risk large, possible realistic mitigating measures, size of risks after these measures, related failures mechanisms.

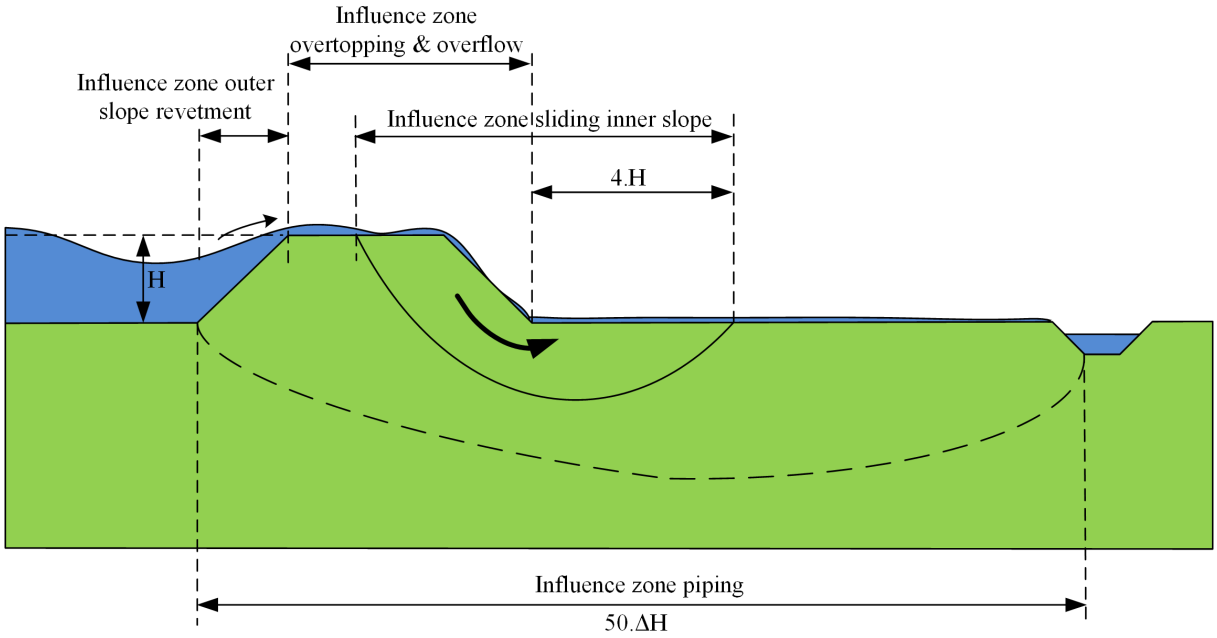

Figure 2.10: Multiple influence zones

Table 2.2: List of risks of wind turbines near flood defences

Construction phase	
1.1	Instability resulting from liquefaction due to pile driving vibrations
1.2	Dynamic loads due to pile driving
1.3	Flow slides resulting from liquefaction (zettingsvloeiing) due to pile driving
1.4	Penetration of impermeable layers (hydraulische kortsluiting)
1.5	Soil consolidation due to pile driving
1.6	Heavy equipment causes vibrations, settlements and track forming
1.7	Construction road traffic damages flood defence
1.8	Excavations temporary works

Exploitation phase	
2.1	Vibrations due to dynamic wind loads
2.2	Flow slide as result of liquefaction by wind related vibrations of turbine
2.3	Higher phreatic line near wind turbine
2.4	Space between foundation and soil can cause seepage
2.5	Space between foundation and soil can cause loss of grass revetment
2.6	Erosion & seepage along cables perpendicular through dike
2.7	Erosion & seepage along cables lateral with dike
2.8	Falling over of wind turbine
2.9	Falling of nacelle/rotor
2.10	Wind turbine blade falling down
2.11	Heavy maintenance equipment consolidates soil
2.12	Maintenance equipment damages flood defence
2.13	Erosion around foundation due to wave attack or overflow

Dismantling phase	
3.1	Several effects of exploitation phase will stay present if foundation piles stay in soil
3.2	Removing the foundations lowers (temporarily) height of defence
3.3	Pile removing: effects of fill material
3.4	Removal equipment damages dike

Wind turbine disturbance zone

The 'risk contour' or 'disturbance zone around a wind turbine' are two names for the same principle. It is a maximum distance from the wind turbine where effects from the wind turbine could be present. The goal of this chapter is to show what could occur in the system Wind turbine - Flood defence and what are the important risks and unknowns. To obtain this conclusion, many effects can be thoroughly researched and used from the mentioned risk studies. But only the important risks and unknowns are of importance. In order to provide a good insight in the risks and at what distance they play a role in risk analysis, it can be useful to use disturbance zones. These disturbance zones or effect zones are schematic around the turbine in Figure 2.11.

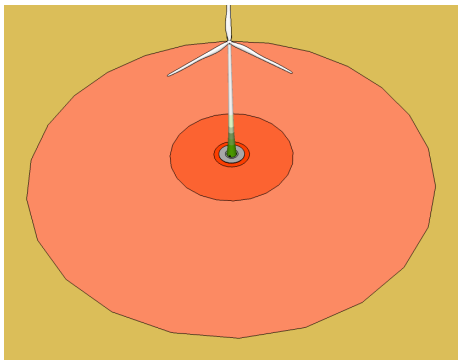

Figure 2.11: Disturbance zones around the wind turbine

In Figure 2.11 the different colors represent disturbance zones where a certain risk is present. Every risk has its own contour around a wind turbine where the risks is present, but for this study this has been combined into 5 zones around the wind turbine. This is the area where almost all effects are of importance. So the further away from the turbine, less effects are important. Right under the turbines foundation, gray in Figure 2.11, all the risks are present. Zone 2 is from the inner to 1/20 times the tip height (TH), this distance is chosen for the effects which play a role around the foundation, which lays usually 1/20th of the tip height around the tower. Zone 3 and 4 and chosen for the effects of parts of the wind turbine falling down, 1/2D is the half of the rotor diameter. This falling distance of 1/2D is chosen due to the possibility of a blade hitting the tower during rotation. If this occurs at with a tip of the blade, which is at a maximal distance of 1/2D, the tower can buckle at that location. At large onshore turbines the diameter and hub height are in the same order of length, this gives a tip height of around 1.5 times the rotor diameter. So when the wind turbine completely falls over it lands over a distance of 1.5 times the rotor diameter. The furthest (yellow) zone from Figure 2.11 is for the wind turbines located at a distance which the possible effects have a negligible risk, here only falling off of a blade is a risk.

So all the risks have been put in a disturbance zone or multiple zones, these can as well be found in Appendix B. In Figure 2.12 all the risks are coupled to the relative distances which correspond with the disturbance zones. These distances from the wind turbine are relative, because they are related to the size of the turbine. Figure 2.11 is on scale, notice Figure 2.12 is not, but the 5 distances correspond in the 2 figures.

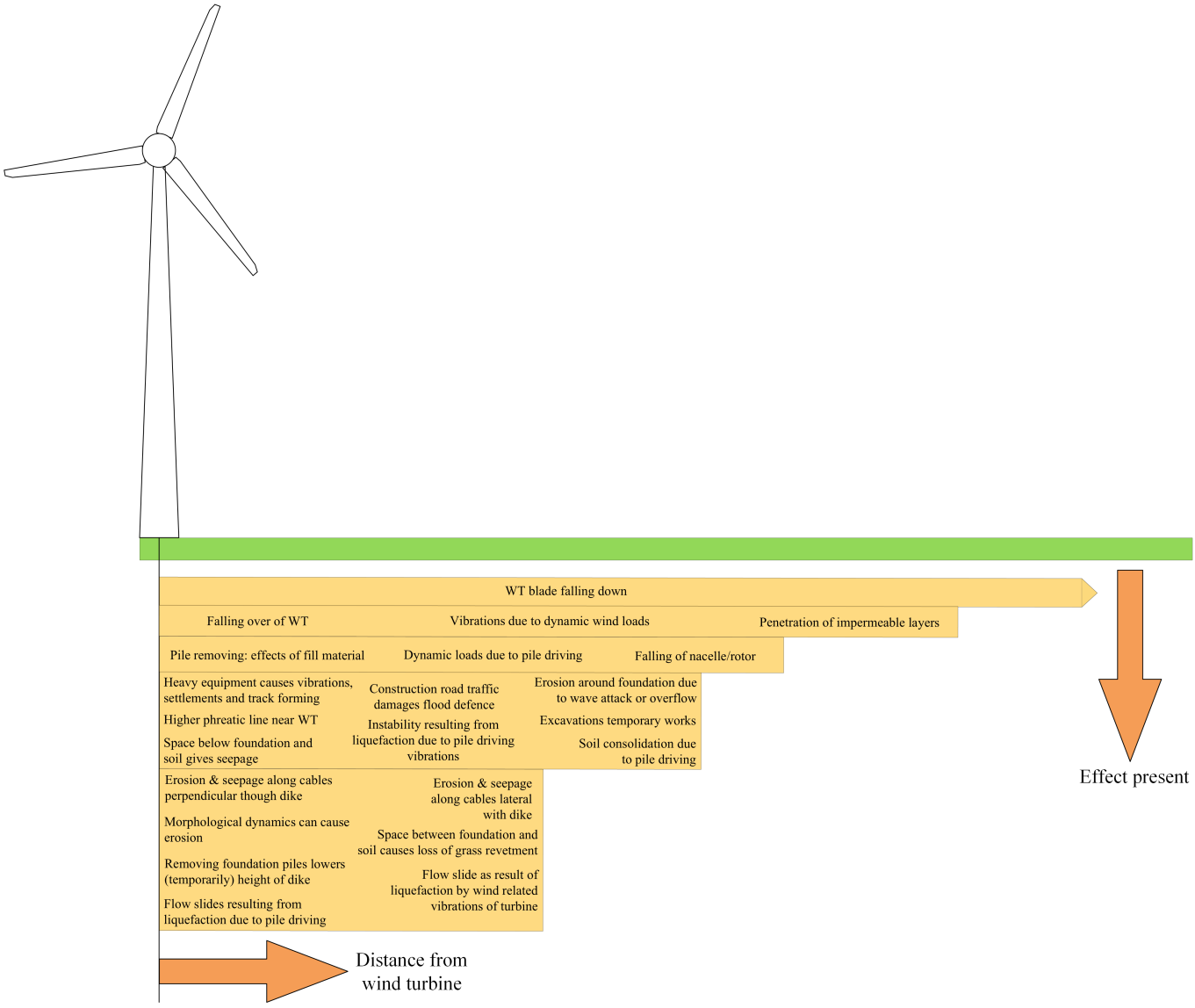

Figure 2.12: Schematization risks of wind turbines regarding flood defences with their relative distances

Filtering of the risks

The high risks have priority in research for most stakeholders. If these risks can be assessed better, better designs are possible. The risks from Table 2.2 & Appendix B are filtered in three steps to obtain the high risks. First the risks which have very small probability of occurrence and only are of interest in very specific situations are filtered out. These are for example risks related to liquefaction. The list complete list can be found in Appendix B.

The second filter looks at the possibility of the use of mitigating measures. Not all risks related to the wind turbines near flood defences are specific for wind turbines near flood defences. The pile driving risks are generic for example. The risks are rather well-known, because there has been much experience on pile driving and these risks and realistic mitigating measures can be used to almost eliminate these risks. Realistic mitigating measures are measures which are not extremely expensive and almost certain will tackle the problem or easily fix them when needed. Also these can be found in Appendix B.

Many of the remaining risks can be lowered significantly by conducting policy. There are multiple ways for wind turbine to cause damage to a flood defence during construction, but this

risk can almost be eliminated if correct policy is conducted. This policy can be a requirement of the use of a maintenance plan. This is the third filter which also can be found in the Appendix B. The second and third filter are closely related and the difference between them is not strict. Several risks can also be filtered in the other filter therefore.

After applying these filters only a handful of important risks remain and these have priority in research. The remaining risks can be found in Table 2.3 and can be split in two categories. The first two risks are related to the dynamic behavior of the wind turbine during exploitation. The other three are related to a structural failure of a part of the wind turbine.

Table 2.3: Remaining important risks from effects of wind turbines

ID	Risk	Description
2.1	Vibrations due to dynamic wind loads	Vibrations caused by dynamic wind loads or extreme peak values can lead to excess pore pressures, liquefaction of boulder clay or clay in the core of the dike. Also reduction of soil characteristics and an extra loading on the soil can occur. The stability of the flood defence can decrease and consolidation can occur.
2.3	Higher phreatic line near wind turbine	The phreatic line near the wind turbines can be at higher level than usual, which affects the stability in a negative way.
2.8	Falling over of wind turbine	A wind turbine which falls over on a flood defence will have a major impact. Revetment, cover layers and profile can deform.
2.9	Falling of nacelle/rotor	A wind turbine loses its nacelle or rotor and falls on a flood defence will have a major impact. Revetment, cover layers and profile can deform.
2.10	Wind turbine blade falling down	A blade can hit at high speed a flood defence. It can cause a crater in the flood defence, damage cover layers and revetment.

Interference disturbance and influence zones

The disturbance zone of the wind turbine which is built near a flood defence can interfere with the influence zone of the flood defence. For each failure mechanism there is a different influence zone, as can be seen in Figure 2.10. Also the disturbance zones of the wind turbine have different distances, see Figure 2.11. So there are several potential interference zones. One of them is presented in Figure 2.13, the interference zone between the zone for the failure mechanism piping and the disturbance zone for vibrations. The interference zone is important for the assessment of the flood defence. The risks in all the interference zones together should be summed up in order to give a judgment on the flood probability.

Permissible additional failure probability by a wind turbine

Custom checks are used for the assessment of flood defences for wind turbines, as there is no prescribed method in WBI2017. The water authorities have different views on how to do this custom check. This is also one of the white spots. In this section an example of a custom check is performed.

For the primary flood defences in Flevoland there is the assumption that there is a 1% probability that the dike will fail, if a blade hits the dike (Fugro Geoservices b.v., 2016). Also for falling of the tower and falling of nacelle with rotor such a percentage is used: 10% probability the dike will fail, if the nacelle hits the dike. The flood probability as consequence of one wind turbine

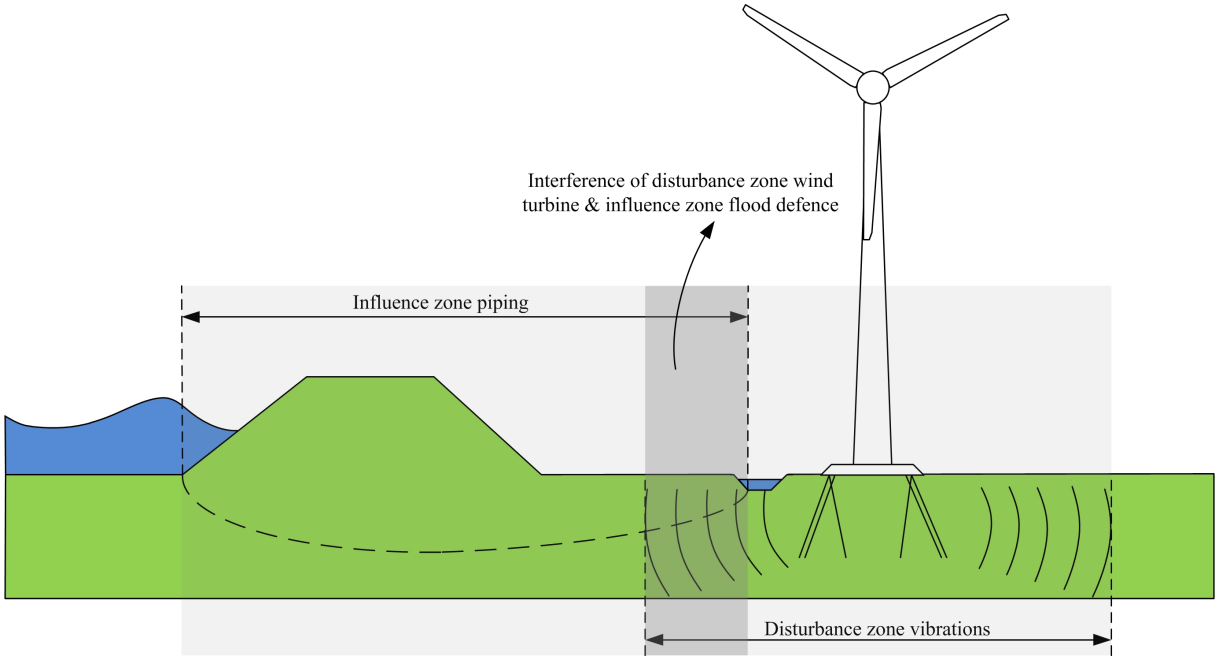

Figure 2.13: Interference of disturbance zone and influence zone

should be lower than the safety standard times a maximal permissible failure probability by one turbine. An option for checking if a wind turbine satisfies the safety standard (Fugro Geoservices b.v., 2016) can be found in Equation 2.1. This is an extreme simplification of the calculation, it is chosen to only show this equation, because showing a complete detailed calculation of the additional failure probability would not make it clearer. In Chapter 7 'Impact on dike failure probability' more detailed calculations on this subject can be found.

$$P_{failure,blade} \times P_{hitting,blade} \times 1\% + P_{failure,tower} \times P_{hitting,tower} \times 10\% \leq P_{safetystandard,segment} \times \omega_{1turbine} \tag{2.1}$$

Where:

$P_{failure,blade}$: Probability that a blade falls of a wind turbine.

$P_{failure,tower}$: Probability that the tower of wind turbine falls over.

$P_{hitting}$: Probability that the falling component hits the dike.

$P_{safetystandard}$: Maximal permissible flooding probability of a dike segment.

$\omega_{1turbine}$: Permissible additional failure probability per wind turbine, often 1%.

In Equation 2.1 the assumption of 1% percent probability the dike will fail is very rough. There are no influence zones used for the different failure mechanisms. All the failure mechanisms have been put in the 1% and 10%.

2.7 White spots

A white spot is a gap in knowledge and has not yet been researched. In every engineering design, assumptions are made to model a system and make reliable designs. For uncertainty

a conservative assumption is often used as a solution. The worst-case scenarios are used to make the design reliable. An example for estimations/assumptions for the calculation of a blade hitting a dike: wind turbine is rotating with the blades perpendicular to the dike, extreme high rotating speed when blade falling in one part off, landing of the blade with an angle at highest possible damage, blade hits the dike at the worst possible location, blade will not splinter, at the time of the impact there is high water, there is no time to repair the damage. All these aspects mentioned show that only for a blade failure there are many white spots.

This is an example for the structural failures, but there are many more white spots, mainly originating from the risks of Table 2.3 and the studies from Section 2.6, see Table 2.4.

Table 2.4: White spots in the system wind turbine near Flood Defences

White spots	**Research potential**
There is only a general failure probability for towers falling over, nacelle falling and blade failures of all turbines in the world used. There is no differentiation in smaller components. (RVO, 2014)	Medium, first extended statistics are needed to have an idea of the failure probabilities of smaller components.
Wind Turbines being built at this moment are much larger (>3 MW) then the last update of the 'Handboek risicozonering windturbines'. Wind turbines have different components which are more reliable than in the past.	High, the difference between the statistic failure probabilities and the ones provided by the manufacturers large, in the order of 10^2, but these manufacturer failure probabilities are not public.
There is no structural use of the influence of the shape of objects hitting the flood defence in risks analyses. The influence of the shape of towers, rotor and nacelle is unclear.	Medium, it can all be researched, but every turbine has different characteristics, so the practical use afterwards might be limited.
Penetration depth of wind turbine components hitting a flood defence. The models used so far all have disadvantages and present doubtful results.	Very high, there is a model which in principle has no disadvantages, but is never used before.
Energy absorption of parts hitting the flood defence is chosen 50% and 75% in different studies, both without substantiation.	Medium, it is only useful for the models used for determination of the crater depth.
Correlation between structural wind turbine failures and high water. Also the correlation between the direction of falling objects and wind speed is unknown.	High, the risk contour is asymmetric if the wind direction and speed is non-uniform. The falling direction distribution is important for all external risks of wind turbines.
Effect of vibrations in the exploitation phase due dynamic wind loads on failure mechanisms.	High, vibrations can have effect on many failure mechanisms. For turbines inside a flood defence research is very relevant.
There is no legal method to determine the additional failure probability of a flood defence by wind turbine failure. Only an advise which has no legal status.	Determine the method to assess wind turbines near flood defences and add it to WBI2017 or OI2014
Water boards struggle with the maximal permissible additional failure probability of wind turbines and have different views on this.	Very high, if there is a clear policy by all water boards, this can benefit all stakeholders.
Excess pore pressures near wind turbines and the effect on the stability.	Medium, this is correlated with vibrations. It should be measured and modeled during storms.

2.8 Research possibilities

Multiple of the white spots from Table 2.4 are worth researching. If the estimations made are very conservative and can lower the flood probability by a factor 10 or more in situations where the flooding probability is not negligible, it is worth researching, because it has a serious impact.

At the time of this study (2017) there is much research going on in this field. The effect of vibrations in the exploitation phase due dynamic wind loads on failure mechanisms is being researched by Paul Hölscher (Hölscher, 2016). Another study on this topic and also the phreatic lines near a wind turbine is being executed by FUGRO (Fugro Geoservices b.v., 2017).

The failure probabilities of the structural elements of a wind turbine can probably be lower than provided in the HRW. For every new turbine the failure probabilities are determined by the manufacturer and they differ. A manufacturer can use more reliable bolts and increase the reliability. All this can be worth researching, but it is hard to provide a generic failure probability, otherwise the HRW would already have provided it.

Relevance of researching penetration depth of a nacelle hitting a flood defence

Only large wind turbines will be built on land in the future and probably many in the north of the Netherlands (Ministerie van Infrastructuur en Milieu, 2014). Therefore a typical Dutch dike in the province of Groningen together with the Enercon E-126 turbine will be used as a case study. The situation of a nacelle falling on a dike will be the main model.

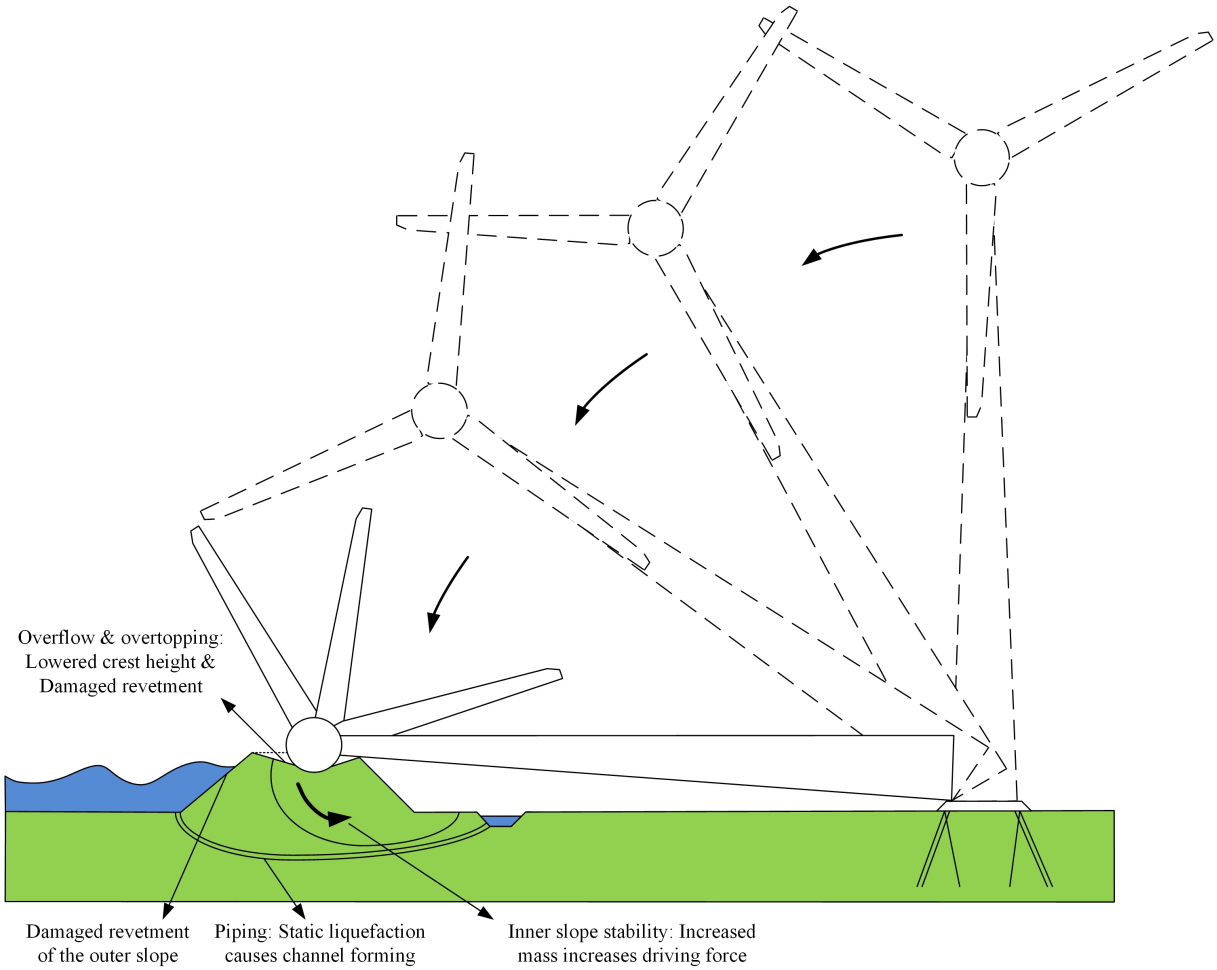

Figure 2.14: Effects of a tower falling down on flood defence

A falling turbine with the nacelle and rotor can damage a dike, see Figure 2.14. Multiple failure mechanisms can be affected by this. Overflow and overtopping are the ones which are the most important in this situation. The crest height will be lowered significantly and the revetment is destroyed if a wind turbine falls on it. A lower wave overtopping discharge is permitted if the revetment is destroyed. A list with the relevant effects on these failure mechanisms is shown in Table 2.5.

To show this, a calculation with Hydra-NL has been made. Hydra-NL can calculate hydraulic loading level (hydraulisch belastingniveau) for a certain location and return periods. The hydraulic loading level consists of a crest level with a certain wave overtopping discharge over the flood defence. For the Zeedijk Groningen at km 57.0, which is near Noordpolderzijl, calculations have been made. This location is chosen as it is one of the preferred locations for wind turbines (Ministerie van Infrastructuur en Milieu, 2014). The crest level is just over NAP +9 m.

Table 2.5: Crater effects on failure mechanisms

Overtopping & overflow
Lowered crest height by soil compaction on top layers.
Static liquefaction causes soil layers under flood defence to compact and lower the crest height.
Destroying of the revetment on crest and slope.
Inner (& outer) slope instability
Mass of nacelle provides extra driving force.
Momentum of nacelle provides extra driving force.
Increased pore pressure lowers the shear capacity.
A flow slide as a result from static liquefaction of the foreshore decreases the resistance of the slope (only outer slope).
Piping
Static liquefaction can cause channel forming.
A flow slide as a result from static liquefaction of the foreshore shortens the piping length.
Outer slope revetment
The revetment is damaged or destroyed by an impact on the crest or outer slope.

Graph 2.15 shows the results of the calculation. The failure probability before the impact was around $1.5 \cdot 10^{-4}$ per year for a discharge of 5 l/s/m. After the impact this probability is around $6.0 \cdot 10^{-2}$ per year due to the lowered crest and lowered maximum wave overtopping discharge. So the failure probability is increased by 400 times in this case. This is the failure probability if no repair works will be conducted. The repair time is dependent on the damage and failure mechanism. The duration of the repair works is in the order of weeks. This lowers the increase in failure probability significantly.

This is only a calculation for a penetration depth of 3 meters, but it can also be 1 meter or 5 meters or in between, in the risk analysis studies they are both found. That is why this white spot is important to research. The difference of the 1 meter and 5 meters penetration provides a difference of overtopping probability of over a factor 15, the exact value cannot be calculated in Hydra-NL because the probability becomes too low.

The difference between those depths in the probability of overtopping is over a factor 15, so it is important to know the penetration depth. In the beginning of this chapter the developments of the wind turbines in the future have been outlined. The hub height and mass of the rotor and nacelle will increase even more. Both of these developments cause a larger penetration depth for future turbines, so the need to know the penetration depth grows.

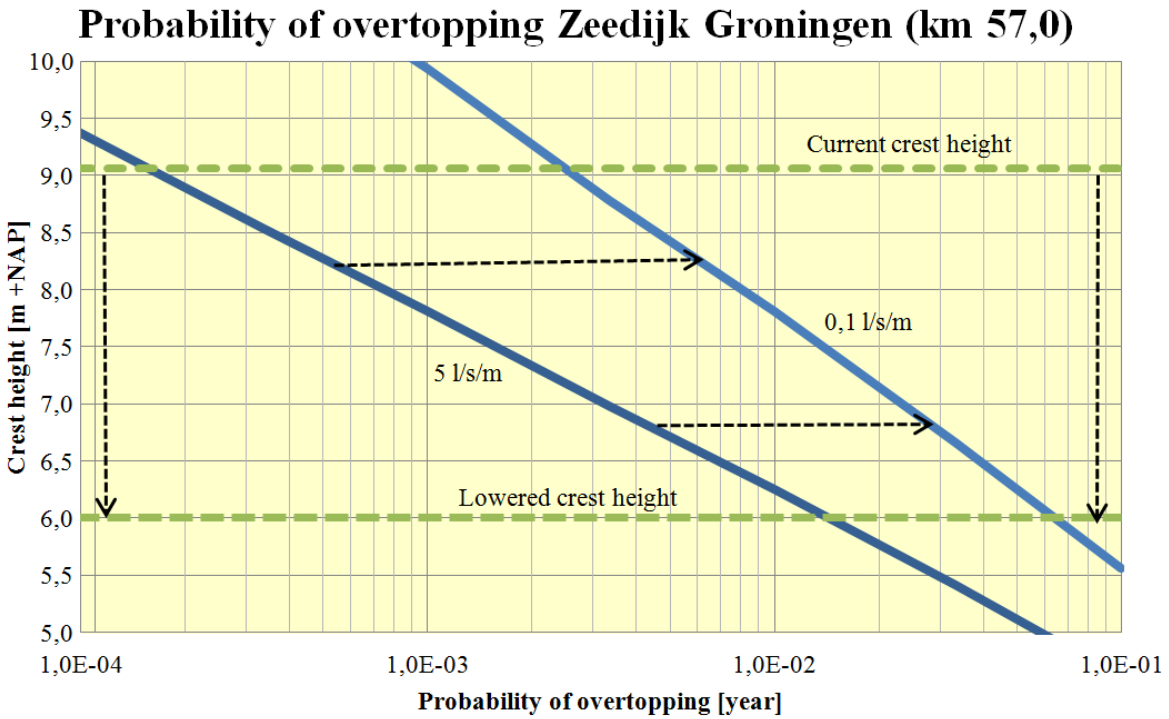

Figure 2.15: Probability of overtopping Zeedijk Groningen with lowered and damaged crest

Chapter 3

Research definition

3.1 Problem statement

The conclusion from Chapter 2 is that several white spots in the system Wind Turbine – Flood Defence are worth researching. The white spot with a very high research potential is the situation when the nacelle hits the flood defence. The problem here is that the influences of falling turbine components on the reliability of a flood defence are not sufficiently enough determined. The flood safety assessment starts with knowing the size of the hole or crater the falling components cause. Only when this crater is known the consequences on the failure mechanisms can be determined correctly. Of all components that can fall down, the nacelle is the one with the most effect. The mass of the nacelle is much higher than that of the blades, so it will cause more damage to the soil. Also the impact velocity is an important parameter at impacts. However, the difference in mass between the components is in a different order and the velocity is in the same order.

Real cases of objects with masses in the order of hundreds of tonnes and a relative low velocity falling on dike bodies are not available. Current models and formulas used for the determination of the crater depth and size have all large disadvantages. This results in estimated craters which can be too deep or too shallow. If the crater depth or size is modeled too high or large, this leads to a higher expected flooding probability than there is in reality. On the other hand if the crater depth in reality will be higher than modeled, the risk of flooding is underestimated.

3.2 Goal of research

The goal of research is to determine the effect on the failure mechanisms of a crater caused by a nacelle falling on a dike. Therefore the crater size and depth will be determined by a model. The dike is the most interesting of all flood defences to investigate because relatively most wind turbines are built near dikes compared to dunes and flood barriers.

This leads to the main research question of this thesis:

'What is the impact of a nacelle of a wind turbine hitting a dike and its effect on the failure probability of a dike?'

3.3 Research questions

In order to obtain an answer to the main research question, several sub research questions need to be answered.

1. Which mechanisms play a role in the crater formation?
2. What is the additional value of the Material Point Method in crater formation?

3. What is the penetration depth and size of a nacelle hitting a dike using the most suitable method?

4. What is the additional failure probability of a dike caused by an impact by a nacelle?

3.4 Research method

First a short theoretical study will be performed to show the previous research and existing models on this topic. Several existing methods have been used in the past to estimate the crater depth. Also the possibilities for scale testing and the use of Finite Element Methods will be examined. After this theoretical study research question 1 and 2 are answered.

The determination of the crater size is done by using the Material Point Method (MPM), which can deal well with large displacements of soil unlike Finite Element Methods. MPM has never before been used for a crater situation with similar potential energy. The software used for MPM is Anura3D, this has been developed for modeling large deformation and soil–water–structure interaction (Rohe & Liang, 2017). First, the processes which cause the crater are analyzed if they are incorporated in the model correctly. Then a sensitivity analysis is performed to see if all parameters work as they should according to the theory. Then a 3D model is used for determining the crater for the flood safety assessment.

When the crater is determined, the results of the model will be compared to the models used in the past to show the differences in penetration depth and size. The conclusions of the MPM results and other models lead to the answer of research question 3.

Then the coupling is made back to flood protection. The crater will be used to make stability analyses and failure probabilities for overtopping and overflow. Then this can be coupled with the failure probabilities of the wind turbine itself to provide a judgment on the flood probability.

From the crater size the coupling will be made to flood protection. The failure mechanisms which are important were presented in Section 2.8: stability of the slopes, overtopping, overflow and damage to the revetment.

The crater size will differ for every wind turbine, dike, falling speed and falling direction. So a case study is performed to limit the variables. Only large wind turbines will be built on land in the future and probably many in the north of the Netherlands (Ministerie van Infrastructuur en Milieu, 2014). Therefore a typical Dutch dike in the province of Groningen together with the Enercon E-126 turbine will be used as a case study. The situation of a nacelle falling on a dike will be the main model. This failure probability assessment gives the answer to research question 4.

Chapter 4

Theory of craters & penetration in soil

4.1 Types of craters

A crater is a bowl-shaped, annular or circular landscape form, often formed in a very short time. This crater can have different causes: a volcano eruption, meteorite impact and an explosion for example. Several of those craters have similarities with the expected crater of a nacelle hitting a dike. Volcano craters differ from impact and explosion craters, because there is no energy transferred from the object to the soil.

Impact craters

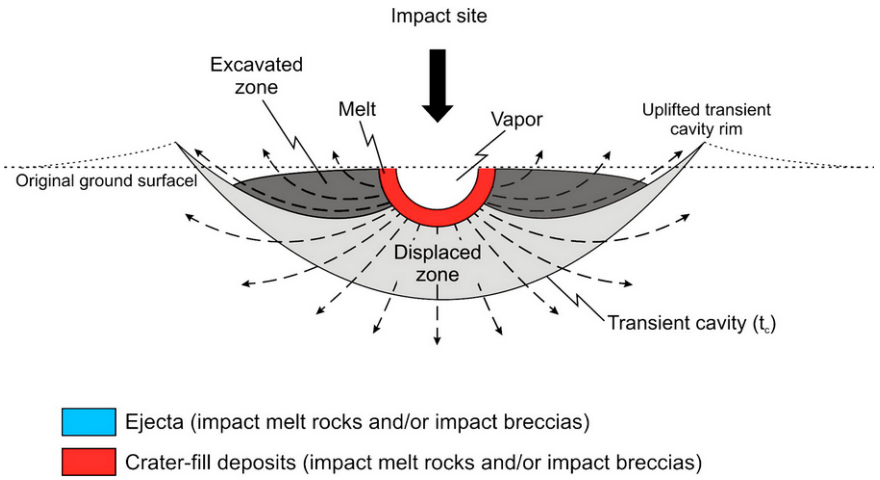

Figure 4.1: Simple terrestrial impact crater (Osinski et al., 2011)

In Earth's history many meteorites have hit the earth surface. If the meteorite is large enough (typically >50 m) it creates an impact crater (Osinski & Pierazzo, 2012). The impact velocity on earth of a meteor is very high, on average 20 km/s (Kenkman et al., 2005). The meteorites have an extreme amount of energy to transfer to the soil due to the very high velocities.

There are multiple impact crater shapes, a simple terrestrial impact crater is shown in Figure 4.1. The process of a simple impact crater formation is described briefly. The projectile penetrates the soil usually no more than 2 times its diameter. The pressures at impact are several thousand times the Earth's normal atmospheric pressure. Next, the extreme amount of kinetic energy of the target is transferred to the soil in the form of shock waves and rarefaction waves. Then the meteorite completely melts and vapors, therefore no meteorite can be found in the crater. The shock wave propagates outwards in the soil and rarefaction waves downward.

Together they create a 'transient cavity expansion', which will be filled in time with material which rolls down from the slopes or the slopes collapse into the crater (Osinski & Pierazzo, 2012). Due to the extreme energy transfer and associated shock waves the impact craters from hyper velocity (3 km/s) projectiles are much larger than subsonic projectiles (330 m/s).

Explosion crater

Figure 4.2: Moment of impact of a missile hitting soil (Tagesschau, 2017)

Craters in the surface created by a (nuclear) bomb, shell, mine or missile are all explosion craters. The principle of the formation of explosion craters is similar to the one from impact craters. But if the bomb is mounted on a missile, the missile will first penetrate the soil, before it explodes. Figure 4.2 provides an insight in the process of the missile penetration. A missile penetrates the horizontal surface with a high velocity. It can be seen that the soil is coming up before the explosion takes place. This part can be similar to a nacelle impact.

At the explosion itself, more soil is pushed aside & compressed and then, in a thousand of a second all the energy is transferred to the surroundings. But the energy that is released is not enough to melt the soil. In Figure 4.3 it can be seen that the crater of a bomb has the same shape as an impact crater by a meteorite.

Figure 4.3: Bomb crater in al-Zapharaneh near Homs, Syria in 2012 (Shaam News Network, 2012)

4.2 Theory of previously used models in flood protection assessments

Analytical solutions for the penetration depth and size have not been developed. It is very difficult to develop these analytical solutions, if not impossible, because it is very complex, so in the near future they are not expected as well (Ma & Zhang, 2009).

For the assessment of a dike, the most important property of a crater is the crater depth. Objects hitting the soil with similar potential energy as a wind turbine falling over are not aplenty registered including the soil type and crater properties. These objects could be e.g. crashing planes or building collapses. So, it is not easy to determine the crater depth in a dike from events in the past. Therefore models have been used to estimate the crater depth.

The models used in the risk analysis studies, mentioned in Section 2.6, are those of: Young, Bernard, Ménard, a Finite Element Method model and a model using the static bearing strength of the soil. These models have not been developed for this purpose and all have their disadvantages for this situation, though they can provide a direction of the penetration depth and give an insight which parameters and processes are important in the crater formation process. Another possibility to approach the crater depth is the use of scale tests. In this section all these models are explained including their backgrounds and disadvantages.

4.2.1 Young penetration equations

The Young penetration equations are developed by Sandia National Laboratories (Sandia) in the USA. These empirical equations are used to predict the depth of penetration into soil and concrete. Sandia's roots go back to World War II in the Manhattan Project: one of Sandia's tasks is to engineer the missiles which can carry nuclear bombs, also known as earth-penetrating-weapons. The Young penetration equations are designed for this purpose in 1967 and updated in 1997. The relations in the formula are a reasoned fit on the measured data, so it is an empirical formula. The data originates from tests executed by Sandia itself. Formula 4.1 is used for falling objects with a velocity below 63 m/s (Young, 1997).

$$D = 0.0008(\frac{m}{A})^{0.7} \cdot S \cdot N \cdot ln(1 + (2.15 \cdot 10^{-4} \cdot V^2)) \tag{4.1}$$

Where D is the depth of the crater, m is the mass of the penetrator, A is the cross-sectional area of penetrator, S is the S-number or index of penetrability, N is the shape factor for the nose or penetrator and V is the velocity of penetrator.

This formula has the following limitations which are of influence if used in the case of a falling nacelle (Young, 1997):

- When the penetration depth is less than 3 calibers (penetrator diameter), the results of the equations are questionable.
- There has never been a lower limit of the velocity defined by Sandia. The velocity of the falling object will be 51.5 m/s maximal for a free fall of 135 m without friction.

4.2.2 Bernard

This semi-theoretical model by Bernard is based on the empirical formula by Young (Bernard, 1975). However it contains a better physical substantiation and uses the equations of motion. The S and N values are the same as those in Young's equations. Also the test database of both formulas is the same. There are two additional coefficients which model the soil behavior, the empirical α-factor and β-factor, which are in the coefficients a, b, c. The equations of motions

are solved by use of the boundary condition that the deceleration in the soil is uniform. The penetration depth is presented by formula 4.2. In Appendix C the equation is described in detail.

$$D(S,V,m) = \frac{1}{c}[-(a+\frac{2}{3}b\cdot V) + \sqrt{(a+\frac{2}{3}b\cdot V)^2 + m\cdot c\cdot V^2}] \tag{4.2}$$

Where d is the projectile diameter, a, b, c are coefficients for the motions of soil.

The limitations of this formula are (Bernard, 1975):

- This formula is developed for earth-penetration-weapons as well, it has the same disadvantages as the Young's equations.

4.2.3 Ménard's dynamic compaction

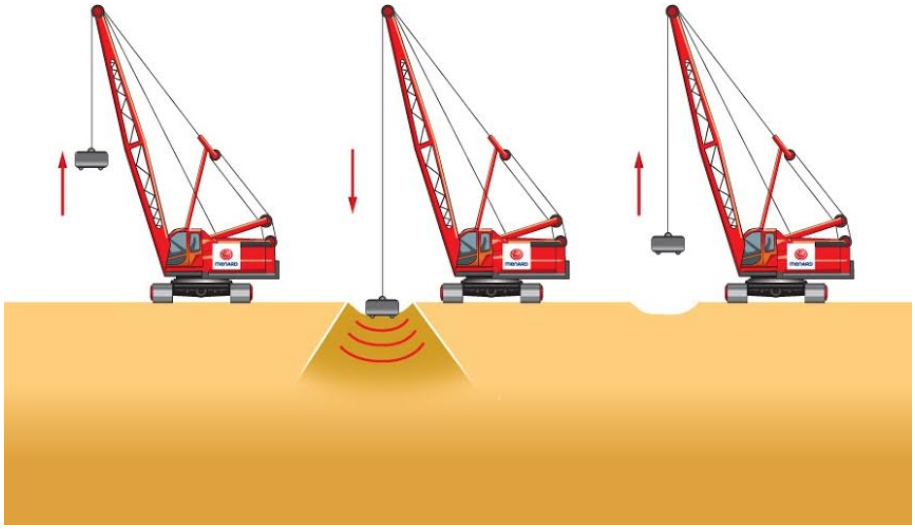

Figure 4.4: Dynamic compaction (Menard Asia, 2017)

The Ménard method is developed to improve the mechanical characteristics of fine saturated soils to a large depth (Ménard & Broise, 1975). The technique used is called dynamic compacting: a large crane drops a mass from a certain height on the surface, see Figure 4.4. Repeated drops of masses, varying from 8 to 20 tonnes and dropping heights of 10 to 40 meter, compact the soil. Ménard did not execute the tests himself: In 1984 Mayne executed tests (Mayne et al., 1984). The soil characteristics differ per location and therefore the tests were performed at different locations all over the world. The use for the model in this study is to look at the results for only one drop. The complete results can be found in Appendix C. The results from the drop tests are presented in Figure C.1, for one drop the result is presented in Equation 4.3.

$$\frac{\delta}{\sqrt{WH}} \sim 0.03 \tag{4.3}$$

Where δ is the penetration depth by Ménard, W is the mass of dropping weight and H is the dropping height.

Also this model has disadvantages:

- The goal of the tests is to compact the soil at large depths, not to know the penetration depth of the object, so probably all the tests are performed at uncompacted soil, for example land reclamations. The dikes in Groningen are compacted already and will behave stiffer.

- The masses used are at maximum 40 tonnes approximately. This is much smaller than the case study in this thesis.
- The dropping height in the tests is approximately 10 to 40 meters, much lower than the case study. So the transferred energy will in the case study much higher, which leads to larger penetration depths.

4.2.4 Static model of bearing strength

The static model of bearing strength is another method to model the penetration depth. The bearing strength is based on the Terzaghi bearing capacity theory (Terzaghi, 1943). The potential energy of the object, mass times height of the object, is used as the load. This energy will be (partly) absorbed by the soil that is displaced. The energy to be adsorbed is equal to the integral of the soil resistance and the penetration of the object. The soil resistance is the bearing strength of the soil. The resistance then is calculated at multiple depths and interpolated. In this method, it is possible to model multiple layers of soil separately. The calculation can be made with (NEN 9997-1:2016 nl, 2016). The energy from the falling nacelle corresponds with a certain penetration depth. In Figure 4.5 the graph shows a relation between the penetration depth and the static bearing capacity. This is just an example calculation of the penetration depth, it is strongly correlated to the soil characteristics used.

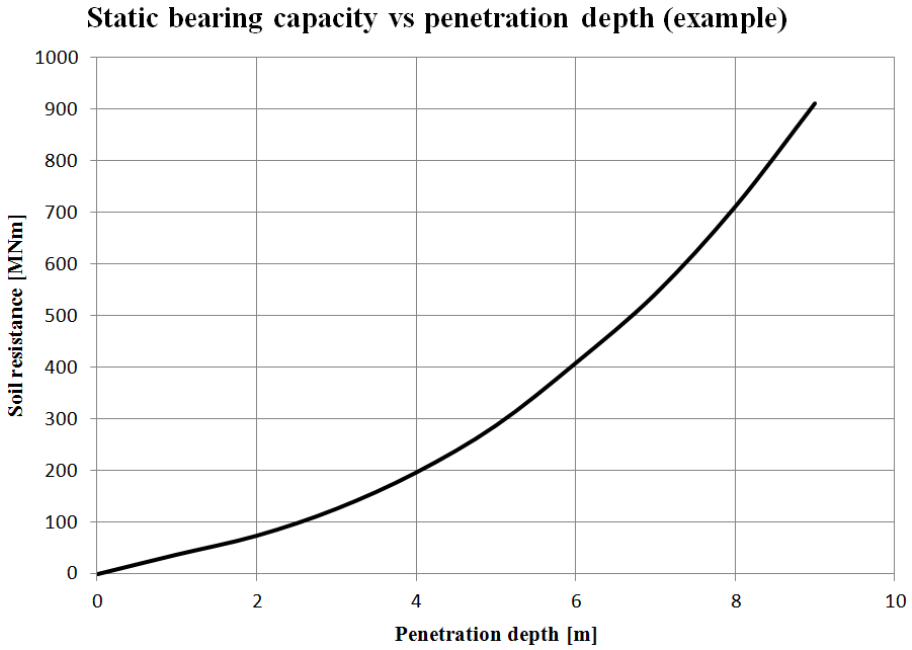

Figure 4.5: Static bearing capacity by NEN 9997-1

There are many disadvantages by this type of calculation, only several are listed:

- In this calculation all impact energy is completely used to deform the soil.
- The dynamic effects are completely ignored, while the formation in reality is very fast.

4.2.5 Scale tests

Scale test could be performed to estimate the crater depth. This could be rather difficult and has disadvantages compared to other models. A centrifuge model is an option, but this is very expensive. Setting up centrifuge models is also complicated and could not be performed within this thesis. Also in this model the validation options are limited.

4.3 Numerical models

Numerical models are widely used for all types of engineering solutions. The best known of these numerical models is the Finite Element Method (FEM). For extreme events which lead to large deformation with multi-phase interaction, finding the correct numerical approach is needed. There are Lagrangian, Eulerian and hybrid methods, which all have different advantages and disadvantages. This section will give an overview of how the numerical models can be categorized.

Lagrangian methods The computational grid of the Lagrangian method is embedded with the material. The mass of each element stays the same during the calculation process, but the volume may change. No material passes between the elements. The main advantage of this method is that it is simpler and more efficient than Eulerian methods. A disadvantage is that mesh distortion can occur, because the mesh follows the material deformation.

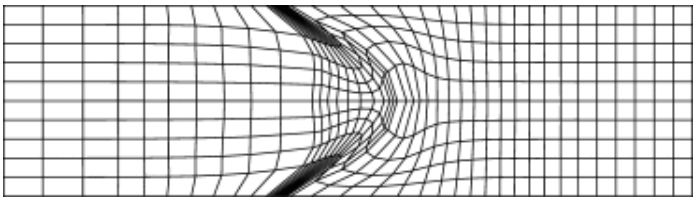

Figure 4.6: Lagrangian grid (Zhang et al., 2017)

Eulerian methods In this method the material flows through the grid and the grid stays at the initial position. Grid distortion cannot occur in this model, so, for large deformation problems, this would be a good model. In the field of computational fluids this method is often used therefore. For modeling the boundary between layers and numerical diffusion, this method has shortcomings. In addition, it cannot model history- and state-dependent material behavior, which is essential for soil mechanical analyzes.

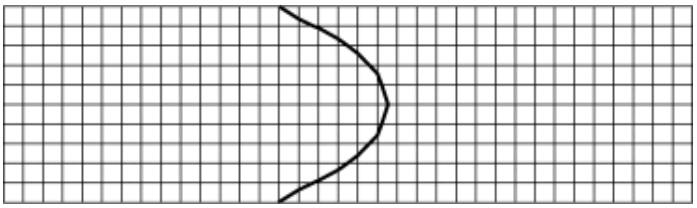

Figure 4.7: Eulerian grid (Zhang et al., 2017)

Hybrid methods In hybrid models the advantages of both the Lagrangian and Eulerian methods are combined. The Lagrangian-Eulerian (ALE) is a well-known one. There is also the particle-in-cell (PIC) method, which is later renamed to Material Point Method (MPM) (Beuth et al., 2010). The MPM will be described in the next section.

Finite element methods Finite Element Methods (FEM) are usually not very suitable for modeling large deformations. Finite elements methods are strong in modeling soil-structure interaction. Plaxis is the most well-known FEM for this purpose in the Netherlands. Nevertheless it also has limitations. There will certainly be large deformation at the impact location and the computation will give severe mesh distortions. This is the case for all Lagrangian FEM with large deformations.

4.4 Material Point Method

4.4.1 Basic concepts of MPM

A numerical model which can be used for large deformation and therefore impact problems is the Material Point Method (MPM). The method has properties of the FEM and particle-based models (MPM Research Community, 2016). As it is a hybrid model, it combines the advantages of the Lagrangian and Eulerian methods. Lagrangian particles are used for the advection, whereas an Eulerian background grid is used for computing the particle interactions. So, in MPM there are two space discretizations. The first is the computational mesh and the second contains the material points (MP), which move through the computational grid. The computational grid is very similar to that of Finite Element Methods. The computational grid has no permanent memory and is only used for calculating the displacements and strains. All the information of the material is stored at the material points. In Figure 4.8 this is summarized.

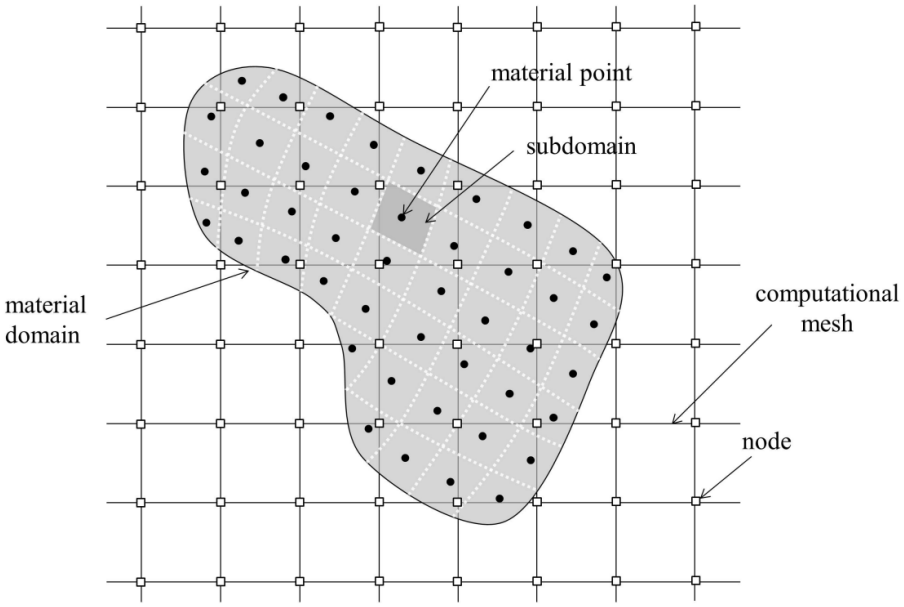

Figure 4.8: Space discretization, nodes of the computational mesh and material points (Yerro, 2015)

The computational scheme of MPM is shown in Figure 4.9. The red dots are the material points, in the figure are 4 material points in an element (a). Before a computational step the information of the material points is transferred to the nodes of the computational mesh. The momentum is working on the nodes and the governing equations are solved (b). Then the information is transferred back to the material points (c). The computational mesh stays in the same position and the position of the material point is updated (d). The material has a new shape and position now.

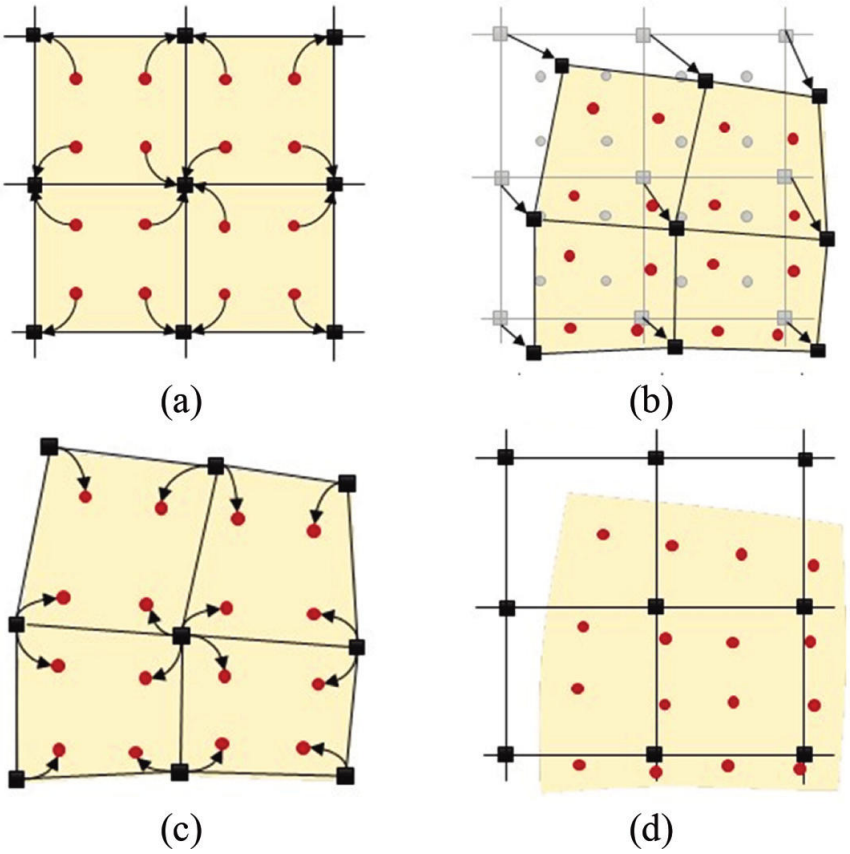

Figure 4.9: Computational scheme MPM

4.4.2 Anura3D

The MPM software used in this thesis is Anura3D, which focuses on soil-water-structure interaction. It can work with pure solids, pure liquids and the coupled combinations. The software works as follows: in the GiD software a mesh is created with all the properties of the geometry and loads. Then Anura3D does the calculations with the input from GiD. Afterwards, the output of Anura3D is post-processed by Paraview. This is schematically shown in Figure 4.10.

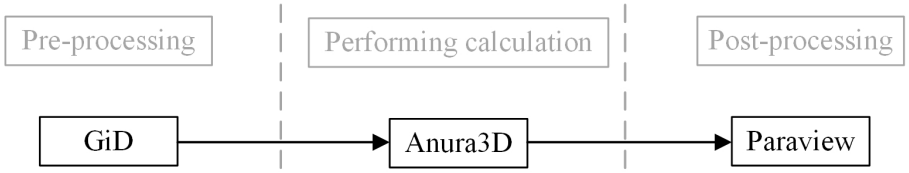

Figure 4.10: Procedure of Anura3D including pre- and post-processing

4.4.3 Disadvantages of MPM and Anura3D

Although MPM is in theory a good method for the determination of the crater depth, it also has disadvantages. The disadvantages mentioned in the list are those of Anura3D. The software is still being developed, so several disadvantages can be dealt with in the future.

- Multiple soil layers can be used. However, material points with different properties sometimes are contributing to the same node. This can lead to complex situations, which might become unrealistic.

- It is not (yet) possible to use a phreatic line in Anura3D, only a phreatic surface. High water, a saturated dike due to intense rainfall and a wind turbine failure can all be correlated to presence of a storm. So, a higher phreatic line in a dike can be related to a wind turbine failure and therefore is interesting to research.
- Coupled calculations with liquids and solids have a long calculation time.
- Larger 3D models will generate much data. Therefore, also the post-processing is time-consuming.
- Skill is needed to create complex models, however, this thesis proves that also with limited prior knowledge on numerical modeling a complex model can be created and used.

4.5 Conclusion

Analytical solutions, results from experiments and data from fallen wind turbines are not available, therefore the penetration depth is estimated by models or empirical formulas which are developed for another purpose than impacts of a large mass with low velocity. Although all models mentioned in this chapter, except for MPM, will probably not give the correct penetration depth, but they do give an insight in which parameters determine the penetration depth.

So it is preferred to include the important parameters in a model. This could be performed in FEM, but for large deformations there is severe mesh distortion. In MPM this problem does not exist. So the additional value of MPM is that it can solve large deformation problems, with considering into account dynamic effects and properties of the object.

Parameters and effects which could have an influence on the crater or penetration depth:

- Soil parameters:
  - Stiffness
  - Cohesion
  - Friction Angle
  - Porosity
  - Degree of saturation
- Object:
  - Impact velocity
  - Mass of the object
  - Area of impact
  - Shape at impact
  - Stiffness of the object
  - Direction of impact
  - Deformation of the object

Chapter 5

Simulation set-up

The goal of the simulations is to estimate the penetration depth of the nacelle hitting a dike and determine the residual profile. As there is no quantitative validation available for impacts on soil, the model first needs to be qualitatively checked. Therefore, first a 2D dike model is used to analyze the processes which occur during impact. To ensure all parameters are working as they should, a 2D model with a horizontal surface is used to for verification of the different parameters. At last, a 3D dike model is used to estimate the penetration depth, to ensure the 3D effects are incorporated.

5.1 Case study

The case study which will be used in the simulation is described briefly here. This case study is similar to a sea dike in the north of province Groningen. This location has been chosen because it has numerous advantages compared to other locations:

- There is a high probability that more turbines will be built near that location in the future, as it is chosen by the Ministry of Infrastructure and Environment as a promising location for the development of wind energy on land (Ministerie van Infrastructuur en Milieu, 2014).
- The geometrical cross-section and the composition of the soil of the dike are similar along the Wadden Sea in Friesland and Groningen, the dike stretches over 100 km. So the results of this study could be used for many locations.
- The dike largely consists of sand, which is the core material in most of the sea dikes in the Netherlands.
- The crest level is relatively high, so probably the effects of the crater are not influenced by the subsoil which is located deeper.

The wind turbine used is the Enercon E-126. Currently this it is the largest onshore wind turbine (Quilter, 2016). There are multiple causes which can lead to a nacelle falling down: i.e. the complete tower falls over or the blades cut the tower and only the top part falls down.

5.2 Domain geometry

The nacelle and dike are both simplified, because a more general solution which is widely applicable is preferred over a very specific case which application is limited. The overview of the geometry is shown in Figure 5.1. The inner slope is 1:3 (vertical:horizontal), outer slope 1:5 and the crest 3 meters wide. In Figure 5.1 the water at the seaside only to show that it is the sea side, it is not used in the simulation. The nacelle is falling vertically and lands with a certain velocity on the crest of the dike.

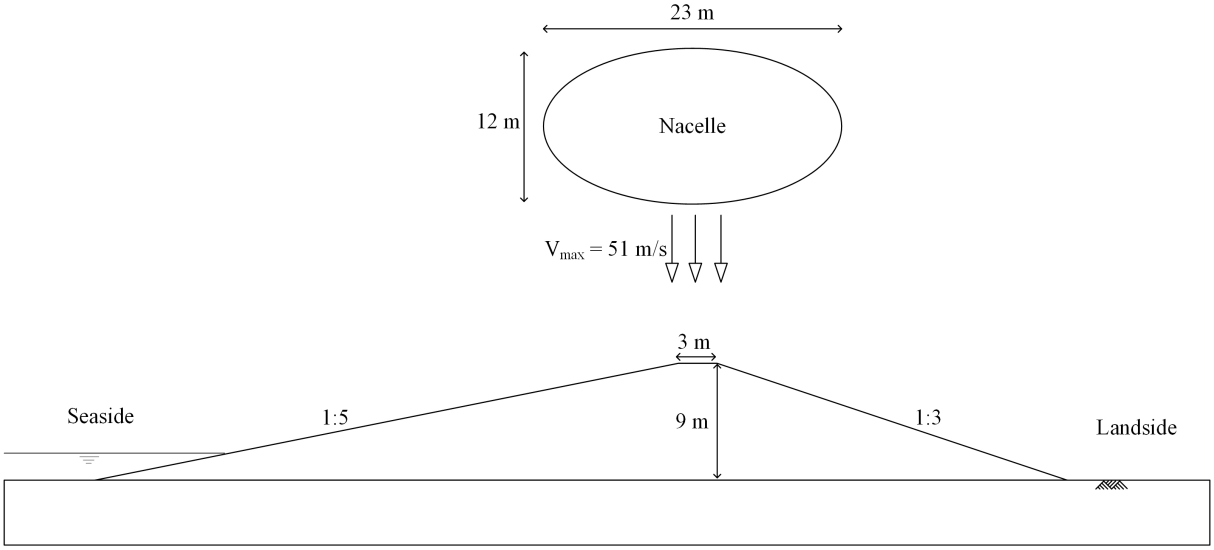

Figure 5.1: Representative dike profile with the Enercon E-126 nacelle falling down

5.2.1 Soil

There are 2 soil geometries considered in this study. One with a completely horizontal surface and the other with a dike profile as can been seen in Figure 5.1.

It is chosen to use only one soil type, in reality the soil is layered with multiple soil types. This is done to keep the model as simple as possible and concentrate on the impact itself and verify whether the model works properly. In reality there is a revetment on the top of the dike, a core of sand and clay layers below. In the MPM model it is chosen to use one uniform soil layer. As this thesis is the first time where an impact problem is modeled, one layer of soil should be proved to be working first, before more detailed features are added.

In addition, the revetment and cover layer will be hit first and will be (partly) destroyed and the soil below it will deform. So, this core material below the revetment is used in the model. The fill material of the dike is medium densely packed sand. In Section 5.4 the soil properties are determined.

5.2.2 Nacelle

When the nacelle of a wind turbine falls down, it hits the surface. The nacelle consists of the rotor and the machine-house. The nacelle of the Enercon E-126 is shown in Figure 5.2. The steel parts are centered around the connection axis between the rotor and the machine-house. So this is where most of the mass is located and the center of gravity lies. The height and width of the nacelle are both 12 m, at the front and back part of the nacelle, there is hardly any mass located, so these parts of the nacelle are neglected in the model. So, the whole nacelle therefore can be modeled as a sphere with a diameter of 12 m. This has the advantage that falling on the side gives the same result as falling on the nose. If the falling nacelle reaches a certain velocity, it could behave similar to a projectile and go with the point down, if there is any pointy component. This is not a likely scenario, so it is neglected.

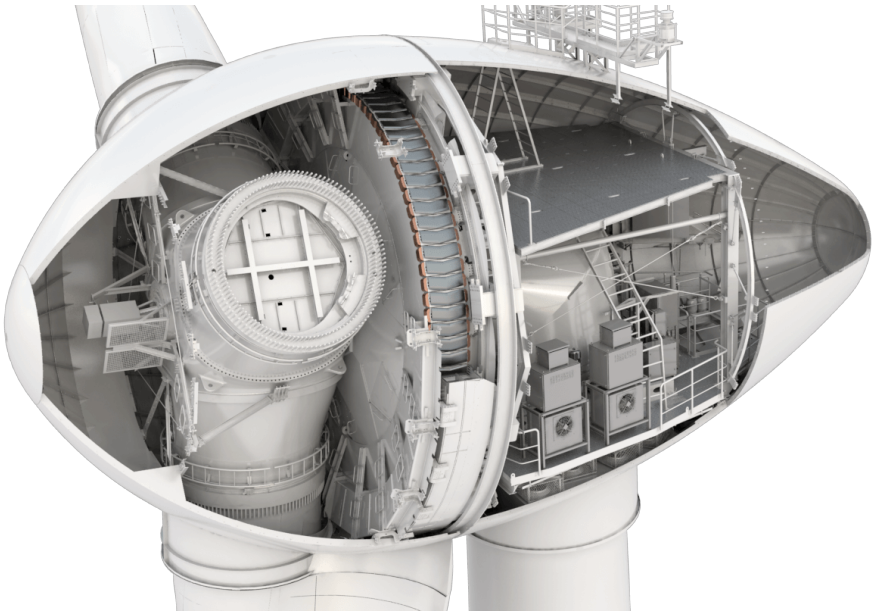

Figure 5.2: Enercon E-126 nacelle

During the impact in reality parts the nacelle will deform. The center where many of the steel parts are located will probably not deform, however, the smaller parts around this center will deform. The hull which is made of a thin layer of steel will deform significantly if the impact velocity is high. In Appendix A the pictures show the deformation of smaller turbines which had a smaller impact velocity. It is chosen not to take the deformation of the nacelle into account, because the mass of the parts which can deform in case of the Enercon E-126 turbine are only a fraction of the total mass of the nacelle.

The mass sphere is shown in Figure 5.3 with the mass uniform distributed within the sphere. If the sphere penetrates a horizontal soil surface and assumed is that the sphere will not deform, it penetrates the soil. In order to make the MPM model as simple as possible, a rectangular shape is used. If the penetration in the soil will be 1 m, the width of the mass which penetrates is 5 meters on average. If the penetration is 2 meters, the average width of the extra part will be 8 meters wide. The total mass which falls down will not affect the size of the boxes. The mass of the top of the Enercon E-126 is shown in Table 5.1. There is another advantage of using blocks instead of using a more round shape. This is explained in Subsection 5.3.6. However a disadvantage of using a box and not a cone is that the shape is of importance for determining the maximum penetration depth, as lowest point of the sphere will determine the maximum penetration depth. From the models from Young and Bernard which are described in Chapter 4, it can be concluded that the shape of the nose is a parameter which determine the penetration.

Table 5.1: Enercon E-126 machine-house, rotor and blade characteristics

Part	**Dimensions**
Width [m]	12
Length [m]	23
Height [m]	12
Weight one blade [t]	26.67
Weight rotor without blades [t]	220
Weight machine-house [t]	348
Total nacelle [t]	568

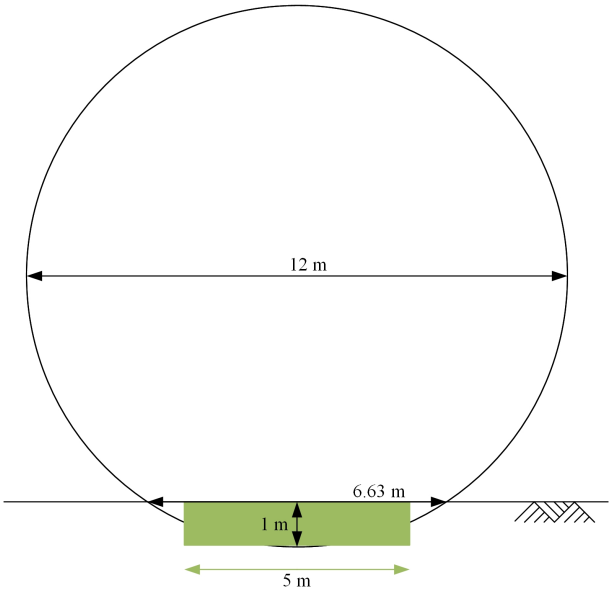

Figure 5.3: Mass modeled as a sphere

5.2.3 Velocity at impact

The theoretical maximal velocity is calculated with the energy balance. The maximal velocity of a free fall is 51 m/s for a height of 135 meters according to 5.1.

$$v = \sqrt{2gh} \tag{5.1}$$

Where v is the free falling velocity, g is the gravitational constant, h is the falling height.

The maximal free falling velocity is higher than the velocity at impact, because there are effects which limit the maximal velocity.

- If the tower falls over completely, the top first will move horizontally, it is vertically constrained by the tower itself. When it then is moved further away from its initial position, the vertical velocity will increase.
- The drag force will increase at higher velocities, which lowers the free fall velocity.
- In addition, there are minor effects which limit the falling height: the mass is seen as a point mass now, in reality it is not. The turbine is built on a foundation which is higher than the ground level. In addition, the dike where the nacelle lands, is higher than the ground level of the turbine.

Because the actual velocity at impact is not easy to estimate, multiple impact velocities have been used in the model to be conservative. It could be useful to make an analysis for the impact velocity at different failure situations and incorporate the factors that decelerate the nacelle.

The velocity together with the mass determines the total energy that can be transferred to the soil. Energy can be lost in the deformation of the nacelle as well. The hull is not very stiff compared to the massive steel parts in the center of the nacelle. If the velocity increases, there will be more energy lost in the deformation as well. Modeling this correctly is difficult and depends on the nacelle used and the velocity at impact as well.

5.3 Meshing the domain

Meshing is the process of transforming the computational domain into discrete cells or elements. At locations where more detailed information is needed the mesh should be finer. The Anura3D software needs to have geometry input created by GiD software. GiD has a function to generate the mesh automatically. However, for the desired solution there are requirements to be met in order to be compatible with Anura3D. The mesh consists only of tetrahedral volumes, because Anura3D only works with those. In 2D the tetrahedrons are recognizable as triangles.

5.3.1 Mesh characteristics

A completely structured very fine mesh will provide the most accurate solution. All tetrahedrons will have the same angle and the least errors will occur in the calculations. However, the calculation time should be as low as possible. For a dike profile and limited calculation time, choices need to be made regarding mesh size.

At the location of the impact, the mesh is the finest, closer to the boundaries of the model the mesh gets coarser, because the area of interest is where the impact and the deformation is. At locations where the mass is passing the elements in the free fall, the mesh is kept structured. This is needed to secure that the mass falls gradually.

The additional space around the soil is needed for material points to move up after the impact.

5.3.2 2D dike profile

The complete mesh of the 2D dike profile is shown in Figure 5.4. In Figure 5.5, a more detailed version of the mesh is shown. The yellow color is where the elements and material points are located, the blue is where the material can move to as well. The mesh is one element deep, so the elements can deform only in 2 dimensions. So, it is in fact a 3D model without 3D feature, therefore it is named 2D. At the top of Figure 5.4 the modeled nacelle can be seen as a box of 5 by 2 meters.

In Figure 5.5 it can be seen that in the dike the mesh is very fine. The height of the elements is 0.5 meter. It is important to have many elements in the dike because most of the deformation takes place right below the impact location. Also finer and more elements provide more nodes to do the calculations at, so the accuracy is better.

There blue elements above the crest of the dike is where the mass block will pass through. Only the part below the block is needed for the impact on the crest. If the impact on the slope is simulated, the block is moved to the side, so it falls on the slope.

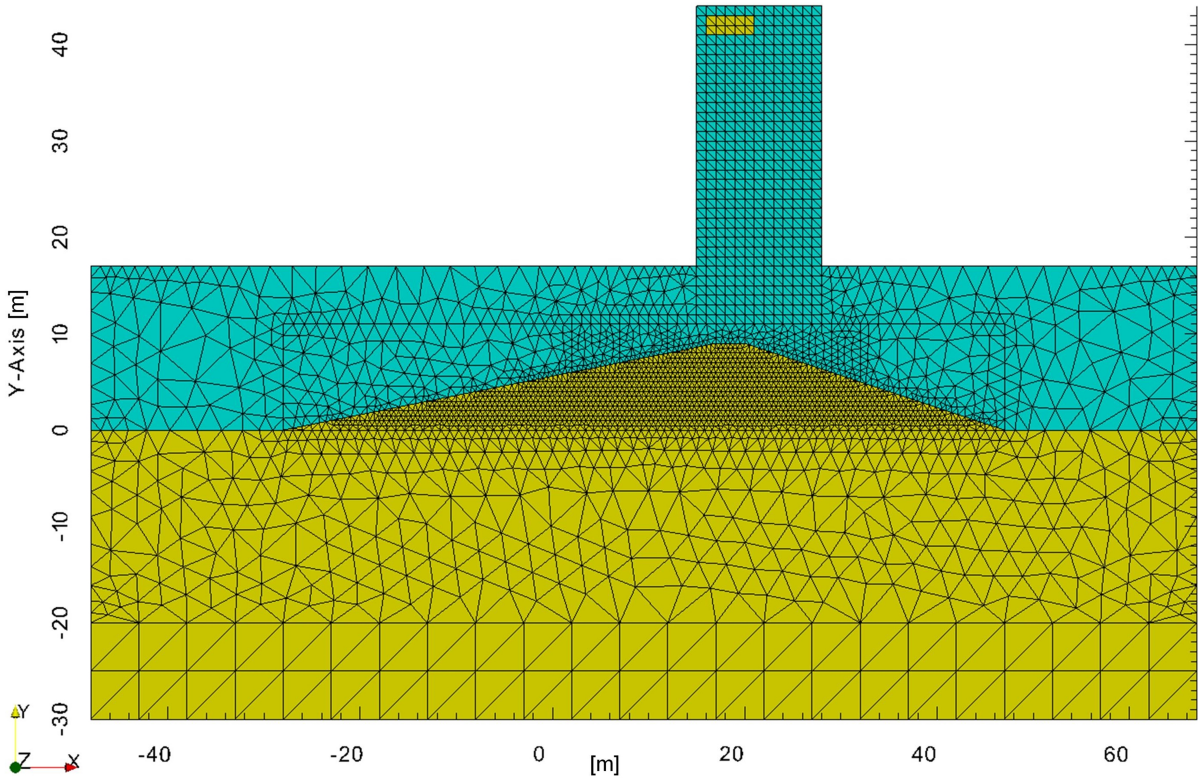

Figure 5.4: Mesh of the 2D dike profile

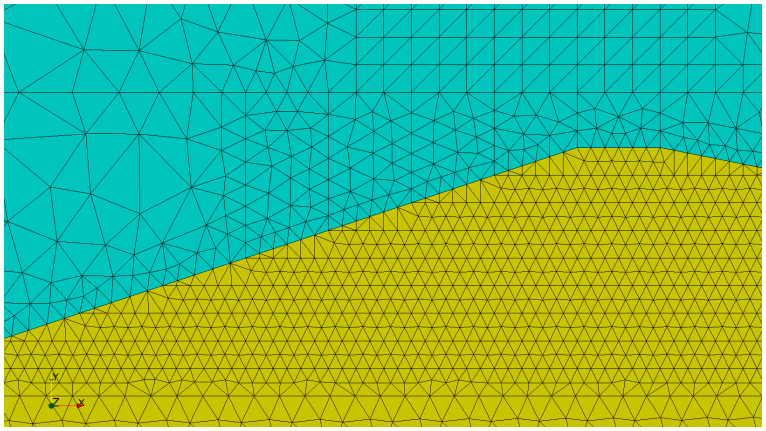

Figure 5.5: Area of interest of the 2D dike profile mesh

5.3.3 2D horizontal surface

This mesh is created for the sensitivity analysis of the MPM model. Different parameters and impact speeds will be used in this sensitive analysis. A horizontal surface has the advantage that the initialization of the stress can be performed much faster and with fewer errors. In the sensitivity analysis many parameters have to be verified, so it is useful have a fast model. Therefore, a horizontal surface is used in this case. This provides a significant reduction of the calculation time. Next to that, the effects of the slopes are eliminated. Also in this model the smallest elements have a height of 0.5 meter, to assure an accurate solution. To ensure no wave will reflect in the area of interest, the model is made deep and wide.

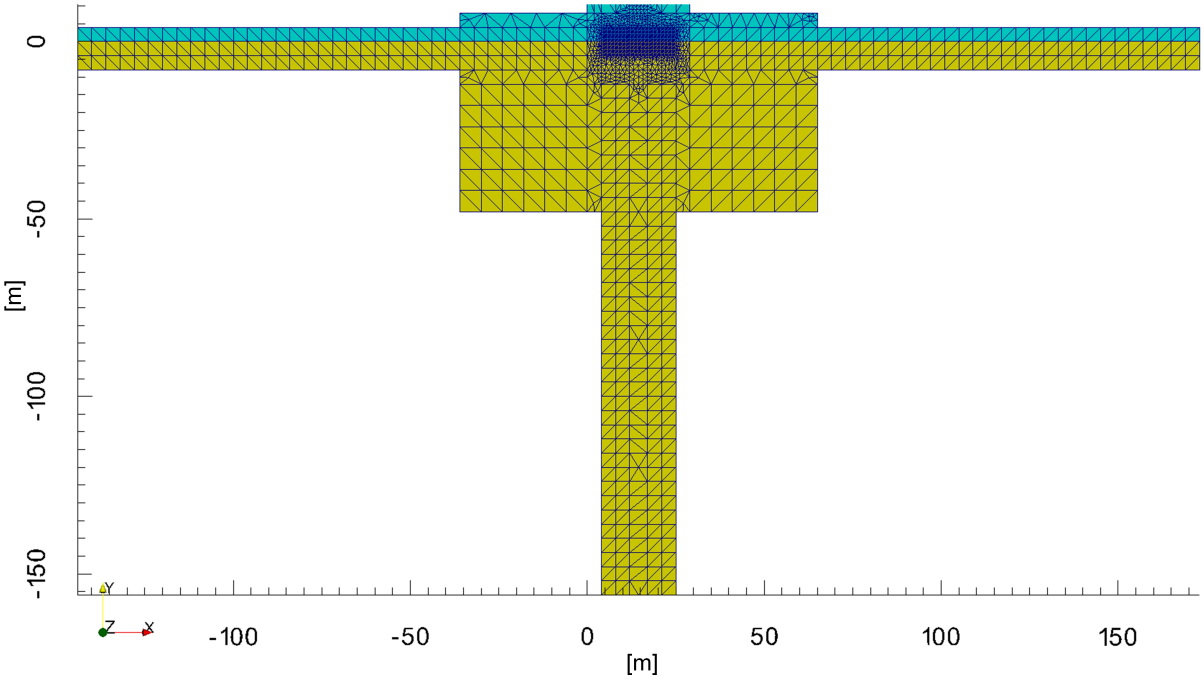

Figure 5.6: Mesh of the 2D horizontal surface

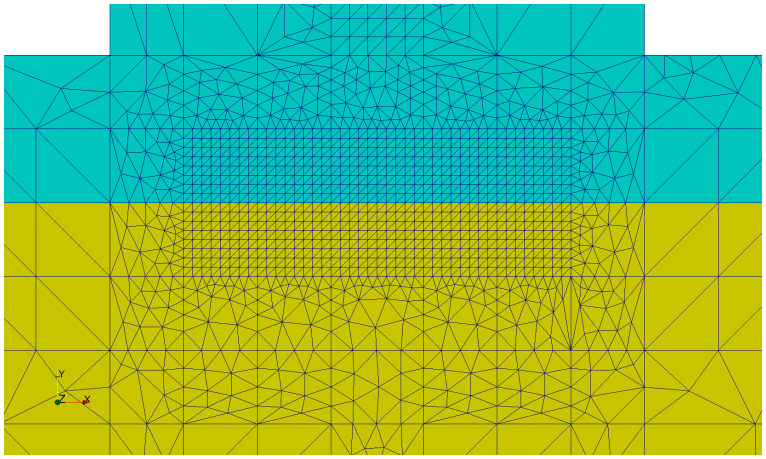

Figure 5.7: Area of interest of the 2D horizontal surface

5.3.4 3D dike profile

The 3D model is shown in Figure 5.8. The mesh is very similar to the 2D dike in Figure 5.4. Fewer elements are present in the X-Y plane. In the Z-direction the model has, instead of 1 element in the 2D, 13 elements: 5 elements in the center originate from the block which has a dimension of 5x5 m in the X-Z plane, 2 times 1 extra element on either side of the impact and 3 wider elements on each side to limit the effect of the boundaries. This provides the model a depth in the Z-direction of 25 meter. This way the shock wave will not reflect immediately. The elements in the dike have a height of 1.0 meter, which is the double of the 2D dike model. If lowers the number of (active) elements by a factor 4, so the calculation time will be lowered. However, the accuracy will decrease as a result.

A 3D model is in most cases better than a 2D model, because reality is in 3D. Though, 3D models have disadvantages. The number of elements and material points increases, therefore also the calculation time and data amount. It is also harder to pre- & post-process 3D models.

The results of the 2D and 3D simulation will be compared and analyzed in Section 6.4.

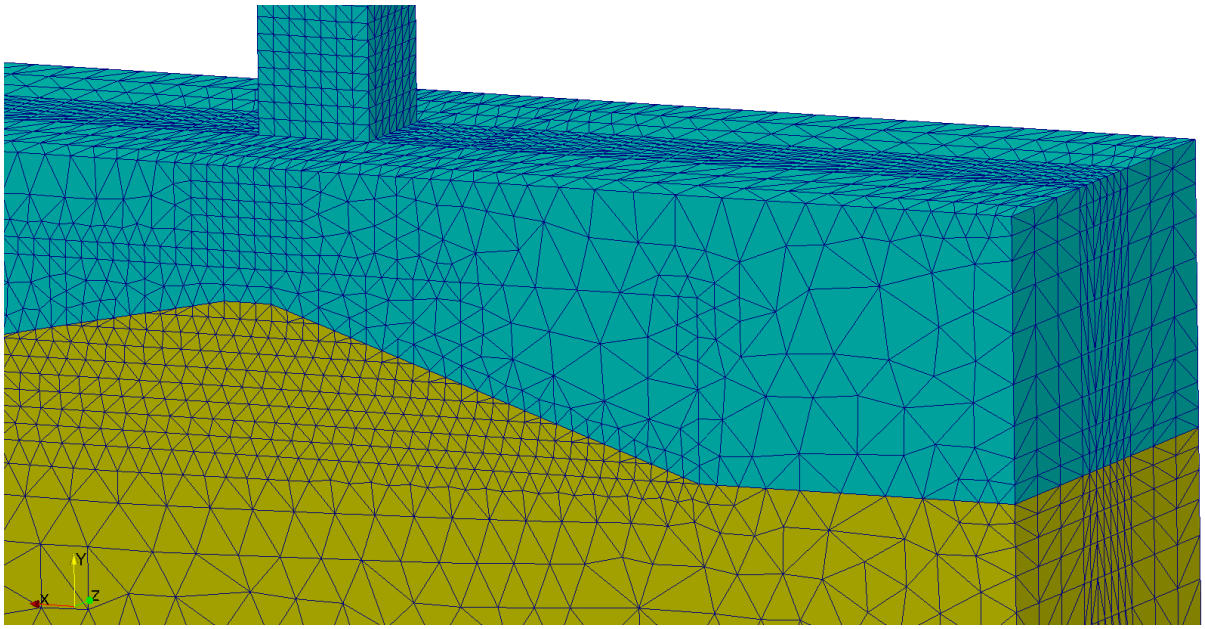

Figure 5.8: Mesh of the 3D dike profile

5.3.5 Boundaries

Numerical models have boundaries at the location where the edge elements are positioned. At these locations the exact stresses in the soil are of minor importance. These boundaries are applied at the nodes. The boundaries can be open, closed or absorbing, the closed boundaries are named fixities as well. Open boundaries will practically be the same as no boundary are applied. Absorbing boundaries absorb stresses and deformation, they are incorporated in Anura3D as Kelvin-Voight model: a purely viscous damper and a purely elastic spring.

At the impact, stresses in the soil are generated. These stresses travel through the soil to the boundary of the model. The goal of the boundaries is to simulate reality where stresses propagate further. So, there should not be unrealistic effects on the model itself. These unrealistic effects can be large settling or large stress reflection. It would be best to have boundaries which behave as perfect dampers, so no stresses are reflected and the material stays in the same position.

The method to do this in the model is to use absorbing boundaries. However, these absorbing boundaries give large numerical issues. The parameters which determine the behavior of the viscous damper and spring have to be changed manually every simulation where other parameters are used, so it is very time consuming as well. Therefore the absorbing boundaries are not used in the model.

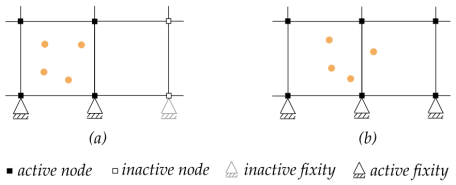

Figure 5.9: Applied fixed boundaries (Al-Kafaji, 2013)

The boundary conditions which do are used are the closed boundaries. The boundaries of the model are fixed in their normal direction, so the waves will reflect at the boundaries, see Figure 5.9. The 2D horizontal model is made large enough to let the reflected waves not influence

the solution. However, the 2D dike profile is not large enough to ensure no wave reflection is occurring. This is not a problem if the reflected stresses do not have a significant effect on the area of interest. This has to be ensured and therefore the reflected stresses are analyzed in Subsection 6.5.2.

5.3.6 Meshing the nacelle

Modeling the shape of the nacelle as a box has the advantage that the model is simple and therefore the least errors can occur in MPM. The mesh of the block and the space below it to the dike are both structured. This has the advantage that the material points can move though the grid without errors. If a pointy or round shape would be used, the mesh of the nacelle would certainly be unstructured. Creating the perfect mesh for this takes a long time. Because it should move through the structured mesh between the block and dike. Errors can occur during this falling process. Using a spherical shape is tried, however, it gave too many complications and errors, to solve within the limited time of this thesis. It does is recommended doing more research on this.

5.4 Material properties

Next to the shape of the dike and nacelle, the materials have been modeled as well. They consist both of only one material in the MPM models.

Steel is the material which is most used in the nacelle, so the material should behave as steel. Ideally, the exact same material properties should be used, because then the effects during the impact need less verification. The material properties of the soil of a similar dike can be found in Appendix E. If more layers are added, the model becomes more realistic. However, it is chosen to only use one layer of soil, because the model needs to be used first with one layer before more complex set-ups are used.

The material properties of the soil and nacelle in the 2D and 3D dike profile are shown in Table 5.2. For the 2D sensitivity analysis, a smaller mass is used to limit the penetration depth. This is for compensating the 3D effects, which will also limit the penetration depth.

Material Properties	**Soil**	**Nacelle**
Type	Solid	Solid
Initial porosity [-]	0.3	0.0
Density solid [kg/m^3]	2650	11400
Material model	Mohr-Coulomb	Linear Elastic
Young's modulus [kPa]	30000	100000
Poisson's ratio [-]	0.3	0.3
Cohesion [kPa]	0	-
Angle of internal friction[°]	30	-
Dilatancy angle [°]	0	-
Tensile strength [kPa]	0	-

Table 5.2: Material Properties

5.4.1 Nacelle

The width is chosen as 5 meters, which originates from the analysis where the nacelle penetrates the top meter, see Figure 5.3. If the nacelle penetrates deeper, the model of the nacelle should be made wider. However, this causes additional complications. The mesh of the nacelle consists of structured elements, so only a layer of elements can be put in top of the block which is wider.

This extra layer will be sticking out and deform upon impact, which in reality will only occur slightly. However, in the model the stiffness or Young's Modulus of the nacelle is much lower than steel, because this increases the calculation speed. This is explained below. Still the most important factor is the amount of energy which is transferred to the soil, so it chosen to only make the block higher and not wider.

In 3D, another dimension is added, so for the area of impact, the width is squared: 25 m^2. In the 3D dike profile the complete mass of 568 tonnes is used. The 2D model is only 1 meter in width, so a fifth of the total mass of 568 tonne is used as the mass material, 114 tonnes. The porosity of the nacelle is 0.0, because it is a solid material without pores.

The used height of the nacelle is 2 meters, this leads to certain density in order to fulfill the requirement of 568 tonnes of mass. In reality, the density of 11400 kg/m^3 would be a rather high value for a solid object, steel only has a density of 7800 kg/m^3. The effect of this higher density together with a smaller solid object than the real nacelle, is that the energy is transferred faster to the soil at the impact. The wave speed of energy is calculated with Equation 5.2.

This higher density will not give an unrealistic result, because in the model a relatively low stiffness or Young's Modulus for the nacelle is used. The lower stiffness slows the energy transmission. So the 2 effects are assumed to cancel each other out, see Equation 5.2. The stiffness of the nacelle is only 100 MPa, much lower than that of steel (2.1 GPa), this is done to control the wave speed in the model. If the wave speed is very high, the time step will be very small. The maximum time step is calculated with the wave speed and the minimal element length. A smaller time step will lead to a longer calculation time. So, a low stiffness is preferred. But it should be high enough, so the nacelle does deform too much or fall apart, at the impact.

$$c = \sqrt{\frac{E}{\rho}} \tag{5.2}$$

Where c is the wave speed, E is the Young's modulus , ρ is the density of the material.

The mass used for the 2D sensitivity analysis is 15 tonnes. This value is chosen as a sort of dummy mass, any value which gives a value with substantial penetration depth can be used.

5.4.2 Soil

Only one soil material is used in the simulation. In Groningen the core of the dike consists mostly of sand. The dike is often covered with a clay layer. Because of the impact, it is assumed that this top layer will be destroyed and will have the same properties as the core material.

Saturated soil or dry soil are the two extreme situations in a dike. The situation in between those extremes: a phreatic line cannot (yet) be used in Anura3D. The governing situation for each failure mechanism can differ. For failure mechanisms water pressure is important for macro-instability for example, a saturated dike could be governing. But the deformation of the dike profile is often more important.

Undrained soil behavior

This is not used in the model, as no saturated soil is used, only dry soil. The behavior of the soil a saturated dike can be drained or undrained. Undrained implies that the water particles are trapped in the pores between the solids. At relative fast impact, which is the case, the water particles will take over the stresses from the impact in the beginning of the impact. Due to the water which behaves incompressible, the deformation will be limited. Short after this period, the effective stresses are lowered and the penetration will increase. The end situation is hard to estimate.

However, for slope-instability the undrained soil behavior is very relevant. The effective stresses will decrease as the water pressure increases. Anura3D should be able to make a fully coupled undrained calculation, however, there is a bug (at the moment) which prevents using this fully coupled calculation. Therefore only dry soil can be used.

Parameters

The parameters which need to be used are determined by the material model, for the nacelle the Mohr-Coulomb model, which is explained in the next subsection. The density of the solids is for most granular soil materials similar: 2650 kg/m^3. The unit weight of the dry soil is than determined by the porosity. A porosity of 30% is used, this leads to a unit weight of 18.55 kN/m^3. The Young's Modulus is chosen as if the sand is loose to medium packed, 30 GPa. It is unclear if the core material is compacted or not. This can vary along a dike segment. Therefore a conservative value is used: loosely to medium packed. The friction angle is chosen as 30 degrees, this is in line with friction angle from the CPT in Appendix E, which is from a similar dike in Friesland. The Poisson's ratio is chosen as 0.3, this usually a good value for soil mechanical analysis. However, it has a disadvantage in this analysis. Because the impact is very short the soil will behave undrained in reality. A higher value, near 0.5 might give a more realistic behavior. The difference between a low (0.0) and high (0.49) Poisson's ratio is shown in Section 6.1. There is no cohesion used, because sand is modeled and that has no cohesion. A small amount of cohesion can be used to limit the number of material points jumping out of the soil. This is tested, however, it gave not the expected result and many material points still jumped out of the soil. Not using dilatancy is conservative, because there will be more deformation without dilatancy in the crater. Sand has no tensile strength, so there is a tension cut-off at 0 kPa.

5.4.3 Material models

The material model determines the mechanical behavior of the soil, so material model should be capable of handling the processes which cause the crater. The deformation of the soil and mass is inherent to the material model. The nacelle is modeled with the Linear Elastic material model and the soil with the Mohr-Coulomb material model.

Linear Elastic The Linear Elastic model is based on Hooke's law of isotropic elasticity. The elastic parameters Young's Modulus and the Poisson's ratio are involved. The model is usually inappropriate to model the non-linear behavior of soil. It does is suitable for simulating structural behavior, therefore, stiff materials such as concrete, rock or steel and often modeled with the Linear Elastic model. The nacelle is very stiff, it consists mainly of steel, and should not have large deformations in the model, so the Linear Elastic model is a suitable material model for this purpose. It is a very simple model, compared to other material models, however, it does transfer the energy at the right wave speed which is most important. In addition, because the Linear Elastic material model is simple to set up and does not need much tweaking, the emphasis can be put on the soil.

Mohr-Coulomb The Mohr-Coulomb model is an Linear Elastic Perfectly Plastic material model, see Figure 5.10. Next to the elastic parameters, there are 2 parameters for the plasticity: c and φ , cohesion and angle of internal friction. Also the angle of dilatancy ψ , can be used. As can be seen in Figure 5.10, there is an elastic part (ε_e) and a perfectly plastic part (ε_p). It is a simple model which is normally used for first-order estimations, so it is suitable for this study (Plaxis, 2016).

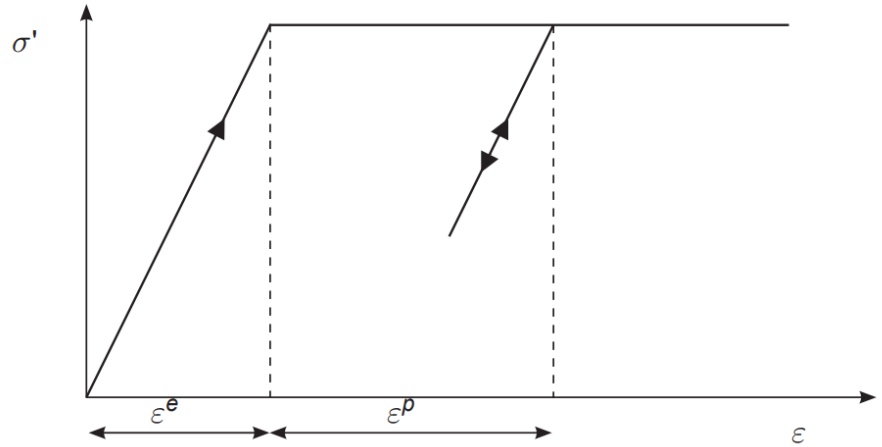

Figure 5.10: Elastic Perfectly Plastic stress-strain diagram

There are disadvantages as well for the Linear Elastic Perfectly Plastic model as it simplifies the soil behavior. Especially the perfectly plastic part is slightly unrealistic. In reality there will be strain softening or strain hardening if the strain increases, it depends situation which of the two occurs. In the case of an impact on sand, strain softening is expected, see Figure 5.11. When the Mohr-Coulomb model is used, the stresses in the MPM model are overestimated, because at the same degree of strain, the stresses are higher.

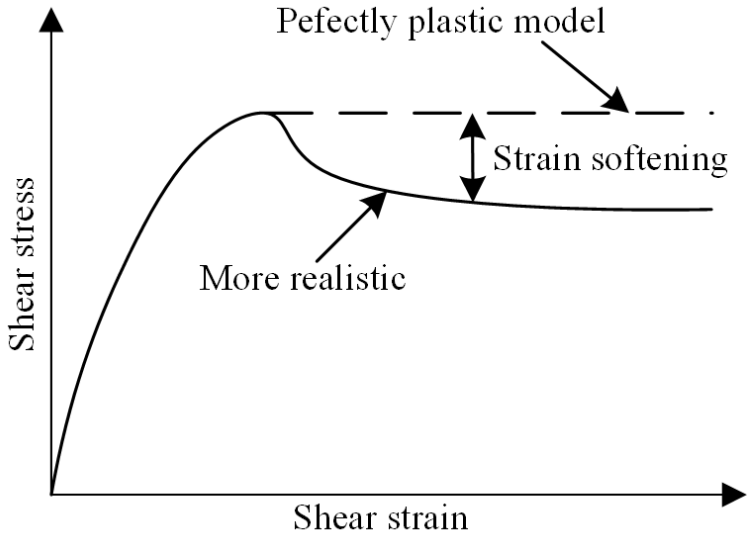

Figure 5.11: Strain softening

5.5 Remarks on set-up & discussion

There have been many assumptions and choices made in this chapter. In this section more background information and reasons for choosing certain assumptions are given. Advantages, disadvantages and methods which can work as well are also discussed in this section.

5.5.1 Kinetic energy at impact

The kinetic energy at impact is an important factor for the depth of the crater. The kinetic energy has two components, the impact velocity and the mass of the object. The mass is more

or less known. The only components that can differ per impact are the blades. Most of the mass of the blades is located near the rotor and might behave as one with the rotor. There are many possibilities that the mass of the blades contributes to the mass at impact, however, there are also many situations where the blades do not contribute to the total mass.

The impact velocity used in the thesis is the free falling velocity, which is the maximum. As stated in Subsection 5.2.3 there are multiple factors which limit the impact velocity, those are all not considered. Because the velocity is squared in the equation for kinetic energy, a lower velocity will have a large influence on the kinetic energy. A good analysis of the impact velocity can give a more realistic penetration depth. However, in the model are different impact velocities used, so, it is more a choice which impact to use, it does not change the behavior of the model.

5.5.2 Soil geometry and profile

The geometry of dikes is differing per location. If a greenfield dike would be built, in the preliminary design it would have an outer slope of 1:5 and an inner slope of 1:3. It turns out that the location of the dike in Groningen has globally these slopes as well. However, at other locations the inner slope is often steeper. With these knowledge, the choice is made to use an inner slope of 1:3 in the model.

There is much variation in the soil profile in the Netherlands. The choice has been made to choose loosely to medium packed sand as the only soil material used in the model. Because the top layer on dikes only has a limited depth and the penetration will be more than only the top layer. The effect of the top layer is neglected in the model, however, the top layer does have an effect on the penetration. It should be taken into account for a better model. If the top layer consists of clay, the penetration will probably will be higher, because clay is less stiff compared to sand. In case a block revetment is present, the opposite will probably happen, less penetration. The top of a dike does not often contain a block revetment, however, the outer slope does.

5.5.3 Dry and saturated soil behavior

In order to make complete failure probability analysis for the dike, a dry, saturated and partly saturated dike should be analyzed. At normal daily conditions the dike will be mostly dry. When water level rises, the dike will become more saturated. High water at the location of the case study is caused by a storm. During a storm there are often longer periods of rain. If this rain will endure for a longer time the dike will get more saturated. The probability that a wind turbine fails is larger during a storm than during normal daily conditions as well. So, both scenarios are important to simulate. It turns out that due to a bug in Anura3D at the moment a fully coupled calculation cannot be made. So, only dry soil is used in the analysis. It has to be mentioned that fully coupled analyses have a much higher computational time as well compared to single-phase materials.

The excess pore pressures which can be modeled in a fully coupled model are important for the dynamic-instability. So, if the bug is fixed, a fully coupled analysis is highly recommended to do.

It is possible to tweak the parameters of dry soil to simulate undrained soil behavior by increasing the Young's Modulus and the Poisson's ratio in example. It is tried to create a model with those parameters, however, it gave not the expected results, so it is chosen to stick to the dry soil behavior.

5.5.4 Expectation of an impact on saturated dike

In this chapter already several aspects of the impact on saturated dike have been elaborated. Here the expectation of an impact on a completely saturated dike is treated, as sort of summary. The penetration in a saturated dike will be different than in a dry dike, because of multiple

aspects. First of all the weight of the saturated dike is higher than a dry dike, so more energy is needed to deform the soil.

Secondly the soil can behave drained and undrained. Sand is permeable, but when the duration of loading is short enough to prevent dissipation of excess pore pressures, the behavior can be seen as undrained behavior. During the very short period of the impact, there soil will behave undrained. Then the stresses in the soil are taken over by the water in the pores in the beginning. The water will behave incompressible during this loading, however this situation is only reality for a fraction of a second. So, the deformation of the saturated soil, technically the water, will be less than of dry soil in the first fraction of a second. The exact moment of this is unknown. After that the effective stresses are lowered by the increased pore pressure. Then the soil will have less resistance against deformation and the penetration increases. It is a possibility that liquefaction can occur after the impact. The penetration of a completely saturated dike therefore is probably higher.

The excess pore pressures lower the effective stresses. For the stability of the slopes the effective stresses are an important part of the resistance against instability. So, dynamic failure of the slopes of the dike can occur. It cannot be estimated if this instability of the slopes occurs during the impact, this is too complex. For this, undrained MPM simulations are needed.

5.5.5 Impact under an angle

In reality, the impact is often not perfectly perpendicular to the surface. There is a horizontal component as well in the velocity of the block. The emphasis in this thesis is on modeling the impact as correct as possible. If an inclined impact would be modeled, the mesh above the dike should have an angle, which leads to multiple complications in the mesh creation. Nevertheless it is possible to overcome all those complications, however, it would take time. An impact under an angle at the crest or inner slope in the sliding direction of the inner slope will lead to a more unfavorable situation than a vertical impact. For wind turbines at the inner side of a flood defence, the only scenario where this can occur is during a buckling of the tower and especially buckling in the bottom half. The probability of occurrence of this scenario is relatively low, so the impact under an angle is not a priority for research.

5.5.6 Shape of the penetrator

In the geometry of Figure 5.3 the penetration depth is estimated 1 meter. If the penetration depth will be larger, the load is spread over more area, because the object that is falling has a more or less round or spherical shape. A solution for this in MPM is to create an additional box on top of the existing box which represents the nacelle. At the moment of impact there the internal forces in the object will be very high. Because the Young's modulus used in model is much lower than in reality, this additional box will deform significantly at impact. It is recommended in further studies to look at the different shapes as well.

The effect of the shape of the penetrator in reality I expect to be limited. The shape which will cause the highest penetration will be the spherical shape, as more pointy shapes are not present in the Enercon E-126 nacelle. In other nacelles this can be the case. The flat shape, which is used in the models, will cause the least penetration. However, the penetration depends as well largely on the width of the penetrator. It is important to note that a higher penetration will cause a smaller crater. The energy which is transferred to the soil is the same for a high and low penetration and is independent of shape of the penetrator.

Chapter 6

Analysis of simulation results

In this chapter the results of the MPM simulations are shown. The results are discussed as well.

6.1 Results 2D dike profile model

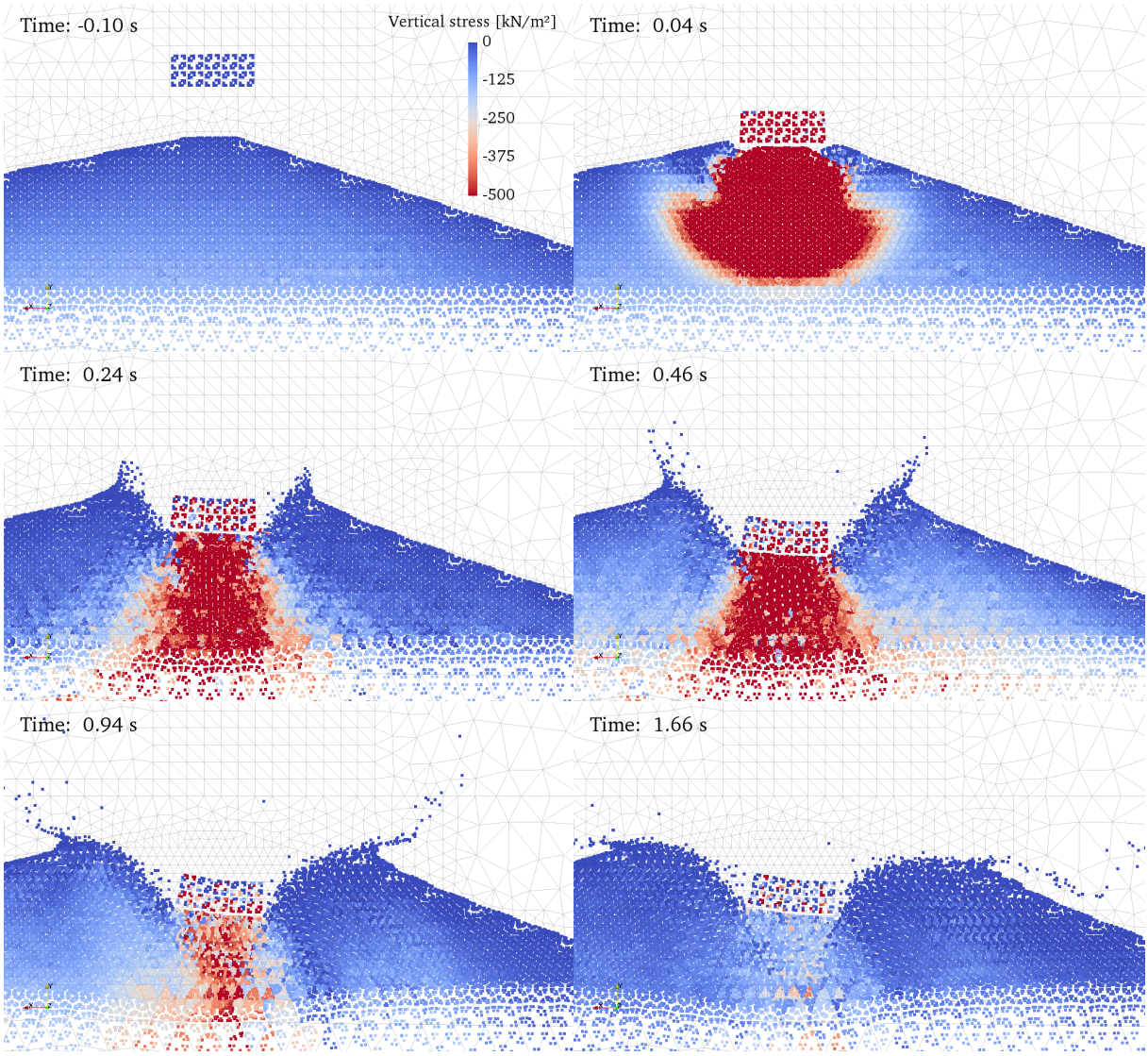

Figure 6.1: Results 2D dike impact

In Figure 6.1 the result of the impact on the crest of a 2D dike model is shown. The different colors of the material points indicate the level of vertical stress. First, there is a static situation with a free falling height of 32 meter, which is the equivalent of an impact velocity of 25 m/s. This velocity is chosen, so the impact is significant and the crater forming processes can be seen clearly and the rough shape of the dike still is intact. The purpose of this simulation is to analyze the model qualitatively.

In the second frame the stress shock wave is recognizable after impact. The graph shows a maximum vertical stress of -500 kPa, but at the material points directly below the mass the stresses are maximal -2000 kPa. These values are negative, because, the Y-axis is oriented upwards positive.

The vertical penetration is at maximum 4.5 meter, this is right below the mass in the soil.

At the sides of the impact the soil seems to move up, but it also moves horizontally. This phenomenon is explained in Figure 6.2. The impact first causes particles to move down. So, there is a compression in the vertical direction, which causes particles to move to the side. Then there is more resistance from the center of the dike, where particles also want to move horizontally. So, the particles away from the center exert stress on particles close to the surface. The closer to the surface the less the resistance is and the soil moves up and to the side. This process is similar to the 'transient cavity' described in Section 4.1.

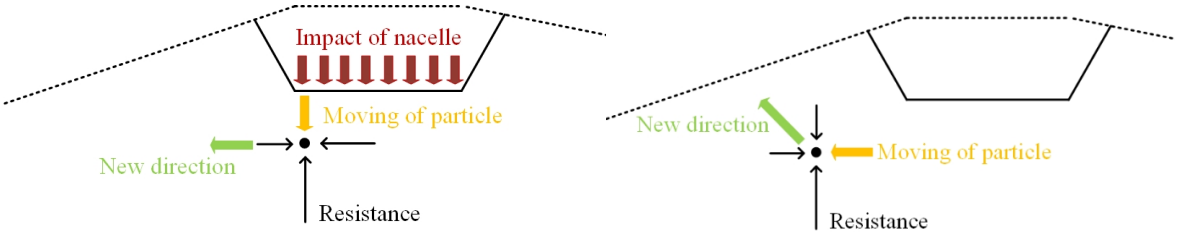

Figure 6.2: Soil moving up and sideways after impact

The fixed boundaries reflect the stresses at the bottom of the model. So, the shock wave which first moves down, later reflects back up, in this simulation after 0.32 seconds. The amplitude of the reflected stress shock wave is the highest at the location where it propagated from, there it is only 10% of the original stress. Alongside the impact the amplitude of the reflected stress shock wave is even much lower, it has hardly any effect on the soil moving up.

The simulation ends at 1.66 seconds after the impact, the crater formation is finished at that time. The residual profile at the end of the simulation shows a flattened top of the slopes, can be seen in Figure 6.1. The soil is pushed away from the top in the other frames. The slopes just next to the mass follow their angle of internal friction after a while. Also it can be seen that in the end the mass is slightly tilted to the inner slope (right slope). This slope (1:3) is steeper than the outer slope (1:5). This causes less resistance at the inner slope for the impact and the highest point in the steady state will be at the milder slope side.

The material points flying in the air appear at most models where material points which have a small mass are at the edge of a model and are given a large acceleration. In addition, the sand has no cohesion or tensile strength, so there is no force to keep the material points at the surface.

A larger version of the last frame of the simulation, which is close to the steady state, is presented in Appendix D.

6.2 Sensitivity analysis

In this section a more quantitative analysis of the results of the simulations is provided. The effect of the stiffness, angle of internal friction, Poisson's ratio, cohesion, porosity, impact mass

Table 6.1: Standard material properties

Properties	**Soil**	**Nacelle**
Material type	Solid	Solid
Initial porosity [-]	0.36	0.0
Density solid [kg/m^3]	2650	3000
Material model	Mohr-Coulomb	Linear Elastic
Young's modulus [MPa]	30	100
Poisson's ratio [-]	0.3	0.3
Cohesion [kPa]	0	-
Angle of internal friction [°]	30	-
Dilatancy angle [°]	0	-
Tensile strength [kPa]	0	-

and impact velocity are analyzed. Those parameters have an effect on multiple mechanisms of the crater formation. The emphasis is on the penetration depth, which is considered most important for the quantitative analysis of the model. The graphs of the development of the penetration depth for each simulation can be found in Appendix D. In this section only the extracted penetration depths from the graphs are presented.

Simulation setup

Most information of the simulation setup can be found in Chapter 5, however, several properties are different in the sensitivity analysis from the 2D and 3D dike profile models.

A 2D horizontal profile is used for the analysis instead of a 3D dike profile model. This is chosen for multiple reasons. The horizontal surface model has a lower calculation time than the 2D dike profile model, this is preferred in this case above a dike profile, because for the sensitivity analysis many simulations have to be run. The model is extended in vertical and horizontal direction, to ensure the reflected waves will not reach the material points where the deformation is measured. These extensions can be seen in Figure 5.6. Also the initialization of the initial stresses of 3D dike profile takes much longer, this is in the order of days for. Another reason is that the goal of the sensitivity analysis is to analyze the effect of the parameters of MPM and in less extend the effects of the parameters in a specific dike.

The standard parameters for the simulations of the sensitivity analysis are shown in Table 6.1. The mass block is smaller and has a lower density compared to the mass block used in the 2D dike profile. The block is 5 meters wide as well, but is only 1 meter in height. The total mass of the block is 15 tonnes, instead of the 2D dike model where it is 114 tonnes. This is chosen to have a penetration depth which is not too large, because in reality the penetration depth will be less than the 4.5 meters from the 2D dike profile. 3D effects will limit the penetration depth, later in this chapter the 3D model is analyzed. The dropping height is 136 meters, which gives an impact velocity of 51 m/s.

Method of determining penetration depth

In the graphs the vertical displacement of material points (MPs) is plotted over time. There are 9 material points for which the displacement in vertical direction is measured. They can be seen in Figure 6.3. The blue points are the MPs of the soil, the red of the nacelle and the 9 MPs in pink measure the displacement. These points are not all in the same horizontal plane, they are spread over 3 different vertical levels, but still close to the surface. This is chosen to ensure there are enough particles which stay in place in the material and do not move relative to their surroundings. MP 3 and MP 5 (the green and purple curve in Figure 6.4) are moving more up

than the MPs next to them, they lost coherence with the MPs of which they first were connected to. So, the material lost the coherence there.

For determining the effects and comparing the results of different parameters, only the plot of one MP is shown. The material point which has the largest deformation is chosen to use in the sensitivity analysis. In Figure 6.5 MP 5 of Figure 6.4 is used for example.

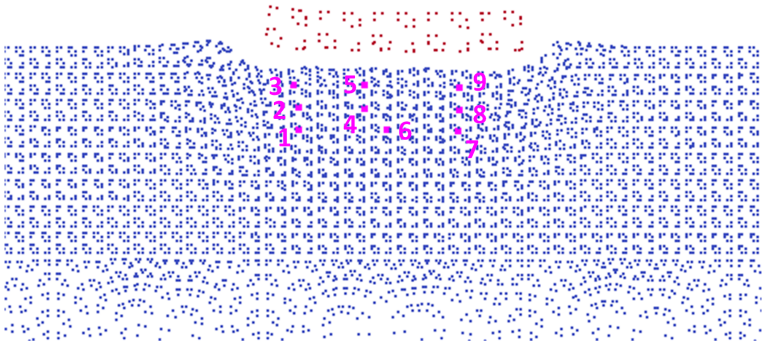

Figure 6.3: Location of the 9 material points in the soil used in the sensitivity analysis

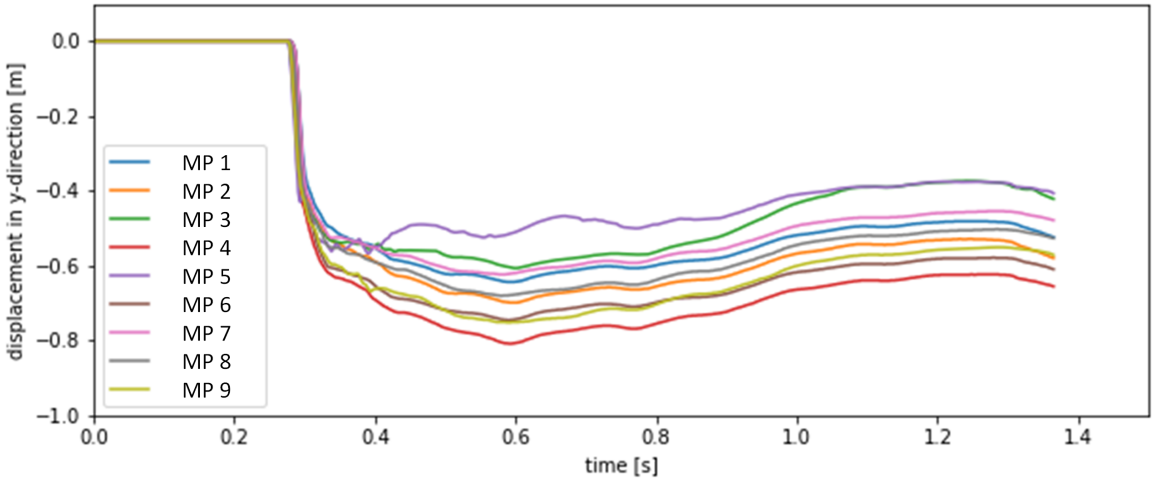

Figure 6.4: Penetration depth with standard material properties

Stiffness of the soil The stiffness of the soil in the Mohr-Coulomb material model is defined by the Young's modulus. A stiffer material will displace less when the same load is applied. So, the penetration depth will be higher for material with a low Young's modulus. The Young's modulus of sand varies from 15 MPa of loosely packed sand to 75 MPa densely packed sand according to table 2.b in (NEN 9997-1:2016 nl, 2016). Next to values within this range, values outside this range have been added as well. The development of the penetration depth in time can be seen in Figure 6.5. The green dashed line is the reference case, the parameters of this reference case can be found in Table 6.1. The penetration depth increases for lower stiffness, as can be seen in the figure, so this is correct according to the theory. An interesting conclusion is that if the Young's modulus is halved, the penetration depth increases in the order of 20%.

Several curves in Figure 6.5 which have a higher penetration depth, bounce up slightly. This effect is caused by elastic behavior of the soil. If more soil which behaves elastically is displaced, more soil will bounce up.

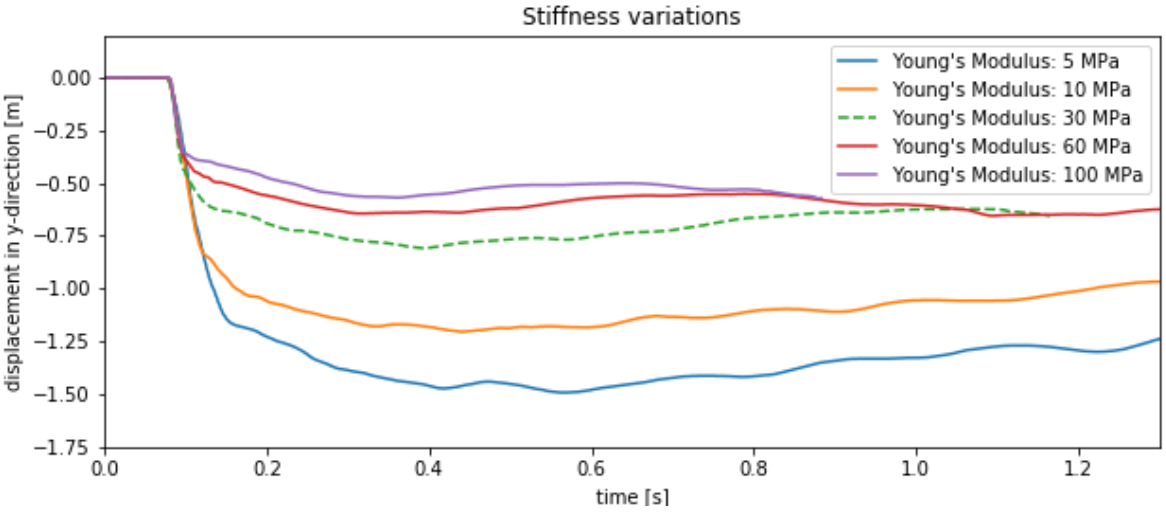

Figure 6.5: Effect of stiffness

Angle of internal friction A higher angle of internal friction will lead to a lower penetration depth. In Figure 6.6 it can be seen that for lower angles of internal friction the penetration increases more than linear. The dashed line is again the reference case. Angles of internal friction below 15 degrees are rarely found. However, for sand an angle of internal friction between 25 and 35 is often a realistic value. The reason that several curves are stopping before others is that in those simulations a material point leave the mesh and the calculation is stopped automatically.

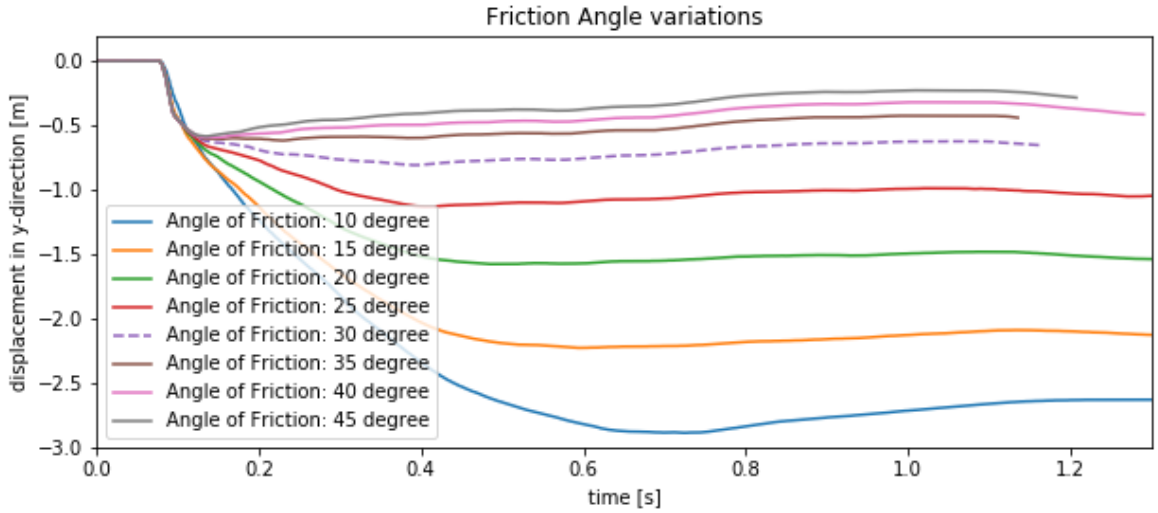

Figure 6.6: Effect of angle of internal friction

Poisson's ratio The Poisson effect is the phenomenon in which a material tends to expand in directions perpendicular to the direction of the compression. So, when the soil is compressed vertically, it expands horizontally. To see if the effect of the Poisson's ratio is incorporated in the model, the width of the crater is a better indication than the penetration depth. In theory it has no significant effect on the penetration depth as well. It is chosen to research two opposite values for the Poisson's ratio. The value of 0.0 is a material similar to cork, 0.49 can be seen as undrained soil behavior. In Figure 6.7 the difference between the Poisson's ratio of 0 and 0.49 are shown. When the ratio is higher, the crater is wider than when the ratio is lower. So, the Poisson's ratio is working as it should as well.

The penetration depth is similar for all Poisson's ratios tested (0.0 - 0.49) and the graphs can be found in Appendix D.

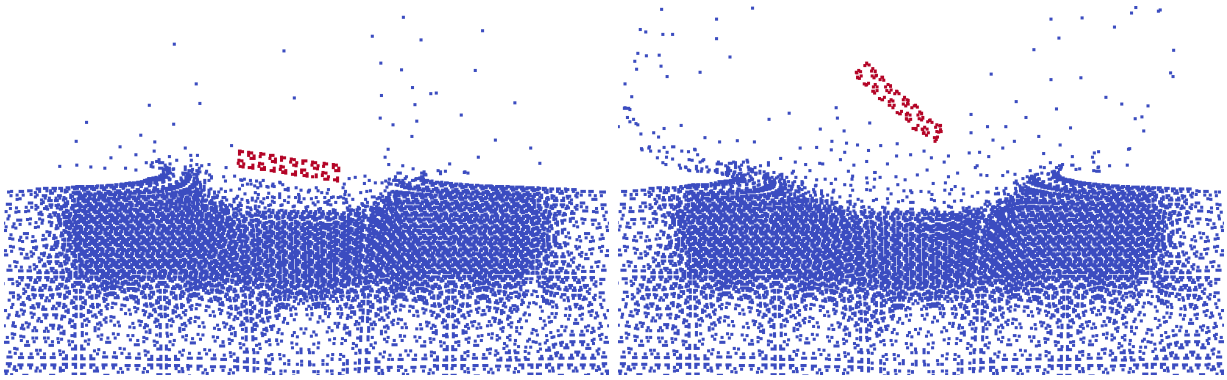

(a) Poisson's ratio: 0.0 (b) Poisson's ratio: 0.49

Figure 6.7: Effect of Poisson's ratio

Unit weight of the soil The unit weight of the sand is incorporated in the model as the porosity. The density of the grains is fixed at 2650 kg/m^3, so the only parameters which have an influence on the weight are porosity and the gravitational constant. The level of saturation could have an influence, however, it is not relevant, because only dry soil is used. In reality, the unit weight of the sand is correlated to the stiffness: densely packed sand is stiffer than loosely packed sand. Nevertheless, looking at the porosity and the penetration depth, this provides more information about the model. In Figure 6.8 it can be seen that the higher the unit weight (and lower the porosity) a lower penetration depth occurs. This effect is caused by the energy balance. A higher mass needs a higher force in order to be displaced than a lower mass.

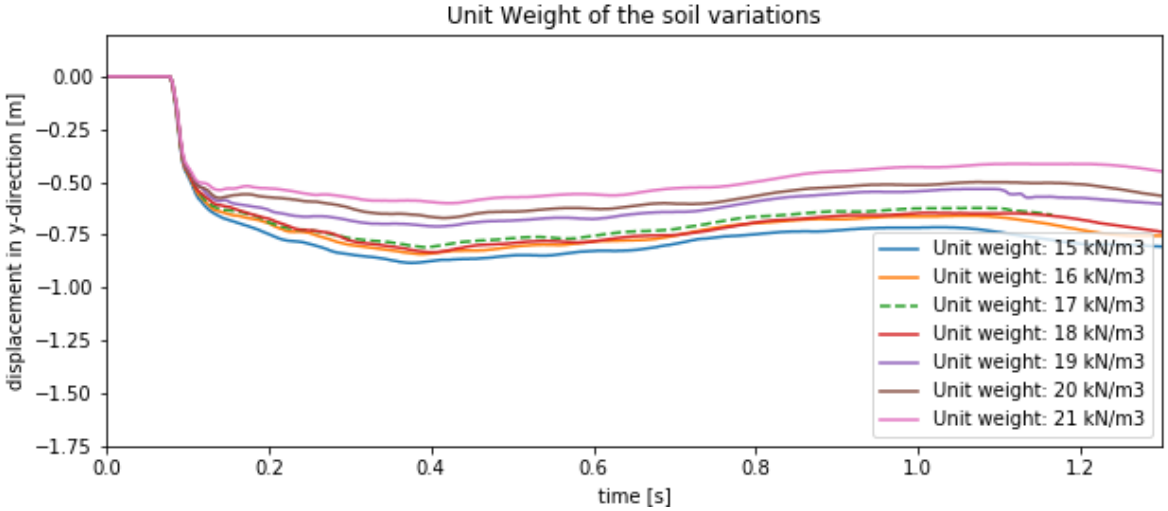

Figure 6.8: Effect of the unit weight of the soil

Weight of the nacelle The weight of the nacelle is very important in these simulations. The weight determines together with the impact velocity the maximal energy that can transferred to the soil. A higher mass causes a higher penetration depth, this is clearly visible in Figure 6.9.

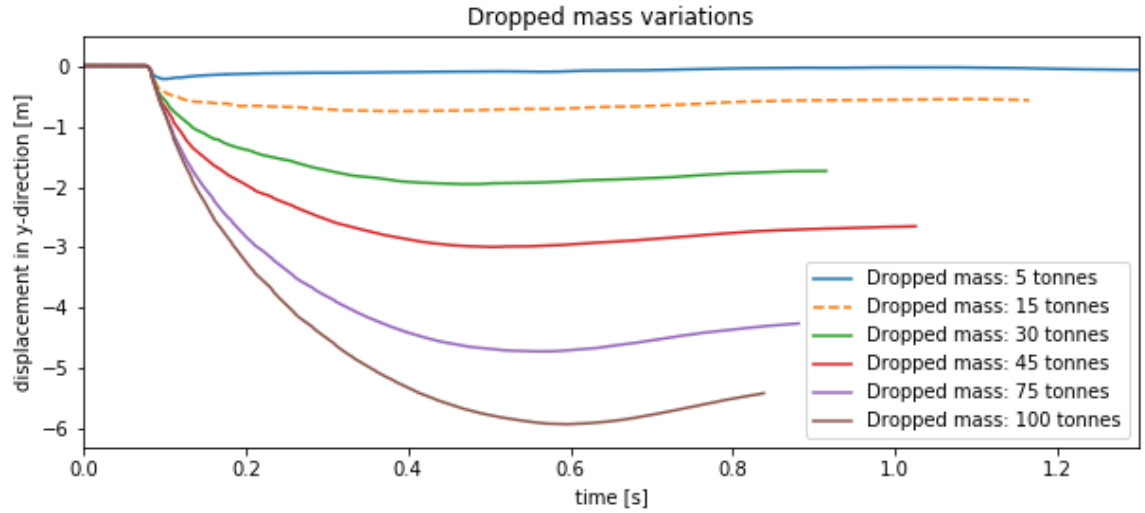

Figure 6.9: Effect of weight of the nacelle

Impact velocity The weight of the nacelle which is falling down is increased to 45 tonnes instead of 15 tonnes in these simulations. This is changed to obtain penetration depths which differ more. The impact velocity has a large effect on the penetration depth, because the velocity is squared in the formula in the kinematic energy equation. The penetration depth increases linearly with the impact penetration depth according to Figure 6.10.

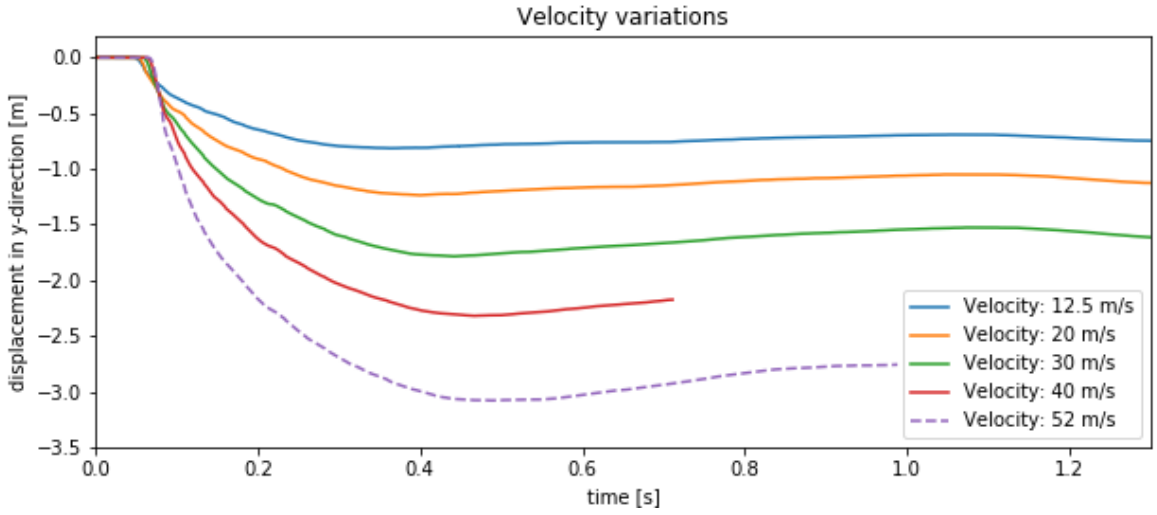

Figure 6.10: Effect of impact velocity

Conclusion sensitivity analysis

It can be concluded that all parameters checked in the sensitivity analysis are working as they should. The sensitivity analysis shows that the governing parameters are the impact velocity, the mass of the penetrating object, the stiffness of the soil and the angle of internal friction of the soil. The unit weight of the soil turns out to be of important for the total energy which needs to be displaced by the object.

6.3 3D simulations

The goal of the 3D simulations is to determine the real penetration depth. The 2D model can be seen as an infinity long dike with an infinitely long nacelle hitting the crest. In the 3D model, the mass which falls down represents the dimensions of the nacelle in 3D. The most important reason to use a 3D model is that the energy and stresses are spread in all three dimensions. In Figure 6.11 a 3D simulation during the crater formation is shown. The crater is still expanding horizontally, while the final penetration depth almost is reached.

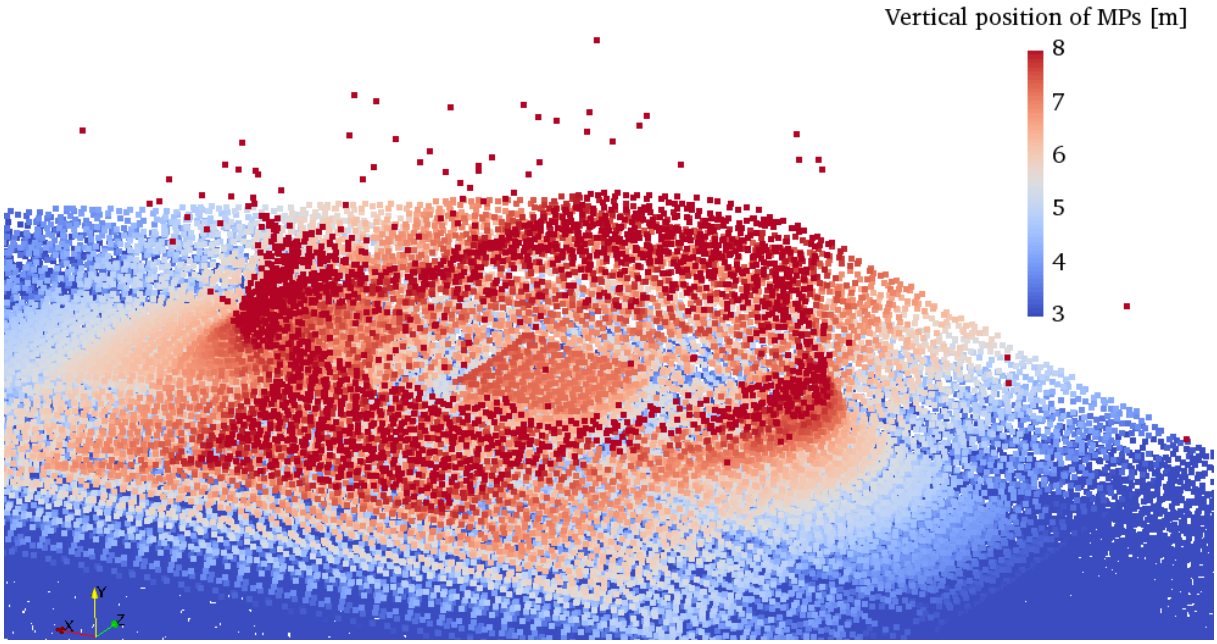

Figure 6.11: Result of the 3D dike impact simulation with material points

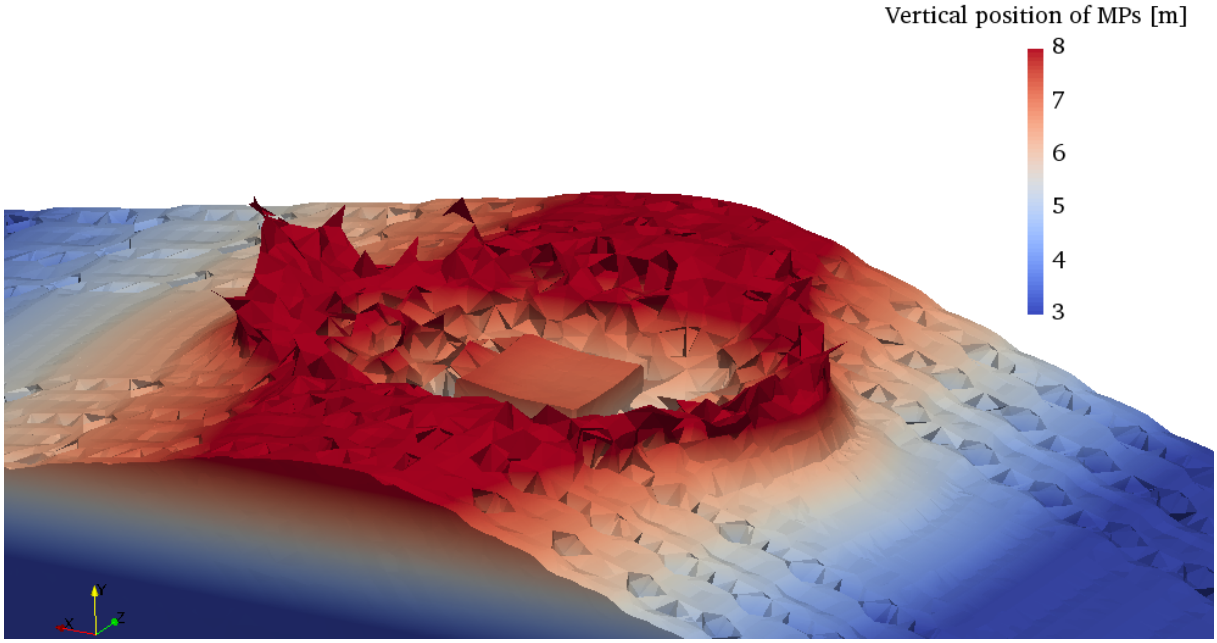

Figure 6.12: Crater forming during the 3D impact by connecting the material points

In Figure 6.12 the material points have been connected again, the crater shape is clearly recognizable here. At the sides of the crater small holes can be seen, this is due to the lower density of material points, in reality the surface would be smooth. The colors of the MPs represent the vertical position of a certain MP. The highest point of the dike was around 8.5 meters in the model. So there is an initial settlement of 0.5 meters before the impact, this is due to gravity loading of the soil. This is a method to establish initial stresses in the soil. The simulation is performed with a falling height of 121 meter. The maximum penetration depth in this simulation is around 3.8 meter, which can be seen in Figure 6.13.

The penetration depth is very sensitive to the impact velocity, as concluded from the sensitivity analysis. In Chapter 4 the different impact velocities are explained. The falling height determines the maximal impact velocity. All sorts of factors limit the impact velocity, so the falling height will provide a conservative estimate of the penetration depth. These depths are shown in Figure 6.13. The derivative of the penetration depth in time just after impact is different for all curves. The derivative is equal to the impact velocity, therefore the curve of the falling height of 121 meters is the steepest.

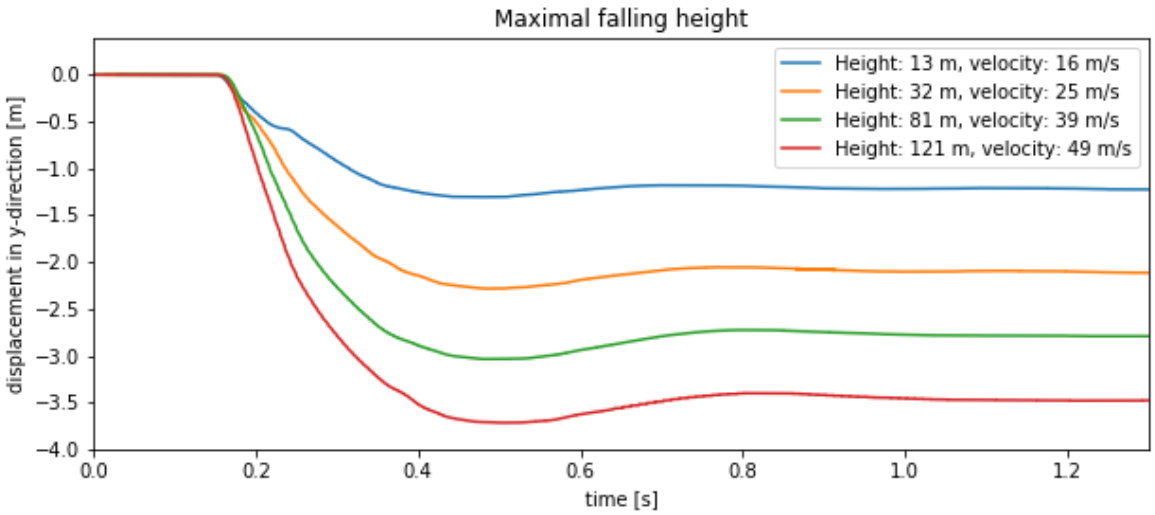

Figure 6.13: Penetration depths of the 3D dike with different falling heights

After the curves in Figure 6.13 go down, they slightly move up again. This is as well caused by the elastic behavior of the soil. The reflection of the stresses at the boundaries could be a cause as well of the soil going up, however, this effect is not significant. The reflection is checked and is elaborated in Subsection 6.5.2 for a 2D dike profile model. For a 3D dike profile model with the same dimensions and an extra dimension, the reflecting stress will be lower. This is due to the effect that stress is spread in an extra dimension, so the amplitude of the reflected shock wave will be lower.

Figure 6.14 presents the interpolated penetration depth of multiple simulations. The moving up of the soil is neglected and the highest maximum depths are chosen from Figure 6.13, the maxima are taken to be conservative and not using the elastic behavior of the soil. From a minimum falling height of 32 meter, a linear trend can be seen in the graph.

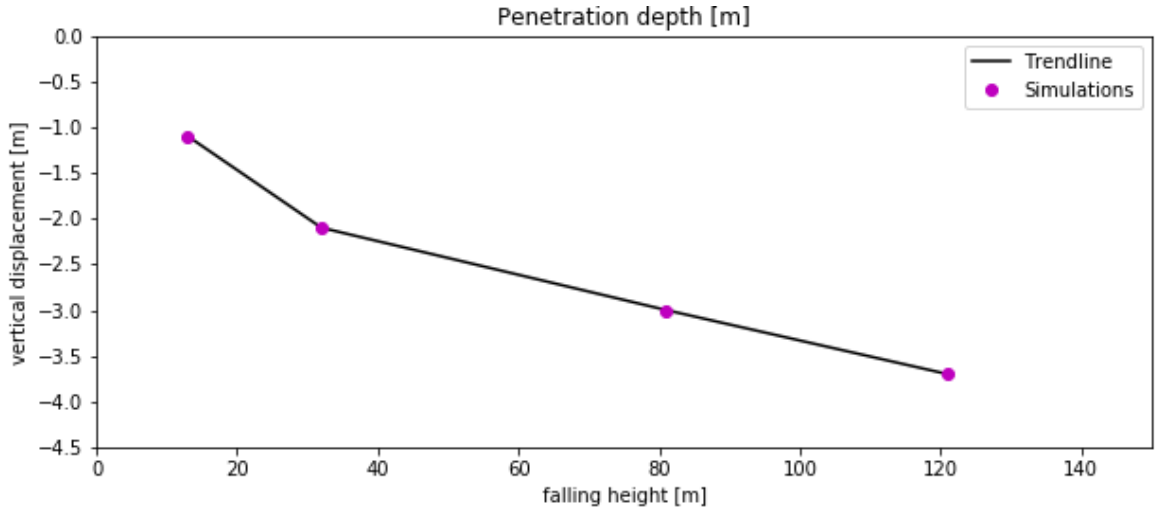

Figure 6.14: Interpolated penetration depths

Shape of crater

In Figure 6.15 the shape of the crater is shown for the 3D simulation with a falling height of 121 meter. The figure is directed in the X-direction, perpendicular to the dike. The flying material points and nacelle have been removed, to focus on the crater itself. The same effects as in the 2D impact simulation of Figure 6.1 can be recognized: transient cavity, slopes stabilizing, compressed soil below the impact and slopes of the dike moving up.

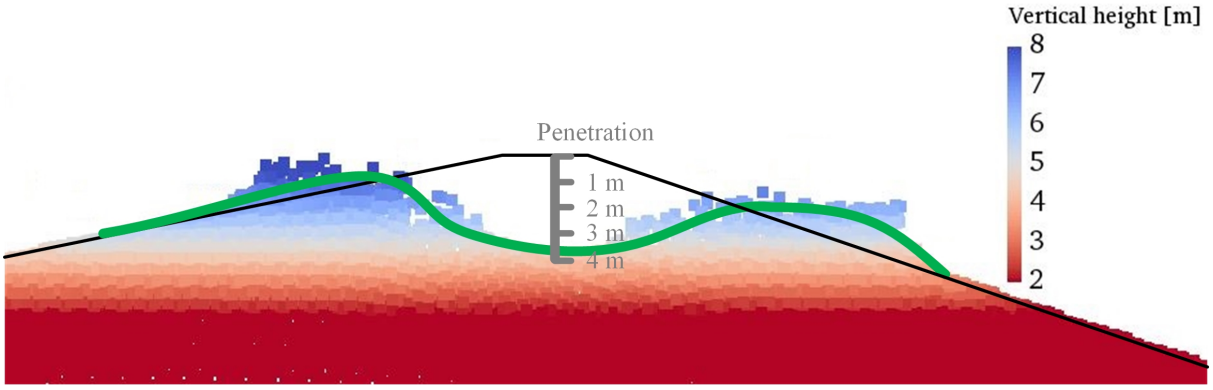

Figure 6.15: Slice of the 3D dike impact simulation

6.4 Difference between 2D and 3D simulations

In Figure 6.16 a 2D and 3D simulation are shown. The impact velocity is in both simulation 25 m/s. The maximum penetration depth of the 2D simulation is 4.5 meters and the 3D simulation 2.1 meter. So the 3D effect in these simulation is large, the penetration depth is more than halved. In 3D the energy is dissipated in both horizontal directions, this causes the lower penetration depth.

Another effect is that total amount of energy is transferred to the soil faster in 3D. The steady state in 2D is reached in 0.9 seconds after impact, while in 3D this is only 0.3 seconds. When the steady state is reached in 0.3 seconds after impact, this would solve the reflecting boundary risk of returning stress shock waves. In the next section more will be elaborated on this phenomenon.

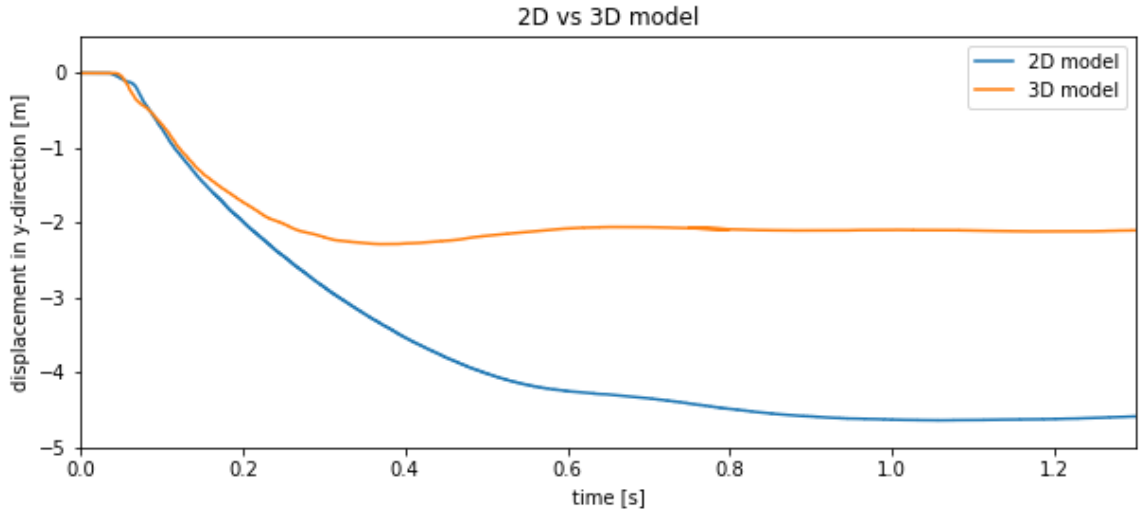

Figure 6.16: Penetration depths of a 2D simulation and a 3D simulation

6.5 Other simulations

6.5.1 Verification analytical falling velocity

To simulate a specific impact velocity, a mass is dropped from a certain height. The velocity should be equal to the analytical falling velocity, see Equation 5.1. The Anura3D software is still being developed, so not all processes have been tested yet. Velocity is the most sensitive parameter as can be concluded from the sensitivity analysis, so for the simulations in this thesis, it is very important to have a correct impact velocity. So, a benchmark has been made for this. In Figure 6.17 the analytical and the MPM fall velocity is shown. The lines exactly match each other, so it can be concluded that the free fall velocity in Anura3D is working as it should.

Figure 6.17: Benchmark free fall velocity

6.5.2 Reflecting boundaries analysis

The MPM models do not have absorbing boundaries. This has the disadvantage that the stress shock waves reflect at the boundaries and return to the soil. This could lead to soil moving up or lowering of the final penetration depth when the stress wave returns to the surface. So, the vertical stresses at multiple locations are checked in the 2D simulation of Figure 6.1. Those 4 locations are shown in Figure 6.18. Only the vertical stresses are analyzed, because they have the most impact the final penetration depth. The highest point is a depth of 12.1 meters below the impact, this is rather low, a higher point could provide more information. However, these points have been analyzed as well and gave too many fluctuations in the stress in order to extract information from it. The lowest point is just 2.8 m above the reflecting boundary.

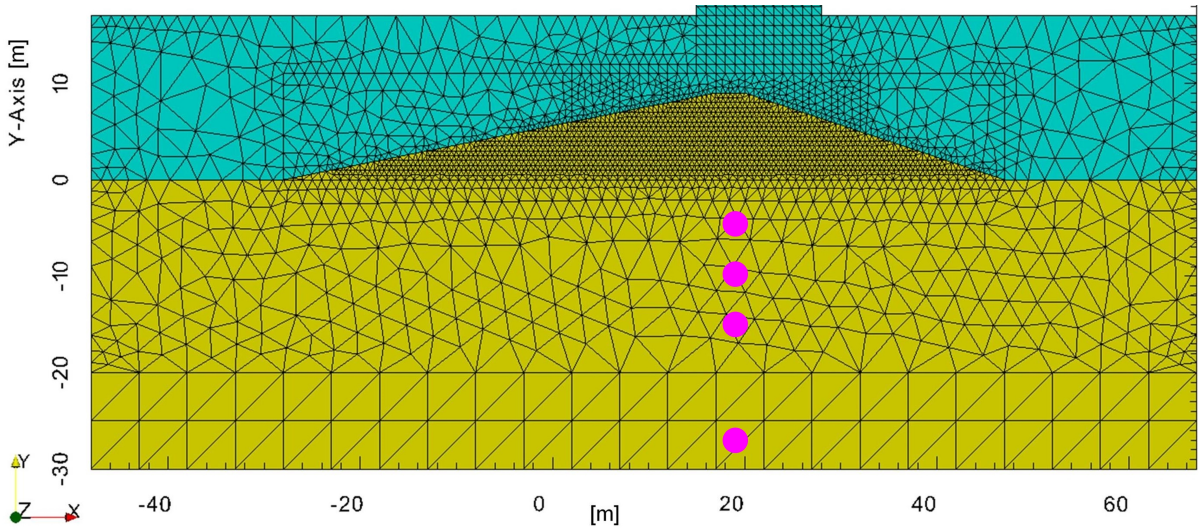

Figure 6.18: Location of the material points for the reflecting boundaries analysis

In Figure 6.19 the vertical stress caused by the impact are shown. The vertical stress is corrected with the initial stress, this normalization is used to show the effect of shock wave. So, the effect of the shock wave is shown, therefore all stresses start at 0 kN/m^2 in Figure 6.19.

In the figure the maximum stress decreases for larger depths. This is due to the fact that the stress spreads in 2 dimensions. When the stress reaches the lowest of the 4 material points, 2.5 meters above the reflecting boundary (37.2 meters below the impact), a near perfect wave shape is recognizable between 0.25 s and 0.65 s. So, the reflecting boundary does what it is meant for. The wave is moving up again which can be seen when the stresses increase positively around 0.6 seconds.

The theoretical time for the shock wave to return to the surface can be calculated with Equation 5.2. The soil has a total height of 38.6 meters at the start of the impact, this leads to 0.7 seconds for the shock wave to return. This can be seen in Figure 6.19. At around 0.7 seconds in the graph the soil might move up gain. Although the stresses are only a fraction of the ones which were present at the impact. At impact the vertical stresses are at maximum over 2000 kN/m^2 (value cannot be obtained from Figure 6.19), the returning absolute difference of the stress is below 500 kN/m^2. This value can be obtained if the difference is taken of the blue curve between the minimum and maximum between 0.6 and 0.8 seconds. No significant change of the penetration depth can be seen in the graph around 0.7 seconds after impact in the 2D simulation of Figure 6.16.

In the Mohr-Coulomb material model tensile stresses cannot occur, in the figure it can seem that these tensile stresses do occur. However, this is not the case, as the graph is normalized for effective stresses. The tension cut-off which is present in the Mohr-Coulomb model is visible is

the blue line at 0.75 seconds. The line is horizontal for a short time, at that time the effective stress is 0. The soil will be moving up there slightly probably.

In this reflecting boundary analysis only the vertical stresses are used. The horizontal stresses are lower, because the impact is vertical. In addition, the distance to the vertical horizontal boundaries, which reflect the horizontal stresses, is specially chosen at a distance from the impact similar to the horizontal bottom boundary. This can be seen in Figure 6.18.

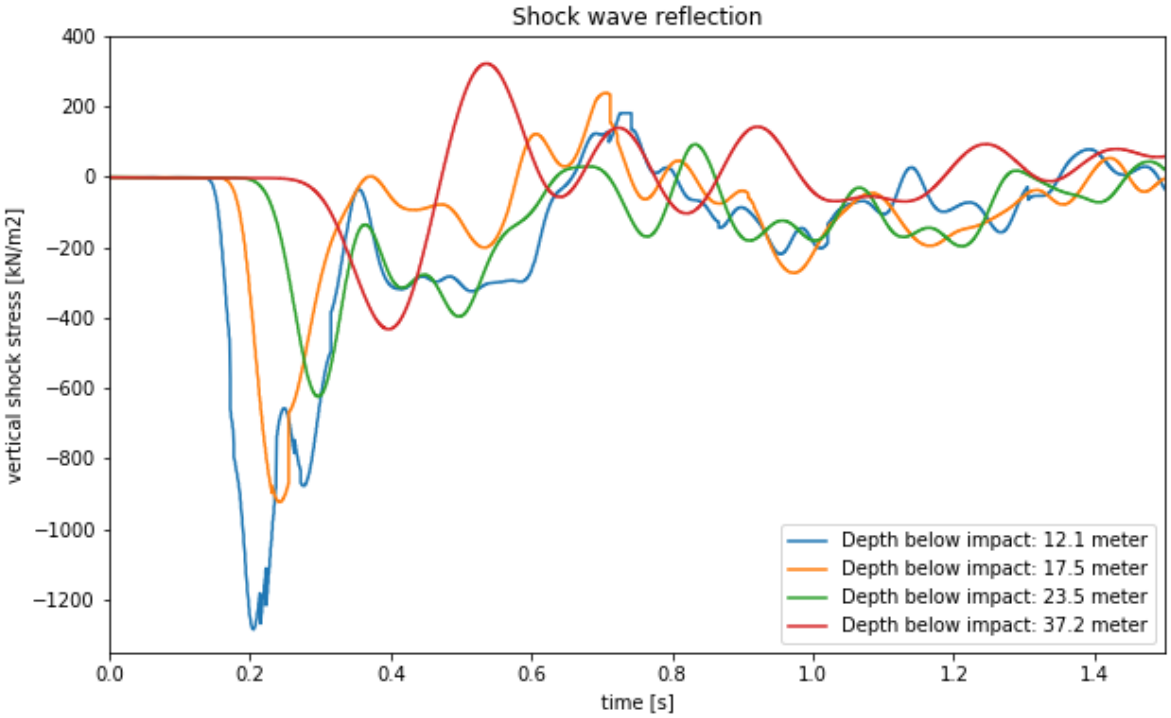

Figure 6.19: Shock wave reflection

6.5.3 Impact on a slope

Instead of the nacelle hitting the crest of the dike, it can hit the slope as well. In Figure 6.20 the box shaped mass falls on the upper part of the inner slope of the dike. The clear red material points show displacements rightwards of larger than 0.3 meter. The sliding plane due to instability of the slope can be recognized. The sliding plane is at the locations where the horizontal displacement is between 0.0 and 0.3 meter, the orange part in the figure. The instability of the inner slope is an important failure mechanism of the dike. In Figure 6.20 the slope is stable after the impact, so no dynamic failure occurs with this dry dike. However, if the slope is steeper and the dike is partly saturated, which is often the case in reality, the dike has a higher probability of becoming unstable.

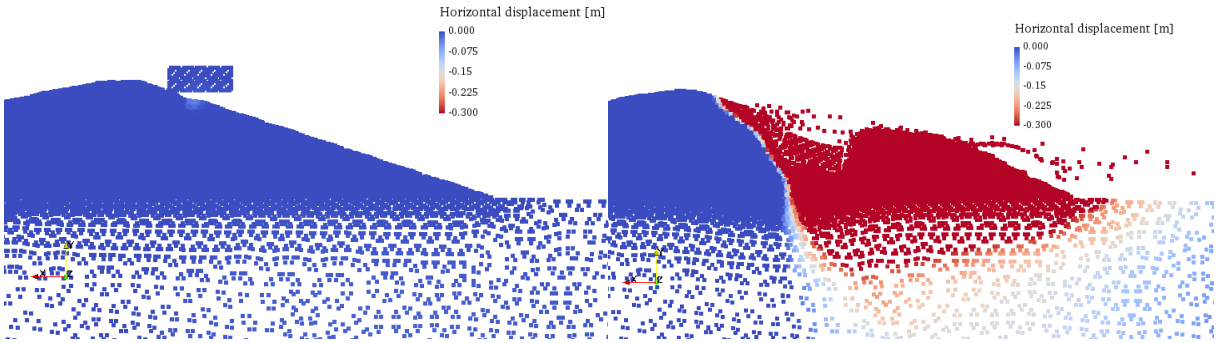

Figure 6.20: Horizontal displacement

Normally when indicating sliding planes, the plastic shear strain is presented. In this case, a figure of the plastic shear strain is trivial. Almost all strain in the simulations is plastic deformation, only a small part is elastic deformation. Due to the impact, there is already a large amount of material around the impact which deforms. The strain of the soil around the impact is much larger than the soil at the sliding circle. Therefore presenting the shear strain has no additional value. The horizontal displacements of Figure 6.20 show the sliding circle clearly.

The crest is damaged, however the residual profile still contains a small part of the crest. Due to the penetration, in the crater very steep slopes arise. The nacelle in the crater prevents the slopes from sliding down. The real shape of the nacelle is important in this process, as the shape of the nacelle determines if sliding in the crater can occur.

It is recommended for further studies to look deeper into impacts on the slope of the dike, especially the dynamic sliding and saturated soil are important to research.

6.6 Comparison with other models

The penetration depths of the other models for determining the penetration depth from Chapter 4 are compared with the MPM penetration depth in Figure 6.21. The parameters used in the other models are similar to the ones used in the MPM simulation. Only for the MPM simulation a dike profile is used, for the other models a horizontal profile is used, which limits the penetration depth.

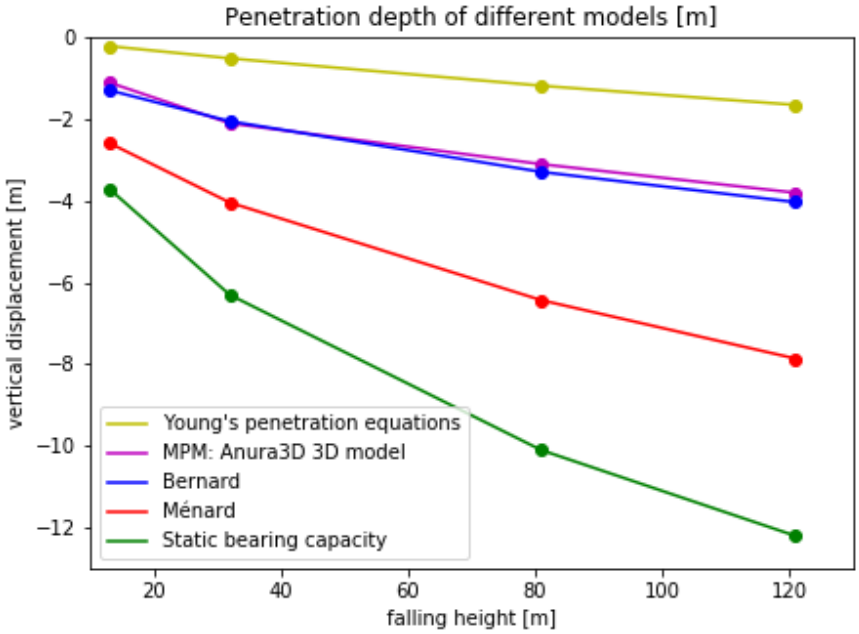

Figure 6.21: MPM compared with other models

The Young's penetration equations do not show the same trend which is present at all the other models: a penetration which flattens if the falling height increases. It is also the only model which underestimates the penetration depth significantly compared to MPM.

The model of the Static bearing capacity overestimates the penetration depth by a factor 3. This model is very different from the MPM and uses other parameters as an input. It is the only model which is not developed for penetration estimations at all.

It seems the Ménard model overestimates the penetration depth as well. This model is only valid for much smaller masses and much smaller penetrations. If the penetration increases, the resistance of the soil increases, so, at the surface there is relatively less resistance and the model is probably more suitable.

The penetration depth of the Bernard model is similar to the MPM simulation, it follows the MPM-plot surprisingly well. Almost all variables used in MPM, are used in the Bernard formulas as well. It is not recommended to use Bernard as verification for the MPM, as stated in Chapter 4: the data it is based on situations with masses and impact velocities of another order. The link between the Bernard formulas and MPM model is interesting to research. Varying the parameters in both formulas can give more insight on the similarities and difference between the two models.

6.7 Conclusion

The Material Point Method turns out to be a good method to determine the size and depth of a crater. The nacelle of the Enercon E-126 turbine can cause at maximum a penetration depth of 3.8 meters on a dry sea dike consisting of sand. There are two impact locations on the dike which can be distinguished: an impact on the crest and an impact on the slope. If the impact is on the crest, both the crest is and large parts of both slopes are affected. The soil below the slopes is lifted up, this causes the revetment to lose its coherence. An impact on the slope will mainly affect the slope and the crest is only limited affected. However, the size and depth of the crater depend largely on the soil characteristics and the potential energy of the nacelle. Those are taken conservative in the model. So, the penetration depth of 3.8 meters is the maximum.

The sensitivity analysis shows that the governing parameters are the impact velocity, the mass of the penetrating object, the stiffness of the soil and the angle of internal friction of the soil. 3D models are preferred over 2D models for determining the penetration depth. There are large 3D effects which are not covered when using 2D models. At last, a saturated dike will probably cause a deeper crater, because the effective stresses are lower compared to a dry dike, this scenario is not considered in this report.

Chapter 7

Impact on dike failure probability

7.1 Introduction

The focus of this chapter is on the results of the research which is performed in the previous chapters: the crater caused by a nacelle impact. In Chapter 6 'Analysis of simulation results' the residual profiles after the impact by a nacelle are presented. These residual profiles provide less flood protection than the original profile. The effect of those residual profiles on the additional failure probability of a dike is analyzed in this chapter.

The assessment in this chapter is based on the method currently used for assessing wind turbines near flood defences. This assessment of the additional failure probability of a dike by a nacelle impact covers only a part of a total flood protection assessment, as only the additional failure probability caused by a nacelle impact is determined. The analogy for hitting probabilities for falling wind turbine blades and towers would be similar to the nacelle impact.

7.1.1 Case study

The dike which is used in this flood protection assessment is the same as in the MPM simulations: The dike is based on a dike in the north of Groningen at the Wadden Sea. The geometrical characteristics are shown in Figure 7.1. The outer slope consists of an asphalt revetment at the lower part of the slope and a grass revetment higher on the slope.

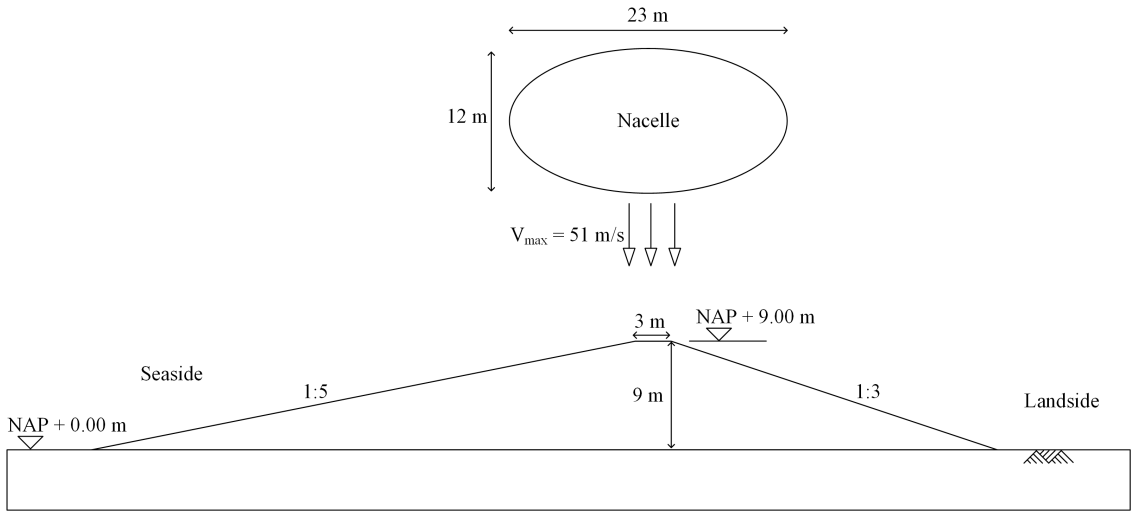

Figure 7.1: Dike profile with the Enercon E-126 nacelle falling down

The same wind turbine is used: the Enercon E-126. The most important characteristics in

this assessment are the hub height of 135 meter, rotor diameter of 127 meters and nacelle mass of 568 tonnes. The center of the wind turbine is place 20 meters from the toe of the dike. The base of the turbine has a radius of 11.5 meters and concrete foundation will be place around the base as well. So, 20 meters is the minimum distance to build this wind turbine near a dike, if a smaller distance is used, it will be technically in the flood defence, which is not within the scope of this thesis.

In the MPM simulations the dike consists purely of medium dense sand. This is the material in the core of the dike, where most of the deformation takes place. The soil profile is different in this assessment than in the MPM model. In reality the soil is layered, so also layered soil is used in the assessment. Another component that is not included in the MPM simulations is a phreatic line. For stability calculations a phreatic line is realistic, so it is incorporated in these calculations.

7.1.2 Advice Expertise Network for Flood Protection

An option for the assessment of the flood defence is given by Expertise Network for Flood Protection (ENW) (ENW, 2014): The additional failure probability of the wind turbines on the flood defence should be negligible small. This can be interpreted as: the maximal permissible additional failure probability of the wind turbine(s) can be:

- 1% of the permissible failure probability per cross-section per failure mechanism.
- 10% of the maximum permissible failure probability on segment level for all NWO's together.

The NWO's are wind turbines in this case. The first requirement is used for one wind turbine and the second for all wind turbines within a segment. At this moment in all failure probability assessments and flood protection assessments, this is the rule of thumb used and therefore it is used in this thesis as well. In the future it might change, because this rule of thumb is only an advice and not part of the WBI2017. At the moment not all water authorities use the policy described above.

7.2 Procedure additional failure probability assessment

7.2.1 Introduction

The procedure used to assess the failure probability of a dike by a wind turbine failure is as follows:

1. Define the safety standard for the flood defence
2. Determine the failure probability of a wind turbine
3. Determine the probability of hitting the flood defence by a nacelle
4. Determine the probability of governing hydraulic loads during a wind turbine failure
5. Determine the damage of the impact by a nacelle
6. Determine the probability of the failure mechanism by the damage caused by a nacelle
7. Compare failure probability of the flood defence with the safety standard

7.2.2 Maximum permissible additional failure probability

The system for the flood protection assessment in this thesis is based on WBI2017. However it is impossible to completely follow the WBI2017 due to limited time, therefore several simplifications are used.

The safety standard consists out of 2 values: the lower threshold value and alert value. For determining the additional failure probability the lower threshold value should be used: 1/1000 per year for segment 6-6, which is the segment at the location of the case study. The alert value is 1/3000 per year, however, it is not needed to use this value, because a wind turbine is not a permanent object and therefore should not be designed as one. The lifetime is of a wind turbine is only around 20 years. The purpose of the alert value is to indicate near future reinforcements.

The safety standard is divided in required failure probabilities (faalkanseis) for each failure mechanisms. This method to divide the safety standard is named failure probability budget division. The default failure probability budget is prescribed, but it can also be tweaked as long as the sum of the failure probability budget factor does not exceed 1 and the same division is used in a segment. Here the standard failure probability budget division is used. This is also the economic the best option according to VNK 2 (KPR, 2016).

Length effect

To determine the required failure probability per failure mechanism, the budget factors per section should be used together with Equation 7.1.

$$P_{req,cs} = \frac{\omega \cdot P_{req}}{N_{cs}} \tag{7.1}$$

$$N_{cs} = 1 + \frac{a_l \cdot L_{segment}}{b_l} \tag{7.2}$$

Where: $P_{req,cs}$ is the required failure probability per cross-section, ω is the failure probability budget factor for a certain assessment track, P_{req} is the safety standard, in this case the lower threshold value, per dike segment, N_{cs} is the length effect factor for a cross-section, a_l is the mechanism-sensitive fraction of the dike segment, b_l is a measure for the intensity of the length effect within the mechanism-sensitive length of the dike segment.

The length effect is created to cope with variability of strength within a dike segment (ENW, 2016). Determining the real strength of a dike for every meter would be a very costly operation, so an estimation is made for sections of the dike. The weakest spot is not known and the strength at that location neither. The geotechnical failure mechanisms macro-instability and piping have a large length effect, due to the high variability in the soil parameters. Mechanisms which are correlated to the hydraulic loads have a small length effect, because they are mostly correlated to the water level and waves, which are similar along the segment. For the length effect factor N_{cs} for macro-instability, Equation 7.2 should be used.

Failure probabilities per mechanism

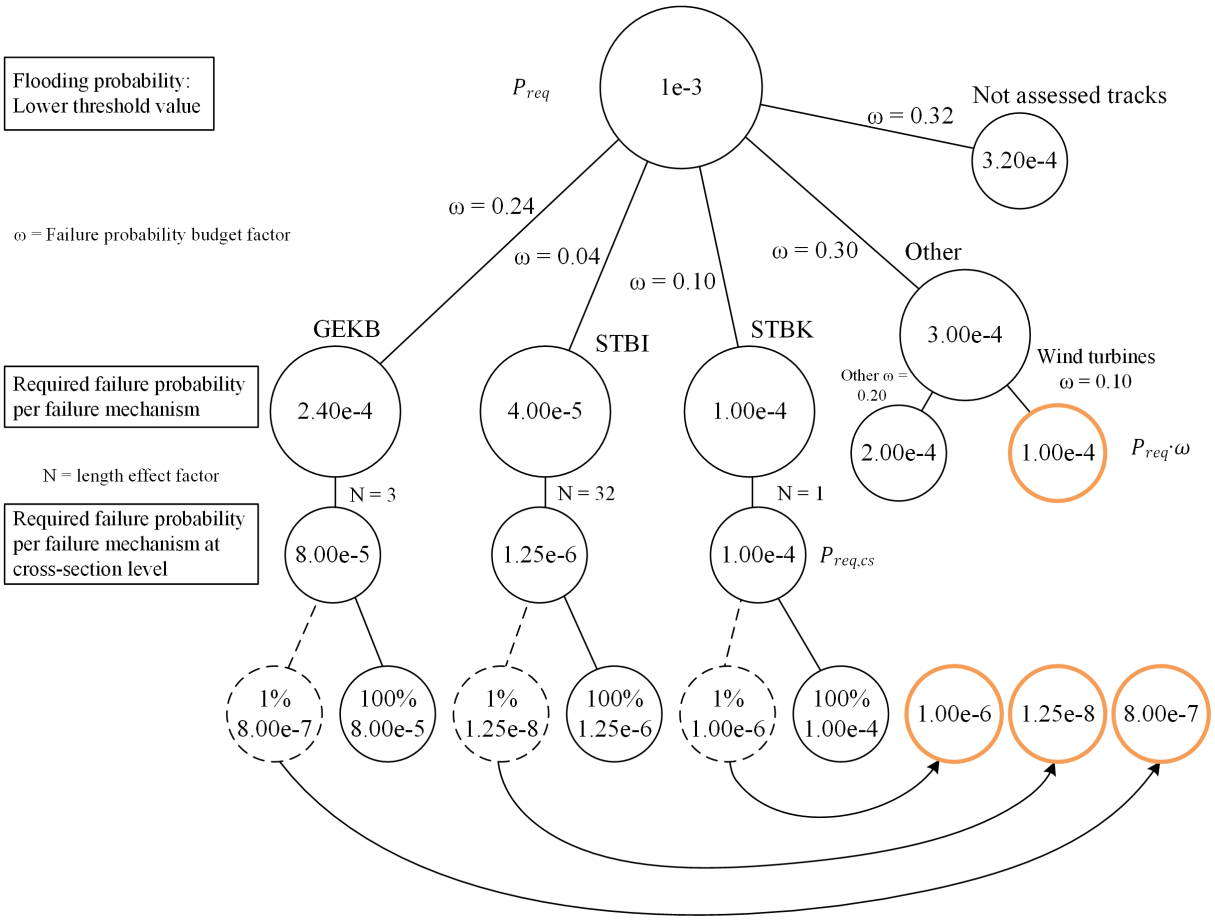

Figure 7.2: Failure probabilities per failure mechanism at cross-section level

In Figure 7.2 it is shown how the maximum permissible additional failure probability can be calculated. The figure is complex, as the system is complex, the elaboration of the figure will take the rest of this subsection and the next subsection.

Figure 7.2 starts with the safety standard or flood probability, which is 1/1000 per year at the location of the case study. This safety standard is divided by the failure probability budget factors in required failure probabilities per failure mechanism. To obtain the required failure probability per failure mechanism at cross-section level the length effect factor is used. This 100% value is used in assessing the dike in case there is no wind turbine. The 1% part is explained in the next subsection.

In this assessment only three assessment tracks are used: GEKB, STBI and STBK. GEKB is an abbreviation for Grass revetment erosion crest and inner slope, also known as overtopping and overflow. The inner slope macro-instability (STBI) is assessed as well. The assessment tracks Grass erosion of the outer slope (GEBU) and other revetment outer slope are assessed together with a failure probability budget factor of 0.10 under the name STBK. The effect of a wind turbine part hitting the outer revetment will be similar for the different revetments, therefore the failure probability budget factors are summed up. The other mechanisms are not assessed quantitatively, because it is assumed that the additional failure probability of an impact on a dike is negligible.

In Figure 7.2 the failure probabilities per mechanism at cross-section level are given for this case. The length effect factor N is 3 for GEKB, this is segment dependent. For STBI the value is

calculated with Equation 7.2: a_l is 0.033, b_l is 50 meters and L is 46.1 kilometers, this gives a N of 32, for STBK this factor is 1. This value of 1 is rather low, this implies that the revetment has hardly any variability in the strength and the hydraulic loads are very similar along the segment. The same holds for the length effect factor for GEKB.

7.2.3 Converting ENW advice to probabilities

The maximum permissible additional failure probability of the dike by a wind turbine is determined with the safety standard, not the actual strength of the dike. In the introduction of this chapter the requirement for the additional failure probability for 1 turbine is given:

- 1% of the permissible failure probability per cross-section per failure mechanism.

The 1% is taken from the 100% required failure probability per failure mechanism at cross-section level. This implies that the total is 101% for each of the three mechanisms. Next, this 1% (dashed circle) is moved to the 'other' assessment track, so the GEKB, STBI and STBK tracks will not exceed the 100% value.

For the failure mechanisms assessed in the assessment, the maximum permissible additional failure probability per wind turbine can be found in Table 7.1 and Figure 7.2. In the next section the actual additional failure probability is calculated for the three mechanisms described. If the value of each mechanism is lower than the 1% value, the wind turbine passed this requirement.

The other requirement from the ENW is:

- 10% of the maximum permissible failure probability on segment level for all NWO's together.

In different words this requirement means that 10% of the occasions that a dike segment fails, it is caused by a wind turbine failure. This requirement depends strongly on the number of the turbines near the flood defence. This is not a problem at first sight, however, for this segment 6-6, which has a length of 46.1 km, there will be a maximum number of turbines near this flood defence.

Table 7.1: Maximum permissible additional failure probability per failure mechanism per wind turbine

Assessment track	**Required failure probability per failure mechanism at cross-section level, 100%**	**Maximum permissible failure probability per wind turbine, 1%**
Grass revetment erosion crest and inner slope (GEKB)	$8.00 \cdot 10^{-5}$	$8.00 \cdot 10^{-7}$
Macro-instability inner slope (STBI)	$1.25 \cdot 10^{-6}$	$1.25 \cdot 10^{-8}$
Revetment failure outer slope (STBK)	$1.00 \cdot 10^{-4}$	$1.00 \cdot 10^{-6}$

In Figure 7.2 it is shown that 10% maximum permissible failure probability on segment level is $1.00 \cdot 10^{-4}$ per year. This is the sum of the maximum permissible additional failure probability of the three mechanisms of all wind turbines together. Again, with the assumption that the other mechanisms, next to the three which are mentioned, have a negligible failure probability. However, there is discussion on the method to obtain this 10%. Because the 10% is on segment level and it is 'filled' with the requirements which are at cross-section level. To go from the cross-section level to segment level is a gray area or white spot. The concerns are: there can be two turbines in one cross-section and not at all cross-sections contain wind turbines. Choosing the right coupling between those maximal permissible failure probabilities is complicated and not in the scope of this thesis. In addition, if the 1% requirement is satisfied for each mechanism, this would imply for segment 6-6 that at least 55 wind turbines can be built near this flood defence (concerning flood protection and only the nacelle impact used). So, it is advised to do more research on this topic.

This is the end of the first step in the assessment procedure of Subsection 7.2.1.

7.3 Probability of possibility of repair

The maximum permissible additional failure probability per mechanism has been determined. Now the actual additional failure probability should be determined. This is performed for every scenario: per failure type (tower and nacelle failure), per hitting zone and per assessment track. This actual additional failure probability of an assessment track is calculated with:

$$P_{f,cs} = P_{f,WT} \cdot P_{hitting|f,wt} \cdot P_{FM|hit} \cdot P_{flooding|FM} \tag{7.3}$$

Where $P_{f,cs}$ is the actual additional failure probability of an assessment track at cross-section level, $P_{f,WT}$ is the failure probability of a wind turbine failure, $P_{(hitting|f,wt)}$ is the hitting probability of wind turbine given a wind turbine failure, $P_{(FM|hit)}$ is the failure probability of failure mechanism given a flood defence has been hit by a wind turbine part, $P_{(flooding|FM)}$ is the flooding probability given a failure of a flood defence.

In this section the method to determine $P_{(flooding|FM)}$ will be elaborated. The value itself differs per hitting zone and per assessment track. In this value the causes of wind turbine failures, residual profile and repair time are incorporated.

Types of dikes

As mentioned in Chapter 2, there are multiple possible causes for a wind turbine failure. The most common ones are: a storm, a fire and a lack of maintenance. It depends on the flood defence which causes are relevant for flood defences. In this section three types of dikes are distinguished:

- Sea dikes, which have a residual profile after an impact and can still protect the land against a flood in daily conditions.
- Lake dikes, which have no residual profile after an impact.
- Large river dikes

In Figure 7.3 the consequences of a failure of three types of dikes are shown.

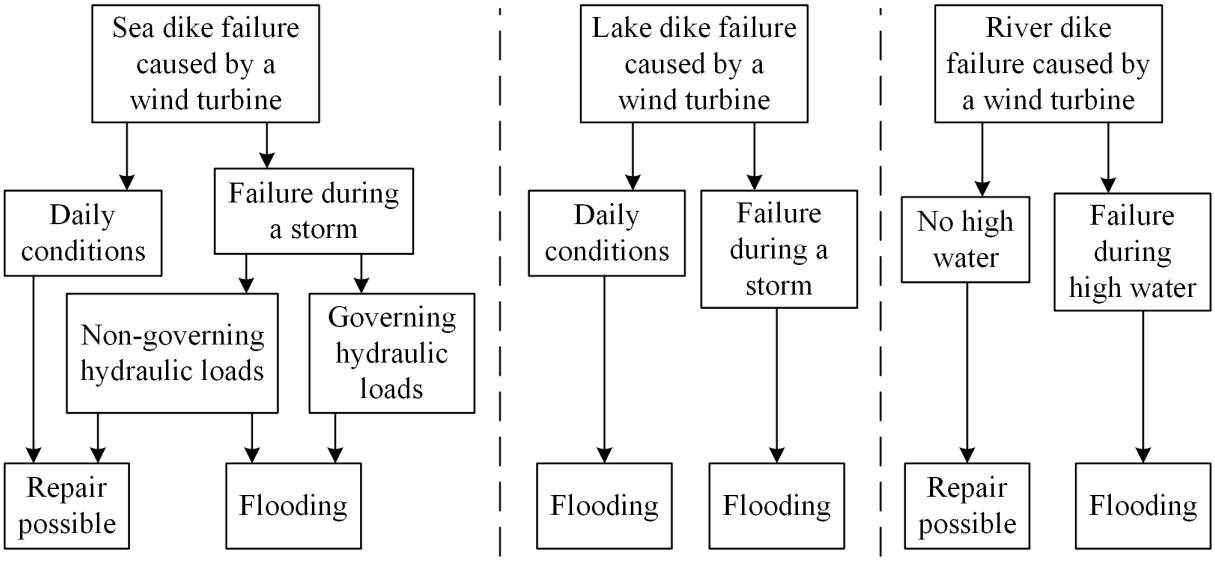

Figure 7.3: Consequences after a failure of three types of dikes

Sea dike

This dike is usually larger than a lake dike. This is because the water level varies more at sea, due to the tide and longer fetch lengths at seas.

If the cause of the wind turbine failure is fire or a lack of maintenance, then the cause of the failure is independent of the presence of a storm, so the failure is during daily conditions. For governing hydraulic loads the presence of a storm is a requirement. The residual profile of a flood defence will be large enough to protect the land during daily conditions, the exact residual profile of the case study is elaborated in Section 7.4. Therefore, in Figure 7.3 the result at daily conditions is 'repair possible'. One could argue that after normal conditions there still can be a storm. If a wind turbine has fallen over or the nacelle with the blades has fallen down, the water authorities will be warned right away. They can repair the dike immediately or later, depending on the severity of the storm which is coming, more is explained later in this section on this subject. This scenario is the lower boundary of the failure probability: $P_{(flooding|FM)} = 0$.

If the failure of a wind turbine is during a storm where the governing hydraulic conditions are present as well, then there will be an immediate flooding. This is the upper boundary of the failure probability: $P_{(flooding|FM)} = 1$. The wind turbine failure is caused by the storm, however it is unknown to which hydraulic loading level this storm will lead. The hydraulic loading level is the height of a dike to prevent a certain amount of overtopping. This storm - hydraulic loading level relation is a gray area in the assessment. The storm can lead to governing hydraulic loads. However, the correlation between a storm and (near) governing hydraulic loads differs per location and is weak. It is weak at the Wadden Sea in Groningen. At other locations with constant high water, at lakes for example, this relation is very strong. An example: in the last 108 years in the Netherlands, there have been 15 storms with the same or stronger wind gusts than the 1953 storm (KNMI, 2017).

So, the correlation between a wind turbine failure and a storm that causes significant hydraulic loads should be determined. The upper and lower boundaries have already been determined, the reality is in between. Later in this section the values used in the assessment are elaborated.

Lake dike

Lake dikes are lower than sea dikes. At a lake dike with polders there is always high water and a failure of a dike by a wind turbine failure will lead to flooding immediately. So, the cause of the wind turbine failure and repair time are irrelevant. However, a smaller dike has advantages, because the hitting zones are smaller and therefore hitting probabilities are lower.

Large river dike

In Figure 7.3 the river dike described is one on the major rivers in the Netherlands. The high water usually last for several weeks at rivers. At normal conditions or at non-high water conditions the dike has no water against it. So, there cannot be a flooding during daily conditions. If this do is the case, it can be seen as constant high water, similar to a lake, and there will probably a flooding, if the dike has not a very large residual profile. So, if there is no foreland on a river dike, it can be seen as dike with constant high water in this figure.

Repair time

In case there is no immediate flooding after a failure of the dike, then the dike can be repaired. The restoration or repair should be finished before a certain hydraulic loading level is reached, which can lead to a flooding if only the residual profile is present. The average repair time differs per failure mechanism. A nacelle is a large heavy object which cannot easily be moved by any crane, special equipment is needed for this. In this assessment the repair time used is 2 weeks for the failure mechanisms GEKB and STBI. For STBK a probability of possibility of repair is used, this is 90% for a failure during daily conditions and 50% during storm conditions.

Next to the repair time, there is a noticing time as well for failure of NWO's. For a wind turbine failure the noticing time is assumed to be negligible short, because the failure of the wind turbine can be seen at the flood defence itself as at the wind turbine as well.

The storm season is an important factor in using the repair time in an assessment. If a failure of the dike is not in the storm season, the probability of flooding will be significantly lower. The probability of a significant hydraulic loading level which is higher than the residual profile is negligible outside the storm season. If a failure of the dike is during a storm, this implies that the failure is during the storm season and the probability of a significant hydraulic loading level is important. In this assessment the duration of the storm season is taken as half of a year, from October 1 to April 1.

Probability of flooding given a failure of the dike

A failure of the dike is caused by failure mechanism that has occurred. However, a failure of a dike does not have automatically lead to a flood. Therefore the factor $P_{(flooding|FM)}$ is used. The method described below is only used in this thesis and has several assumptions. The idea behind the method is shown in Figure 7.4.

First of all, it is assumed that half of the failures of wind turbines occur during daily conditions and the other half during storm conditions. This is conservative according to the statistics from Caithness Windfarm are analyzed (RVO, 2014).

If the impact is during daily conditions, the repair time is important. During this period the hydraulic loading level can be reached which is higher than the residual profile. For a profile with a residual height of NAP +5.2 m for example, the return period of this hydraulic loading level is 10 years, see Figure 7.11.

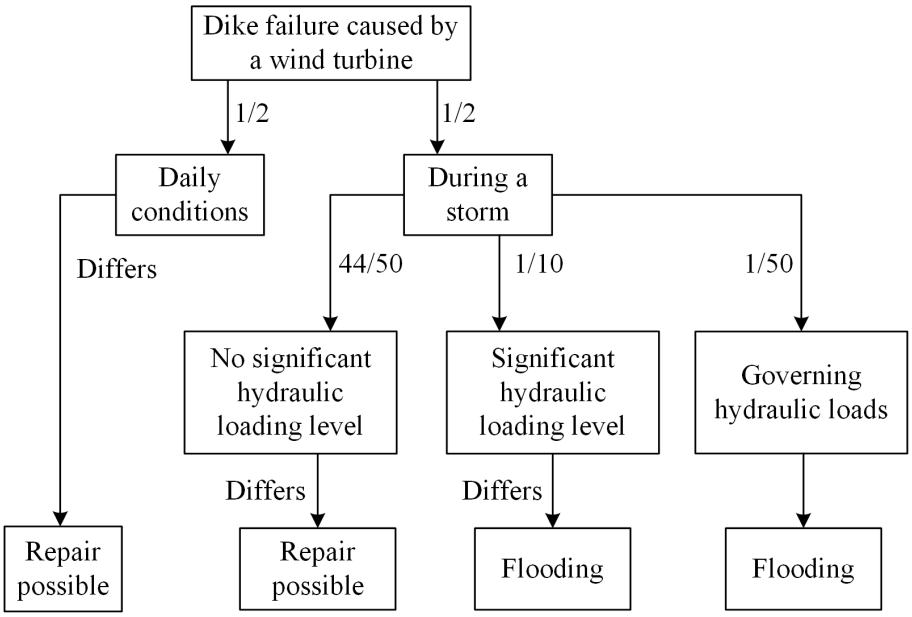

Figure 7.4: Method to determine the $P_{(flooding|FM)}$

For a failure during storm conditions the situation is split into three scenarios: one where the governing hydraulic loads are present, one where a significant hydraulic loading loads are present, but not the governing loads and one where the storm causes no significant hydraulic loading level.

The most important scenario is when the governing hydraulic loads will occur, because, it will immediately lead to a flooding. This probability that these governing hydraulic loads are present in a storm is chosen as 1 in 50 storms where a wind turbine can fail. This value is chosen for the following reason. There were in the past 108 years 15 storms which were stronger than the 1953 storm (KNMI, 2017). The 1953 storm caused by far the highest hydraulic loading level in 108 years, its return period is 300 years. The governing hydraulic loads in the case study have a return period of 1250 years, see Figure 7.11. Assuming that at least a storm which caused the 1953 flooding is needed for causing the return period of 1250 years, the probability that a storm which causes the wind turbine failure and governing hydraulic loading level is 15/1250 or 1/83. So, 1/50 which is used in this case study is conservative. However, the relation between a storm and hydraulic conditions differs per location. In this analysis the relation is assumed the same for Zeeland and Groningen.

If the storm causes a water level set-up and waves, the significant hydraulic loading level can be reached, the probability of this is assumed to be 1/10 per storm. This significant hydraulic loading level does not always reaches the level of the residual profile, therefore in Figure 7.4 it is named 'Differs'.

The last scenario is when no significant hydraulic loading level will be reached. This is when the storm does not cause a water level set-up or waves at a significant level for example. The wind turbine can fail in any storm, it has no relation with the hydraulic conditions. This holds for example for every storm not coming from the north-west in this case study. Therefore, a rather large part of probability goes to this scenario.

7.4 Results of wind turbine failures on the flood defence

7.4.1 Failure probability of a wind turbine

In Section 2.4 this subject is treated more in detail. The water authorities use the 'Handboek Risicozonering Windturbines' as the source for the failure probability which fits their conservative philosophy. The failure probabilities of wind turbines of the latest, 2014 v3.1, are used in this assessment. There are three types of failures to distinguish: Falling of nacelle and/or rotor, Falling over of wind turbine/ tower failure, Falling of a blade/ blade failure. Falling of the tower implies falling of the nacelle. In the first two the nacelle is falling, so those are the 2 scenarios used. Falling of a blade is not considered in this failure assessment, however, it described how this can be incorporated in Chapter 8 'Conclusions & Recommendations'.

The failure frequencies of wind turbines can be found in Table 7.2. The Ministry of Infrastructure and the Environment decided the 95% reliability percentile should be used in flood protection assessments (RVO, 2014), which are as double as high as the mean values.

Table 7.2: Failure frequencies per turbine per year

Scenario	Mean value	95% reliability percentile
Falling of nacelle	$1.8 \cdot 10^{-5}$	$4.0 \cdot 10^{-5}$
Tower falling over	$5.8 \cdot 10^{-5}$	$1.3 \cdot 10^{-4}$

7.4.2 Hitting zones

Here step 3 of the procedure starts. The hitting zones are the zones where nacelle can land where in it affects the failure mechanisms.

Influence zones have been described in short in Chapter 2. For the specific dike with the three failure mechanisms/ assessment tracks which are considered in this flood protection assessment 4 zones are distinguished. If piping would be considered quantitatively, there should be an extra zone added on the inner side.

The 4 hitting zones are shown in Figure 7.5, the figure is schematic, not on scale. Zone A covers the whole outer slope, which has a horizontal width of 45 meter. The crest has a width of 3 meters and can be recognized by the blue color. The inner slope is divided in 2 zones, for the sake of inner slope-instability. If the nacelle lands in the lower part of the inner slope, the failure mechanism macro-instability inner slope is less affected. The mass of the nacelle is high and this will contribute to the resistance against sliding if it rests on the soil in the resistance part of the profile. An impact in zone C do can contribute to a failure of the inner slope.

Next to those 4 zones, an extra zone is used. This is zone B+ which can replace zone B, it consists out of the crest with 5 meters added on both sides. So, the total width is 13 meters and it overlaps zone A and C slightly. This extra zone is used for the GEKB assessment track. If the center of gravity impacts slightly next to the crest, it will still impact the crest, as the penetration is bowl shaped. So, if the impact is slightly next to the crest, it has the same effect as an impact on the crest in fact.

7.4.3 Hitting probabilities of the hitting zones

The HRW describes how to the probability or frequencies of the hitting zones can be described. Determining the hitting zone can be performed very detailed with probability density functions and different center of gravity of objects. If a very detailed analysis is performed, the results will still be similar to a simple analysis, therefore the analysis is kept simple.

When only the nacelle falls down, maximal falling distance is 1/2 times the rotor diameter. The probability of falling at a location within the risk contour is taken equal at every location.

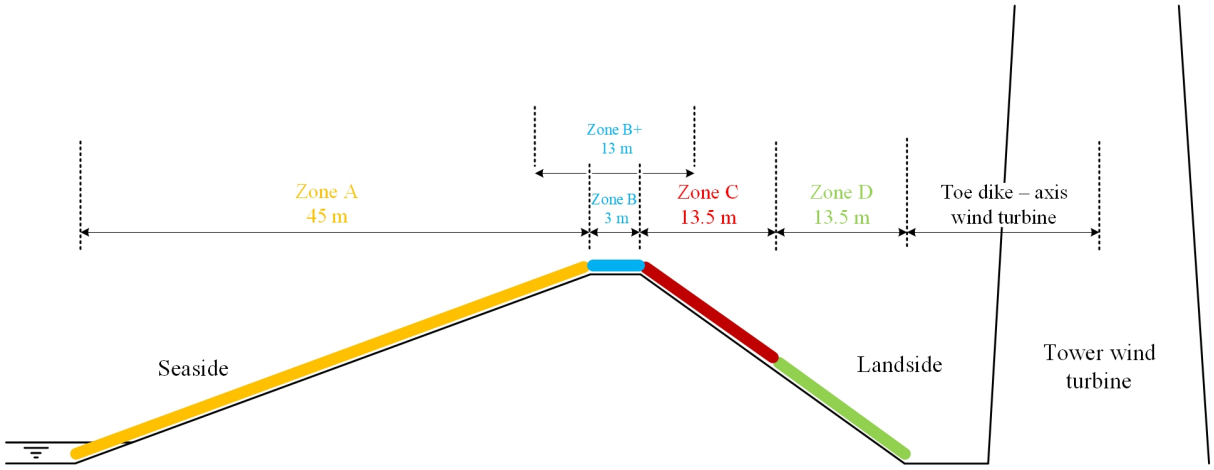

Figure 7.5: Hitting zones of the dike

The scenario of the tower falling over is more complicated. Most probably the tower falls over (almost) completely caused by a failure at the base of the tower. If this is the case, the nacelle will land at distance of the tower height from the base. However, it is possible that the tower buckles halfway the tower. Then the nacelle will fall anywhere between the base of the wind turbine and the maximum hitting distance. This maximum hitting distance depends on the foundation height, width of the tower at the base, hub height and height of the nacelle.

The nacelle will cause much more damage than a tower itself can do: it has a higher concentrated mass and higher falling velocity. So, the tower itself will cause a much smaller crater which is probably almost negligible compared to the crater of a nacelle. However the tower can seriously damage revetments, so this is taken into account in this flood protection assessment.

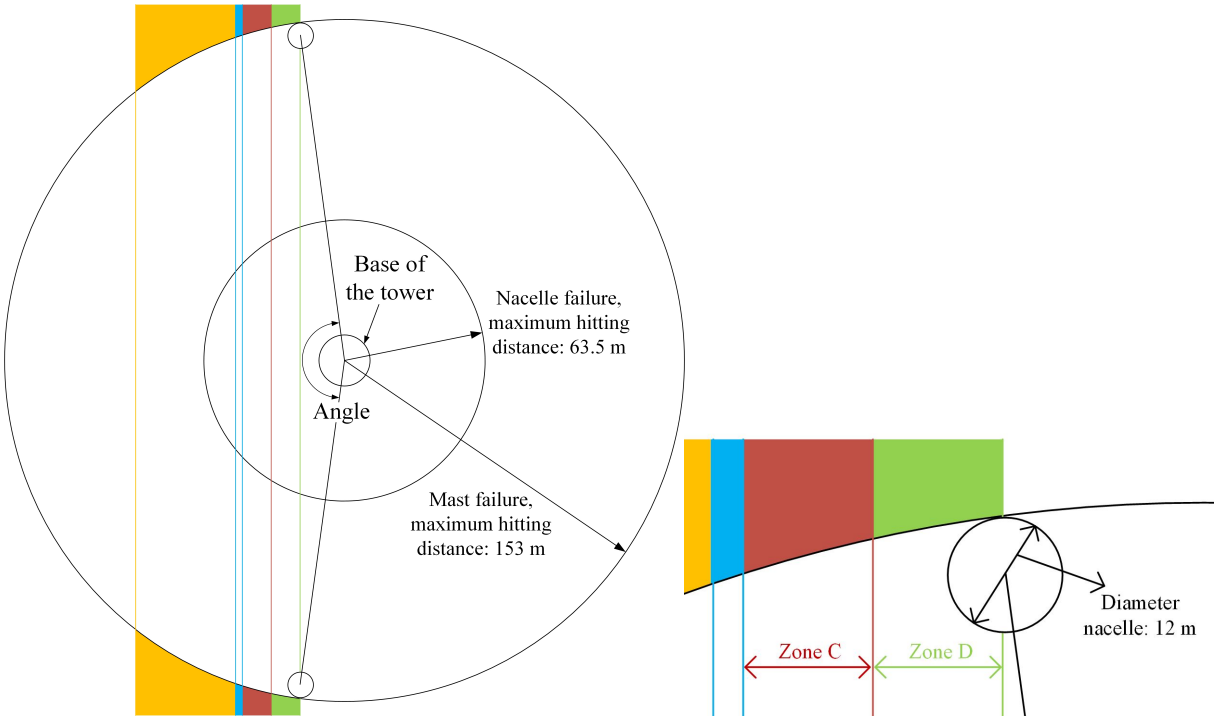

Figure 7.6: Risk contour for the tower falling over with the nacelle hitting zone D

In Figure 7.6 the risk contour of the wind turbine completely falling over is shown. This figure is on scale, with the axis of the wind turbine at a distance of 20 meters from the toe of

the dike. The angle will become smaller if the turbine is placed further from the toe. However if the location of the wind turbine is changed from 20 to 40 meters from toe, for most hitting zones there will be hardly any change in the hitting probability. In the scenario where only the nacelle falls down, moving the turbine further away has a larger impact.

In Table 7.3 the hitting probabilities are given. These values are the probability that the center of gravity of the nacelle hits a zone, given a failure.

Table 7.3: Probability of hitting a zone of the dike, with the center of the turbine 20 meters from toe

	Only nacelle failure	**Tower failure: only nacelle hits dike**	**Tower failure: tower or nacelle hits dike**
Zone A: Outer slope	$6.38 \cdot 10^{-2}$	$1.69 \cdot 10^{-1}$	-
Zone B: Crest	$1.94 \cdot 10^{-2}$	$1.23 \cdot 10^{-2}$	$3.96 \cdot 10^{-1}$
Zone B+: Crest	$1.03 \cdot 10^{-1}$	$2.99 \cdot 10^{-2}$	$4.07 \cdot 10^{-1}$
Zone C: Upper inner slope	$8.41 \cdot 10^{-2}$	$5.33 \cdot 10^{-2}$	-
Zone D: Lower inner slope	$1.23 \cdot 10^{-1}$	$5.77 \cdot 10^{-2}$	-

7.4.4 Effect of impacts & craters on the dike profile

Impact on the crest

In Chapter 6, the damage by a nacelle on the crest is determined qualitatively and quantitatively, both in 3D. The maximum penetration depth at the crest of the dike can be extracted from Figure 7.7. This depth is presented for multiple falling heights. The maximum falling height of the Enercon E-126 nacelle on a 9 meters high sand dike is around 124 meters. This is very close to the calculated 121 meters falling height, with corrections for limited impact velocity, the penetration depth of 3.8 meters is a good approximation. After lowering the crest height, the nacelle will still lay in the crater. The weight of the nacelle will cause static stresses on the soil.

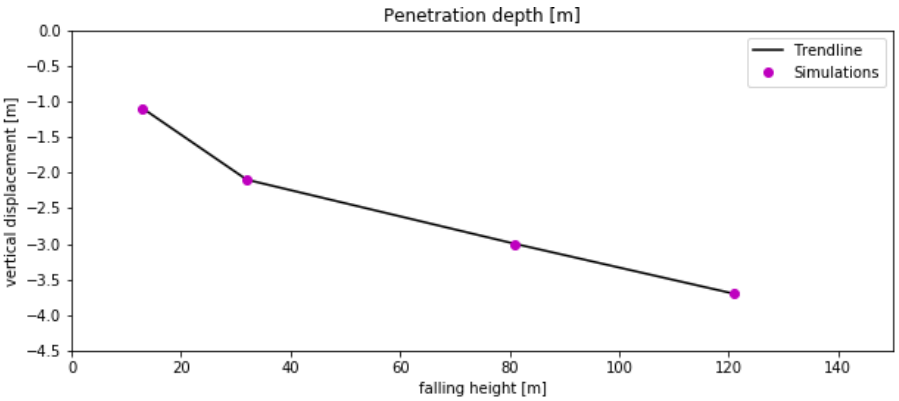

Figure 7.7: Interpolated penetration depths of an impact on the crest

In Figure 7.8 the crest is shown after the impact by a nacelle which fell from the hub at a falling height of 121 meter. The flying material points and nacelle have been removed from the plot. The green line shows where the soil is packed and can be regarded as the surface, the black line shows the dike profile before the impact.

After the impact, the revetment is destroyed as well. It can be assumed that the revetment area which is near the impact is destroyed and cannot fulfill the function of protecting the underlying soil. This holds for grass revetments as for asphalt revetments as well. At block revetments the stones can be pushed out due to the soil below it is moving upwards.

The shock wave which will develop can also cause damage to the dike as it can trigger (indirect) failure mechanisms such as instability of the foreshore. The shock wave can also affect the water pressures and consequently the effective stresses in the soil. In the plots of Figure 7.8 and Figure 7.9 there no sign of macro-instability of the inner or outer slope. So at a completely dry dike no dynamic failure will occur. However, if there was saturated soil, there might be instability, it is recommended to research. More on this is elaborated in Subsection 7.5.4.

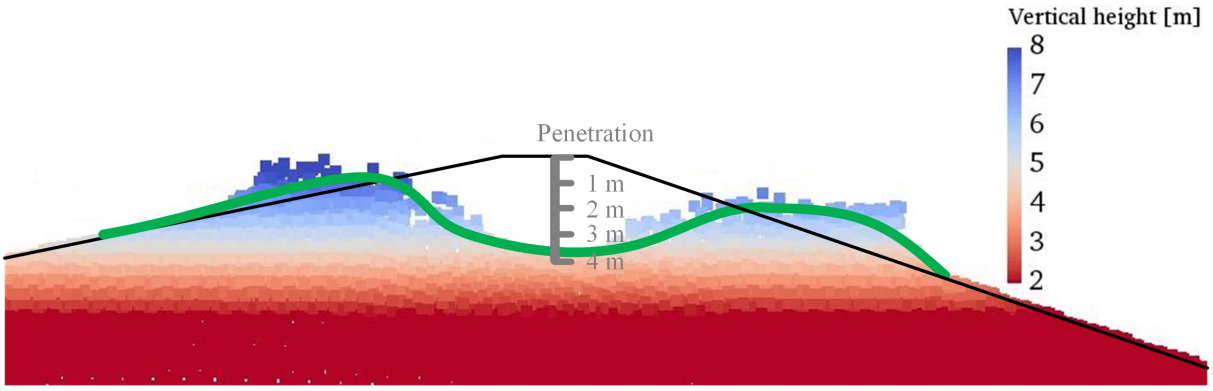

Figure 7.8: Residual profile after an impact at the crest

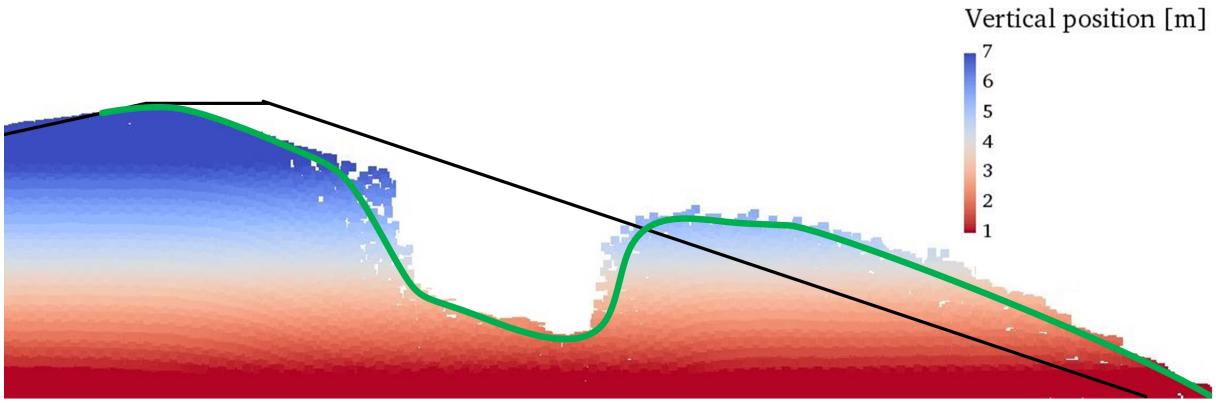

Figure 7.9: Residual profile after an impact at the slope

Impact on inner & outer slope

If the nacelle falls on the inner slope, the 2D simulation on the slope can be used, because it is similar to a 3D simulation with a slightly higher mass, the process which occur are similar, however, the penetration depth differs slightly. The shape of the crater after impact is shown in Figure 7.9. The nacelle of 5 meters in width has fallen 1 meter from the crest at the inner slope. The effect on the outer slope of an impact at the inner slope is negligible. But the crest do is lowered slightly, so the revetment on the crest has no residual strength. The impact in Figure 7.9 is near the crest, and still it has an effect on the full length of the slope: at the top the crest height is lowered at the inner side, a crater in the middle and soil pushed up below the crater. So at every location of the revetment on the inner slope is destroyed by the impact.

An impact on the outer slope is not simulated, however, the impact on inner slope of Figure 7.9 can give enough information. The inner slope has an inclination of 1:3, the outer slope 1:5. The effect on the outer will be less, so it is conservative to use the information of the impact on the inner slope for the outer slope impact as well.

7.4.5 Summary effects of wind turbine failures on the hitting zones

Table 7.4: Summary effects of wind turbine failures on the hitting zones

	Nacelle impact	**Impact of tower itself**
Zone A	Crater in outer slope Revetment outer slope destroyed Crest destroyed	Does not occur
Zone B/B+	Crater in the crest, Crest is lowered significantly Revetment destroyed at inner and outer slope to the level of penetration	Revetment destroyed on the crest
Zone C	Crater in inner slope Crest revetment destroyed Revetment destroyed at upper part of the inner slope	Does not occur
Zone D	Crest remains intact Crater at the lower part of the inner slope Revetment of the inner slope destroyed	Does not occur

7.5 Assessment per failure mechanism

7.5.1 Erosion crest and inner slope

The erosion of the crest and inner slope is assessed with the maximum overtopping discharge. The maximum overtopping discharge is dependent on multiple factors. Several important are: hydraulic loads, crest level height, steepness of the outer slope and quality of the revetment on the crest and inner slope. A combination of these factors determines the probability of a certain overtopping discharge.

Hydra-NL can calculate with the hydraulic loading level the height of the crest which is needed to withstand a certain maximum overtopping discharge. This calculation can also be used the other way around: the probability can be calculated by interpolation with the input of a crest level, see Figure 7.11.

Impact on the crest

After the impact of a nacelle on the crest, a crater will develop and the new surface will be as shown in Figure 7.8. In the simulation there is no revetment used, which in reality is present, this can limit the amount of soil moving up.

Due to the impact, the soil at the top of the outer slope (left in Figure 7.8) moved upwards. Within this process there is a high probability that the revetment loses strength. A slope without any resistance against erosion will erode easily. The maximum penetration is 3.8 meters and the original height of the dike was NAP +9 m. Below the level of the maximum impact, at a level of NAP +5.2 m, the soil and therefore the revetment as well, stays in position. So the residual height of the dike at NAP +5.2 m is used without a revetment on top of the crest. Also at a higher location no horizontal crest can be determined, only peaks in the soil can be seen. If the highest point would be taken, the first wave which would overtop would erode the crest. In Figure 7.10, the residual profile is colored yellow which is used for the GEKB assessment track.

Zone B+ is created solely for this assessment track. The hitting probabilities are calculated for the center of gravity of the nacelle. If the nacelle lands just on the inner slope, it will still

impact the height of the crest. If the center of gravity lands 5 meters from the crest the impact is still seen as a crest impact. Therefore hitting zone B+ is used instead of hitting zone B. For the assessment track STBI, an impact on crest is not governing.

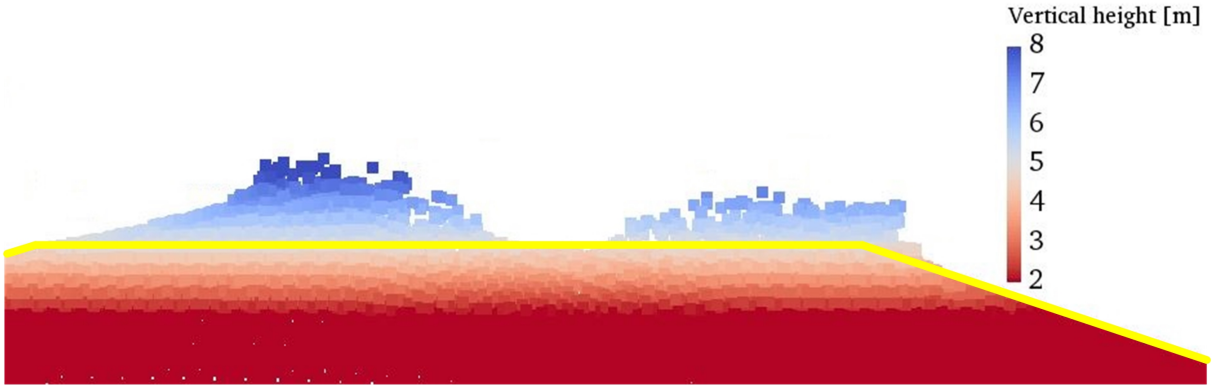

Figure 7.10: Residual profile for GEKB

The tower of the wind turbine is also used in the assessment track GEKB. It is assumed the tower will destroy the revetment, however, it does not lead to a crater. It could be researched in the future if it leads to a crater, however, the prediction is that the size and depth of this crater is limited. The tower will only hit the crest (hitting zone B), the other zones are not affected, this is because the tower will always hit the highest point and will do limited damage if the nacelle hits first, which is always the case at the other hitting zones. The tower is assumed to be a stiff structure, which is valid for most towers. If the tower is falling over and the nacelle lands at the seaside of the crest, then the tower will hit only the crest as this is the highest point. As well when the nacelle hits the crest or the inner slope, the tower stays connected to the nacelle and the tower will not hit the inner slope. Therefore the tower can only hit the crest.

Impact on the inner slope

The impact on the slope does not directly impact the crest height, therefore only the revetment is damaged as a result of the impact. The height of the residual profile stays at NAP +9.0 m, this can be seen in Figure 7.9. The maximum overtopping discharge as a result of a damaged revetments is 0.1 l/s/m (RWS, 2014), this holds for every scenario in Table 7.5.

7.5.2 Design high water level & Hydraulic loading level

The design high water (maatgevend hoog water) level is the maximum still water level at a certain return period, in this case this is the lower threshold value of the safety standard. A Hydra-NL calculation has been performed to calculate the design high water level. The flooding probability is 1/1000 per year, this leads to a design high water of 4.95 meters at the location of the case study. The value of the design high water level is needed for the stability calculations.

The hydraulic loading level determines the height of the crest required for a certain overtopping discharge. The level is dependent on the waves, dike profile and orientation to the waves. The hydraulic loading level calculation in Hydra-NL gives a probability of overtopping. According to OI2014v4 a discharge of 5 l/s/m is 'safe value' for a Dutch dike with a grass revetment (RWS, 2014)

After an impact the crest and inner slope are damaged/destroyed and the crest might be lowered. If there is no revetment a value of 0.1 l/s/m should be used. The lowering of the crest is 3.8 meter, as is concluded in Subsection 7.4.4. For an original crest height of NAP +9 m, this leads to a residual crest height of NAP +5.2 m. The probabilities of overtopping which belong to the hydraulic loading level are shown in Figure 7.11, in the figure as well as the lowered crest level is indicated.

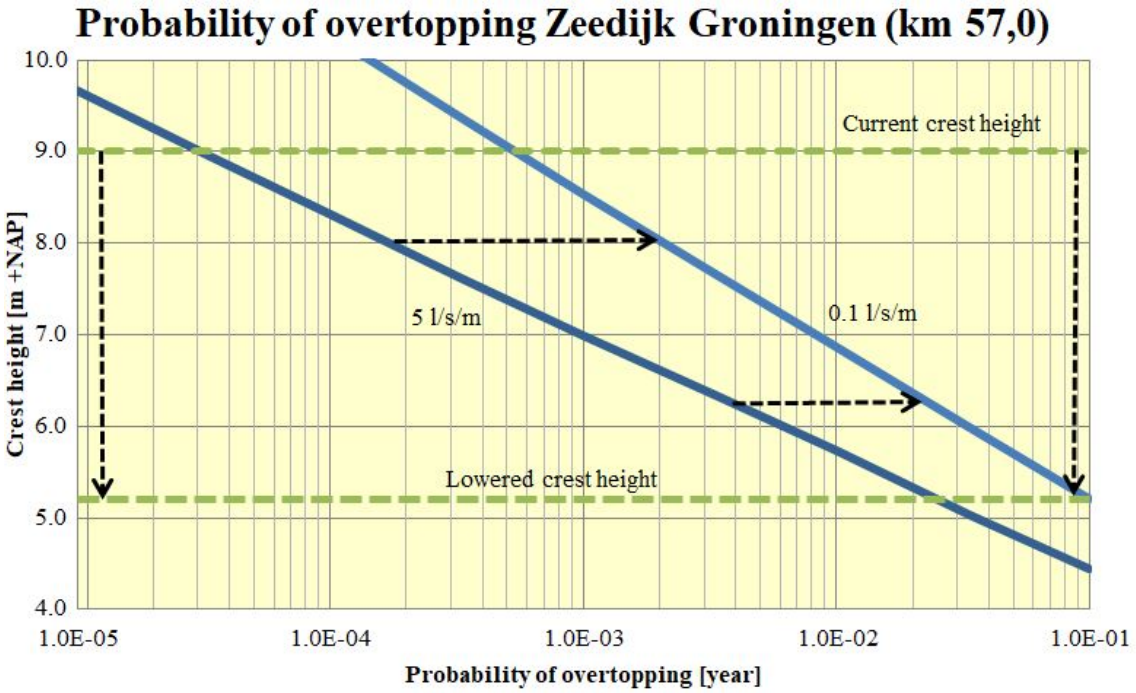

Figure 7.11: Probability of overtopping

7.5.3 Soil profile

For the stability calculations, a layer of clay or peat can influence the stability significantly. Therefore, a layered soil profile is used. A cone penetration test (CPT) from a similar location is used to determine soil layers: the northern Wadden Sea dike in Friesland. Although this is not exactly the same location, the soil profile is assumed to be similar. The soil profile contains sand, sandy clay and stiff clay. In Appendix E the CPT and complete soil geometry and characteristics can be found.

Additional failure probability GEKB

Table 7.5: Additional failure probability GEKB

Scenario	$P_{f,WT} \cdot P_{hitting\|f,wt}$ [per year]	Level residual profile [NAP +m]	$P_{FM\|hit}$ [-]	$P_{flooding\|FM}$ [-]	$P_{f,cs}$ [per year]
Nacelle failure, nacelle falling on zone B+	$3.37 \cdot 10^{-6}$	5.20	$1.00 \cdot 10^{-1}$	$6.53 \cdot 10^{-2}$	$2.20 \cdot 10^{-8}$
Nacelle failure, nacelle falling on zone C	$4.19 \cdot 10^{-6}$	9.00	$5.50 \cdot 10^{-4}$	$1.03 \cdot 10^{-2}$	$2.37 \cdot 10^{-11}$
Nacelle failure, nacelle falling on zone D	$4.91 \cdot 10^{-6}$	9.00	$5.50 \cdot 10^{-4}$	$1.03 \cdot 10^{-2}$	$2.78 \cdot 10^{-11}$
Tower failure, tower falling on zone B	$5.15 \cdot 10^{-5}$	9.00	$5.50 \cdot 10^{-4}$	$1.03 \cdot 10^{-2}$	$2.91 \cdot 10^{-10}$
Tower failure: nacelle falling on zone B+	$6.93 \cdot 10^{-6}$	5.20	$1.00 \cdot 10^{-1}$	$6.53 \cdot 10^{-2}$	$4.53 \cdot 10^{-8}$
Tower failure, nacelle falling on zone C	$7.33 \cdot 10^{-6}$	9.00	$5.50 \cdot 10^{-4}$	$1.03 \cdot 10^{-2}$	$4.15 \cdot 10^{-11}$
Tower failure, nacelle falling on zone D	$7.50 \cdot 10^{-6}$	9.00	$5.50 \cdot 10^{-4}$	$1.03 \cdot 10^{-2}$	$4.24 \cdot 10^{-11}$

The total additional failure probability for the assessment track GEKB is the sum of the 7 scenarios of Table 7.5: $6.77 \cdot 10^{-8}$ per year. The 1% requirement is $8.00 \cdot 10^{-7}$ per year. This leads to a percentage of 0.08%, so the requirement is met.

7.5.4 Inner slope stability

Excess pore pressures

Multiple processes occur during and after the impact: the shock wave starts to propagate in vertical and horizontal direction, as can be seen in Figure 6.1. After a few meters down, the shock wave reaches the phreatic line in the dike. To which location this shock wave will reach and have a significant impact on the excess pore pressure is not clear. However it is important to know the level of excess pore pressures. If these excess pore pressures are high, then the effective stresses are decreased significantly. This is important, because the resistance against slope-instability is partly determined by the friction caused by the effective stresses at the passive plane. Lowering of the phreatic line at the landward side of the dike is a solution to decrease the effects of this mechanism. Another solution could be to use mitigating measures such as using a sheet pile wall which cuts through the sliding plane.

An option to calculate the excess pore pressures is using the empirical relation between accelerations of earthquakes and excess pore pressures in the dike (Deltares, 2014). However the acceleration in the case of a nacelle falling on the dike will be higher and there will only be a single shock, instead of multiple shocks at an earthquake. MPM might be able to give a solution on the excess pore pressures, however, a phreatic line is not incorporated and the excess pore pressures do not work yet as they should in the case of a dike. Also the results might be questionable due to the extreme shock wave for which the models are not designed.

It is recommended for further research to look deeper into these excess pore pressures after an extreme impact. The focus should be on which locations are influenced by the shock wave and in what degree they are influenced.

Assessment method

To fully calculate the inner slope stability, 3 situations should be analyzed, according to Deltares when assessing earthquakes at flood defences (Deltares, 2016b). Two of those methods can be used for an impact of a nacelle hitting the flood defence as well:

1. The first situation is directly after the impact when the final degree of liquefaction is maximal. This situation should be calculated statically with excess pore pressures: Spencer method and horizontal equilibrium should be used.

2. Static drained situation, usually Bishop or Spencer is used for this.

As described above, the excess pore pressures are required for this calculation. These are not available, so only method 2 is used in this thesis.

With the use of D-Geo Stability the slope stability is determined. At the determination of the crater with MPM, several conservative estimations have been used. Therefore, the real penetration depth will be between the calculated crater and the situation without a crater. For stability, a deeper crater creates a more stable situation for the slopes. Therefore the most unfavorable penetration depth will be used, which is the scenario without penetration. In Appendix E the stability of different shapes from different crater depth is given.

The weight of the nacelle has a large influence on the stability. The mass of the nacelle is 568 tonnes, spread over an effective area of 25 square meters for a 3D situation, this gives a uniform distributed load is 223 kN/m. The phreatic line is determined with 'Technisch Rapport Waterspanningen bij dijken' (TAW, 2004). The phreatic line which is used is the one which is advised for rough estimations.

Calculation method

The calculation method is described briefly, details on the calculation can be found in the Schematiseringshandleiding Macrostabiliteit of the WBI2017 (Rijkswaterstaat, 2016a). The goal is to obtain an additional failure probability for every scenario, nacelle falling on the hitting zones i.e. With equations 7.4, 7.5 and 7.6 the failure probability per scenario can be determined.

$$\gamma_R = \gamma_b \cdot \gamma_d \cdot \gamma_m \cdot \gamma_n \tag{7.4}$$

$$\gamma_n = 1 + (\beta_{req,cs} - 4.0) \tag{7.5}$$

$$\beta_{req,cs} = -\Phi^{-1}(P_{req,cs}) \tag{7.6}$$

Where: γ_R is the stability factor or safety factor, γ_b is the schematization factor, γ_d is the model factor, γ_m is the material factor, γ_n is the damage factor, $\beta_{req,cs}$ is the reliability index for a cross-section.

The D-Geo calculations have been performed with the Mohr-Coulomb (MC) model, this implies to a model factor of 1.10. The schematization factor and material factor are both taken 1.0. Equation 7.5 normally is not used any more in WBI2017, because the Critical State Soil Mechanics (CSSM) is the preferred model. The difference between the MC and CSSM is that MC works with drained soil behavior and CSSM with undrained behavior. Due to limited time in this thesis the simpler MC method is used.

Impact on the crest

Different craters are considered for the stability of the inner slope. The slopes within the crater are modeled similar to Figure 7.8. Next to no penetration and the maximum penetration of 3.8 meters, a crater with a depth of 2 meters is considered. No penetration by the nacelle in this scenario the governing situation. The shape of the crater will stabilize the situation, therefore no penetration will give the lowest stability factor. This stability factor is for no penetration 1.03, for 2 meters of penetration 1.28 and for 3.8 meters penetration 1.45, in Appendix E the sliding circles are shown of all calculations. The damage factor is 0.94.

Impact on the slope

For the impact on the slope, only an impact on the upper part of the inner slope is relevant. If the impact would be at the lower part, then the slope will have more resistance against sliding in the static situation. The weight of the nacelle will lead to higher effective stresses and more resistance in the passive plane.

The analogy of the impact on a crest is used for the slope as well. For this scenario two situations are considered: full penetration and no penetration. The crater of the full penetration is governing according to the D-Geo Stability calculations which can be found in Appendix E.

Determining the governing sliding circle is complicated. The crater creates 2 new 'crests', the sliding circle can be chosen at the 3 locations therefore, as can be seen in Figure 7.12. In the figure the highest point is still a residue of the 'old' crest.

The first is the global sliding circle which starts at the 'outer' crest and ends at the inner side of the dike, it is completely orange in Figure 7.12, which indicates a higher stability factor compared to circle 2 and 3, which are red. The second is the sliding circle which starts at the very top of the residual crest and ends on the lowest point of this outer slope, recognizable as the left red plane. The third lies within this red plane and starts halfway the slope and ends also at the lowest point of the outer slope.

A choice has to be made which sliding circle is going to be used. The most conservative choice is circle 3, as it has the lowest stability factor: 0.75. The second sliding circle can be used as well and has a higher stability factor, however, with the requirement that the overtopping will be negligible. The stability factor for the impact on a slope therefore is 0.75. In sliding circle 2 the stability factor is 0.97. The damage factor is 0.68.

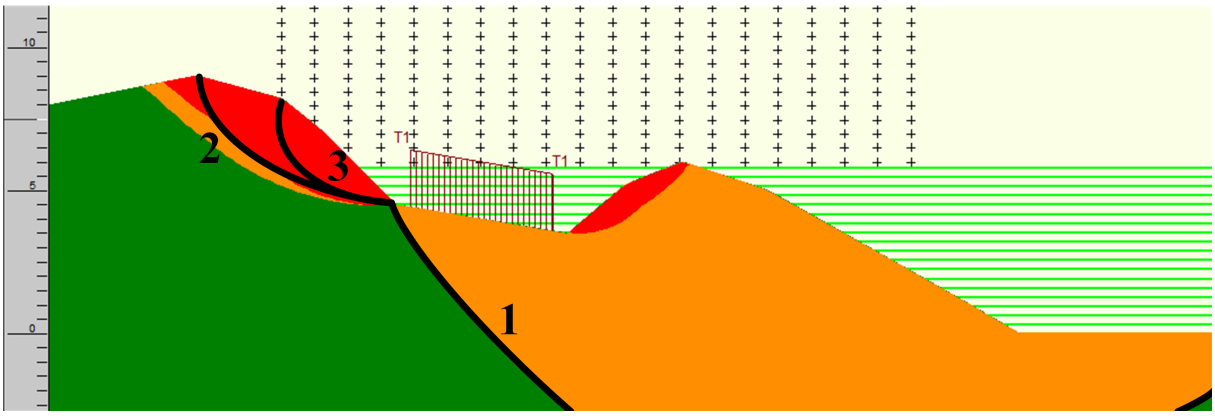

Figure 7.12: Stability overview after an impact at the slope with 3.8 meters penetration

Additional failure probability STBI

Table 7.6: Additional failure probability STBI

Scenario	$P_{f,WT} \cdot P_{hitting\|f,wt}$ [per year]	Stability factor γ_R	β_{cs}	$P_{FM\|hit}$ [-]	$P_{flooding\|FM}$ [-]	$P_{f,cs}$ [per year]
Nacelle failure, nacelle falling on zone B	$7.77 \cdot 10^{-7}$	1.03	3.51	$2.24 \cdot 10^{-4}$	$6.53 \cdot 10^{-2}$	$1.13 \cdot 10^{-11}$
Nacelle failure, nacelle falling on zone C	$1.36 \cdot 10^{-5}$	0.75	1.55	$6.03 \cdot 10^{-2}$	$1.03 \cdot 10^{-2}$	$8.44 \cdot 10^{-9}$
Tower failure, nacelle falling on zone B	$4.92 \cdot 10^{-7}$	1.03	3.51	$2.24 \cdot 10^{-4}$	$6.53 \cdot 10^{-2}$	$7.19 \cdot 10^{-12}$
Tower failure, nacelle falling on zone C	$7.33 \cdot 10^{-6}$	0.75	1.55	$6.03 \cdot 10^{-2}$	$1.03 \cdot 10^{-2}$	$4.55 \cdot 10^{-9}$

The total additional failure probability for the assessment track STBI is the sum of the 4 scenarios of Table 7.6: $1.30 \cdot 10^{-8}$ per year. The 1% requirement is $1.25 \cdot 10^{-8}$ per year. This leads to a percentage of 1.04%, so the requirement is not met.

7.5.5 Revetment of the outer slope

The revetment consists of a combination of grass and an asphalt revetment. This assessment track is the combination of all revetment assessment tracks. It is chosen to do this, as the result of an impact is for all revetments is the same: failure. If the nacelle hits the outer slope, the revetment is assumed to be destroyed or damaged. Only if the revetment would be damaged during normal daily conditions or non-governing hydraulic loads, then a repair time is used.

Next to hitting zone A, an impact in hitting zone B will lead to a revetment failure as well. This is shown in shown in Table 7.4.

Additional failure probability STBK

Table 7.7: Additional failure probability STBK

Scenario	$P_{f,WT} \cdot P_{hitting\|f,wt}$ [per year]	$P_{flooding\|FM}$ [-]	$P_{f,cs}$ [per year]
Nacelle failure, nacelle falling on zone A	$2.55 \cdot 10^{-6}$	$1.95 \cdot 10^{-1}$	$4.98 \cdot 10^{-7}$
Nacelle failure, nacelle falling on zone B	$7.77 \cdot 10^{-7}$	$6.53 \cdot 10^{-2}$	$5.07 \cdot 10^{-8}$
Tower failure, nacelle falling on zone A	$2.20 \cdot 10^{-5}$	$1.95 \cdot 10^{-1}$	$4.28 \cdot 10^{-6}$
Tower failure, nacelle falling on zone B	$1.60 \cdot 10^{-6}$	$6.53 \cdot 10^{-2}$	$1.04 \cdot 10^{-7}$

The total additional failure probability for the assessment track STBI is the sum of the 4 scenarios of Table 7.6: $4.93 \cdot 10^{-6}$ per year. The 1% requirement is $1.00 \cdot 10^{-6}$ per year. This leads to a percentage of 4.93%, so the requirement is not met. The main cause of this higher percentage is that there is almost no repair possible if the revetment is hit. It it assumed that the probability

of repair after a STBK failure during daily conditions is 90%. For a failure during a storm event, this is assumed only 50%.

7.5.6 Other mechanisms

Next to the three assessment tracks which are quantitatively assessed in this chapter, there are more failure mechanisms which need to be checked. This is done only qualitatively, because it is estimated that those failure mechanisms are of minor importance compared to three described above.

Outer slope stability The failure mechanism macro-instability of the outer slope is triggered by a sudden drop down of the water level. It is an indirect mechanism, because when the water level is low, it will not lead to a flooding immediately. The trigger can be the impact by a nacelle as well. The probability of this in combination with a sudden drop down of the water level is considered negligible. The static situation with the nacelle resting on the slope with a crater is not considered a risk as well, because the complete slope has a steepness of 1V:5H. The dynamic failure is similar to that of the inner slope-instability, it is recommended to do more research on the excess pore pressures.

Piping This failure mechanism is typical relevant for river dikes, less for sea dikes. Piping has three mechanisms which all should occur in order to have a failure (Deltares, 2016a). These mechanisms are uplift, heave and backward erosion. Falling wind turbine parts can affect the uplift criterion.

Uplift is caused by a large hydraulic head over the cohesive layer at the inner side of the flood defence. The upward pressure can exceed the weight of the cohesive blanket layer. Then this blanket is lifted up and it ruptures (Jonkman & Schweckendiek (eds), 2015). The impact of a nacelle on the inner side of a flood defence, can damage this blanket severely, so the blanket is penetrated at the impact. In that case the uplift criterion is fulfilled and only the other 2 criteria remain.

A piping failure caused by a wind turbine failure can be prevented. A fallen wind turbine part will probably be noticed if there is a levee guard present, usually this is the case during high water conditions. Piping only occurs at long periods of high water, so if during this period it is checked if sand particles are washed near the crater, mitigating measures can be taken, placing sand bag rings around the crater i.e. If uplift is prevented or solved with measures, the follow-up mechanisms heave and backward erosion cannot occur. Therefore the risk of this failure mechanism is considered negligible.

Instability foreland by static liquefaction Considering the case study in Groningen, instability of the foreland is an indirect failure mechanism that might occur after a nacelle impact. Sliding of the foreland can lead to a shorter piping length and a decreased resistance against outer slope-instability (Deltares, 2014). Static liquefaction is the behavior of saturated loosely packed granular material as a thick fluid by an instant loading. This instant loading can be anything: an earthquake, wind turbine falling over or even stamping of feet. During the liquefaction the slope will slide down and transforms to a very gentle slope (i.e. 1V:10H to 1V:20H). A requirement for this is that the soil material is loosely packed granular material and the slope is relatively steep (>1V:4H).

In the dynamic morphological active area of the Wadden Sea, the morphology changes regularly. The exact locations where the instability is a risk is hard to determine. Therefore all location where no salt march is present in front of the dike, are vulnerable to this failure mechanism. Measures to limit the risk are: using a sheet pile wall, using a geotextile at the foreland.

These measures are expensive and are usually only used if the risk of the occurrence of the failure mechanism is large. Using a geotextile for a wind turbine near a dike is not economic feasible.

The risk of the instability of the foreland should remain as small as possible. There are not many mitigating measures which are economic feasible, because the failure mechanism is indirect. So, it is important to restore the foreland as fast as possible after a failure, so the probability of occurrence of follow-up mechanisms is kept as small as possible.

7.6 Overview

In this section the overview of the additional failure probabilities is given. In addition, options for optimizations are given. The choice of using those optimizations is a political choice and is not made in this assessment. Note: the damage by the wind turbine blades and dynamic instability of a saturated dike are not taken into account.

7.6.1 Comparison with requirements from ENW

In Subsection 7.1.2 the requirements from Expertise Network for Flood Protection (ENW) to allow wind turbines near flood defences for the sake of flood protection are given. Those are:

- 1% of the permissible failure probability per cross-section per failure mechanism.
- 10% of the maximum permissible failure probability on segment level for all NWO's together.

In Figure 7.2 the values of the maximum permissible additional failure probabilities are elaborated. There the values of the maximum permissible additional failure probabilities are determined.

Requirement for 1 wind turbine

Table 7.8 shows the overview of the additional failure probabilities per assessment track at cross-section level. In the case study the center of the turbine is built 20 meters from the inner toe. This is minimum distance from the toe to build a turbine. The wind turbine would not satisfy the flood protection requirement for the assessment tracks STBI and STBK. GEKB does satisfy the 1% requirement per wind turbine.

Table 7.8: Summary additional failure probability for 1% requirement

Track	**Maximum permissible additional failure probability** $P_{req,cs}$ **[per year]**	**Actual additional failure probability** $P_{f,cs}$ **[per year]**	**Actual Additional failure probability 1 turbine [%]**
STBI	$1.25 \cdot 10^{-8}$	$1.30 \cdot 10^{-8}$	1.04
GEKB	$8.00 \cdot 10^{-7}$	$6.77 \cdot 10^{-8}$	0.08
STBK	$1.00 \cdot 10^{-6}$	$4.93 \cdot 10^{-6}$	4.93

For STBI or instability of the inner slope, the additional failure probability is slightly higher than maximum permissible. However, dynamic failure has not been taken into account, which will increase the failure probability even more.

The assessment track GEKB which accounts for overtopping and overflow, has relatively the lowest additional failure probability of the three assessment tracks. This is due to the residual profile after an impact and repair possibilities. The dike is relatively large and will retain height after an impact.

The additional failure probability of the stability of the revetment or STBK is too high as well. This is partly caused by the fact that the dike has failed when a nacelle hits the revetment. If the blades would be taken into account as well, the failure probability would be even higher. The repair possibilities are limited, because the damaged part zone of the dike is open the sea.

Requirement on all wind turbines in a segment

This requirement is on segment level, so it will sum the actual additional failure probabilities of the assessment tracks at cross-section level. The maximum permissible additional failure probability on segment level is 10% or $1.00 \cdot 10^{-4}$ per year. The maximum number of turbines which can be constructed within a segment can be determined by this requirement and is shown in Figure 7.13. It is assumed that the cross-section is the similar along the whole segment and the turbines are placed at the same distance from the toe. Only the three assessment tracks which have been used in the assessment are used in this 10% requirement. It is assumed that the other assessment tracks have a negligible additional failure probability, this should be validated. This is because those tracks should be added as well in the sum for the 10%. Assuming that those assessment tracks have a negligible additional failure probability, the maximum number of turbines is 19. This is only for the flood protection part of the consideration. There are many other regulations regarding wind turbines.

Figure 7.13: Maximum number of turbines within the 10% failure probability requirement

Number of turbines	**Actual additional failure probability [%]**
1	0.50
5	2.51
10	5.01
20	10.03
50	25.07

7.6.2 Optimizations

The 1% requirement is not met. Optimizations can be used to lower the actual additional failure probabilities. Those optimizations should be verified, which is not performed in this assessment. The choice of using those optimizations is a political choice for the water authorities.

In Eurocode 0 there is a load combination factor ψ which accounts for loads which will not be present simultaneous (NEN, 2011). A similar factor or method also can be used in this flood protection assessment. Only one or several loads or probabilities are taken at their 95% reliability percentile. Several optimizations are suggested which lead to more realistic additional failure probabilities. The method to determine the new actual additional failure probabilities is by tweaking the input parameters.

In Table 7.9 the list can be found with the new additional failure probabilities for the three assessment tracks. In Table 7.10, the values of the new additional failure probabilities at cross-section level at given. The first row shows the standard additional failure probability as it determined in the assessment above.

Table 7.9: Suggestions for optimization

ID	Suggested optimization
1	This is the standard method without optimizations. The additional failure probabilities are determined in the assessment above.
2	The distance of center of the wind turbine to the toe is in the assessment 20 meters. This can be increased to any distance, however, building close to the dike will have advantages which have been elaborated in Chapter 2. To give an indication of the effect of constructing wind turbine further from the toe, the distance is doubled to 40 meters. The hitting probability is lowered by this optimization
3	For a nacelle failure, the maximum hitting distance is 1/2 times the diameter of the rotor. However, the probability of falling at that location is small. The blades can cut the tower with their tip. However, this is often regarded as a tower failure instead of a nacelle failure. The hitting distance of a nacelle/rotor failure probably is less. This can have a significant impact on the hitting probability of the zones. Therefore the maximum hitting distance of 1/4 times the diameter is used. in this optimization.
4	Turbine failure probabilities given by manufacturers are far lower than the outdated 95% reliability percentile failure probabilities of the HRW. The water authorities can require a certain structural quality of a wind turbine, so there is room for improvements. In addition, the 50% reliability percentile can be used as a value in the assessment. The 50% reliability percentile of the manufacturers is used as optimization.
5	For the stability factor of STBI after an impact on zone C, the factor is 0.75, however, as described in Subsection 7.5.4, a value of 0.97 can be used as well, if there is hardly any overtopping, which is often the case.
6	The repair time is chosen 2 weeks for GEKB and STBI in the assessment, which is rather long. If measures are taken, the effect of lowering the repair time to 5 days is shown.
7	For the assessment track STBK there is not a repair time used, but a repair probability. If these probabilities are increased by a factor 10, the result is shown. For a failure during daily conditions the repair probability would become 99% and for the repair probability for a failure during the storm season 95%, in case there are no significant hydraulic conditions during the failure.
8	Multiple suggestions can be used to lower the additional failure probability. If the suggestions with ID 3, 4 and 5 are combined, this is the additional failure probability for each mechanism.

Table 7.10: Suggested optimization of additional failure probability

ID	Suggested optimization	$P_{f,additional}$ STBI [%]	$P_{f,additional}$ GEKB [%]	$P_{f,additional}$ STBK [%]
1	Reference case, determined in the assessment	1.04	0.08	4.93
2	Move the wind turbine 20 meters more land inward	0.62	0.05	3.90
3	Half the maximum falling distance of the nacelle	0.36	0.06	4.39
4	Use 50% WT reliability percentile instead of 95%	0.46	0.04	2.20
5	Increase stability factor for the inner slope impact	0.02	0.08	4.93
6	Repair time lowered from 14 to 5 days	1.03	0.08	4.93
7	Repair probability for STBK increased by a factor 10	1.04	0.08	1.96
8	Combination of ID 3, ID 4 and ID 5	0.00	0.03	1.96

The additional failure probabilities with use of the suggested optimization are lower than the original ones, as can be seen in Table 7.10. Number 8 is a combination of optimizations, it shows that for STBI and GEKB the additional failure probabilities can be decreased significantly. However, for STBK it is not possible to lower the additional failure probability significantly, reducing the repair probability by a factor 10 will only lower the failure probability by 60% (4.93 to 1.96).

The optimization that will always work is moving the turbines more land inward, because the hitting probability will decrease. So, if wind turbines are permitted depends on the distance between the wind turbine and the flood defence. This can be seen by optimization 2 where location of the turbine is moved more land inward.

7.6.3 Discussion

In this flood protection assessment several assumptions and choices have been made which have an impact on the output. The most important ones are discussed in this subsection.

Maximum permissible additional failure probability

The ENW determined two requirements for wind turbines near flood defences. However, the following requirement leaves space for discussion: 10% of the maximum permissible failure probability on segment level for all NWO's together. If the sum is taken of all additional failure probabilities at cross-section level for each mechanism, it is not a very strict requirement. If in this case study the 1% requirement is satisfied, at least 50 turbines can be constructed along the dike. So, the requirement does not limit the number of turbines. There should be clearer requirements which do not leave space for interpretation.

Tower failures

To assess a tower failure correctly, a better failure analysis of the tower can be made. The probability of failure at multiple points along the tower could be used for example. The effect of the concrete and steel tower could be determined as well. Several scenarios are possible when a

concrete tower hits the crest: the concrete parts can split, stay connected or bounce off the dike. For steel towers there are multiple scenarios as well. It all depends on the construction method of the towers.

Stability calculations

The penetration depth is not determined for a saturated dike. In reality in the case of a severe storm, the dike will be (partly) saturated. The impact of a nacelle on a saturated is a very important scenario. The penetration will probably more and it has a large impact on the excess pore pressures. The slope stability will be much lower in the case of saturated dike and especially with excess pore pressures.

For the stability calculations the Mohr-Coulomb model is used, while the Critical State Soil Mechanics is preferred in this case study. The results might be different, this should be researched.

Assessment of stability of the outer slope revetment

The additional failure probability of the STBK assessment track does not satisfy the 1% requirement from ENW. If this assessment is researched more in detail, it will probably satisfy the requirement. In this assessment there is only one hitting zone used for the outer slope. Creating more hitting zones will help, because then the effect of the crater is not on the whole outer slope.

Relation between storm and hydraulic conditions

The relations between a storm and hydraulic conditions is very important in this assessment. As stated in this chapter the relation between a storm and governing hydraulic conditions is weak. It has an extreme impact on the additional failure probability. Therefore it is important to look at the statistical relation between a storm and hydraulic conditions at this location. The limited time prevented doing this analysis in this thesis.

Fully probabilistic approach

A probabilistic approach is needed for determining the governing hydraulic conditions during a storm. This is a very complex analysis where much room for improvement is. Perhaps a better coupling between failure of the wind turbine during storm conditions can be made.

Incomplete assessment

The assessment is not complete, only the impact of a nacelle hitting the flood defence is determined. The impact of blades should be determined as well to make a full assessment of the falling parts. The below ground level failures which have been described in Chapter 2 should be considered as well in order to make full flood protection assessment.

7.6.4 Conclusion

There is no legal method to determine the additional failure probability of a flood defence by an impact of a nacelle. The method currently used is the one prescribed by the Expertise Network for Flood Protection: a requirement for the additional failure probability at cross-section level per failure mechanism and a requirement on segment level. Overtopping & overflow, inner slope-instability and instability of the revetment are considered as the governing failure mechanisms for the additional failure probability. When using only conservative assumptions, one of the requirements is not met for an Enercon E-126 turbine built directly at the inner side of a sea dike in Groningen. However, with using more realistic assumptions, the additional failure probability for each assessment track can be lowered significantly. Still, for the failure mechanism instability of the outer slope revetment it is hard to satisfy the requirement. In addition, special attention is needed in case a dike section is sensible for instability of the foreland caused by static liquefaction. In the end, the wind turbine can be moved further inland to lower the hitting probability of the flood defence, this will decrease the additional failure probability.

Chapter 8

Conclusions & Recommendations

There are many white spots concerning wind turbines near flood defences. The white spots in determining the risk of wind turbines are given in the Section 'Recommendations'. In the Section 'Conclusions' the answers on the research questions and main research questions are given.

8.1 Conclusions

Which mechanisms play a role in the crater formation?

A crater created by meteorites and earth-penetrating-weapons have similarities with the impact crater caused by a nacelle falling down. The amount of transferred energy is the main factor for the size and depth of the crater. Secondly, the soil characteristics have an effect on the crater formation. The shape of the penetrator is mainly an important factor for the crater depth. The crater formation has different stages to distinguish: directly after the impact, most of the energy is transferred from the object to the soil and the transient crater is formed. Later, there are small landslides at the inner side of the crater due to unstable slopes. When this process has finished, the well-known crater shape remains.

What is the additional value of the Material Point Method in crater formation?

Analytical solutions, results from experiments and data from fallen wind turbines are not available, therefore the penetration depth is estimated by models or empirical formulas. However, currently used models and formulas are developed for other purposes than modeling the impact of an object similar to a nacelle, which has a large mass and low impact velocity. So, the results from those models and formulas are questionable. Finite elements methods are strong in modeling soil-structure interaction and deformations. However, at modeling large deformations severe mesh distortions will occur. The Material Point Method can handle large deformations, which is essential in the case of a nacelle impact. Because the Material Point Method is fully dynamic, the forming process can be simulated as well.

What is the penetration depth and size of a nacelle hitting a dike using the most suitable method?

The Material Point Method turns out to be a good method to determine the size and depth of a crater. The nacelle of the Enercon E-126 turbine can cause at maximum a penetration depth of 3.8 meters on a dry sea dike consisting of sand. There are two impact locations on the dike which can be distinguished: an impact on the crest and an impact on the slope. If the impact is on the crest, both the crest is and large parts of both slopes are affected. The soil below the slopes is lifted up, this causes the revetment to lose its coherence. An impact on the slope will mainly affect the slope and the crest is only limited affected. However, the size and depth of the

crater depend largely on the soil characteristics and the potential energy of the nacelle. Those are taken conservative in the model. So, the penetration depth of 3.8 meters is the maximum. The sensitivity analysis shows that the governing parameters are the impact velocity, the mass of the penetrating object, the stiffness of the soil and the angle of internal friction of the soil. 3D models are preferred over 2D models for determining the penetration depth: there are large 3D effects which are not covered when using 2D models. At last, a saturated dike will probably cause a deeper crater, because the effective stresses are lower compared to a dry dike, this scenario is not considered in this report.

What is the additional failure probability of a dike caused by an impact of a nacelle?

There is no legal method to determine the additional failure probability of a flood defence by an impact of a nacelle. The method currently used is the one prescribed by the Expertise Network for Flood Protection: a requirement for the additional failure probability at cross-section level per failure mechanism and a requirement on segment level. Overtopping & overflow, inner slope-instability and instability of the revetment are considered as the governing failure mechanisms for the additional failure probability. When using only conservative assumptions, one of the requirements is not met for an Enercon E-126 turbine built directly at the inner side of a sea dike in Groningen. However, with using more realistic assumptions, the additional failure probability for each assessment track can be lowered significantly. Still, for the failure mechanism instability of the outer slope revetment it is hard to satisfy the requirement. In addition, special attention is needed in case a dike section is sensible for instability of the foreland caused by static liquefaction. In the end, the wind turbine can be moved further inland to lower the hitting probability of the flood defence, this will decrease the additional failure probability.

Main research question

Answering of all the sub questions leads to answering the main research question of this thesis:

'What is the impact of a nacelle of a wind turbine hitting a dike and its effect on the failure probability of a dike?'

If the nacelle hits the soil, it will cause a significant crater if the impact is on the crest or inner slope of a dike. The case study is an Enercon E-126 turbine built directly at the inner side of a sea dike in Groningen. The Material Point Method turns out to be a good method to determine the size and depth of this crater. The impact of the crater reaches further than only the location of the impact, the soil around the crater moves up due to the impact as well. When using only conservative assumptions, the flood protection requirements are not satisfied. However, with using more realistic assumptions, the additional failure probability for each assessment track can be lowered significantly. In the end, the wind turbine can be moved further inland to lower the hitting probability of the flood defence, this will decrease the additional failure probability.

8.2 Recommendations

8.2.1 Verification and validation

For risks where the probability of occurrence is low and the consequences are large, it is difficult to determine the consequences exactly. Because it is unlikely that a wind turbine falls exactly on the crest of dike, tests should be performed. Tests with high masses dropped at a height of the hub height of a wind turbine could provide a verification of the model, however, getting a mass at such a height is very expensive and complicated. Models with lower masses do can be tested and verified, however this still will be scale tests and not full scale tests.

It is recommended to verify impact simulations from MPM in reality. Those tests can be on a much smaller scale, because the MPM model can be created in any possible size .

8.2.2 MPM impact modeling

- In this thesis 2D and 3D simulations are run. Running a 3D model takes a long time, in this case it took more than 10 times longer than to run a 2D simulation. The slice in the center of the impact of the 3D simulation is the governing one and used for flood protection assessments. Compared to the 2D model, only the energy dissipation is in more directions in the 3D model. It is useful to determine the method for obtaining in a 2D simulation the same results as in a 3D simulation.

- Only the nacelle of an Enercon E-126 is used, however, it will be useful to know the effect of smaller turbines as well. Nacelle of geared turbines have a much smaller mass than gearless turbines and are more often built at the moment. A database or table can be created with the results. Different impact velocities can be simulated as well. This way, an indication can be given of the size and depth of the crater. However, the effect of different soil characteristics should be considered as well.

- The impact on a slope can be researched further, as only one simulation for a slope is performed in this thesis. Already in that simulation the sliding plane was visible. Multiple slopes can be tested to get a better insight in the dynamic slope-instability.

- A fully coupled calculation with liquids and solid should be performed to get an insight in the behavior of the excess pore pressures. The penetration in saturated soil is recommended to research as well, as large storms often also bring large amounts of rain which can saturate a dike. At the moment of running the simulations, there was a bug in the software which prevented performing this simulation in this thesis.

- The effect of the shape of the penetrator is not taken into account, in reality the penetrator has a round shape at the impact. This could possibly lead to a different crater shape and depth. The effect of an inclined impact should be researched as well.

- The penetration depth of the Bernard model is similar to the MPM simulation, it follows the MPM-plot surprisingly well. Almost all variables used in MPM, are used in the Bernard formulas as well. The link between the Bernard formulas and MPM model could be researched. Varying the parameters in both formulas can give more insight on the similarities and difference between the two models.

8.2.3 Flood protection assessment

- There is no legal method to determine the additional failure probability of a flood defence by an impact of a wind turbine failure. This makes that there can be a discussion on the assessment method. It is recommended to create an assessment method with a legal status.

It should leave no or much less room for interpretation. This way the initiators of wind farms have a better view on the feasibility of wind farm regarding flood protection.

- This study is dedicated to the nacelle from chapter 3 on. The same can be done for the failure of the blades. The risk of falling blades cannot completely be neglected. However, there are many conservative assumptions used in current flood protection assessments. This leads to the assumptions that blades can do damage to a flood defence. If pictures of failure are analyzed, it can be concluded that the blades will cause very little damage to the flood defence. So, it is recommended to look at all those conservative assumptions and their probability of occurrence. Those assumptions are: real probability of overspeed, bouncing of the blade at the soil, probability of each angle of impact and fragmentation of the blades at different impact velocities and different revetments. Then it can be interesting to research the penetration depths of the blades with taken into account the probability of all previous points.

- It is recommend doing more research on the excess pore pressures and effect on slope-instability and liquefaction. There is research going on at the excess pore pressures in dikes by induced earthquakes, at several points the impact of a nacelle is similar, however, at many others it is not. It is not clear to which distance the 100% excess pore pressures will reach after a large impact.

- The assumption that during the storm that causes the wind turbine fails, also the governing hydraulic loading occurs, these events are not fully dependent. This relation is very weak at the Wadden Sea in Groningen. At other locations with constant high water, lakes, this relation is very strong however. The hydraulic loading level that occurs is partly caused by a storm or the wind speed. This assumption has a major impact on the additional failure probability. It leads to situations where a wind turbine in the Noordoostpolder near a small dike leads to the same risk as one in Groningen at a large sea dike, which is not the reality. A method can be researched which deals with this phenomenon.

- The probability that a wind turbine fails during a storm is not known. At locations which have at normal hydraulic conditions no water against the dike, a failure of the wind turbines does not cause a significant additional failure probability. So it is recommended to research more on the cause of wind turbine failures.

- The 'handboek risicozonering windturbines' is outdated. The failure probabilities of wind turbines are orders smaller than the values which are currently used in flood protection assessments. Using the HRW as a source for wind turbine failures increases the failure probability of the flood defence significantly. An update of the HRW could be made or another source can be used for the failure probabilities of wind turbines.

- The risk of instability of the foreland by static liquefaction is not well-known. At the location of the case study in Groningen, this failure mechanism is a significant risk. It can be triggered by an earthquake or an impact by a nacelle. More research is needed to know when this mechanism occurs.

- In the assessment in this thesis a sea dike has been been assessed. For lake and river dikes a small difference has been pointed out. This should be expanded to a full assessment to show the differences. For the failure mechanism stability of the revetment, a lake dike will have less additional failure probability. The hitting zone of the outer slope is smaller, because the dike is often smaller and the slope is steeper.

Appendix A

Pictures of damage

In this appendix pictures of wind turbines that had a failure are shown. Most of it are tower failures and a single is a nacelle failure. The pictures do not show a large crater below the impact. This is due to that the wind turbines shown are smaller and the nacelle has a lower mass than the Enercon E-126.

Figure A.1: Tacke TW 600 Windmill with LM19 –Blades, January 2017, Saxony, Germany (Williams, 2017)

Figure A.2: Nordex N80 2.5 MW, February 2015, Country Down, Northern Ireland (Cou, 2017)

Figure A.3: Siemens 3MW-101, October 2016, Hawaii, United States of America (Mau, 2016)

Figure A.4: Siemens SWT-2.3-108, November 2016, Ocotillo, United States of America (Raferty, 2016)

Figure A.5: Vestas V112, 3 MW, December 2015, Verlanda, Sweden (Ver, 2016)

Appendix B

Risks table

In this appendix the risk database is given. It consists out of 4 pages. The results have been used in chapter 2. The risks that can be managed and used in the filters in chapter 2 are in this appendix as well.

ID	Risk	Description by sources	Zone	Size related? Height, mass & foundation (3 is highly, 1 is not)
Construction				
1.1	Instability resulting from liquefaction due to pile driving vibrations	De door heiwerkzaamheden veroorzaakte trillingen kunnen leiden tot verweking van de keileemkern of los gepakte zand in de waterkering en daarmee tot instabiliteit van de waterkering.	1 till 2	3
1.2	Dynamic loads due to pile driving	De dynamische belastingen (zone circa 50 m op basis van expert judgement) ten gevolge van het heien kunnen leiden tot afname van de stabiliteit van de waterkering.	1 till 3	3
1.3	Flow slides resulting from liquefaction (zettingsvloeiing) due to pile driving	De door heiwerkzaamheden veroorzaakte trillingen kunnen aan de Waddenzeezijde/IJsselmeerzijde, bij aanwezigheid van een onderwatertalud en een zettingsvloeiingsgevoelige voorland (aanwezigheid van een los gepakte fijnkorrelige zandlaag met geringe relatieve dichtheid), leiden tot het optreden van zettingsvloeiing in het voorland en daarmee mogelijk tot bezwijken van de waterkering.	1	3
1.4	Penetration of impermeable layers (hydraulische kortsluiting)	Door de installatie van palen kan kortsluiting ontstaan tussen watervoerende grondlagen met daartussen een afsluitende laag. Door kortsluiting kan kwel toenemen en kan de kans op optreden van piping toenemen.	2 till 4	1
1.5	Soil consolidation due to pile driving	De door heiwerkzaamheden veroorzaakte trillingen kunnen leiden tot zetting door verdichting/inklinking van het dijklichaam en/of dieper gelegen zandlagen. Daarbij kunnen zettingsverschillen optreden. De hoogte van het dijkprofiel kan afnemen met enkele decimeters.	1 till 2	2
1.6	Heavy equipment causes vibrations, settlements and track forming	Samendrukking en verlaagde doorlatendheid van de grond	1 till 2	3
1.7	Construction road traffic damages flood defence	Bij betreding van de waterkering met zwaar bouwverkeer (o.a. de heisteling en kranen) zou schade kunnen ontstaan aan de waterkering en bekleding en daarop aanwezige infrastructuur.	1 till 2	2
1.8	Excavations temporary works	Ten behoeve van het plaatsen van de funderingspoer en het aanleggen van kabels en leidingen zullen tijdelijke ontgravingen nodig zijn, welke de waterkering tijdelijk verzwakken met kans op afschuiven, doorsnijding van afsluitende lagen of lokale erosie.	1 till 2	2
Exploitation				
2.1	Vibrations due to dynamic wind loads	Trillingen door cyclische windbelastingen of extreme piekbelastingen kunnen leiden tot verhoogde waterspanningen, verweking van keileem of zand in de dijkkern, verminderde grondeigenschappen en extra belasting op de grond. Hierdoor kan de stabiliteit van de waterkering door afschuiven nadelig worden beïnvloed en/of kan zetting optreden.	1 till 4	3
2.2	Flow slide as result of liquefaction by wind related vibrations of turbine	De door wind veroorzaakte trillingen van een windturbine kunnen, bij een verwekingsgevoelig voorland (aanwezigheid van een los gepakte fijnkorrelige zandlaag met geringe relatieve dichtheid) aan de Waddenzeezijde/IJsselmeerzijde, leiden tot het optreden van zettingsvloeiing in het voorland en daarmee mogelijk tot bezwijken van de waterkering.	1	2
2.3	Higher phreatic line near WT	De freatische lijn kan in de nabijheid van windmolens (door opstuwing) hoger liggen dan normaal, waardoor de stabiliteit nadelig kan worden beïnvloed.	1 till 2	3
2.4	Space below foundation and soil gives seepage	Door het optreden van verschilvervormingen kunnen kieren ontstaan tussen de constructie en omringende grond. Hierbij wordt gedacht aan het ontstaan van ruimte onder de funderingsplaat door zetting van de ondergrond en het ontstaan van ruimte tussen de funderingspalen en de ondergrond (afsluitende lagen) door horizontale beweging van de palen. Door de holle ruimtes kan kortsluiting ontstaan en/of kan de kwelweglengte worden verkort. Daarnaast is het mogelijk dat er een hogere freatische watersland ontstaat wat een negatieve invloed heeft op micro- en macrostabiliteit.	1 till 2	1
2.5	Space between foundation and soil causes loss of grass revetment	Door het optreden van horizontale en verticale verschilvervormingen, kan tevens de aansluiting tussen de funderingsconstructie en de bekleding sterkte verliezen. Als gevolg hiervan kan lokale erosie optreden bij golfaanval aan de buitenzijde en stroming aan de binnenzijde.	1	1
2.6	Erosion & seepage along cables perpendicular through dike	Bij kabels die de waterkering kruisen kan (door zetting), afhankelijk van de ligging, de kans op geconcentreerde erosie (kanaalvorming) toenemen;	1	1
2.7	Erosion & seepage along cables lateral with dike	Bij kabels parallel aan de waterkering kan de kwel en/of erosie nadelig worden beïnvloed.	1	1
2.8	Falling over of WT	Bij het omvallen van een windturbine op de waterkering, zal deze aanzienlijke schade aan de waterkering kunnen veroorzaken. Er dient in dat geval rekening te worden gehouden met beschadiging van bekleding, deklagen en deformatie van het dwarsprofiel.	1 till 4	3

Figure B.1: Risk database (1)

ID	Risk	Description by sources	Zone	Size related? Height, mass & foundation (3 is highly, 1 is not)
2.9	Falling of nacelle/rotor	Indien de rotor of gondel losraakt en de waterkering treft, zal deze aanzienlijke schade aan de waterkering kunnen veroorzaken.	1 till 3	3
2.10	WT blade falling down	Bij breuk van een rotorblad of deel daarvan (door bijvoorbeeld overbelasting, defecte componenten of bliksemінslag) zal het bladdeel), indien dit op de waterkering terecht komt, schade aan de deklaag van de waterkering kunnen veroorzaken. Ook kan dit een gat veroorzaken in de kering.	1 till 5	3
2.11	Heavy maintenance equipment consolidates soil	Samendrukking en verlaagde doorlatendheid van de grond	1 till 2	3
2.12	Maintenance equipment damages flood defence	Bij betreding van de waterkering met zwaar onderhoudsverkeer (bijvoorbeeld bij vervanging van grote onderdelen zoals rotorbladen) kan schade ontstaan aan de waterkering en daarop aanwezige infrastructuur.	1 till 2	2
2.13	Erosion around foundation due to wave attack or overflow	Aansluitingen van harde constructieonderdelen (funderingspoer) op het dijk- lichaam kunnen extra gevoelig zijn voor materiaaluitspoeling door geconcentreerde oppervlakteafstroming bij neerslag of golfoverslag. Bij plaatsing van windturbines op het buitentalud van een waterkering vormen de aansluitingen extra gevoelige punten voor erosie/materiaaluitspoeling bij golfaanval. Op het binnentalud kan erosie optreden door stroming.	1 till 2	3
During and after dismantling				
3.1	Some effects of exploitation phase will stay present if foundation piles stay in soil	Indien de fundering geheel of deels achterblijft, zullen verschillende effecten die een rol (kunnen) spelen in de beheer- en exploitatiefase ook van toepassing (kunnen) zijn in de periode na demonteren van de turbine. Hierbij wordt bijvoorbeeld gedacht aan kwelwegverkorting bij doorsnijding van slecht waterdoorlatende lagen, door optreden van verschilzetting of door degradatie van het beton.	1 till 3	3
3.2	Removing foundations lowers (temporarily) height of defence	Het verwijderen van het funderingsblok, inclusief het bovenste deel van de funderingspalen tot een niveau van 2m onder de bovenkant van de bekleding zou gevolgen kunnen hebben voor de functionaliteit van de waterkering: Bij het verwijderen verandert het dwarsprofiel (lokale verlaging/versmalling inclusief verwijderen van de bekleding) en daarmee mogelijk ook (tijdelijk) de hoogte en stabiliteit van de waterkering.	1	3
3.3	Pile removing; effects of fill material	Het verwijderen van de fundering inclusief de volledige paalfundering zou gevolgen kunnen hebben voor de functionaliteit van de waterkering: bij het verwijderen van de palen dienen de gaten met geschikt materiaal te worden gevuld. Bij vervanging van palen door opvulmaterialen (bentoniet, cement o.i.d.) kunnen niet alle effecten worden weggenomen.	1 till 3	3
3.4	Removal equipment damages dike	De door de sloopwerkzaamheden veroorzaakte belastingen kunnen de functionaliteit van de waterkering tijdelijk beïnvloeden. Hierbij wordt gedacht aan beïnvloeding van de stabiliteit van de waterkering door betreding van zwaar materieel en eventueel veroorzaakte trillingen.	1 till 2	2

Zone 1:On flood defence, till the inner toe
Zone 2: 1/20 x tip height of the turbine
Zone 3: 1/2 x rotor diameter
Zone 4: Tip height
Zone 5: From tip height and further
STBK: Stabiliteit bekleding: stability of revetment, can have an effect on multiple failure mechanisms

Figure B.2: Risk database (2)

ID	Risks known (5 is known, 1 is unknown)	When is the risk substantial?	Realstic mitigating measures	Risk after mitigating measures (5 is high, 1 small)	source_1	source_2	Failure mechanism_1	Failure mechanism_2	Failure mechanism_3
1.1	4	Boulder clay (keileem) or loosely packed sand	Non-vibrating pile driving system	1	Afsluitdijk + Krammer	NOP	Sliding inner+ outer slope		
1.2	5	Non-vibrating pile driving system	Non-vibrating pile driving system	1	Afsluitdijk + Krammer		Sliding inner+ outer slope		
1.3	4	Boulder clay or loosely packed sand and slope larger than 1:4	Non-vibrating pile driving system	1	Afsluitdijk + Krammer	NOP	Erosion first bank		
1.4	4	Polders	not needed	1	Afsluitdijk + Krammer	NOP	Piping		
1.5	5		Non-vibrating pile driving system	1	Afsluitdijk + Krammer		Overflow/overto pping		
1.6	5		Heavy, wide construction roads and repair damage. Construction in low season	1	NOP	Krammer	Overflow/overto pping	Sliding inner+ outer slope	
1.7	5	If stability of dike is low	Agreement with contractor on damage repair, possible pile foundations for cranes, parts coming from water	1	Afsluitdijk + Krammer		Erosion outer slope	Sliding inner+ outer slope	STBK
1.8	5	High water pressures in layers below, polders	Calculations for stability, sheet piles and location of cables should be good. Construction in low season.	1	Afsluitdijk + Krammer	NOP	Erosion inner slope	Piping	STBK
2.1	1	depends on foundation (interaction with pile distance, conrete, mass tower, turning speed)	Larger foundation, higher safetyfactors, do more calculations	5	Afsluitdijk + Krammer	NOP (Noordoostp older)	Many mechanisms		
2.2	1	slope 1 on 4 etc. If water gets locked up between foundation and low permeable layer	no	1	Afsluitdijk + Krammer		Erosion first bank		
2.3	3		Make a drainage system	5	Afsluitdijk + Krammer	Haringvliet	Sliding inner+ outer slope		
2.4	3	If large deformation develop around the foundation	Apply skirt or add soil when needed	2	Afsluitdijk + Krammer	NOP	Piping	Sliding inner+ outer slope	
2.5	4	when turbines is on dike	There are regulations for cables and pipes near flood defences which cover this risk	1	Afsluitdijk + Krammer		STBK		
2.6	3	Pipe in clay layers	There are regulations for cables and pipes near flood defences which cover this risk	1	Afsluitdijk + Krammer		Piping		
2.7	3	Pipe in clay layers	There are regulations for cables and pipes near flood defences which cover this risk	1	Afsluitdijk + Krammer		Overtopping		
2.8	1	Polders		5	Afsluitdijk + Krammer		Overflow/overto pping	Sliding inner+ outer slope	STBK

Figure B.3: Risk database (3)

ID	Risks known (5 is known, 1 is unknown)	When is the risk substantial?	Realstic mitigating measures	Risk after mitigating measures (5 is high, 1 small)	source_1	source_2	Failure mechanism_1	Failure mechanism_2	Failure mechanism_3
2.9	1	Polders		5	Afsluitdijk + Krammer		Overflow/overto pping	Sliding inner+ outer slope	STBK
2.10	1			5	Afsluitdijk + Krammer		Overflow/overto pping	STBK	
2.11	5		Heavy, wide construction roads and repair damage. Construction in low season	1	NOP	Krammer	Overflow/overto pping	Sliding inner+ outer slope	
2.12	5	If stability of dike is low	Agreement with contractor on damage repair, possible pile foundations for cranes, parts coming	1	Afsluitdijk + Krammer		Erosion outer slope	Sliding inner+ outer slope	
2.13	5		Erosion resistent connections	2	Afsluitdijk + Krammer		STBK		
3.1	3	see those other ID's		2	Afsluitdijk + Krammer		Multiple mechanisms		
3.2	4	Low height of flood defence.	Remove only the top part of the piles	1	Afsluitdijk + Krammer		Piping	Sliding inner+ outer slope	
3.3	2	many piles	Remove only the top part of the piles	4	Afsluitdijk + Krammer		Multiple mechanisms		
3.4	5	If stability of dike is low	Agreement with contractor on damage repair, possible pile foundations for cranes, parts coming from water	1	Afsluitdijk + Krammer	0	Erosion outer slope	Sliding inner+ outer slope	STBK

Zone 1:On flood defence, till the inner toe
Zone 2: 1/20 x tip height of the turbine
Zone 3: 1/2 x rotor diameter
Zone 4: Tip height
Zone 5: From tip height and further
STBK: Stabiliteit bekleding: stability of revetment, can have an effect on multiple failure mechanisms

Figure B.4: Risk database (4)

Risks with very small probability & only occur in specific situations

ID	Risk / Effect	Situation risk is present
1.1	Instability resulting from liquefaction due to pile driving vibrations	Boulder clay or loosely packed sand
1.3	Flow slides resulting from liquefaction (zettingsvloeiing) due to pile driving vibrations	Boulder clay or loosely packed sand and slope larger than 1:4
1.4	Penetration of impermeable layers (hydraulische kortsluiting)	In polders and impermeable layers, but risk is extremely small
2.2	Flow slide as result of liquefaction by wind related vibrations of turbine	Boulder clay or loosely packed sand and slope larger than 1:4
2.4	Space below foundation and soil gives seepage	Very small risk
2.14	Morphological dynamics can erode the area around the foundation	If the foundation is built in the water in a morphological active area

Well known risks from other construction projects

ID	Risk / Effect	Mitigating measure
1.2	Dynamic loads due to pile driving	Use of non vibrating pile driving system
1.8	Excavations temporary works	Calculations for stability, construction outside storm season
3.3	Pile removing: effects of fill material	Risks are known, because this is done often

Risks which can be eliminated or controlled by policy

ID	Risk / Effect	Measure
1.5	Soil consolidation due to pile driving	Use of non vibrating pile driving system
1.6, 2.11	Heavy equipment causes vibrations, settlements and track forming	Heavy, wide construction roads and repair damage. Construction in low season
1.7, 2.12, 3.4	Construction road traffic, maintenance & removal equipment damages flood defence	Agreement with contractor on damage repair, possible pile foundations for cranes, parts coming from the water
2.5	Space between foundation and soil causes loss of grass revetment	A skirt can be applied around the foundation
2.6	Erosion & seepage along cables perpendicular through dike	There are regulations for cables and pipes near flood defences which cover this risk
2.7	Erosion & seepage along cables lateral with dike	There are regulations for cables and pipes near flood defences which cover this risk
2.13	Erosion around foundation due to wave attack or overflow	Construct erosion resistance connections around the foundation
2.15	Lack of maintenance on the WT causes increased failure probabilities	Make a plan for the responsibility of the maintenance and dismantling if needed in advance
3.1	Some effects of the exploitation phase will stay present if foundation piles are not removed	Same as other measures mentioned and regular inspections
3.2	Removing foundations lowers (temporarily) height of defence	Remove only the top part of the piles and

Figure B.5: Filtered Risks from the database

Appendix C

Penetration model equations

This appendix gives the equations for the different models given in Chapter 4.

C.1 Young's penetration equations

For $V < 61$ m/s:

$$D = 0.0008(\frac{m}{A})^{0.7} \cdot S \cdot N \cdot ln(1 + (2.15 \cdot 10^{-4} \cdot V^2)) \tag{C.1}$$

For $V \geq 61$ m/s:

$$D = 0.00018(\frac{m}{A})^{0.7} \cdot S \cdot N \cdot (V - 30.5) \tag{C.2}$$

where:

- D: Penetration depth
- m: Mass of penetrator
- A: Cross-sectional area of penetrator
- S: S-number or index of penetrability
- N: Nose Performance Coefficient
- V: Velocity of penetrator

The S-number depends on the targeted material. There are different formulas for concrete, rock, ice and soil. The soil is of most interest in this thesis and can be found in Table C.1.

Table C.1: Soil S-numbers for Young's penetration equations (Young, 1997)

S-number	Target Description
2 - 4	Dense, dry, cemented sand. Dry caliche. Massive gypsite and selenite deposits.
4 - 6	Gravel deposits. Sand, without cementation. Very stiff and dry clay.
6 - 9	Moderately dense to loose sand, no cementation, water content not important
8 - 10	Soil fill material, with the S-number range depending on compaction.
5 - 10	Silt and clay, low to medium moisture content, stiff. Water content dominates penetrability.
20 - 30	Very soft, saturated clay. Very low shear strength.
30 - 60	Clay marine sediments, either currently (Gulf of Mexico) or recent geologically (mud deposits near Wendover, Utah).
> 60	It is likely that the penetration equations do not apply.

Young has given a formula for the Nose Performance Coefficient, Bernard has written it out in table which gives more insight in the values of the coefficient. This table is given in Table C.2. Due to the fact that the formula is created mainly for bombs, most values for N are rather high in the table. In the case study they are near Flat or Hemisphere.

Table C.2: Nose Performance Coefficient (Bernard, 1975)

Nose Shape	Nose Length-to Diameter Ratio	N
Flat	0	0.56
Hemisphere	0.5	0.65
Cone ogive**	1	0.82
Tangent	1.4	0.82
Tangent ogive	2	0.92
Cone	2	1.08
Tangent ogive	3	1.11
Tangent ogive	3,.5	1.19
Step cone	3	1.28
Biconic	3	1.31
Inverse ogive	3	1.32
Cone	3	1.33

C.2 Bernard method

$$D(S,V,w) = \frac{1}{c}[-(a + \frac{2}{3}b \cdot V) + \sqrt{(a + \frac{2}{3}b \cdot V)^2 + m \cdot c \cdot V^2}] \tag{C.3}$$

Where:

- D: Penetration depth
- m: Mass of penetrator
- V: Velocity of penetrator
- $a = \dfrac{\alpha \cdot d}{S \cdot N}$

- $b = \frac{d}{S \cdot N} \cdot \sqrt{\frac{3}{7} \cdot \beta \cdot m}$
- $c = \frac{\beta \cdot d^2}{S^2 \cdot N^2}$
- d: Projectile diameter
- S: S-number or index of penetrability, same as in Young's formula
- N: Nose Performance Coefficient, same as in Young's formula

For the empirical coefficients $\alpha = 2.2\text{e}6$ N/m and $\beta = 2.8\text{e}7$ N/m^3. These are universal constants, independent of projectile parameters and soil properties.

C.3 Ménard method

$$\frac{\delta}{\sqrt{WH}} \sim 0.03 \tag{C.4}$$

Where:

- δ: Penetration depth by Ménard
- W: Mass of dropping weight
- H: Dropping height

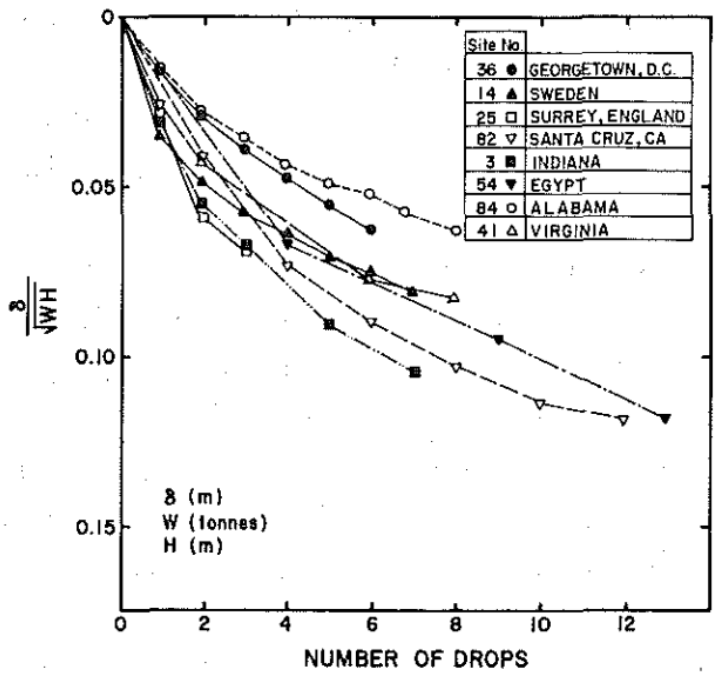

Figure C.1: Dynamic compacting results by Mayne (Mayne et al., 1984).

Appendix D

Sensitivity analysis graphs

The sensitivity analysis is based on a 2D horizontal soil surface. The standard parameters are given in Table D.1. Of all simulations in the sensitivity analysis multiple material points (MPs) have been selected. They are located at different locations below the surface. If there is high variability between the MPs in a graph, then that MP has probably 'jumped out' of the rest of the material.

Properties	**Nacelle**	**Soil**
Type	Solid	Solid
Initial porosity [-]	0.0	0.36
Density solid [kg/m^3]	11400	2650
Material model	Linear Elastic	Mohr-Coulomb
Young's modulus [kPa]	100000	30000
Poisson ratio [-]	0.3	0.3
Cohesion [kPa]	-	0
Friction Angle [°]	-	30
Dilatancy angle [°]	-	0
Tensile strength [kPa]	-	0

Table D.1: Material Properties

D.1 Friction angle

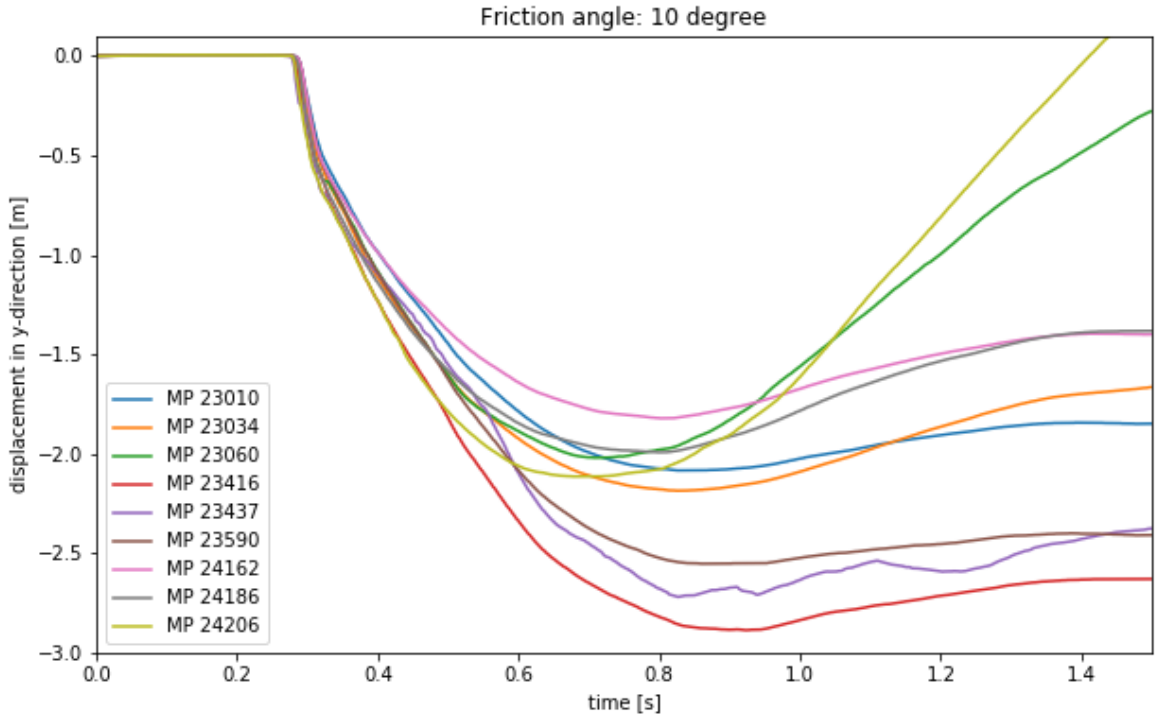

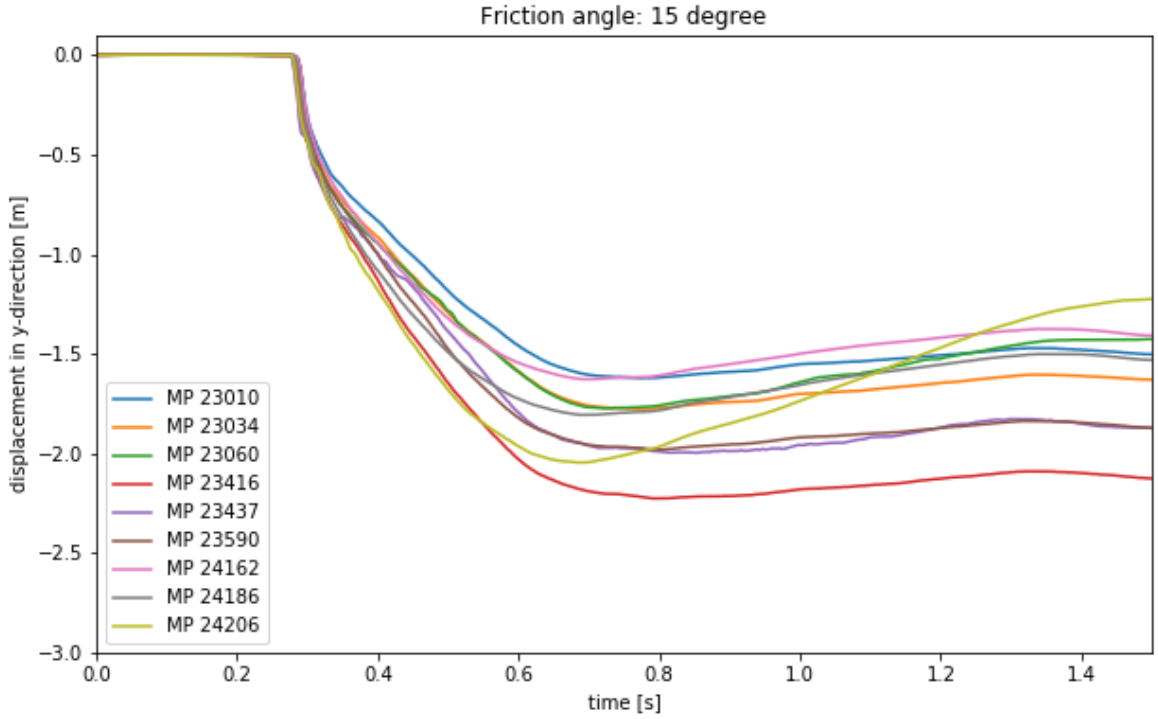

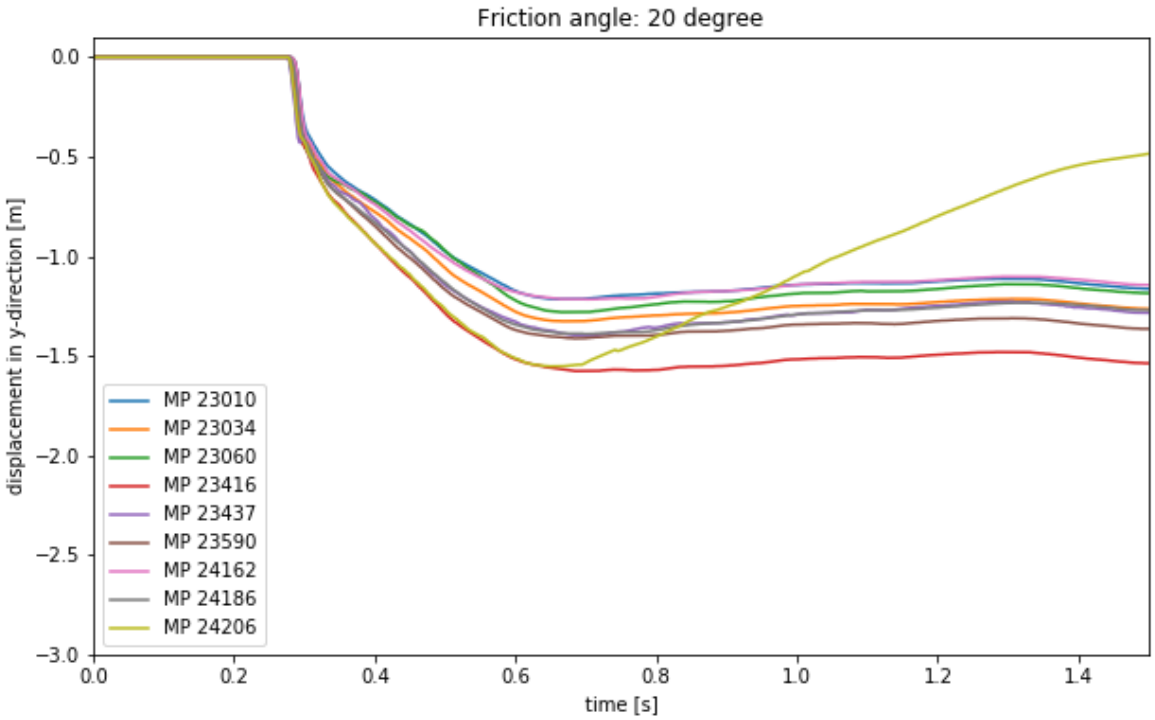
Friction angle: 20 degree
displacement in y-direction [m]
time [s]
MP 23010
MP 23034
MP 23060
MP 23416
MP 23437
MP 23590
MP 24162
MP 24186
MP 24206

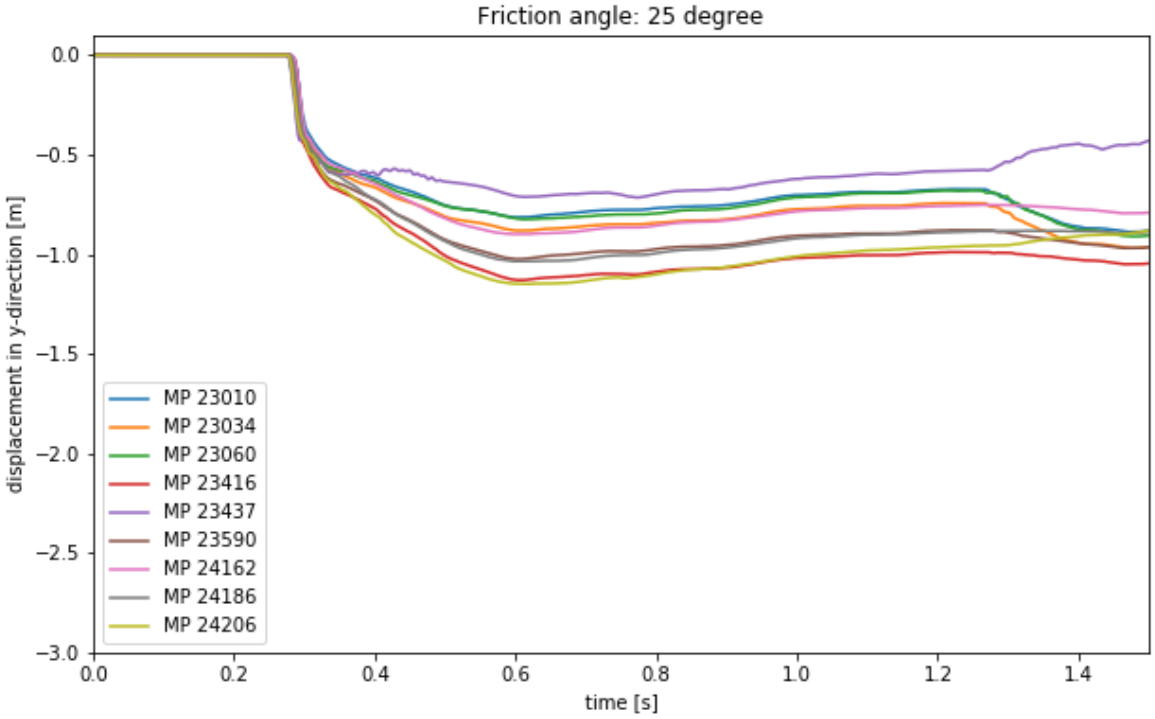
Friction angle: 25 degree
displacement in y-direction [m]
time [s]
MP 23010
MP 23034
MP 23060
MP 23416
MP 23437
MP 23590
MP 24162
MP 24186
MP 24206

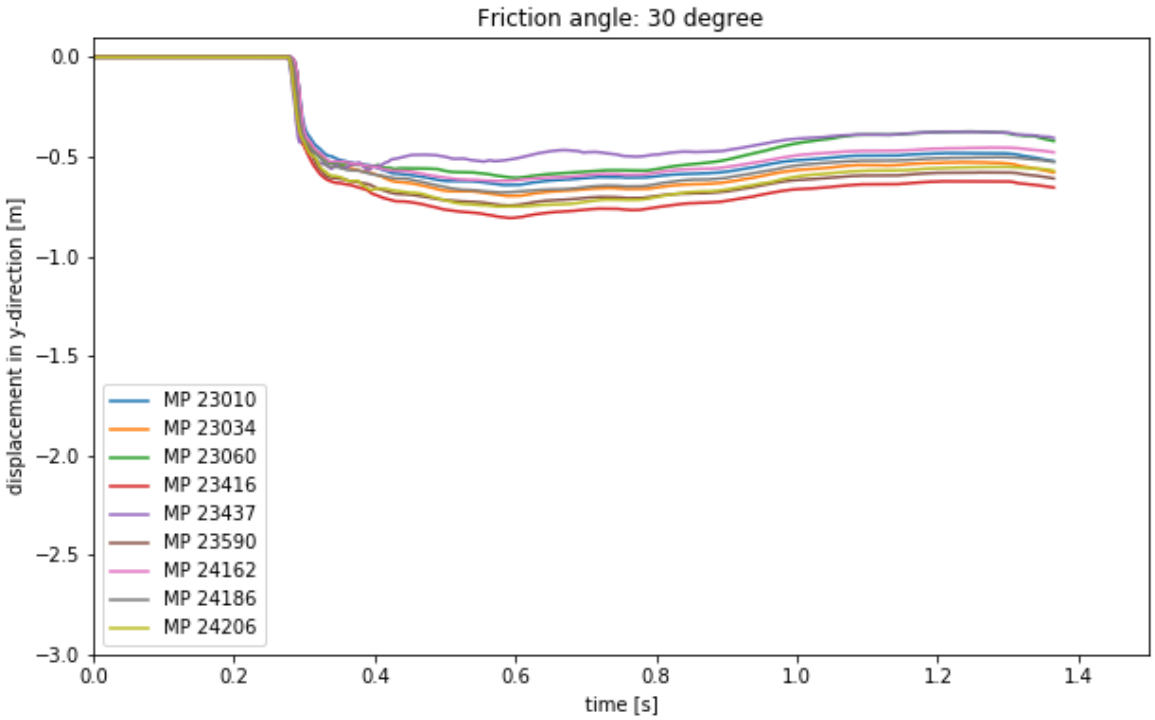
Friction angle: 30 degree
displacement in y-direction [m]
time [s]
MP 23010
MP 23034
MP 23060
MP 23416
MP 23437
MP 23590
MP 24162
MP 24186
MP 24206

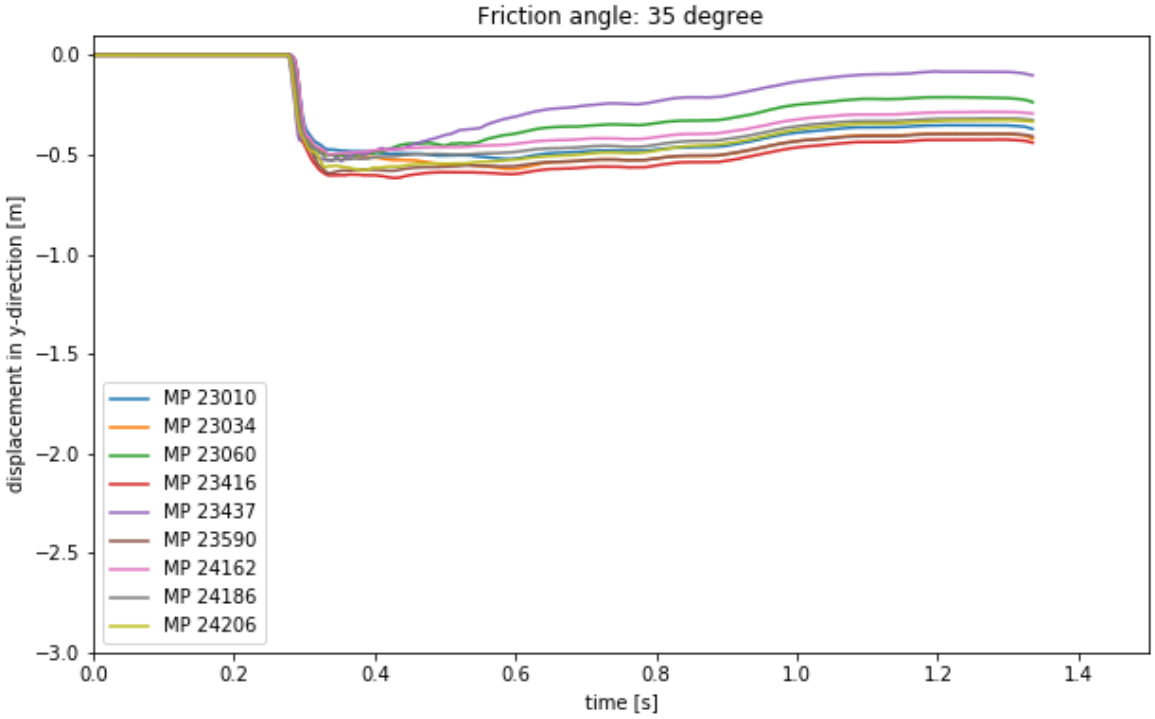
Friction angle: 35 degree
displacement in y-direction [m]
time [s]
MP 23010
MP 23034
MP 23060
MP 23416
MP 23437
MP 23590
MP 24162
MP 24186
MP 24206

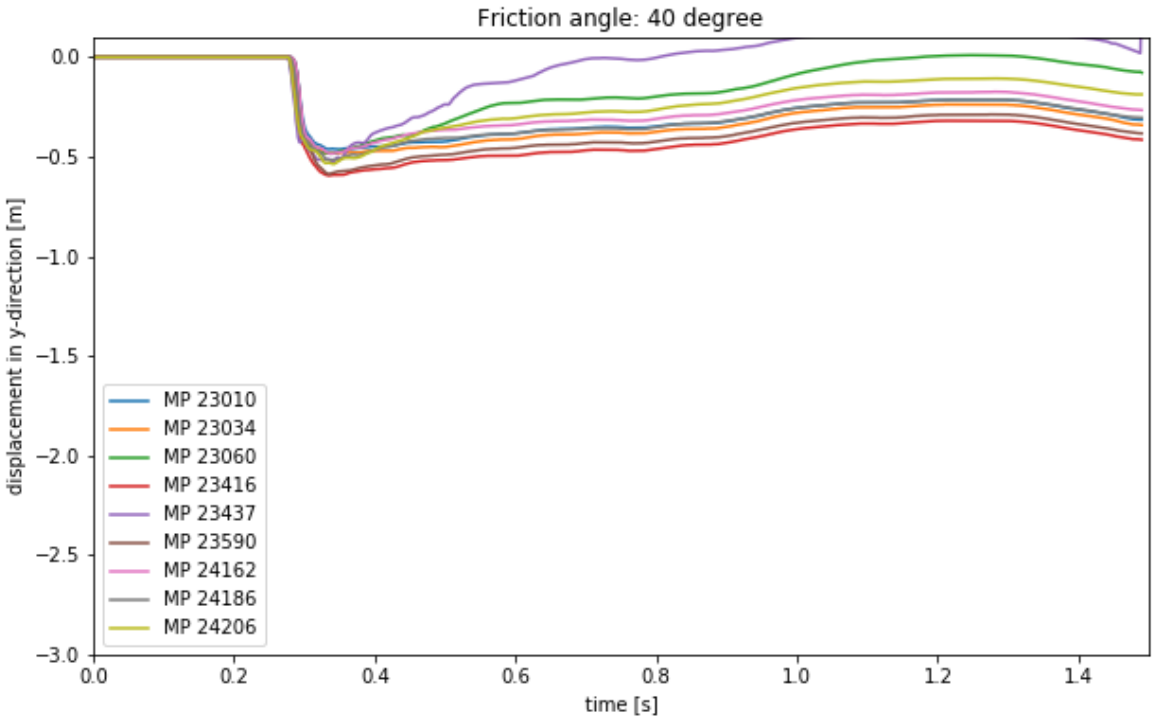
Friction angle: 40 degree
displacement in y-direction [m]
time [s]
MP 23010
MP 23034
MP 23060
MP 23416
MP 23437
MP 23590
MP 24162
MP 24186
MP 24206

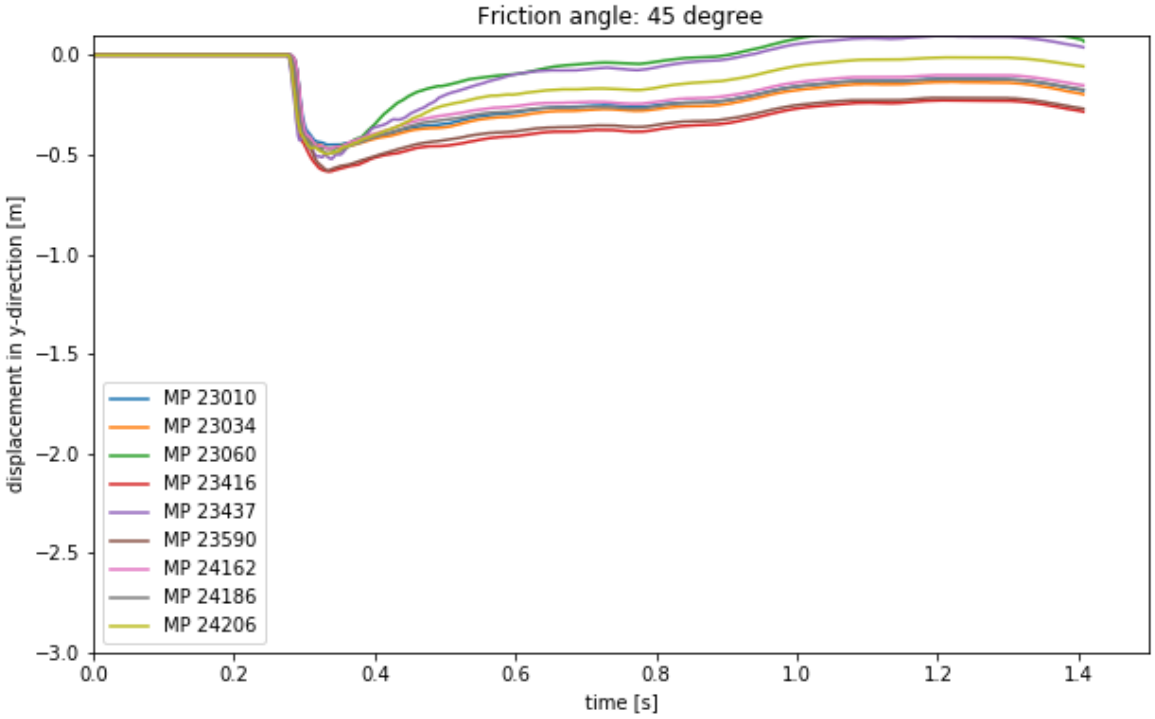
Friction angle: 45 degree
displacement in y-direction [m]
time [s]
MP 23010
MP 23034
MP 23060
MP 23416
MP 23437
MP 23590
MP 24162
MP 24186
MP 24206

D.2 Poisson's ratio

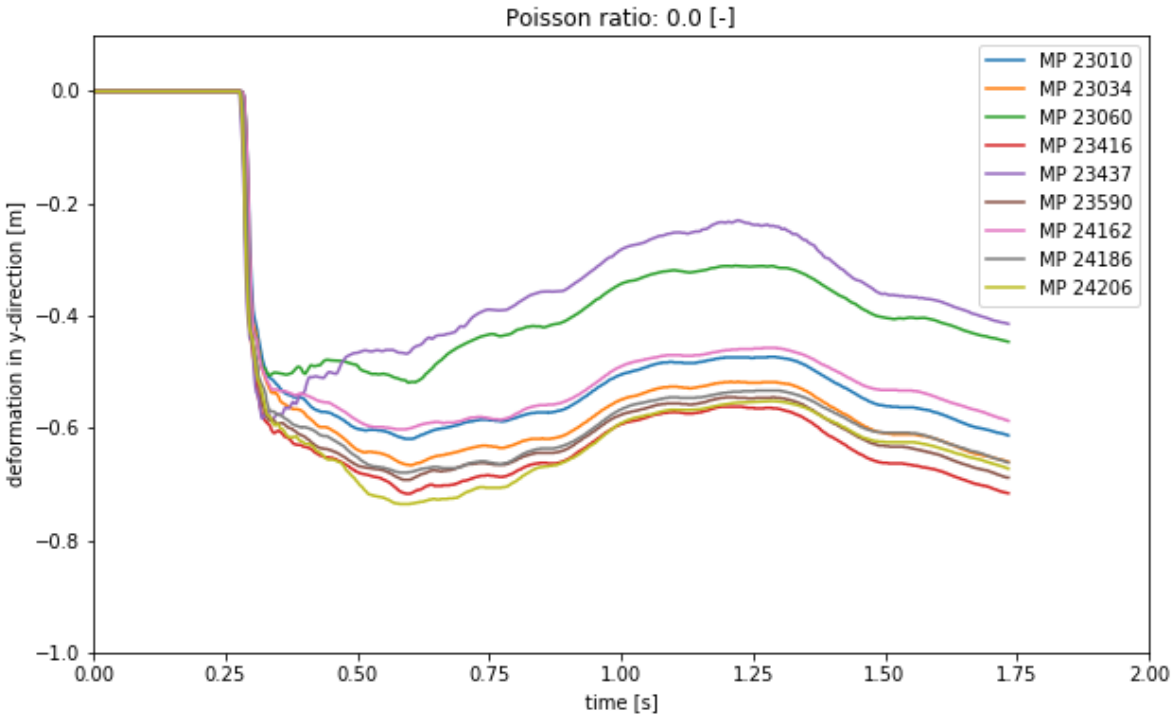

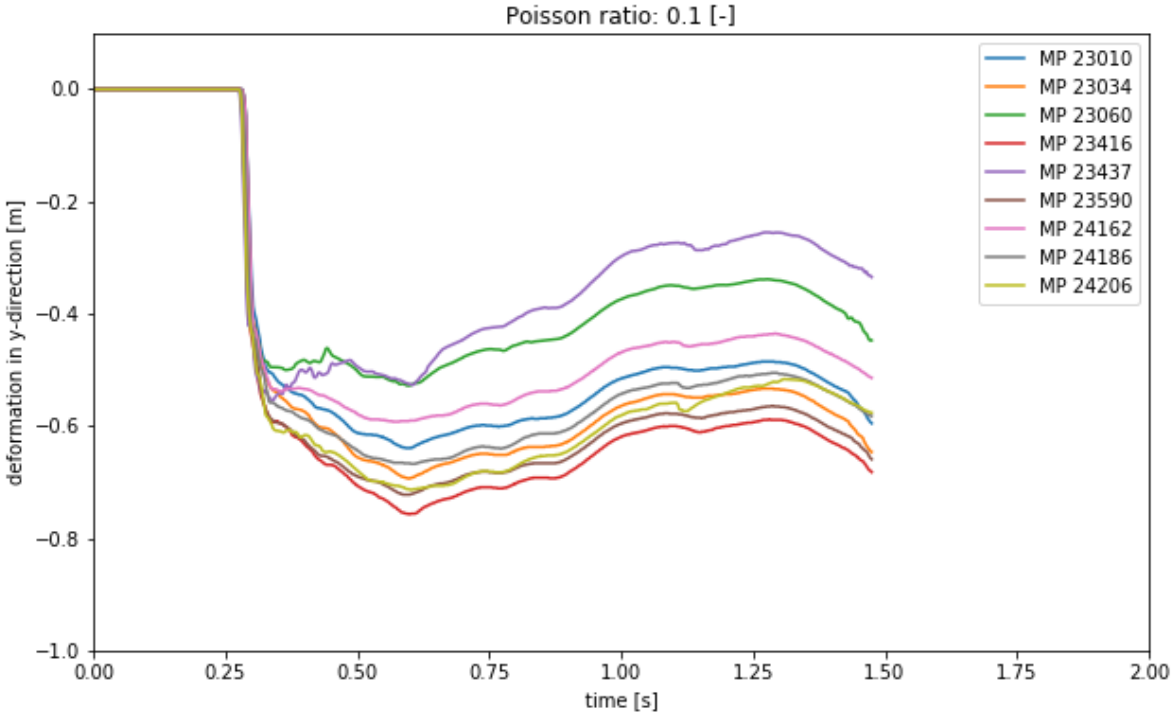

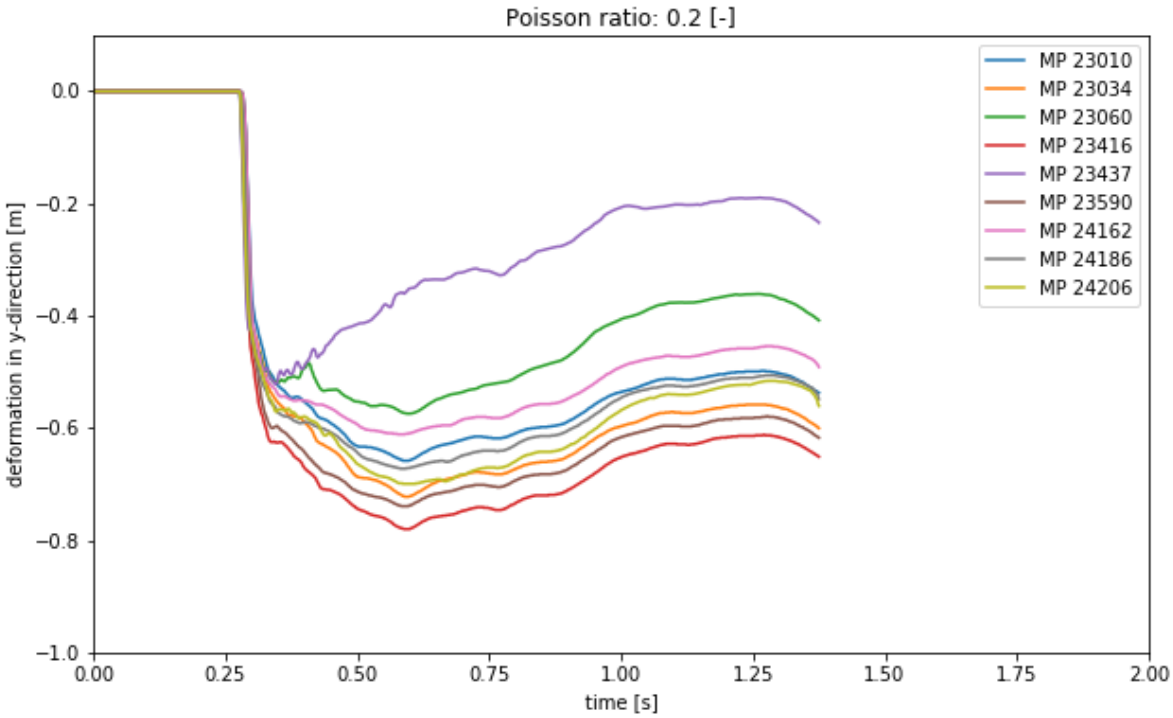
Poisson ratio: 0.2 [-]
deformation in y-direction [m]
time [s]
MP 23010
MP 23034
MP 23060
MP 23416
MP 23437
MP 23590
MP 24162
MP 24186
MP 24206

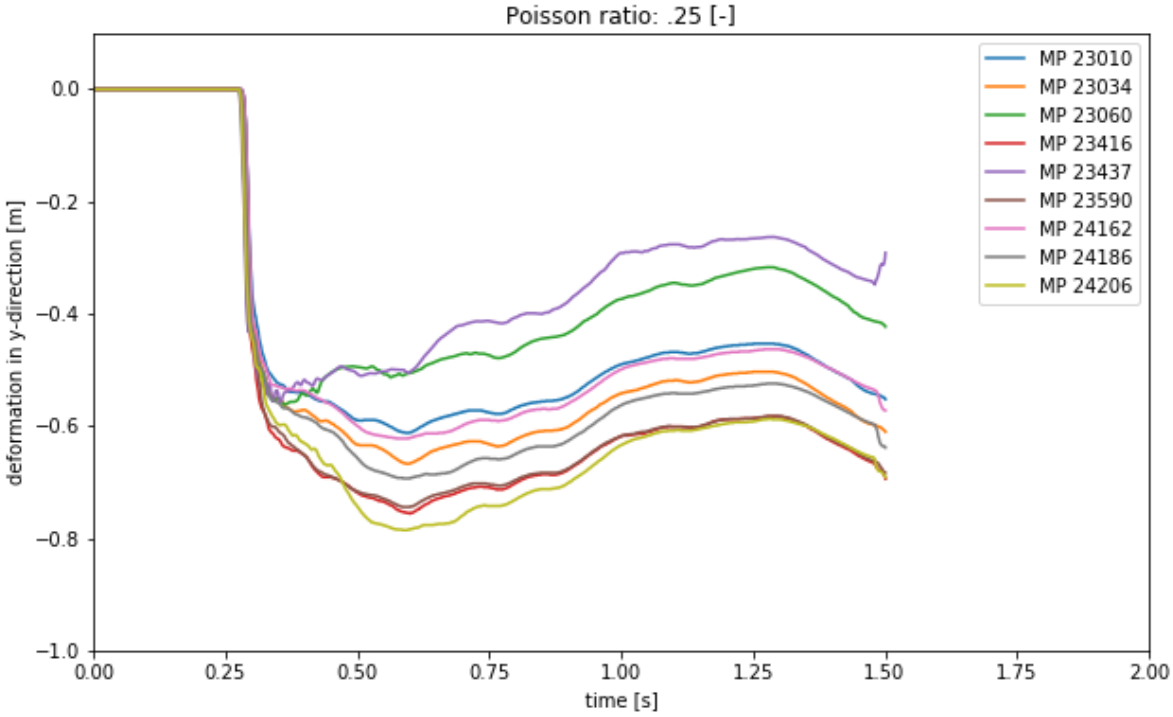
Poisson ratio: .25 [-]
deformation in y-direction [m]
time [s]
MP 23010
MP 23034
MP 23060
MP 23416
MP 23437
MP 23590
MP 24162
MP 24186
MP 24206

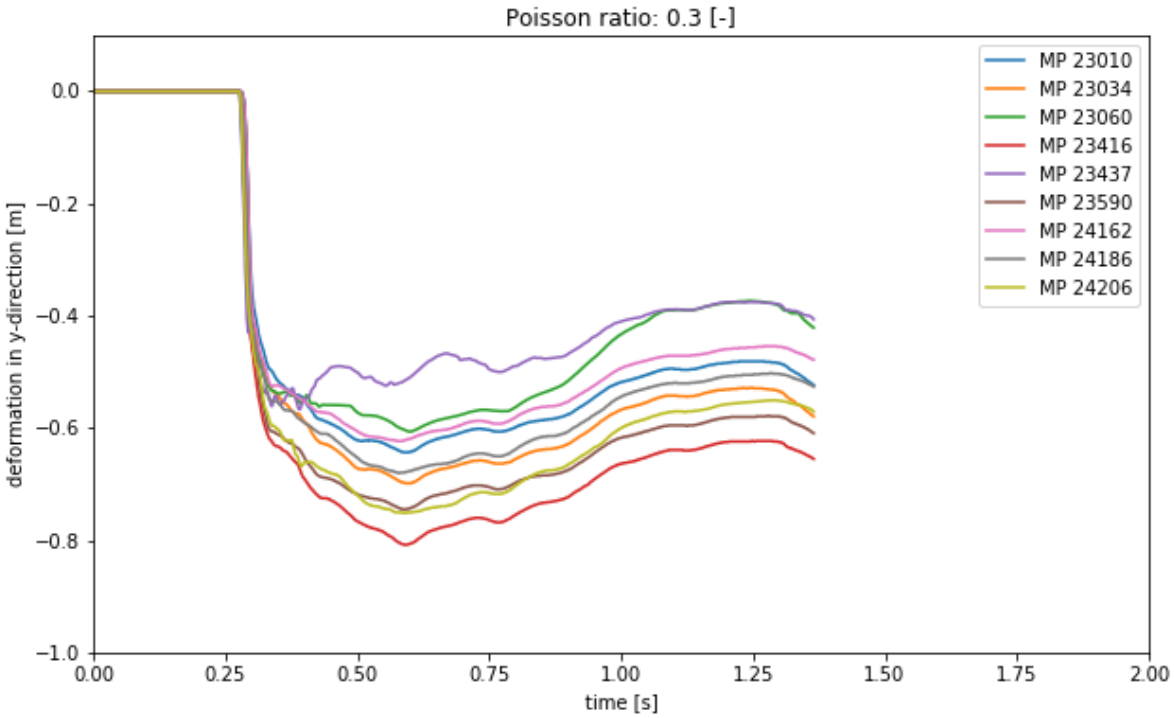
Poisson ratio: 0.3 [-]
MP 23010
MP 23034
MP 23060
MP 23416
MP 23437
MP 23590
MP 24162
MP 24186
MP 24206
deformation in y-direction [m]
time [s]
0.0
−0.2
−0.4
−0.6
−0.8
−1.0
0.00
0.25
0.50
0.75
1.00
1.25
1.50
1.75
2.00

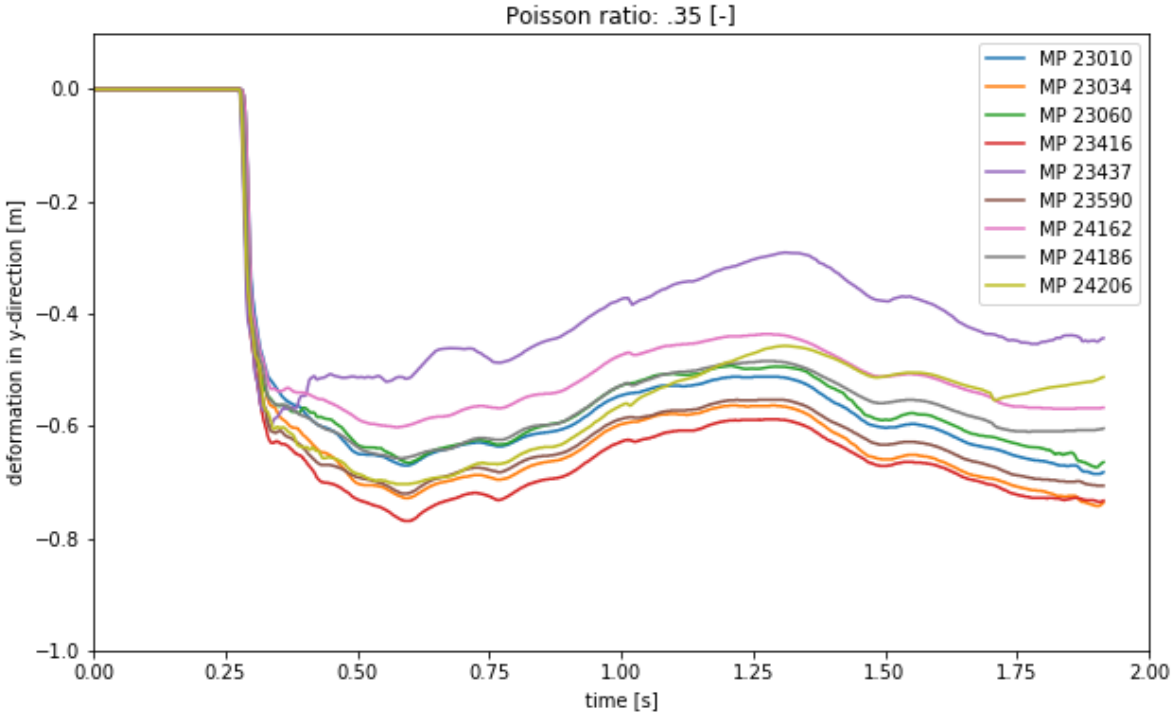
Poisson ratio: .35 [-]
MP 23010
MP 23034
MP 23060
MP 23416
MP 23437
MP 23590
MP 24162
MP 24186
MP 24206
deformation in y-direction [m]
time [s]
0.0
−0.2
−0.4
−0.6
−0.8
−1.0
0.00
0.25
0.50
0.75
1.00
1.25
1.50
1.75
2.00

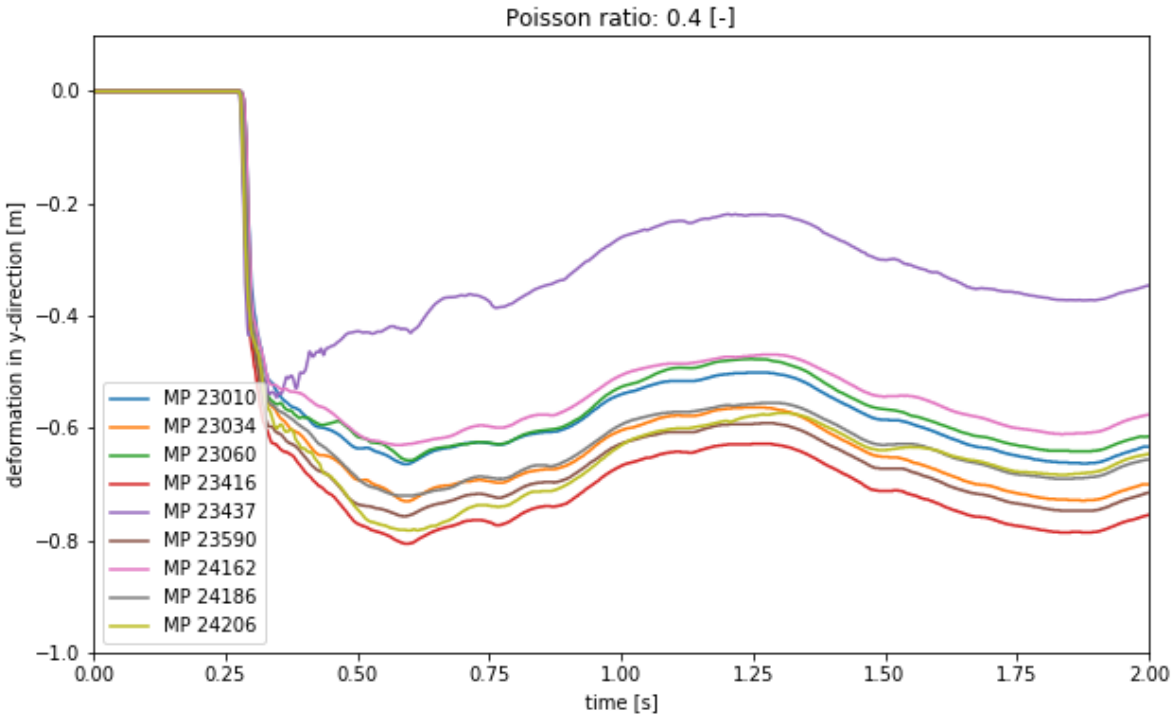
Poisson ratio: 0.4 [-]
deformation in y-direction [m]
time [s]
MP 23010
MP 23034
MP 23060
MP 23416
MP 23437
MP 23590
MP 24162
MP 24186
MP 24206

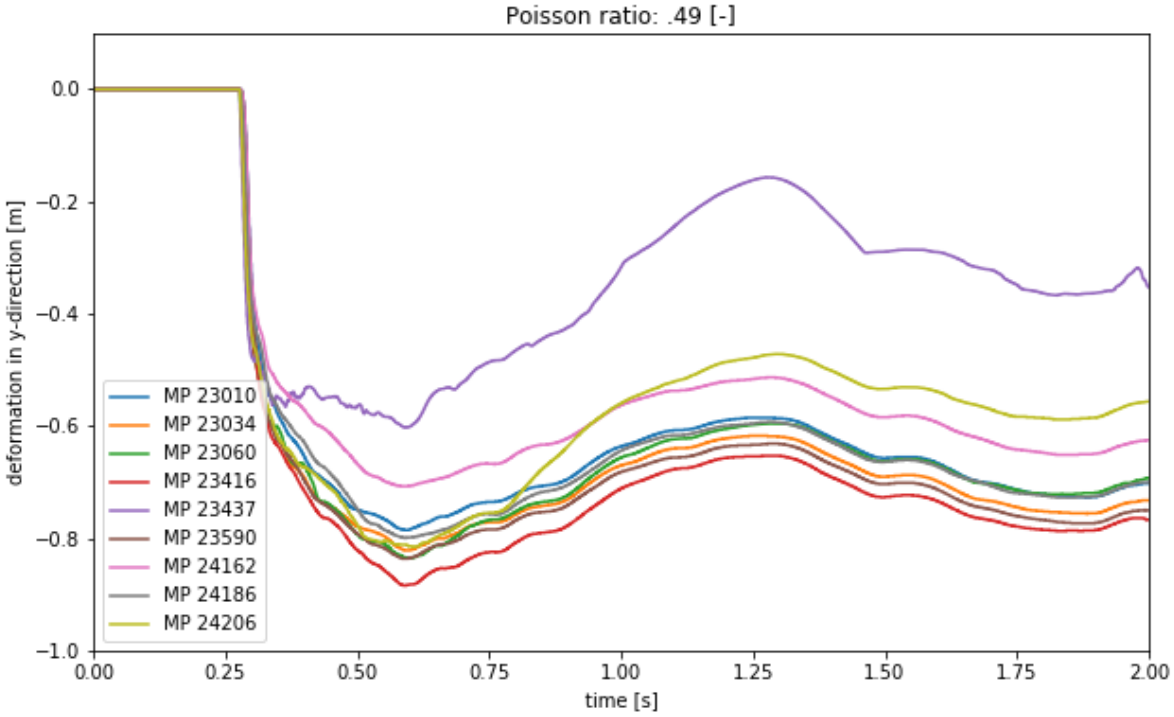
Poisson ratio: .49 [-]
deformation in y-direction [m]
time [s]
MP 23010
MP 23034
MP 23060
MP 23416
MP 23437
MP 23590
MP 24162
MP 24186
MP 24206

D.3 Stiffness

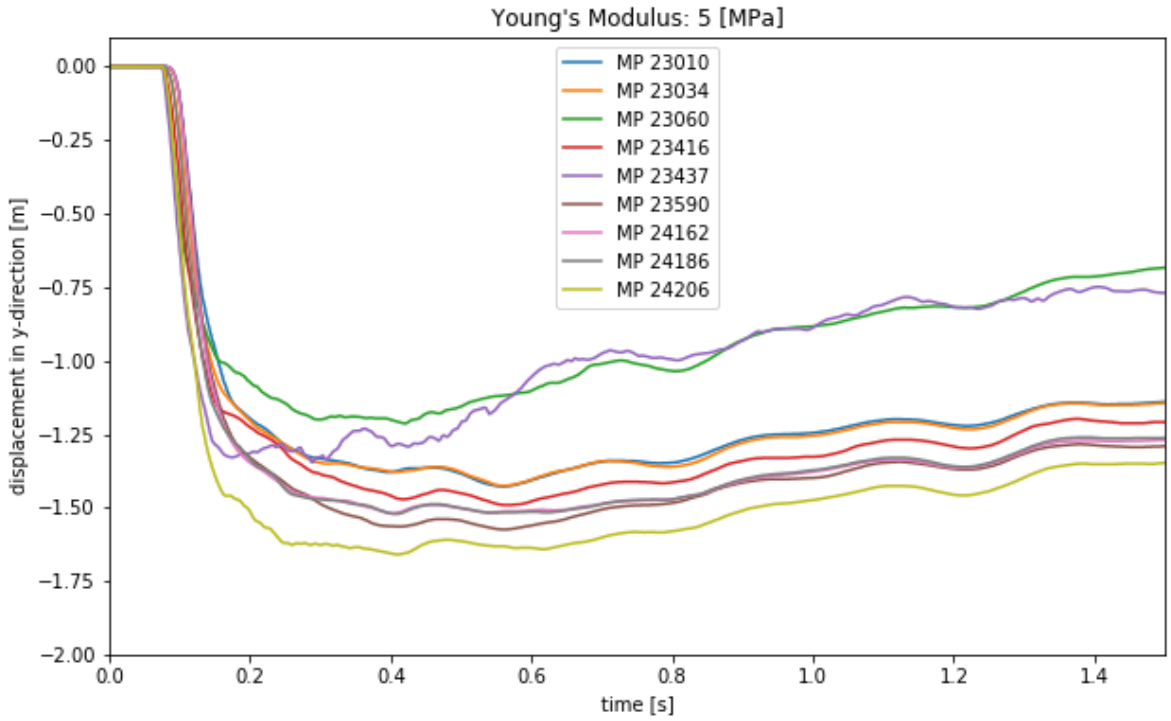

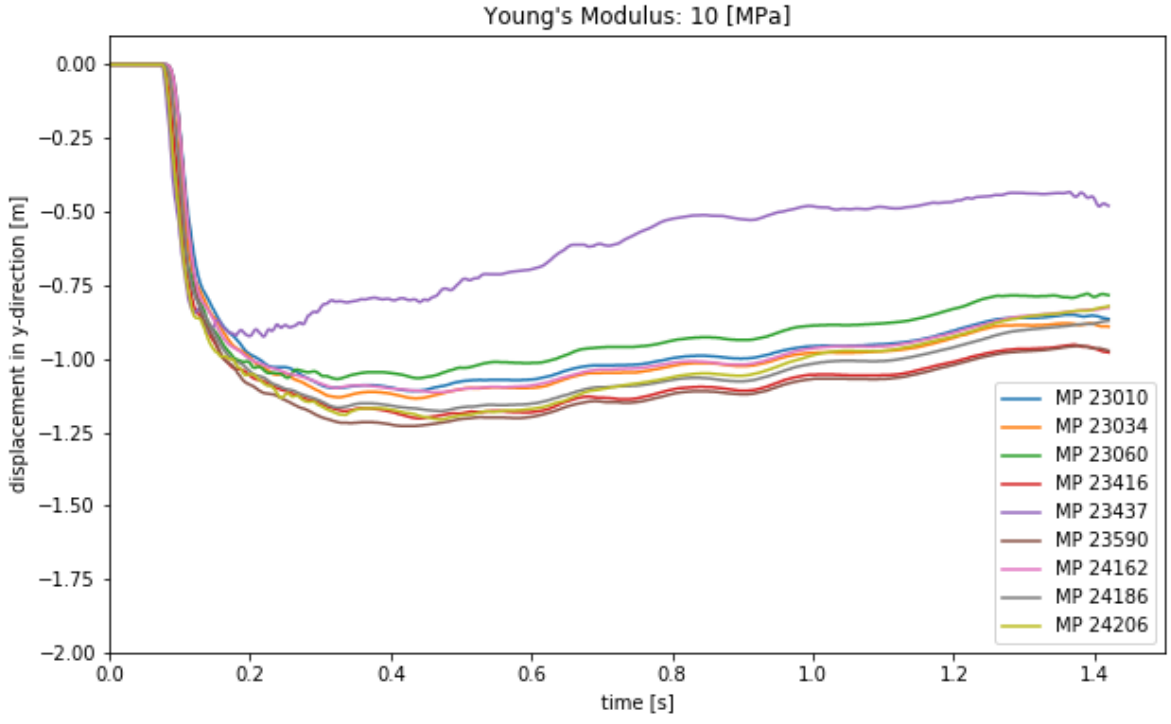

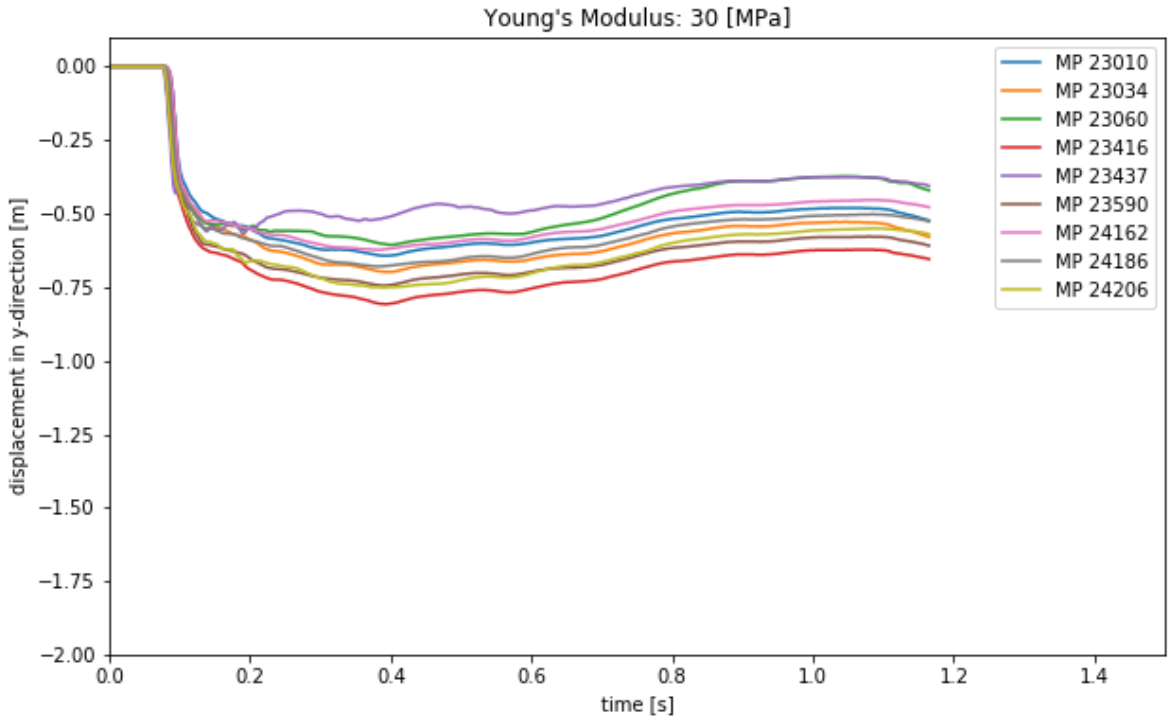
Young's Modulus: 30 [MPa]
displacement in y-direction [m]
time [s]
MP 23010
MP 23034
MP 23060
MP 23416
MP 23437
MP 23590
MP 24162
MP 24186
MP 24206

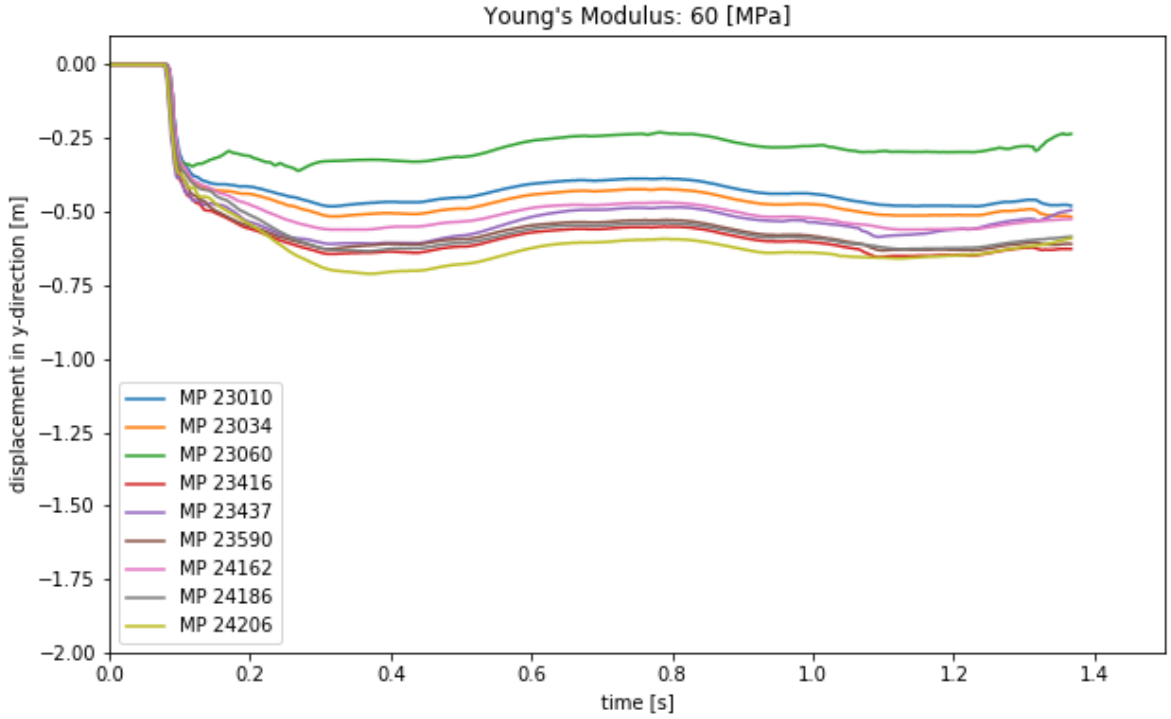
Young's Modulus: 60 [MPa]
displacement in y-direction [m]
time [s]
MP 23010
MP 23034
MP 23060
MP 23416
MP 23437
MP 23590
MP 24162
MP 24186
MP 24206

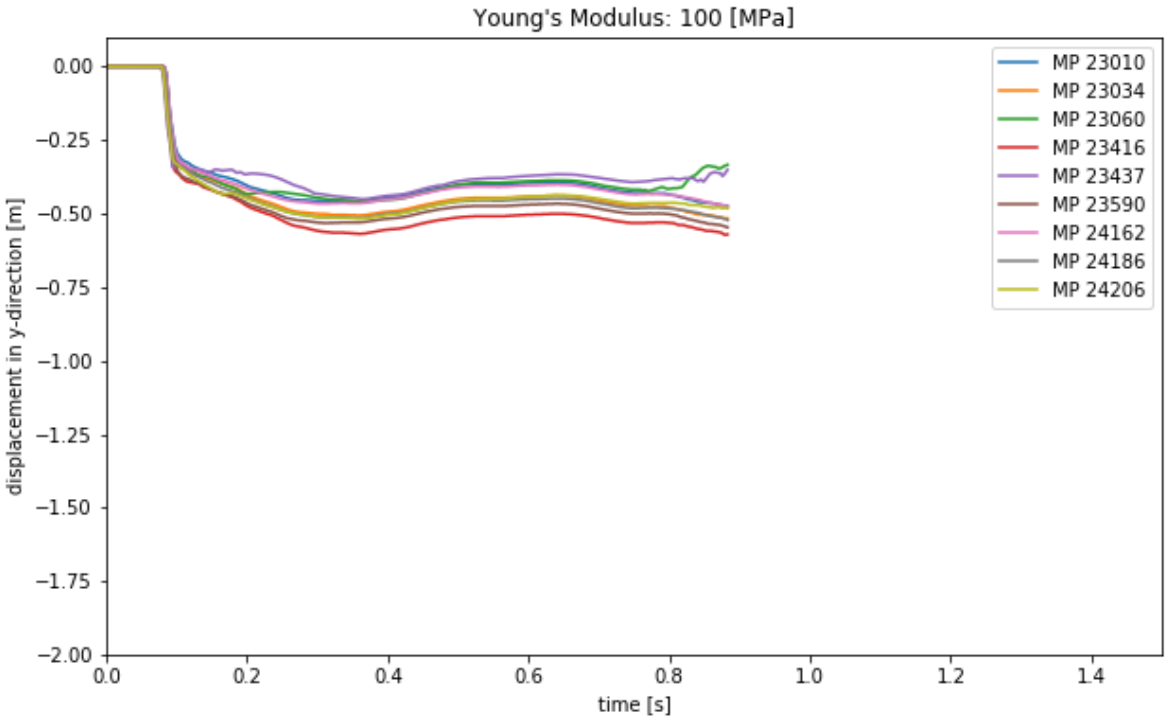

D.4 Unit weight of the soil

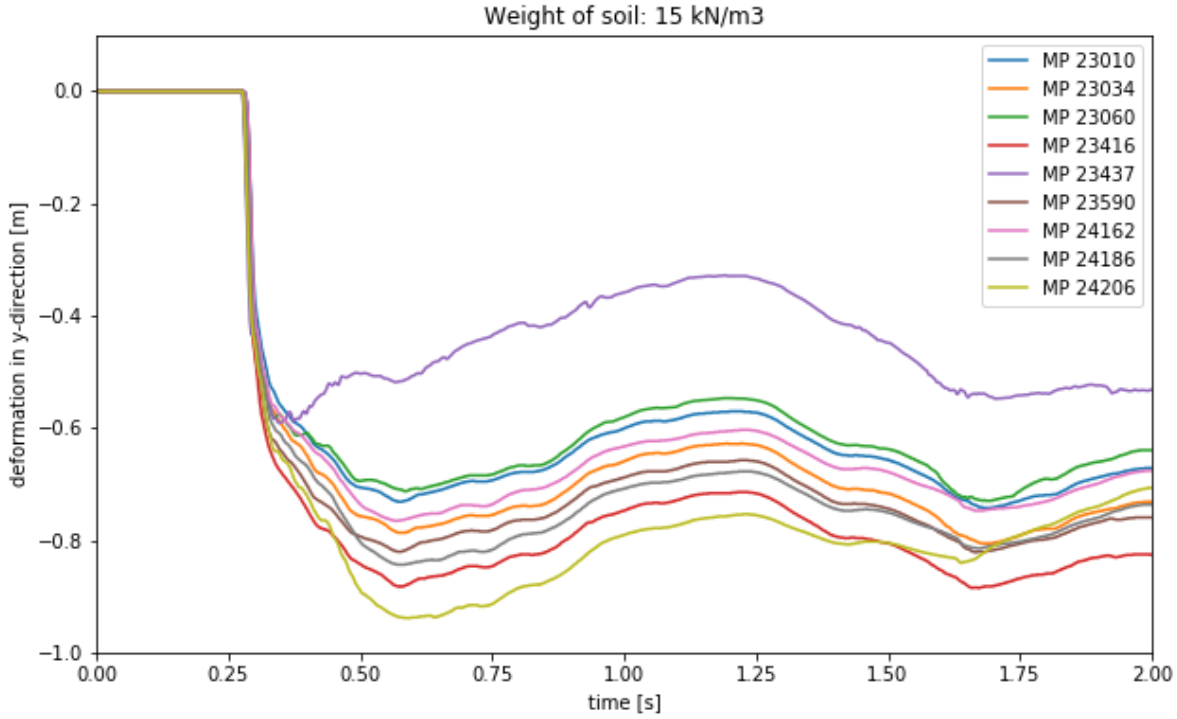

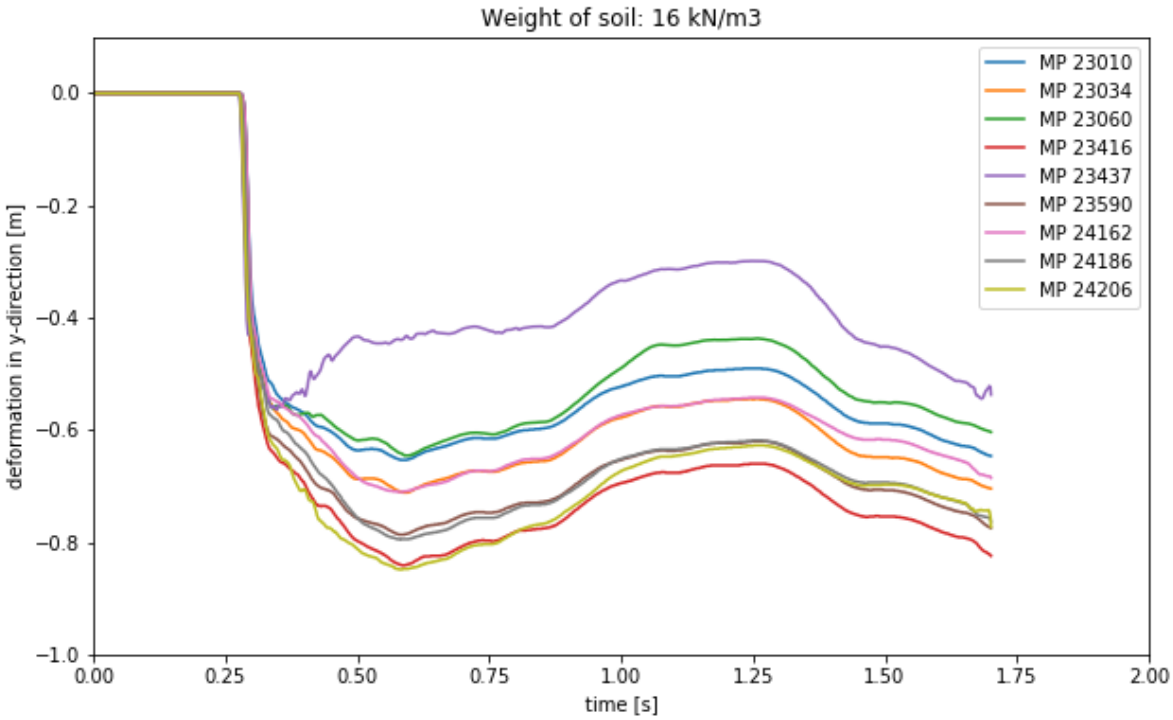
Weight of soil: 16 kN/m3
MP 23010
MP 23034
MP 23060
MP 23416
MP 23437
MP 23590
MP 24162
MP 24186
MP 24206
deformation in y-direction [m]
0.0
−0.2
−0.4
−0.6
−0.8
−1.0
0.00
0.25
0.50
0.75
1.00
1.25
1.50
1.75
2.00
time [s]

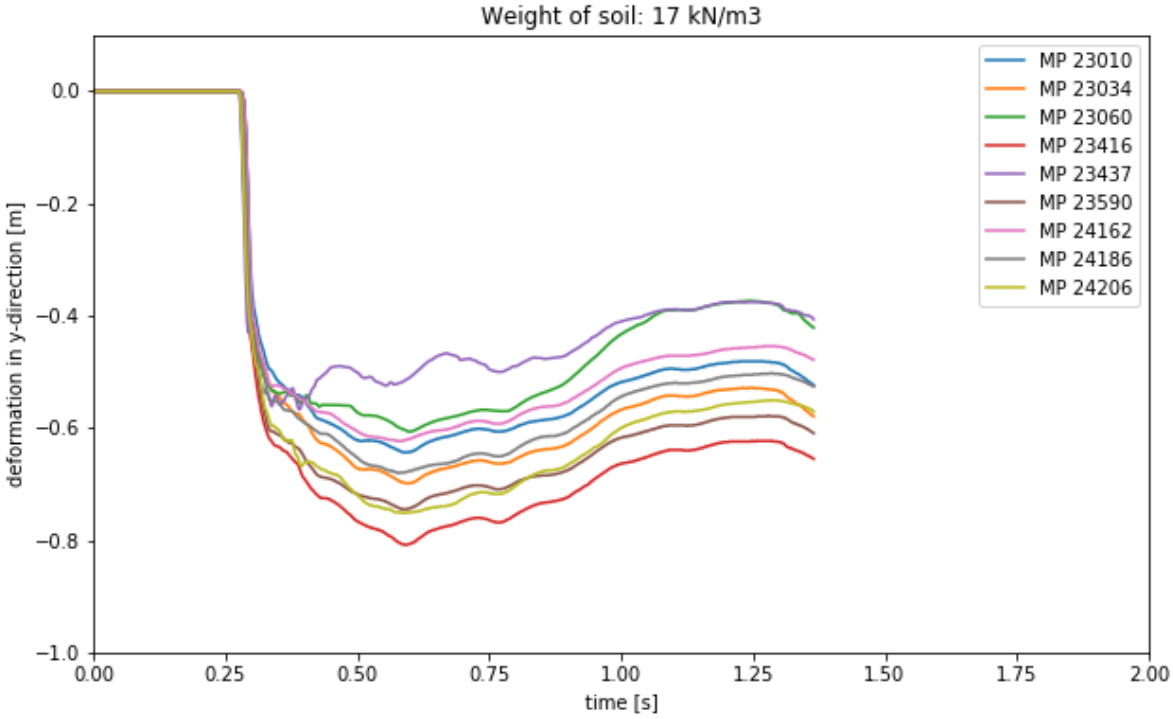
Weight of soil: 17 kN/m3
MP 23010
MP 23034
MP 23060
MP 23416
MP 23437
MP 23590
MP 24162
MP 24186
MP 24206
deformation in y-direction [m]
0.0
−0.2
−0.4
−0.6
−0.8
−1.0
0.00
0.25
0.50
0.75
1.00
1.25
1.50
1.75
2.00
time [s]

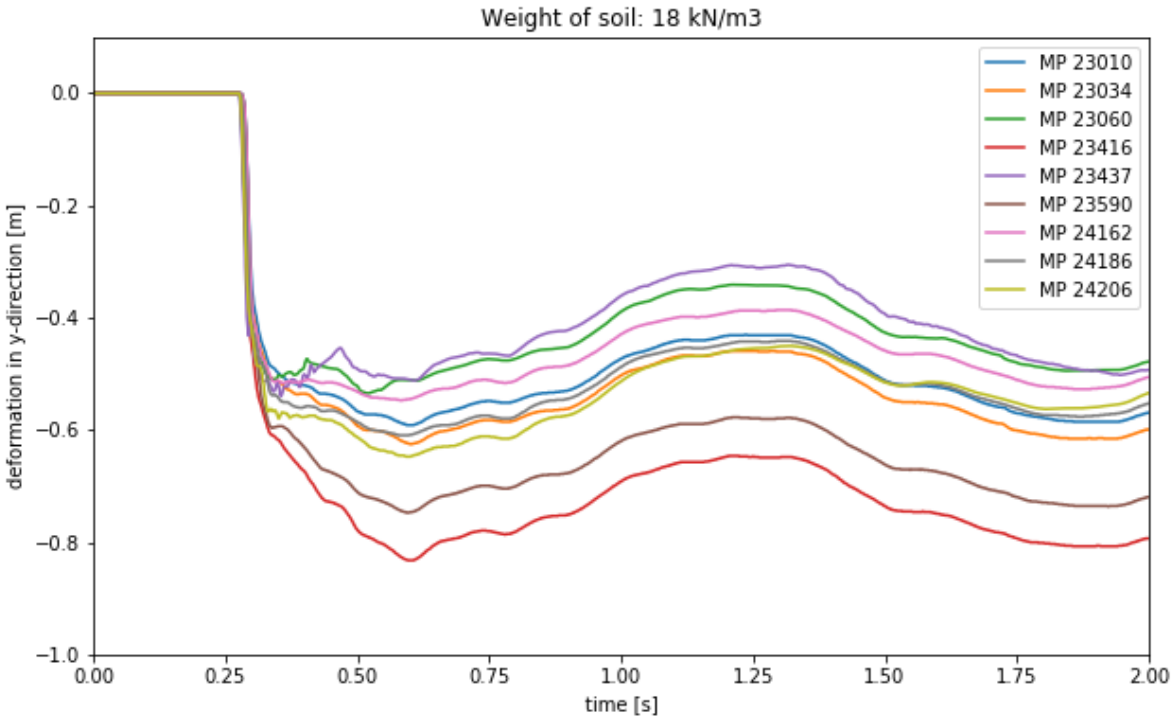
Weight of soil: 18 kN/m3
MP 23010
MP 23034
MP 23060
MP 23416
MP 23437
MP 23590
MP 24162
MP 24186
MP 24206
deformation in y-direction [m]
time [s]
0.0
−0.2
−0.4
−0.6
−0.8
−1.0
0.00
0.25
0.50
0.75
1.00
1.25
1.50
1.75
2.00

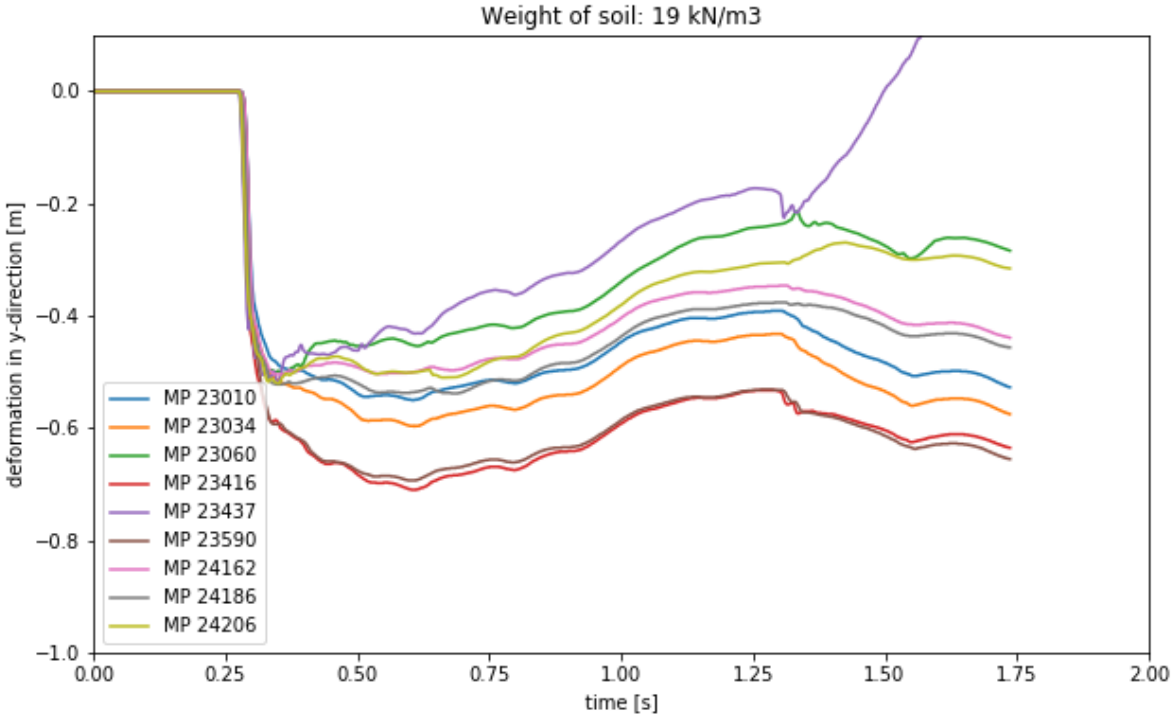
Weight of soil: 19 kN/m3
MP 23010
MP 23034
MP 23060
MP 23416
MP 23437
MP 23590
MP 24162
MP 24186
MP 24206
deformation in y-direction [m]
time [s]
0.0
−0.2
−0.4
−0.6
−0.8
−1.0
0.00
0.25
0.50
0.75
1.00
1.25
1.50
1.75
2.00

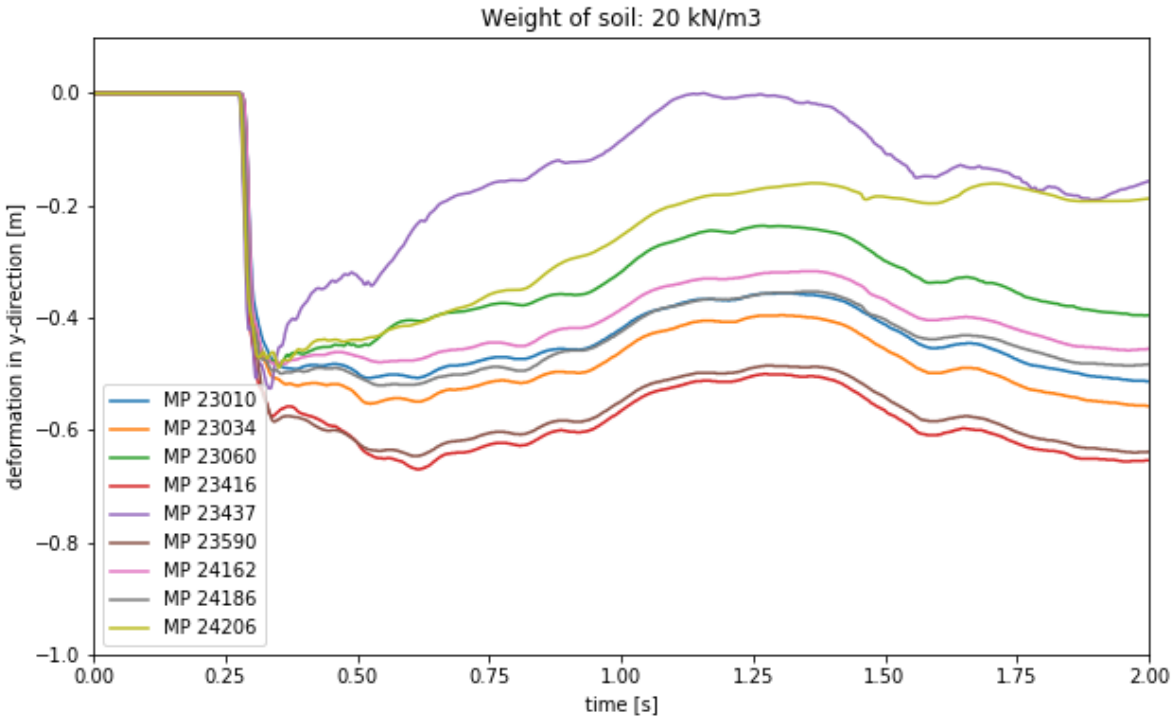
Weight of soil: 20 kN/m3
deformation in y-direction [m]
time [s]
MP 23010
MP 23034
MP 23060
MP 23416
MP 23437
MP 23590
MP 24162
MP 24186
MP 24206

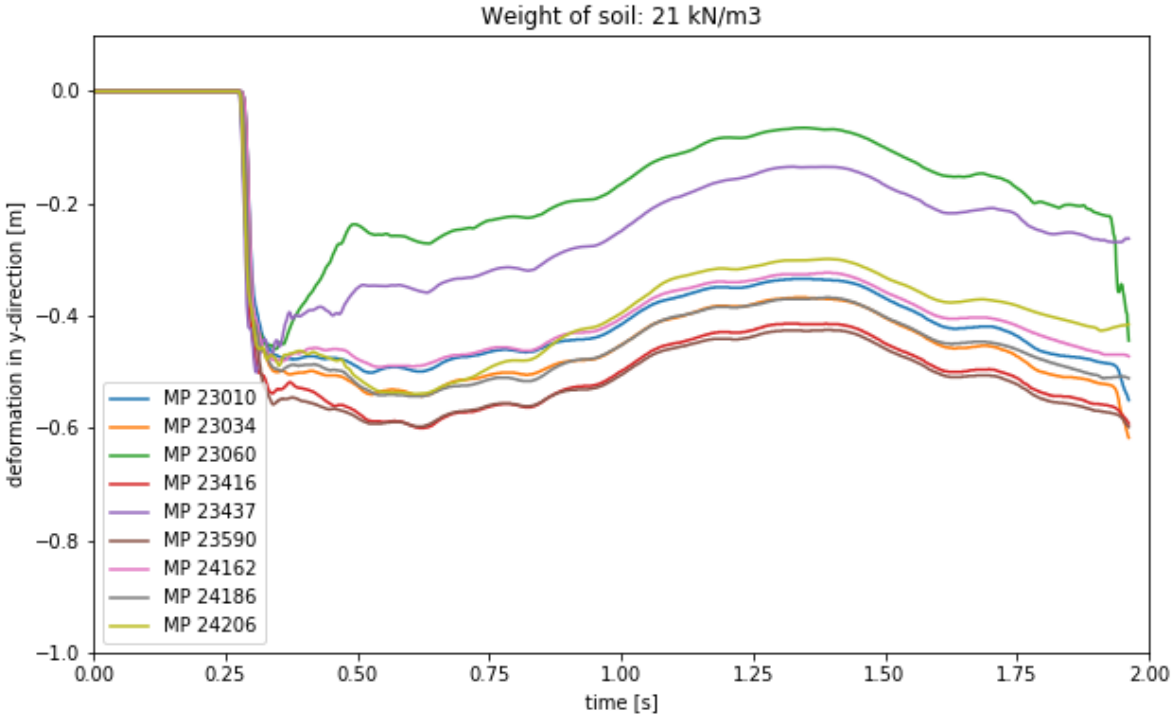
Weight of soil: 21 kN/m3
deformation in y-direction [m]
time [s]
MP 23010
MP 23034
MP 23060
MP 23416
MP 23437
MP 23590
MP 24162
MP 24186
MP 24206

D.5 Mass of the nacelle

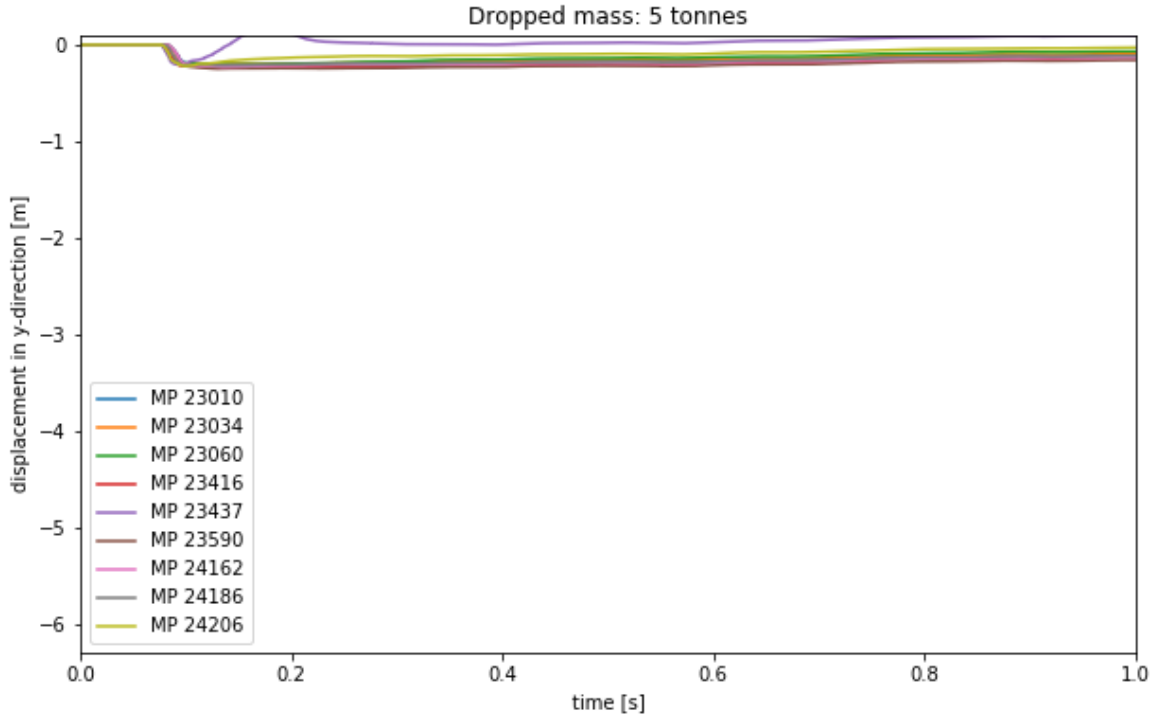

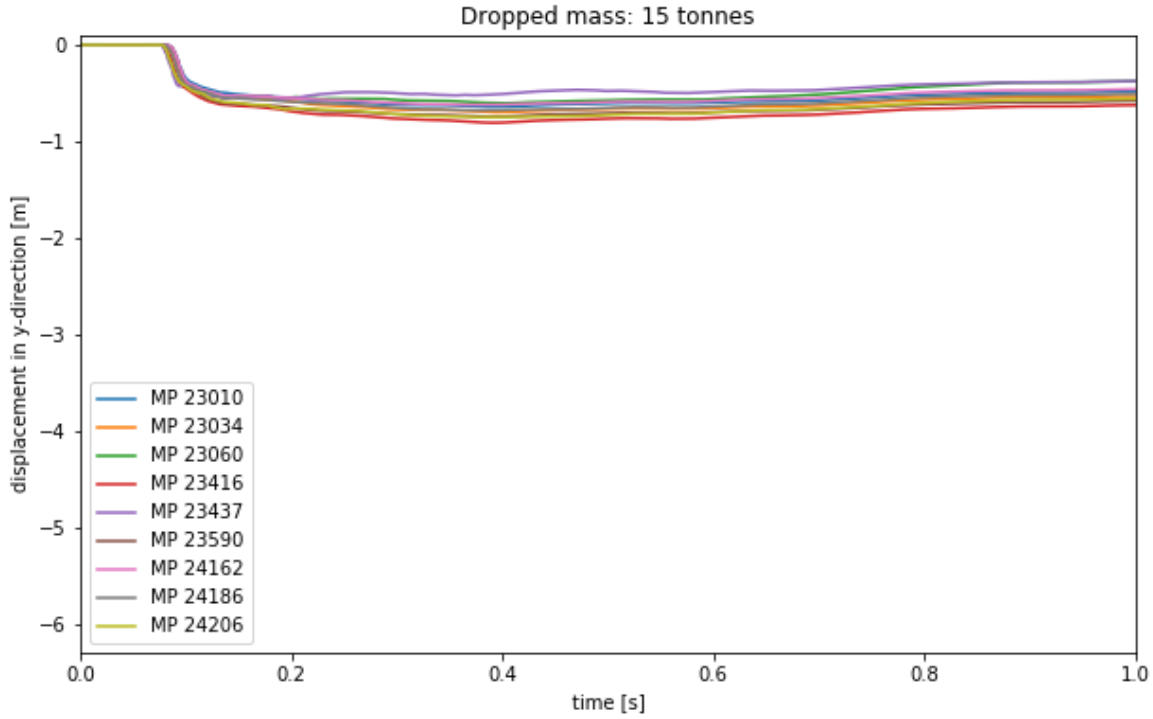

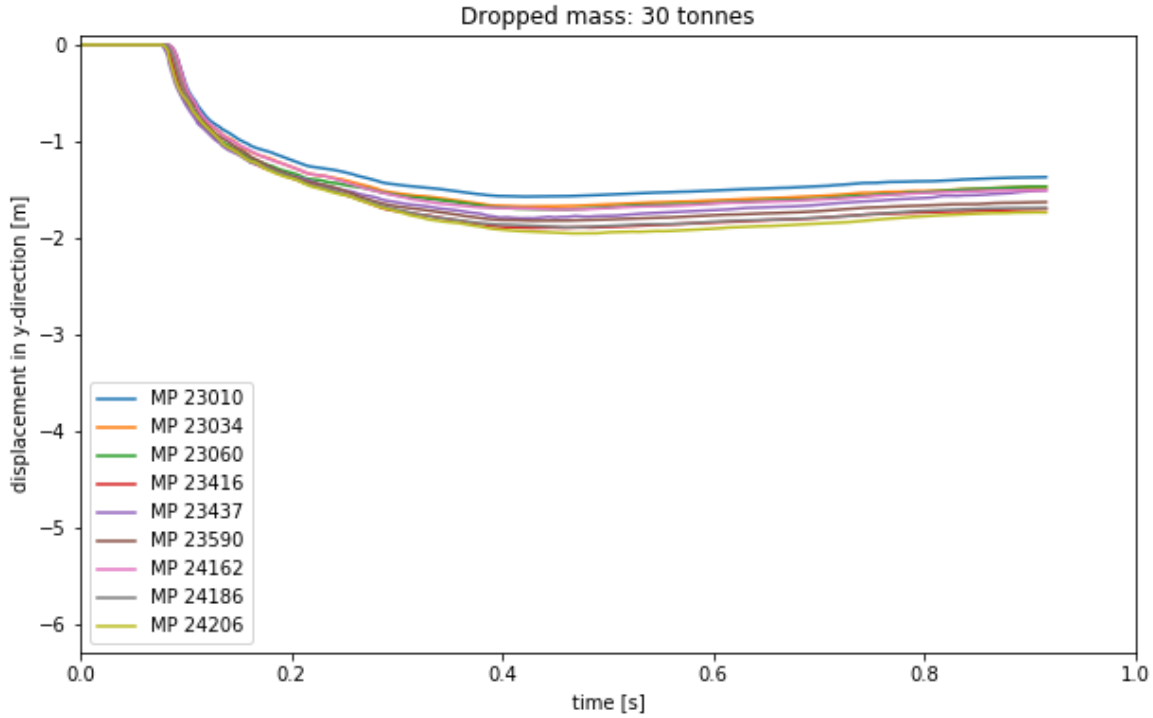
Dropped mass: 30 tonnes
displacement in y-direction [m]
time [s]
MP 23010
MP 23034
MP 23060
MP 23416
MP 23437
MP 23590
MP 24162
MP 24186
MP 24206

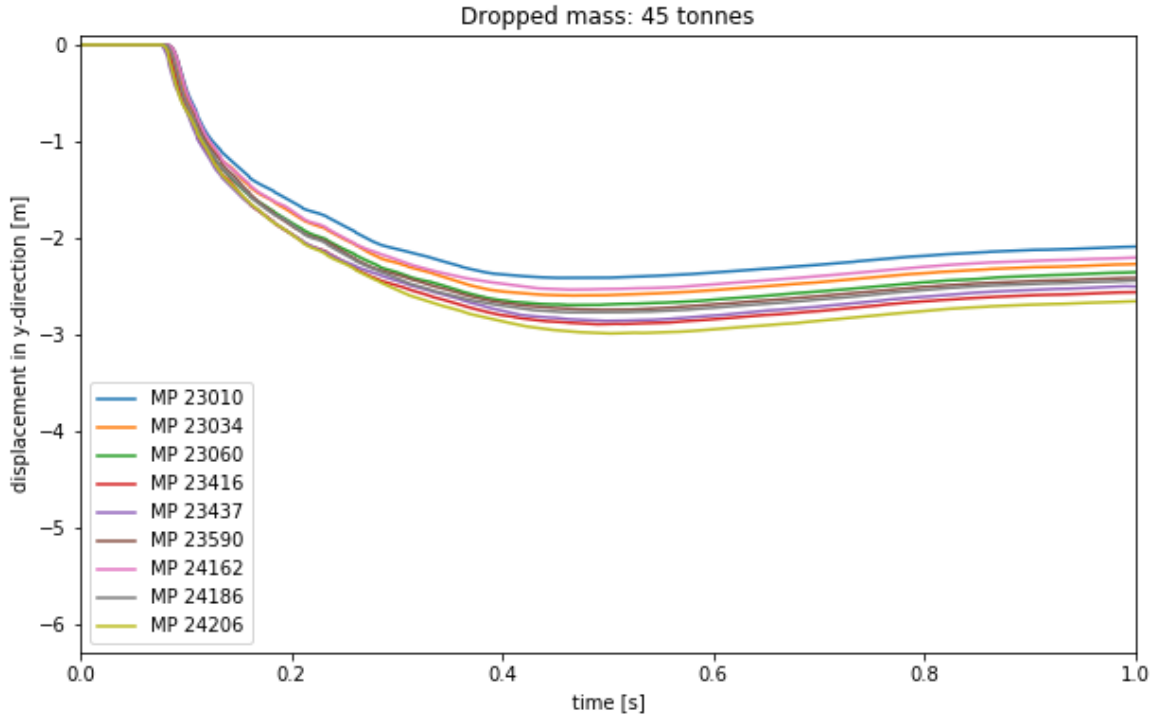
Dropped mass: 45 tonnes
displacement in y-direction [m]
time [s]
MP 23010
MP 23034
MP 23060
MP 23416
MP 23437
MP 23590
MP 24162
MP 24186
MP 24206

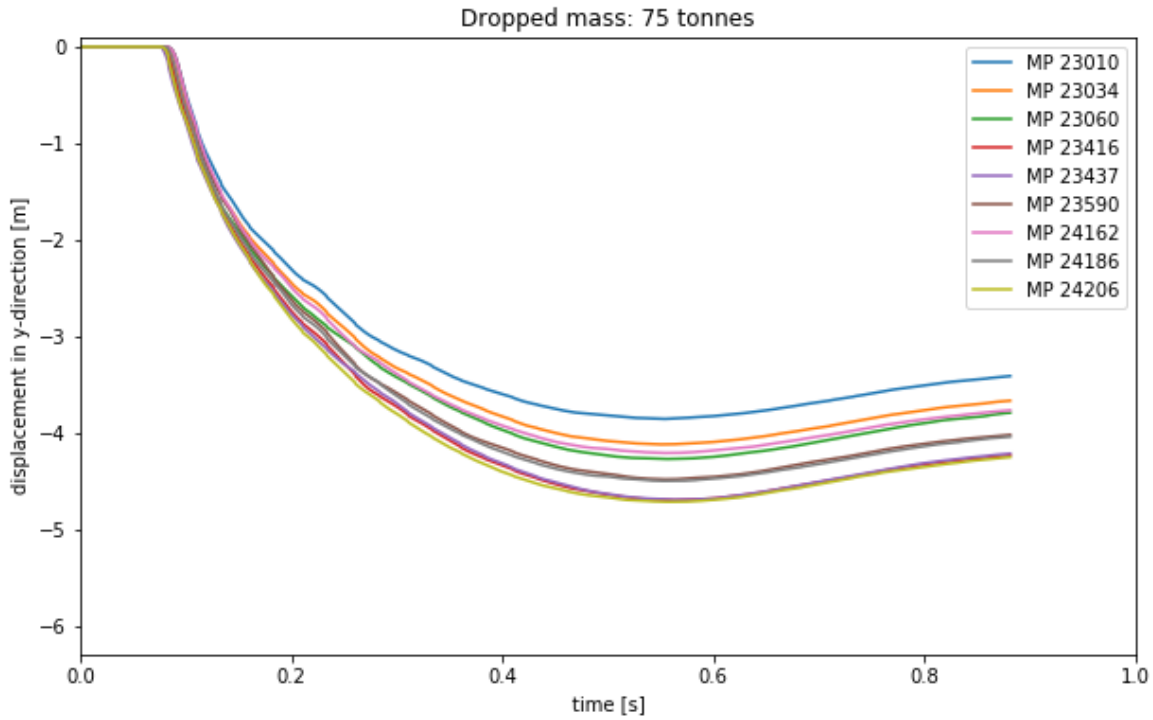
Dropped mass: 75 tonnes
displacement in y-direction [m]
time [s]
MP 23010
MP 23034
MP 23060
MP 23416
MP 23437
MP 23590
MP 24162
MP 24186
MP 24206

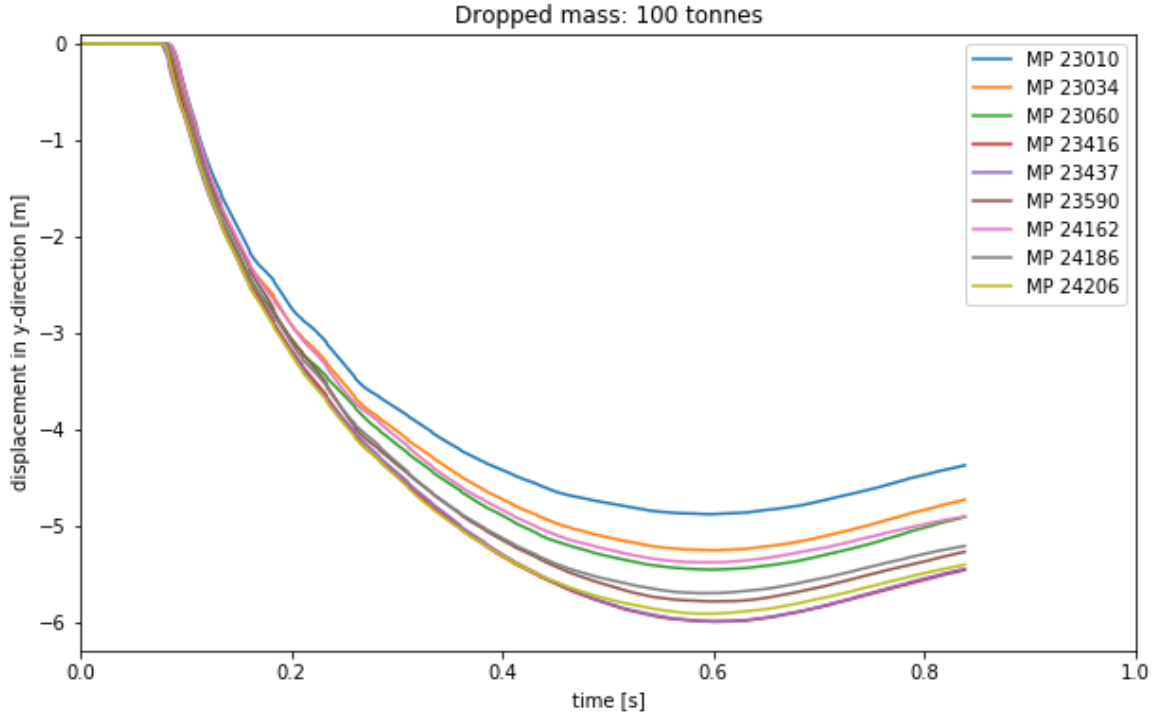
Dropped mass: 100 tonnes
displacement in y-direction [m]
time [s]
MP 23010
MP 23034
MP 23060
MP 23416
MP 23437
MP 23590
MP 24162
MP 24186
MP 24206

Appendix E

Stability Calculations

E.1 Soil profile

In Figure E.1 the soil profile which is used for the stability calculations is shown. The source is the DINOloket. The Cone penetration test is from a similar dike as in the case study described. The location of the cone penetration test was at the Frisian part of the Wadden sea dike (Koehol). It shows that the crest level is NAP +9 m, exactly the same as in the case study. Table E.1 shown the properties which are derived from Figure E.1.

Table E.1: Soil layers and properties

Layer number	**Top NAP** [m]	**Material name**	**Gam usat** [kN/m3]	**Gam sat** [kN/m3]	**Cohesion** [kN/m2]	**Phi** [degrees]	**Dilatancy** [degrees]
7	9.00	Sand	18.00	20.00	0.00	30.00	30.00
6	1.00	Sandy Clay	20.00	20.00	1.00	30.00	0.00
5	-1.50	Stiff Clay	19.00	19.00	13.00	22.50	0.00
4	-4.50	Sandy Clay	20.00	20.00	1.00	30.00	0.00
3	-7.00	Sand	18.00	20.00	0.00	30.00	30.00
2	-11.00	Sandy Clay	20.00	20.00	1.00	30.00	0.00
1		Sand	18.00	20.00	0.00	30.00	30.00

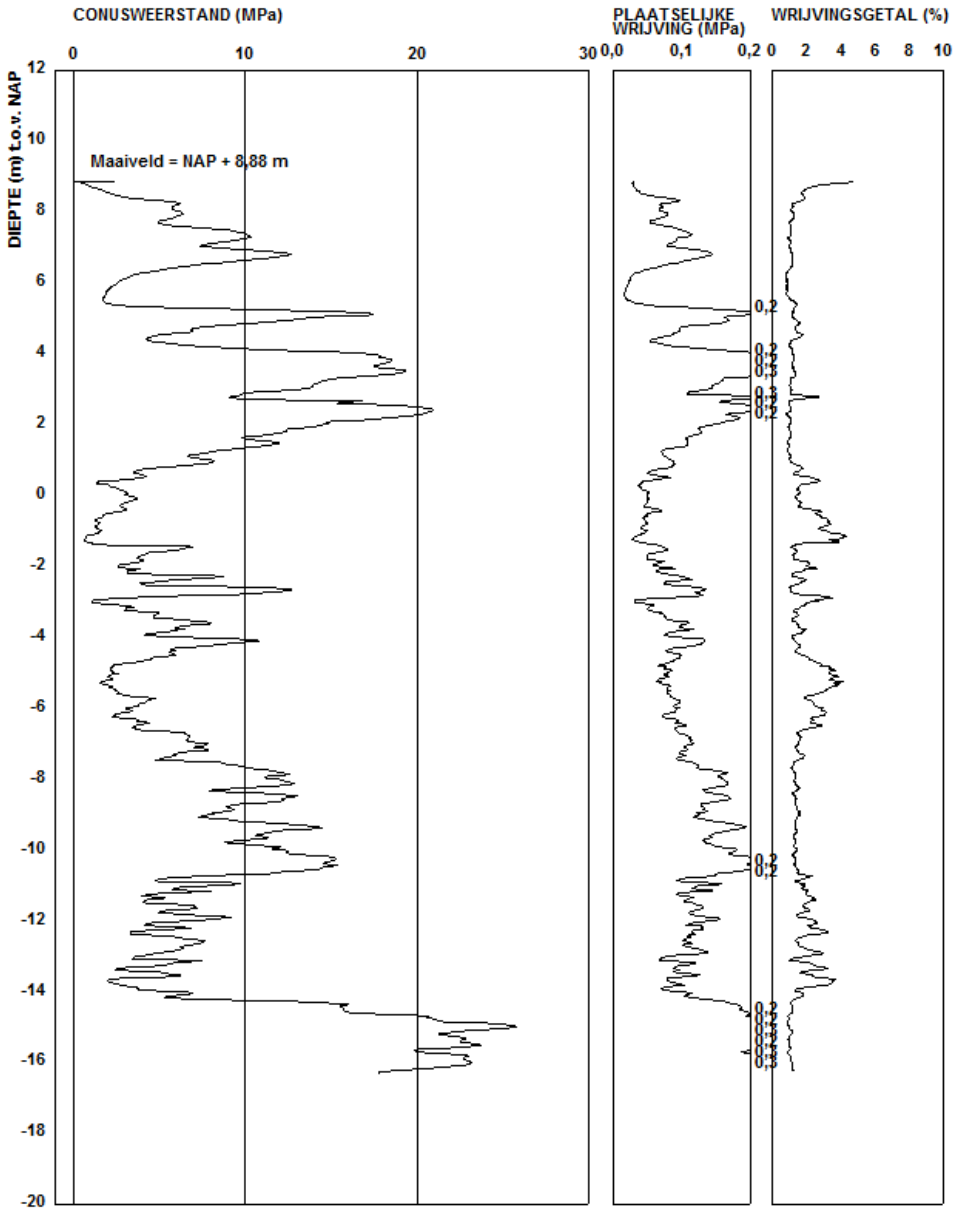

Figure E.1: Cone penetration test

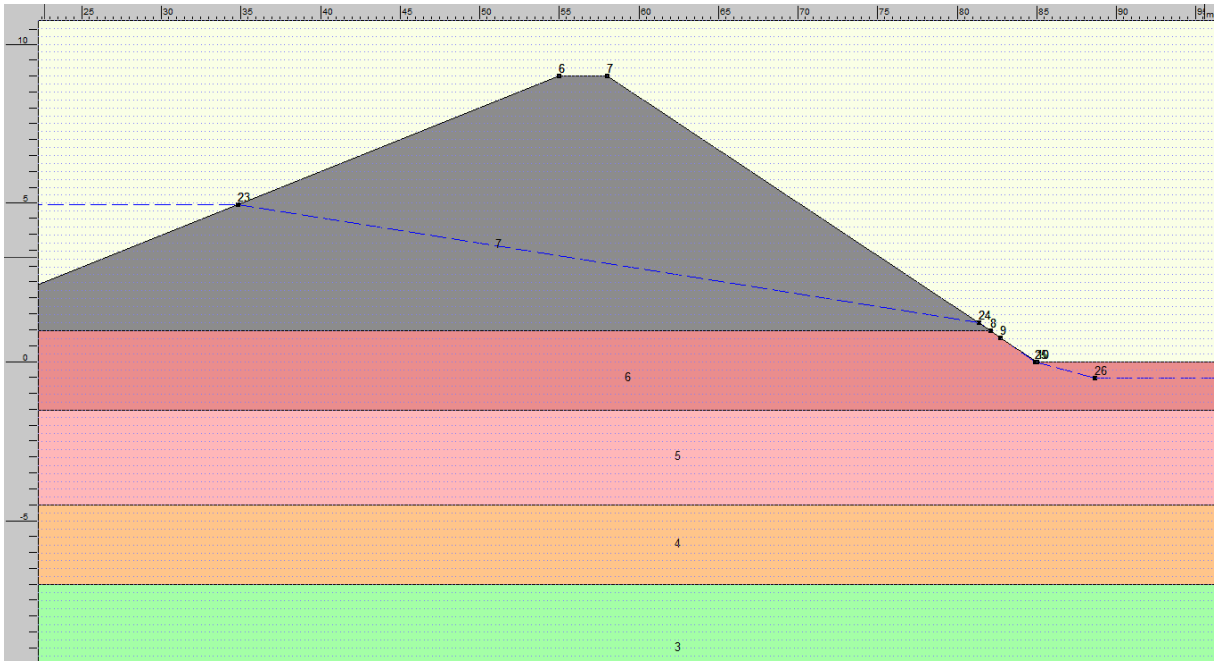

Figure E.2: Soil geometry

E.2 Slope-instability after impact on the crest

Impact on the crest without penetration

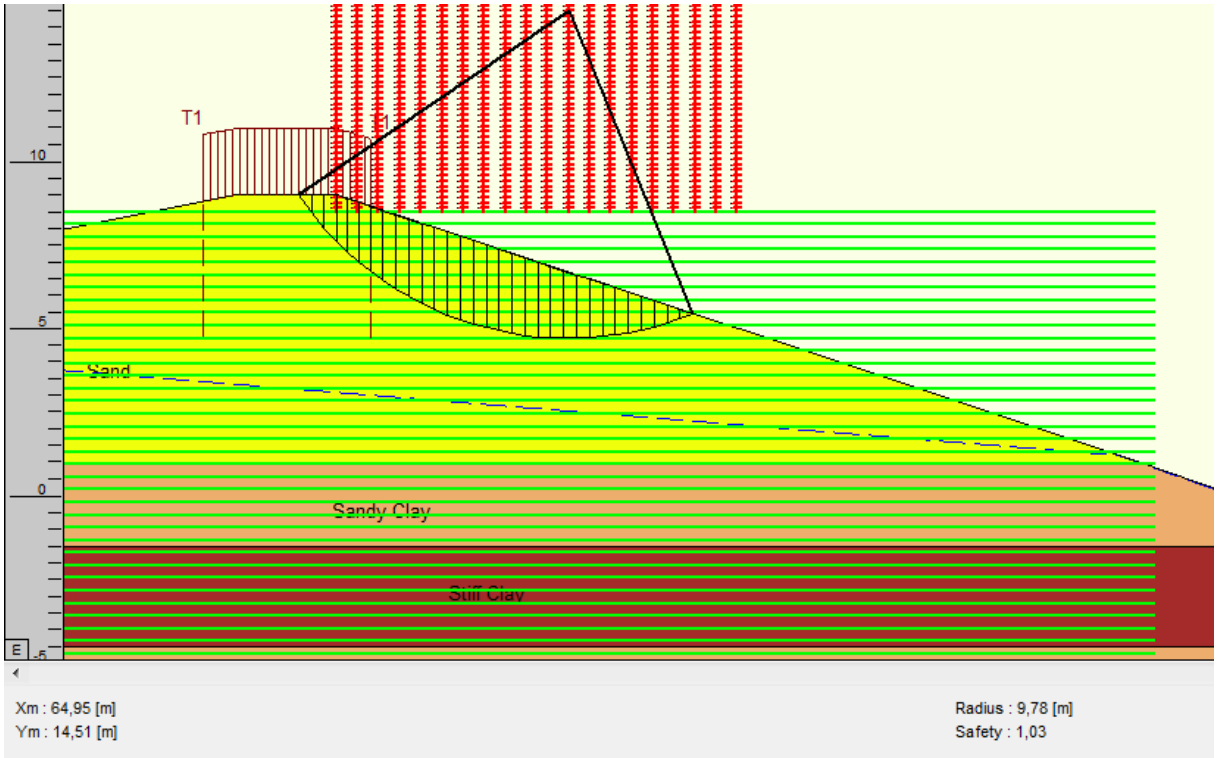

Figure E.3: Inner slope stability after crest impact without penetration

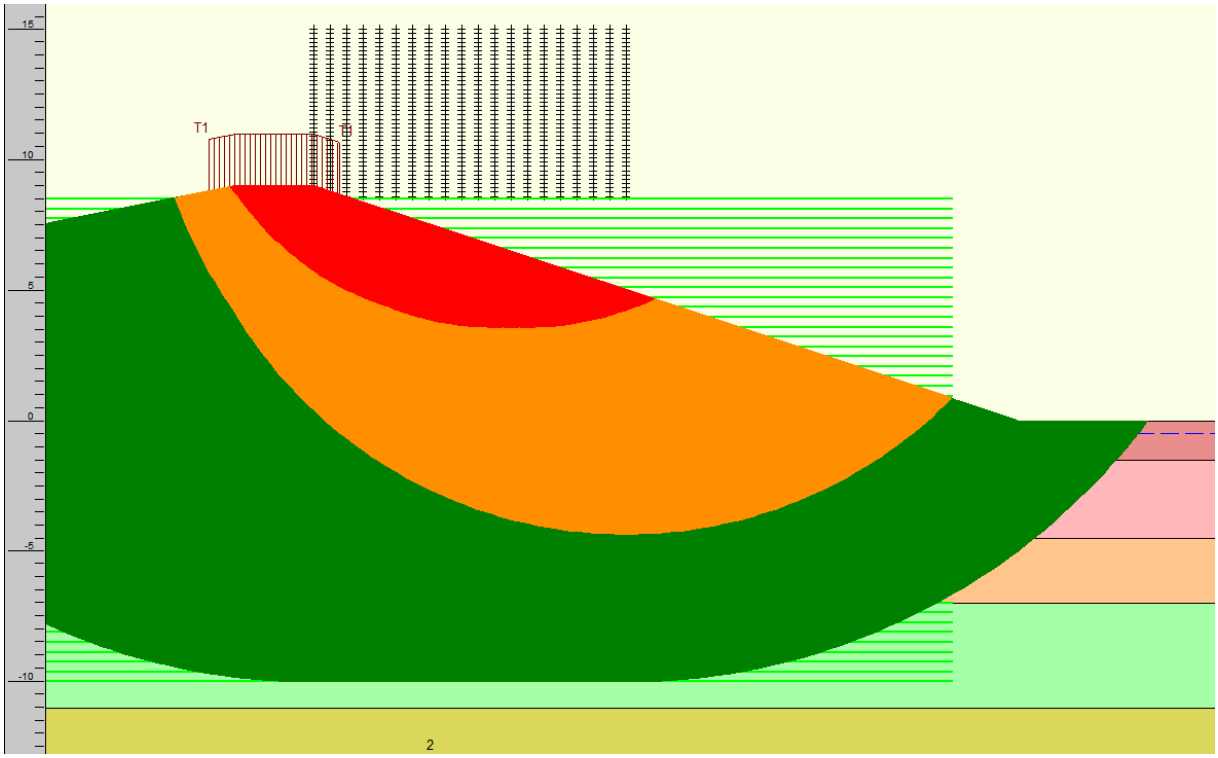

Figure E.4: Stability overview after an impact at the crest without penetration

2.0 meters penetration at the crest

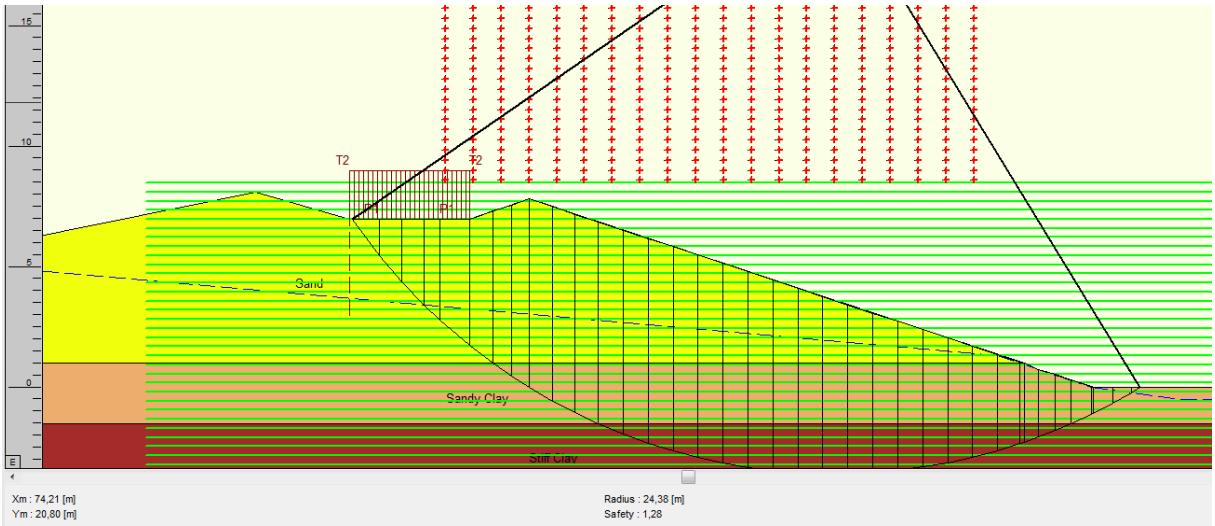

Figure E.5: Inner slope stability after 2 meters penetration at the crest

3.8 meters penetration at the crest

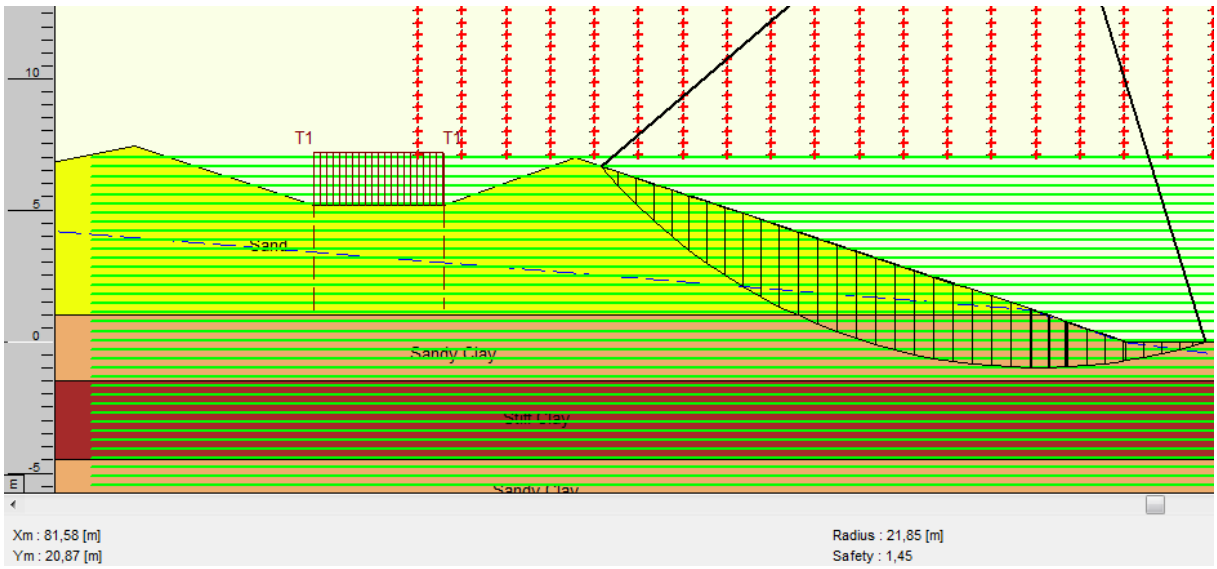

Figure E.6: Inner slope stability after 3.8 meters penetration at the crest

E.3 Slope-instability after impact on the slope

No penetration

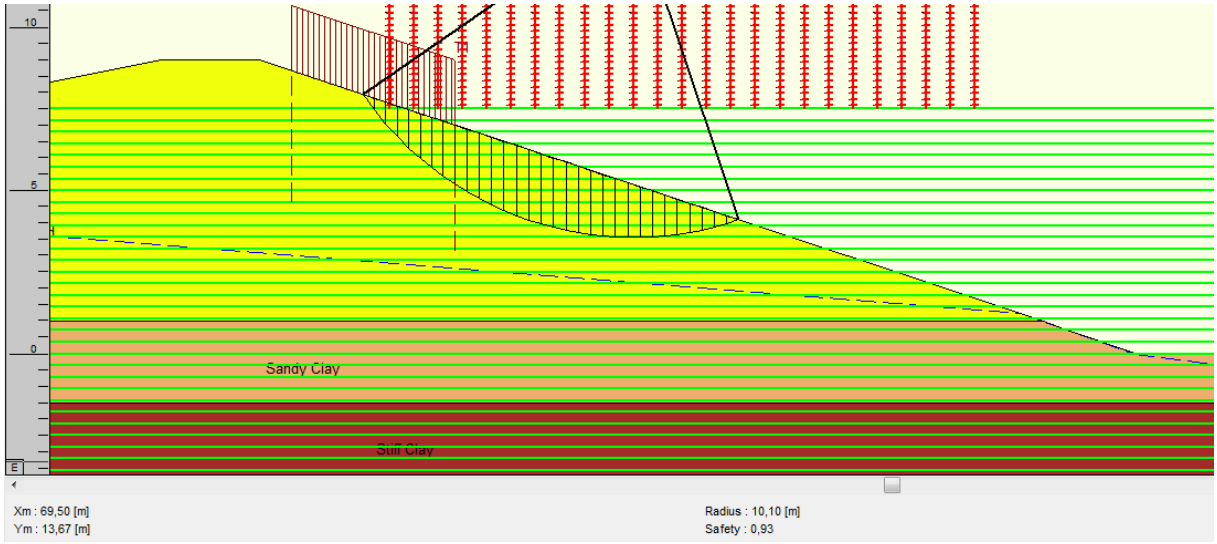

Figure E.7: Inner slope stability after no penetration at the slope

With penetration

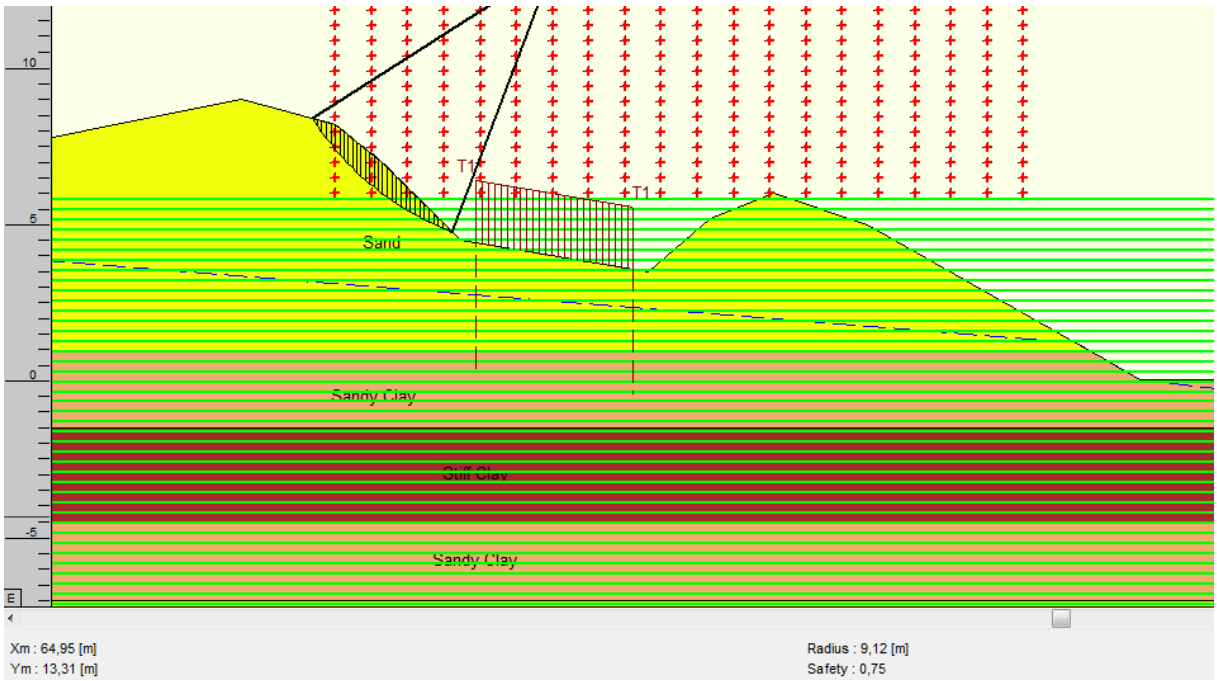

Figure E.8: Inner slope stability after 3.8 meters penetration at the slope, smallest sliding circle

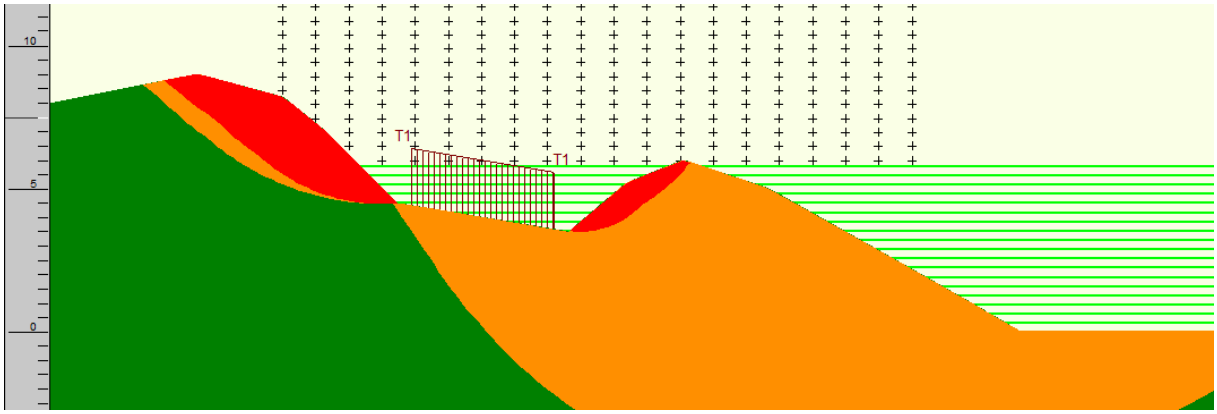

Figure E.9: Stability overview after an impact at the slope with 3.8 meters penetration

Bibliography

(2016). 290 Tonne Vestas Wind Turbines Dropping Like Giant Wounded Flies. (Accessed: 2017-06-27).
URL https://stopthesethings.com/2016/01/01/290-tonne-vestas-wind-turbines/-dropping-like-giant-wounded-flies/

(2016). Haringvlietdam Noord ongeschikt voor windmolens. (Accessed: 2017-04-12).
URL http://www.groothellevoet.nl/nieuws/actueel/58298/haringvlietdam-noord-ongeschikt-voor-windmolens

(2016). Kahuku Wind Generation Lease & Maui Wind Turbine Disaster. (Accessed: 2017-06-27).
URL http://www.ililani.media/2016/10/blnr-hearing-tomorrow-kahuku-wind.html

(2017). De bouw is begonnen! (Accessed: 2017-04-12).
URL http://www.windparkkrammer.nl/horizontale-hdd-boring-is-bouw-echt-begonnen/

(2017). Wind turbine keels over in County Down. (Accessed: 2017-06-27).
URL http://www.bbc.com/news/uk-northern-ireland-38845082

Al-Kafaji, I. K. J. (2013). *Formulation of a Dynamic Material Point Method (MPM) for Geomechanical Problems*. Ph.D. thesis.

Ashuri, T., Zaaijer, M. B., Martins, J. R. A., & Zhang, J. (2016). Multidisciplinary design optimization of large wind turbines - Technical, economic, and design challenges. *Energy Conversion and Management*, *123*, 56–70.
URL http://dx.doi.org/10.1016/j.enconman.2016.06.004

Bernard, R. S. (1975). Development of a projectile penetration theory. Tech. rep.

Beuth, L., Więckowski, Z., & Vermeer, P. A. (2010). Solution of quasi-static large-strain problems by the material point method. *International Journal for Numerical and Analytical Methods in Geomechanics*, *35*(13), n/a–n/a.
URL http://doi.wiley.com/10.1002/nag.965

Deltares (2014). Groningse kades en dijken bij geïnduceerde aardbevingen. Tech. rep.

Deltares (2016a). Fenomenologische beschrijving. Tech. rep.

Deltares (2016b). Seismisch Dijkontwerp: Protocol voor Eemshaven-Delfzijl. Tech. rep.

ENW (2014). Advies Windturbines op de primaire waterkering Oostpolderdijk. Tech. rep.

ENW (2016). *Grondslagen voor hoogwaterbescherming*.

European Commission Research & Innovation (2013). Energy research. (Accessed: 2017-04-05).
URL https://ec.europa.eu/research/energy/print.cfm?file=/comm/research/energy/nn/nn{_}rt/nn{_}rt{_}wind/article{_}1101{_}en.htm

Fugro Geoservices b.v. (2008). Effecten op de waterkering Windpark Noordermeerdijk Noordoostpolder. Tech. Rep. november.

Fugro Geoservices b.v. (2012). Verkenning risicofactoren windturbines nabij waterkeringen zuiderzeeland. Tech. rep.

Fugro Geoservices b.v. (2016). Generiek afstandscriterium voor windturbines bij primaire waterkeringen in flevoland. Tech. rep.

Fugro Geoservices b.v. (2017). Trillingen van windturbines in exploitatiefase bij waterkeringen. Tech. rep.

Grontmij (2016). Milieueffectrapport Dijkverbetering Eemshaven-Delfzijl. Tech. rep.

Hau, E. (2006). *Wind Turbines: Fundamentals, Technology, Application, Economics*. URL `http://books.google.com/books?id=KeNEAAAAQBAJ{%}7B{&}{%}7Dpgis=1`

Hölscher, P. (2016). Dynamisch gedrag van een on-shore windturbinefundering. *Vakblad Geotechniek*, (4), 8–13.

Jonkman, S., & Schweckendiek (eds), T. (2015). *Flood Defences Lecture Notes CIE5314*.

Kenkman, T., Hörz, F., & Deutsch, A. (2005). *Large meteorite impacts III*. Geological Society of America.

KNMI (2017). Zware stormen in Nederland sinds 1910. (Accessed: 2017-10-19). URL `https://www.knmi.nl/nederland-nu/klimatologie/lijsten/zwarestorm`

KPR (2016). Faalkansbegroting. Tech. rep.

Ma, S., & Zhang, X. (2009). Material Point Method for Impact and Explosion Problems. *Computational Mechanics*, (pp. 156–166).

Mayne, P. W., Jones, J. S., & Dumas, J. C. (1984). Ground response to dynamic compaction. *Journal of Geotechnical Engineering*, *110*(6), 757–774.

Ménard, L., & Broise, Y. (1975). Theoretical and Practical Aspects Dynamic Consolidation. *Géotechnique*, *25*(1), 3–18.

Menard Asia (2017). Dyanmic compaction. (Accessed: 2017-06-27). URL `http://www.menard-asia.com/`

Ministerie van Infrastructuur en Milieu (2014). Structuurvisie Windenergie op land. Tech. rep.

MPM Research Community (2016). Scientific Manual Anura3D. Tech. Rep. May.

National Geographic (2013). Windpark Irene Vorrink. URL `http://www.nationalgeographic.com/magazine/2013/09/rising-seas-coastal-impact-climate-change/`

NEN (2011). NEN-EN 1990: Grondslagen van het constructief ontwerp. Tech. rep. URL `https://www.nen.nl/NEN-Shop/Norm/NENEN-1990A1A1-C22011-nl.htm`

NEN 9997-1:2016 nl (2016). *NEN Connect: NEN 9997-1: Geotechnisch ontwerp van constructies - Deel 1: Algemene regels*. URL `https://connect.nen.nl/`

NOS (2016). Recordaantal windmolens gebouwd. (Accessed: 2016-01-05).
URL http://nos.nl/artikel/2078776-recordaantal-windmolens-gebouwd.html

Osinski, G., Tornabene, L. L., & Grieve, R. A. F. (2011). Impact ejecta emplacement on terrestrial planets. *Earth and Planetary Science Letters*, *310*(3-4), 167–181.
URL http://linkinghub.elsevier.com/retrieve/pii/S0012821X11004675

Osinski, G. R., & Pierazzo, E. (2012). *Impact Cratering*. John Wiley & Sons, Incorporated.

Plaxis (2016). Material Models Manual. Tech. rep.

Pondera Consult (2009). MER Windpark Noordoostpolder Algemeen Deel. Tech. rep.

Provincie Zuid-Holland (2009). Vuistregels voor het beheerdersoordeel bij de toetsing van niet-waterkerende objecten.

Quilter, J. (2016). 10 of the Biggest Turbines. (Accessed: 2017-03-23).
URL http://www.windpowermonthly.com/10-biggest-turbines

Raferty, M. (2016). Wind Turbine Collapses in Ocotillo. (Accessed: 2017-06-27).
URL http://www.eastcountymagazine.org/wind-turbine-collapses-ocotillo

Rijkswaterstaat (2015). Beleidsregel voor het plaatsen van windturbines op , in of over rijkswaterstaatswerken.

Rijkswaterstaat (2016a). Schematiseringshandleiding Macrostabiliteit WBI2017. (december 2016).

Rijkswaterstaat (2016b). *WBI2017: Bijlage I Procedure Regeling primaire waterkeringen 2017*.

Rijkswaterstaat (2016c). *WBI2017: Bijlage III Sterkte en veiligheid Regeling primaire waterkeringen 2017*.

Rohe, A., & Liang, D. (2017). Modelling large deformation and soil water struture interaction with material poind method: Briefing on MPM2017 conference. *Journal of Hydrodynamics, Ser. B*, *29*(3), 393–396.
URL http://www.sciencedirect.com.tudelft.idm.oclc.org/science/article/pii/S1001605816607485

Royal HaskoningDHV (2012). Onderzoek technische mogelijkheden windturbines Afsluitdijk: Verkenning van de technische haalbaarheid. Tech. Rep. december.

Royal HaskoningDHV (2013). Toets primaire waterkering: Windpark Krammer te Bruinisse. Tech. rep.

Royal HaskoningDHV (2014). Toets primaire waterkering: Windpark Krammer te Bruinisse Voorkeursalternatief. Tech. rep.

RVO (2014). Handboek Risicozonering Windturbines v3.1.
URL http://ebooks.cambridge.org/ref/id/CBO9781107415324A009

RVO (2016). Monitor Wind op Land 2015.

RWS (2014). Achtergrondrapport Ontwerpinstrumentarium 2014v4. Tech. rep.

Sánchez de Lara García, J. P. (2013). *Wind turbine database: Modelling and analysis with focus on upscaling*. Ph.D. thesis, Chalmers University of Technology.

SenterNovem (2005). Windkaart van Nederland. Tech. rep.

Shaam News Network (2012). Crater at al-Zaphara neh near Homs, July 7, 2012. (Accessed: 2017-06-26).
URL http://darkroom.baltimoresun.com/2012/07/july-8-photo-brief-roger-federer/-wins-seventh-wimbledon-title-rebels-seize-towns-in-eastern-democratic/-republic-of-congo/{#}22

Shahan, Z. (2014). History of Wind Turbines. (Accessed: 2017-03-27).
URL http://www.renewableenergyworld.com/ugc/articles/2014/11/history-of-wind-turbines.html

Sociaal-Economische Raad (2013). Energieakkoord voor duurzame groei. Tech. Rep. September.

Tagesschau (2017). Sendung: tagesthemen 29.08.2017 22:15 Uhr.
URL http://www.tagesschau.de/multimedia/sendung/tt-5467.html

TAW (1998). *Fundamentals on water defences*.

TAW (2004). Technisch Rapport Waterspanningen bij dijken. Tech. Rep. september.

Terzaghi, K. (1943). *Theoretical Soil Mechanics*. Hoboken, NJ, USA: John Wiley & Sons, Inc.
URL http://doi.wiley.com/10.1002/9780470172766

US Department of Energy (2014). Inside of a wind turbine. (Accessed: 2017-04-02).
URL https://energy.gov/eere/wind/inside-wind-turbine-0

Willenbacher, M. (2012). Repowering bietet immenses Potenzial.

Williams, D. (2017). Collapse of wind turbine under investigation. (Accessed: 2017-06-27).
URL http://www.powerengineeringint.com/articles/2017/01/collapse-of-wind-turbine-under-investigation.html

Witteveen+Bos (2016). Milieueffectenstudie windpark Eemshaven-West: Deelrapport Waterveiligheid. Tech. rep.

Yerro, A. (2015). *MPM modelling of landslides in brittle and unsaturated soils*. Phd thesis, Universitat Politecnica de Catalunya.
URL http://upcommons.upc.edu/handle/2117/102412

Young, C. W. (1997). Penetration Equations. Tech. rep.

Zhang, X., Chen, Z., Liu, Y., Zhang, X., Chen, Z., & Liu, Y. (2017). Applications of the MPM. In *The Material Point Method*, (pp. 231–263).
URL http://www.sciencedirect.com.tudelft.idm.oclc.org/science/article/pii/B9780124077164000089

Acronyms and glossary

ENW	Expertise Network for Flood Protection
GEKB	Gras erosion crest and inner slope
HRW	Handboek risicozonering windturbines
MPM	Material Point Method
Nacelle	Housing machine on top of the tower of a wind turbine
NWO	Non water retaining object
STBI	Instability of the inner slope
STBK	Erosion of the outer slope revetment
WBI2017	Wettelijk Beoordelings Instruarium 2017
WT	Wind Turbine

Symbols

Symbol	Description	Units
a_l	Factor for the mechanism-sensitive fraction of the dike segment	–
A	Cross-sectional area falling object	m^2
a,b,c	Coefficients for the motions of soil	–
$\beta_{req,cs}$	Reliability index for a cross-section	–
b_l	Measure for the intensity of the length effect within the mechanism-sensitive length of the dike segment	–
γ_b	schematization factor	–
γ_d	Model factor	–
γ_m	Material factor	–
γ_n	Damage factor	–
γ_R	Stability factor or Safety factor	–
c	Wave speed	m/s
δ	Penetration depth by Ménard	m

D	Penetration depth	m
d	Projectile diameter	m
E	Young's modulus	GPa
g	Gravitational constant	m/s^2
H	Height of dropping	m
h	Falling height	m
m	Mass of falling object	kg
N_{cs}	Length effect factor	–
N	Nose performance coefficient	–
$P_{f,cs}$	Actual additional failure probability of an assessment track at cross-section level	$year^{-1}$
$P_{f,WT}$	Failure probability of a wind turbine failure	$year^{-1}$
$P_{failure,blade}$	Probability that a blade falls of a wind turbine	$year^{-1}$
$P_{failure,tower}$	Probability that the tower of wind turbine falls over	$year^{-1}$
$P_{flooding\|FM}$	Flooding probability given a failure of a flood defence	–
$P_{FM\|hit}$	Failure probability of failure mechanism given a flood defence has been hit	–
$P_{hitting\|f,wt}$	Hitting probability of wind turbine given a wind turbine failure	–
$P_{hitting}$	Probability that the falling component hits the dike	$year^{-1}$
$P_{req,cs}$	Required failure probability per cross-section	$year^{-1}$
ρ	Density	kg/m^3
S	Penetrability of target	–
V	Velocity falling object	m/s
v	Maximal free falling velocity	m/s
ω	Failure probability budget factor	–
$\omega_{1turbine}$	Permissible additional failure probability per wind turbine	–
W	Mass of falling object	t